Loughborough University

This item is held in Loughborough University's Institutional Repository (https://dspace.lboro.ac.uk/) and was harvested from the British Library's EThOS service (http://www.ethos.bl.uk/). It is made available under the following Creative Commons Licence conditions.

creative commons

COMMONS DEED

Attribution-NonCommercial-NoDerivs 2.5

You are free:

- to copy, distribute, display, and perform the work

Under the following conditions:

Attribution. You must attribute the work in the manner specified by the author or licensor.

Noncommercial. You may not use this work for commercial purposes.

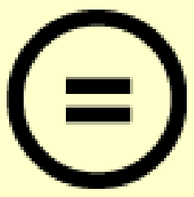

No Derivative Works. You may not alter, transform, or build upon this work.

- For any reuse or distribution, you must make clear to others the license terms of this work.
- Any of these conditions can be waived if you get permission from the copyright holder.

Your fair use and other rights are in no way affected by the above.

This is a human-readable summary of the Legal Code (the full license).

Disclaimer

For the full text of this licence, please go to:
http://creativecommons.org/licenses/by-nc-nd/2.5/

THE INHIBITION OF CALCIUM CARBONATE PRECIPITATION IN WATER SOFTENING

by

MOHAMMED HUSSEIN AL-MAWLAWI

A Doctoral Thesis

submitted in partial fulfilment of the requirements

for the award of Doctor of Philosophy of the

Loughborough University of Technology

AUGUST 1979

Supervisor: Dr. R. J. Akers

Department of Chemical Engineering

© by M. H. AL-Mawlawi (1979)

"In the name of Allah, the Beneficient, the Merciful"

And your Lord has decreed that you worship none but Him and that you be dutiful to parents. If one of them or both of them attain old age in your life, say not to them a word of disrespect, nor shout at them, but address them in terms of honour.

And lower unto them using the wing of submission through mercy, and say: "My Lord! Have mercy on them both as they cherished me in childhood."

The Holy QUR'ĀN

This thesis is respectfully dedicated to

MY MOTHER

for without her encouragement over the years none of this would ever have been achieved.

I hereby certify that I am responsible for the work submitted in this thesis and that the original work is my own except as specified in the acknowledgements or footnotes.

ACKNOWLEDGEMENTS

I would like to thank my supervisor, Dr. R. J. Akers, for his stimulating help, guidance, invaluable suggestions and encouragement during the period of my study; to Professor D. C. Freshwater, for providing the research facilities.

I would also like to thank the academic staff of the Department of Chemical Engineering, in particular the Particle Technology Group for their friendship and many valuable technical discussions.

My thanks are due to the technical staff, in particular the particle sizing laboratory technicians, for their help patience and ingenuity.

My thanks are also due to my family, for their help, patience and encouragement during my stay in the U.K.

Last, but not least, I thank all my friends, at Loughborough and Anstey, for the very pleasant and unforgettable time that I have had with them.

CONTENTS

SUMMARY

The cold-lime water softening reaction was simulated by the precipitation of calcium carbonate following the addition of lime water to prepared solutions of calcium bicarbonate. A laboratory batch crystalliser was used. The overall rate of calcium ion removal was followed using an ion selective electrode and samples were removed for Coulter Counting to enable the variation in crystal size with time to be studied. The effect on the crystallisation rate due to some organic materials likely to be present in raw water or added during processing was studied. These experiments were done with and without added calcium carbonate to simulate conditions in a retained sludge type of reactor.

The calcium ion measurements enabled the induction period before precipitation, the half life of the precipitation and the precipitation rate to be determined. High molecular weight polyacrylamides of anionic, cationic and nonionic type, had no significant effects whereas an extract of water humic substance and low molecular weight polyacrylate had a marked effect on the induction period, half life and precipitation rate. A starch was intermediate in its effects. The optimum does and the adsorption isotherms of the flocculants on calcium carbonate were also determined. The crystal size distribution over the range 2-37 μm was determined by Coulter Counter for several runs. Although high product recovery was obtained attempts to use the population balance method for a detailed study of the nucleation kinetics were less successful.

From the results obtained possible reasons for the observed differences in inhibition behaviour were discussed, with particular reference to the solution diffusivity of the species concerned.

TABLES

FIGURES

NOMENCLATURE

a	activity
a	particle radius
a	sieve aperture
a_i	surface area of the ith face of a crystal
A	constant dependent on the ionic diameter (see eq. 2.3)
A	Hamaker constant
A	pre-exponential factor
A, A_s	surface area
Δc	concentration driving force or overall supersaturation ($C - C^*$)
C	concentration in bulk solution
C^*	equilibrium saturation concentration
C_D	drag coefficient
C_i	solution concentration at crystal solution interface (see eq. 4.26)
CO_3	carbonate alkalinity
C_r	concentration of solution in equilibrium with crystal size, r.
C_∞	concentration of solution of solution in equilibrium with crystal size infinity.
$C_{(0)}$	initial concentration
$C_{(t)}$	$[Ca^{++}]$ at time, t.
$C_{(\infty)}$	$[Ca^{++}]$ at completion of precipitation
C_V	coefficient of variation
d	particle diameter
D	coefficient of diffusion (diffusivity)
e	electron charge
E	activation energy
E	extinction

g	gravitational acceleration
G	linear crystal growth rate
G	velocity gradient
$\bar{G}$	mean velocity gradient
ΔG	overall free energy
$\Delta \bar{G}$	free energy of activation for crystal growth (see eq. 4.18)
ΔG_d	free energy of activation for diffusion of molecules
$\overline{Gt}$	Camp number
h_f	hydraulic head loss
ΔH^*	enthalpy of process
H^+	hydrogen concentration
H	depth of clarification zone (see eq. 3.1)
H	Plank's constant
H	surface-surface distance between two spherical particles.
HCO_3	bicarbonate alkalinity
I	intensity of transmitted light
I_o	intensity of incident light
I_s	saturation index
J	nucleation rate
k	Boltzmann's constant
k	second order rate constant
K	specific reaction rate constant (see eq. 4.4)
K_d	mass transfer coefficient for the diffusion step in crystal growth
K_o	pre-exponential factor (see eq. 4.4)
K_r	surface integration rate coefficient
K_G	overall mass transfer coefficient

K_{sp} solubility product

K'_{sp} corrected solubility product

K_w, K_1, K_2 dissociation constants

K'_w, K'_1, K'_2 corrected dissociation constants

L crystal size

m mass of solid deposited

m methyl orange alkalinity

M mole (gm equivalent/litre)

n order of growth process

n number of ions required to form critical nucleus (see eq. 4.13)

n, n^o population density (number/ml/micron)

n_1 number of molecules per unit volume of system (see eq. 4.17)

n_i number of molecules or ions, i, per unit volume

N Avogadro's number

N cumulative number distribution

N measure of agitation (see eq. 4.21)

N number of nuclei (see eq. 4.13)

N^o number of particles per unit volume

N^o_o initial (t = o) number of particles per unit volume

pA p operates on A and is equal to - log A

pH_s saturation pH value

P phenolphthalein alkalinity

$\bar{P}$ power dissipated in fluid motion

P pressure

P_o ambient pressure

P_r vapour pressure over liquid droplet of radius, r.

P_∞ equilibrium saturation vapour pressure

Q	flow rate
r	interaction distance between two spherical particles
r	radius of spherical particles (or droplet)
r_c	critical nuclear size
R	gas constant
R_e	Reynold's number
R_g	overall growth rate (see eq. 4.41)
S*	critical supersaturation
S_i	supersaturation ratio (C/C*)
Δs^*	entropy of process
T	total alkalinity
T	absolute temperature
t	time
$\bar{t}$	mean detention time
t_i	relaxation time
t_n	time required for the formation of stable nucleus
t_g	time required for the nucleus to grow to detectable dimensions
$t_{\frac{1}{2}}$	half life
t_∞	time for completion of precipitation
U	relative velocity between crystal and solution
U_t	terminal velocity
V	valence
V	volume
V	molal volume
V	crystalliser volume
V	desorption rate (see eq. 5.3)
V_o	overflow rate

V_A attractive force

V_{max} energy barrier

V_R repulsive force

V_r liquid flow due to velocity gradient

V_T total energy of interaction

w_v work to form the body of a particle (or droplet)

w_s work necessary to form the surface of a particle (or droplet)

W total work necessary to form a stable nucleus

X_j cluster of size, j.

Z counter ion valence

Greek Alphabet

α accommodation coefficient

α angle of contact

α collision efficiency

α kinematic viscosity

γ activity coefficient

γ_i surface energy of the ith face

δ thickness of boundary layer (laminar film)

ε adsorption coefficient

ζ zeta potential

Θ fraction of surface area covered with polymer

μ ionic strength

ρ density

σ absolute supersaturation ($= S_i = -1$)

τ induction period

Φ factor less than unity

Ψ potential

Ψ_o surface potential

Ψ_δ Stern potential

Γ surface excess

Abbreviations

[ ]	moler concentration
C.S.T.	capillary suction time
F.A.	fulvic acid
H.A.	humic acid
H.S.	humic substance
H.S.(6)	humic substance six hazen units
H.S.(60)	humic substance sixty hazen units
imm.	immediately
min.	minutes
MS	median size
M.Wt.	molecular weight
p.p.m.	part per millions
PAM	polyacrylamide
(+) PAM	cationic polyacrylamide (FO 115 PD 1200)
(O) PAM	nonionic polyacrylamide (FA 20H MAX 2)
(-) PAM (L)	Anionic polyacrylamide, low charge (FA 60H MAX 6)
(-) PAM (H)	Anionic polyacrylamide, high charge (FA 200-5)

CHAPTER ONE

Introduction

Daily, industry and municipalities are demanding millions of cubic metres of water which have to be treated to remove dissolved inorganic and organic substances and suspended solids.

Although technology exists to treat some of these contaminants, many of the processes developed are still too expensive. Low cost processes may be improved by better design and more efficient operation. Most of the currently used methods of removing impurities from raw water involve precipitation, agglomeration and flocculation and this research investigates some aspects of the combined removal of suspended solids and hardness forming dissolved salts.

Water hardness presents many problems to water users. Hardness is defined as the sum of all multivalent cations in solution. From a practicle standpoint, only Ca^{+2} and Mg^{+2} need to be considered since in most waters they are present in an overwhelming majority. For domestic use the principal reasons for advocating softening have been soap-saving, better washing conditions, and the prevention of hot water heater scaling. With the advent of synthetic detergents the first two reasons have lost much of their importance. Industrial users soften waters to meet process requirements, which are many and varied. For example, low-pressure boilers require hardness levels below 20 p.p.m., and hardness must be virtually absent in electric[1] and

high-pressure boiler feed water.

Lime addition is one process where precipitation is the predominant mechanism for removal of hardness, with the subsequent formation of calcium carbonate.

Lime treatment of hard water is frequently complicated by problems of excessive dosage, incomplete precipitation and poor settling. Several organic materials likely to be present in raw water or added during processing may affect the precipitation reaction.[2,3,4]

Flocculants are able to agglomerate the fine suspended solids into particles that will settle more readily than non-flocculated ones. The two categories of flocculants are metal flocculants or coagulants and polymeric flocculants. Flocculation lowers the suspended solids of water applied to the filters and fosters softening efficiency by flocculating and removing fine $CaCO_3$ particles so that these particles are not dissolved during subsequent recarbonation and pH adjustment.

Metal coagulants form inorganic polymers after addition to water. Those commonly used are aluminium and iron salts. Generally, 20 p.p.m. or less of an iron or aluminium salt is used.

Natural and synthetic macromolecules have been used successfully as aggregating agents in water treatment. Essentially the polyelectrolytes are long-chain organic molecules with molecular weights up to about 15 million, and most having, at intervals along the chain, ionic chemical groups which carry electrical charges. These

charges may be either positive (cationic) or negative (anionic).

There are many publications dealing with the use of these and other flocculants; useful general papers are those by Akers[5], Kitchener[6], Thomas[7], Gale[8], and Purchas[9].

The main use of polymeric flocculants in the treatment of raw water is as flocculant aids where they are used to facilitate the separation of alum or iron flocs. They can however be used as primary flocculants for high turbidity waters. There are many reports that dissolved organic substances inhibit the precipitation of sparingly soluble salts and the purpose of this research was to investigate this with regard to lime softening in the presence of polymeric flocculants and some other organic materials. In lime softening alum is commonly used to aid removal of the calcium carbonate and the possibility of the replacement of alum by polymeric flocculants is considered, as well as effects from their use in preceding separation processes.

CHAPTER TWO

Reduction of Dissolved Solids

2.1 Introduction

Waters are said to be hard when they contain appreciable amounts of the dissolved salts of calcium and magnesium. Temporary hardness is due to the bicarbonates of calcium and magnesium and can be precipitated by boiling. Permanent hardness is due to the sulphates of calcium and magnesium which cannot be precipitated by boiling.

Hardness in water (in industrial plant) gives rise to the formation of hard heat-resistant scale on heating surfaces of steam boilers, and in cooling systems. The decomposition of bicarbonates by heat evolves carbon dioxide which may give rise to metallic corrosion in boilers and if carried forward in steam, may cause corrosion in steam condensing systems.

Some of the more economical methods for reducing total hardness and alkalinity in water to as low a value as possible involve precipitation, agglomeration. One process where precipitation is the predominent mechanism for reducing the hardness and alkalinity in water, is the cold-lime water softening process, in which the addition of lime precipitates the calcium and magnesium salts as calcium carbonate and magnesium hydroxide respectively. These precipitates may then be removed from the water by sedimentation and filtration.

The precipitation of calcium carbonate and magnesium hydroxide in the lime-water softening process is basically

a crystallisation process. The kinetics of crystallisation are a controlling step.

Processes for accelerating these precipitation reactions have been developed, particularly that of causing the products of softening to deposit on crystallisation nuclei in a very short period of time. This research has focused on a study of this process. Comparatively little information of a theoretical nature is available in the literature, but enough practical information exists to make the process extremely interesting.

2.2 Methods of Reduction of Dissolved Solids

A perfect water for boiler-feed use is one which will not deposit any scale-forming substances, will not corrode metal of boilers or appurtenances, and will result in neither priming nor foaming. Such water is seldom obtainable except by artificial purification, whereby the impurities which may cause scale, corrosion or other undesirable effects are removed or charged to less objectional products.

2.2.1 Cold Lime - Soda Ash Method

The use of lime and soda ash in water softening processes dates back to the mid 1800's. The simple chemical reactions involved when calcium hydroxide, in the form of saturated lime water, or as cream of lime, is added to the water to remove calcium bicarbonate and magnesium bicarbonate (temporary hardness):

$$Ca(HCO_3)_2 + Ca(OH)_2 \longrightarrow 2\ Ca\ CO_3 + 2\ H_2O$$

$$Mg(HCO_3)_2 + Ca(OH)_2 \longrightarrow Mg\ CO_3 + CaCO_3 + 2\ H_2O$$

$$Mg\ CO_3 + Ca(OH)_2 \longrightarrow Mg\ (OH)_2 + CaCO_3$$

Non-carbonate hardness (permanent hardness) is removed by addition of lime and soda ash and precipitation of calcium carbonate and magnesium hydroxide. The reactions are:

$$MgSO_4 + Na_2CO_3 + Ca(OH)_2 \longrightarrow Mg(OH)_2 + CaCO_3 + Na_2SO_4$$

$$CaSO_4 + Na_2CO_3 \longrightarrow CaCO_3 + Na_2SO_4$$

$$MgCl_2 + Ca(OH)_2 \longrightarrow Mg(OH)_2 + CaCl_2$$

The lime-soda process is not very effective in cold waters containing less than 100-150 p.p.m. of hardness[10], expressed as calcium carbonate, unless a sludge-blanket or sludge-recirculation type of plant (see 2.3.1 and 2.3.2) is employed. At the lower concentrations, the degree of supersaturation obtained when the precipitants are added may be small so that the calcium and magnesium compounds tend to be precipitated slowly and incompletely. Such water can be softened more conveniently by ion exchange (see 2.2.2).

If the process is carried out at a temperature of 70°C or higher, the hardness may be reduced to a very low figure, e.g. of the order of 10-20 p.p.m. $CaCO_3$, but the cold process is less efficient and the hardness is not reduced below 50-70 p.p.m. $CaCO_3$.

Usually, the reaction between the hardness and the softening reagents is incomplete in the time available, with the result that the water is supersaturated with

respect to calcium carbonate and magnesium hydroxide and delayed precipitation, principally of calcium carbonate, may occur in pipelines, filter equipment, etc., following the softening plant. Water supersaturated with respect to calcium carbonate is commonly referred to as being "unstable" (i.e. unstable in respect of calcium carbonate solubility equilibrium), since slight physical changes may cause equilibrium to shift with precipitation of calcium carbonate.

In water free from carbon dioxide, calcium carbonate has a solubility of 6 p.p.m. at 25°C[11]. In practice crystallisation equilibrium is not attained in the time available and considerable amounts of $CaCO_3$ remain in solution in excess of this theoretical solubility, i.e. in supersaturation. This excess calcium carbonate may subsequently precipitate in other items of plant giving deposits in pipes and placing extra demand on filters. This phenomenon is termed 'post precipitation'.

The practical solubility of calcium carbonate is commonly taken to be 35 p.p.m. as $CaCO_3$, or five times the theoretical value[12]. The calcium carbonate solubility equilibrium is extremely important in water treatment and will be dealt with more fully later (see 2.4).

2.2.2 Cold Lime - Followed by Ion Exchange

The Zeolite, or base-exchange, and cold lime processes may be combined to a method which is claimed to posses the advantages of both. This process gives a water which is

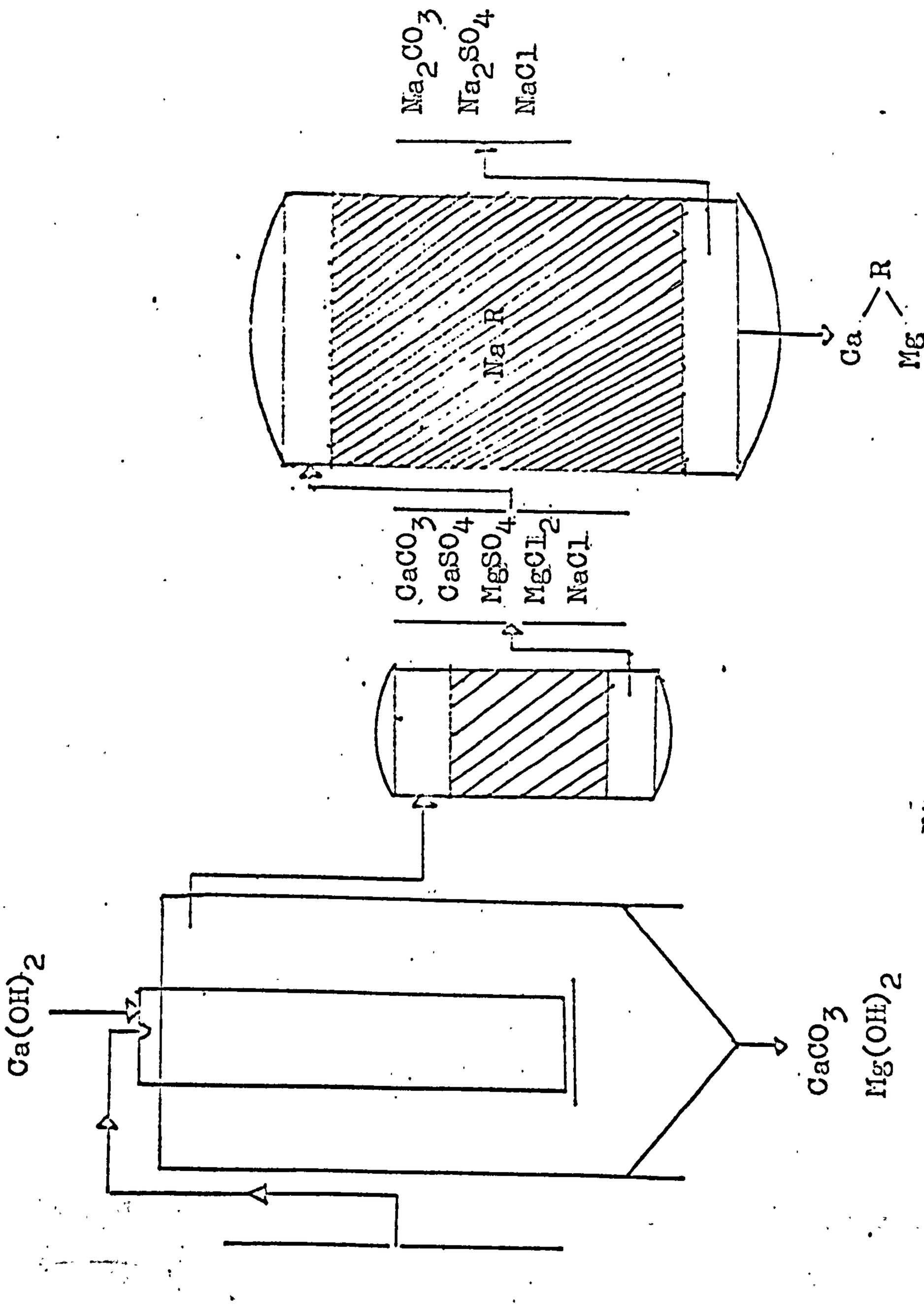
Na_2CO_3
Na_2SO_4
NaCl
R
Na
R
Ca
Mg
$CaCO_3$
$CaSO_4$
$MgSO_4$
$MgCl_2$
NaCl
$Ca(OH)_2$
$CaCO_3$
$Mg(OH)_2$
$Ca(HCO_3)_2$
$Mg(HCO_3)_2$
Mg SO_4
Ca SO_4
Mg Cl_2
NaCl

Fig. 2.1

suitable for use as feed to low and medium pressure boilers, since it does not contain appreciable quantities of any scale-forming substances other than silica.

The Zeolites are either naturally occurring minerals or synthetic products, but all are hydrated sodium aluminium silicates which under suitable conditions will give up the combined basic radical in exchange for a basic radical from the water. As the process is reversible, when the Zeolite ceases to soften water it can be regenerated by treatment with brine solution.

Zeolites have been almost entirely replaced by synthetic resin ion exchange materials which may be used in lime-base exchange softening or using anion and cation resins for complete demineralisation.

2.3 Methods of Accelerating the Lime-Softening Process

The precipitation of calcium carbonate from calcium bicarbonate solutions according to the reaction

$$Ca(HCO_3)_2 + Ca(OH)_2 \longrightarrow 2\ CaCO_3 + 2\ H_2O$$

has been studied extensively in connection with the lime process for water softening. It has generally been shown that the rate of precipitation is slow, requiring several hours to approach completion[13,14] and can be accelerated considerably by stirring[14,15], increasing the temperature[15], and initiating precipitation by seeding[16,17].

In practice, a crystal-seeding process, which involves the precipitation of reaction product on the surface of seed crystals, has been found to improve the filterability

and settleability of various industrial-waste sludges[18,19,20] and accelerate the process of the softening reactions toward equilibrium.

This process of "seeding" the saturated solution to promote the formation of large precipitates may be carried out in three ways.

2.3.1 Sludge Blanket Process

The use of a sludge blanket for conditioning water softening precipitates was first described by Spaulding[21] and his work led to an improved design of reaction and settling tank. Behrman and Green[22] reported that when a mixture of raw water and softening chemicals are stirred in contact with previously precipitated sludge, the chemical and physical reactions involved are materially accelerated, both as to completeness and as to the time required. The patents of Koyl[23], Sutro and Booth[24], and Green and Behrman[25] show both appreciation of the beneficial effect of previously precipitated sludge and successively closer approach to a practical method of securing this effect.

The advantages of sludge contact are even more important in many water treatment applications where coagulation is required. Space savings made possible by the use of higher rising rates, with the resultant saving in concrete for basin construction which usually results in an installed cost less than that of a conventional plant using separate mixing, flocculation and sedimentation basins.

In the "sludge contact" process the treated water is filtered upwardly through a suspended blanket of sludge[10,26] (see fig. 2.2), composed of previously formed precipitates. The intimate contact of the treated water with a large mass of the solid phase prevents supersaturation and the reactions are completed substantially. A retention or reaction period of one hour is sufficient and, therefore, a plant occupying less space than for the conventional process may be employed. However, as in the conventional process (fig. 2.1), it is necessary to dispose of a by-product, in the form of calcium carbonate sludge.

The water to be softened enters the central mixing compartment (fig. 2.2.a), is well mixed with the softening reagents and is discharged from the central compartment to the outer compartment in which a predetermined level of the concentrated sludge is maintained. The water passes upwardly through the sludge blanket at a controlled rate of flow. The suspended blanket of sludge serves virtually as a floating filter bed, and a high degree of clarification is claimed. The sludge settles out in the concentration compartment and is removed continuously at a concentration of 4-5% solids and may be thickened to as much as 15% solids.

The second type (fig. 2.2.b) consists of a hopper-bottomed tank, in which floc formation takes place under the influence of induced hydraulic current; the water passes from the flocculation zone through the suspended floc blanket.

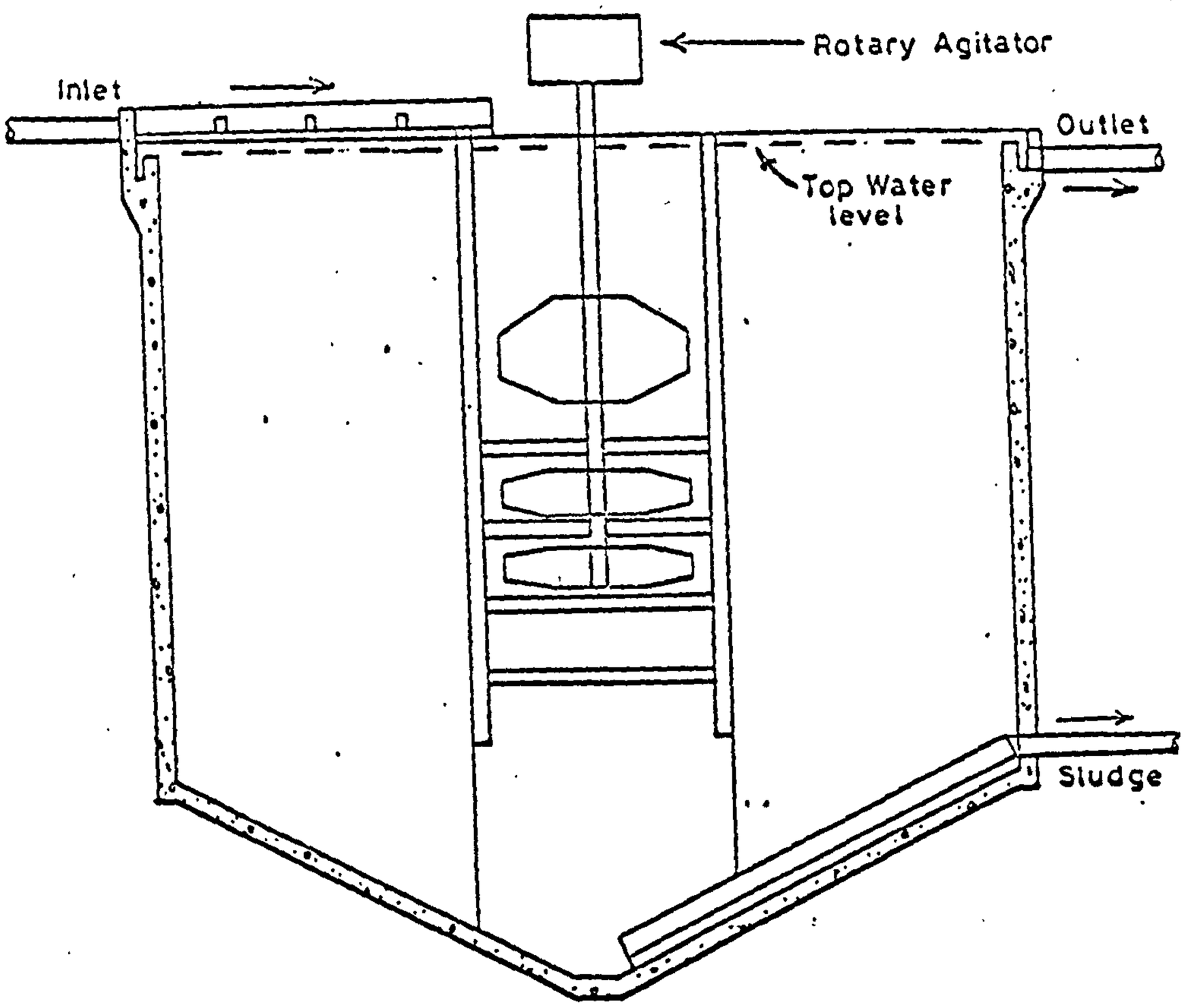

(a)

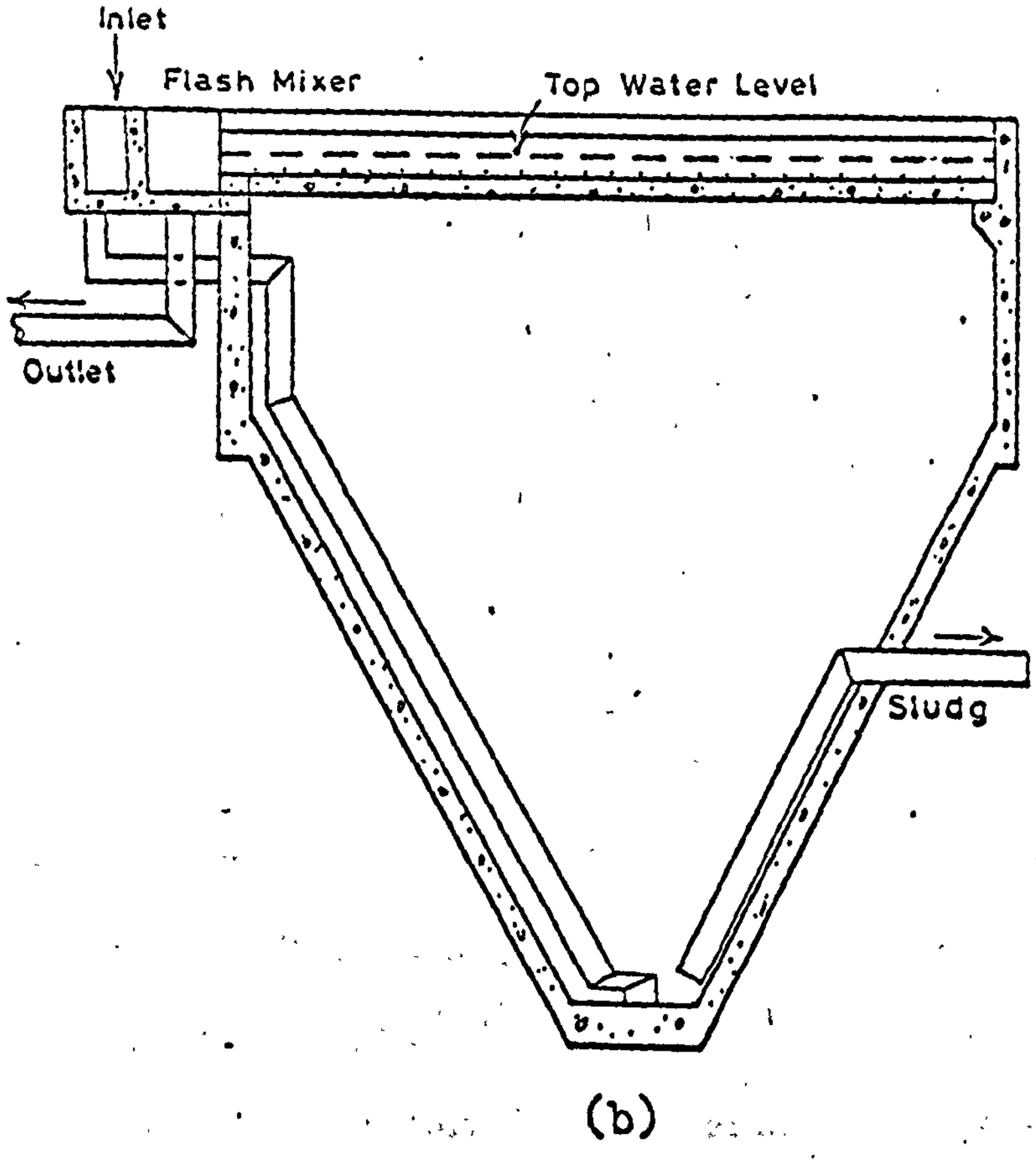

(b)

Figure 2.2: (a) Circular Sludge Blanket with Radial Flow.
(b) A Typical Sludge Blanket Clarifier.

2.3.2 Sludge Recirculation Process

In the sludge recirculation process the contact between preformed sludge and the raw water and reagents, is brought about by recirculation of the preformed sludge without actual flow through a sludge blanket (see fig. 2.3).

The basic features of sludge recirculation systems are a reaction zone equipped with a rapid mixer and a clarification zone. The sludge is drawn from the bottom of the clarification zone and then enters the reaction zone.

Typical results with a sludge recirculation type softener in which calcium carbonate is removed selectively by precipitation by lime, are confirmed by Lawrance[27]. Sludge recirculation showed a higher chemical efficiency than did treatment without the recirculation; the Jar tests and the plant scale experiments indicated that sludge recirculation reduces hardness 20 per cent below that experienced without sludge recirculation under otherwise identical condition provided that suspended sludge were maintained at 0.6 per cent. He found that even greater benefits would be obtained using higher suspended sludge concentration up to 5 or 6 per cent. Additional benefits he confirmed were lower phenolphthalein alkalinity and lower Langelier saturation index.

A similar sludge-recycle process has been studied by Judkins and Wynne[17]. They found sludge recirculation improves the filterability and settleability of large quantities of sludge composed of 85-95 per cent calcium carbonate and varying amounts of magnesium hydroxide in

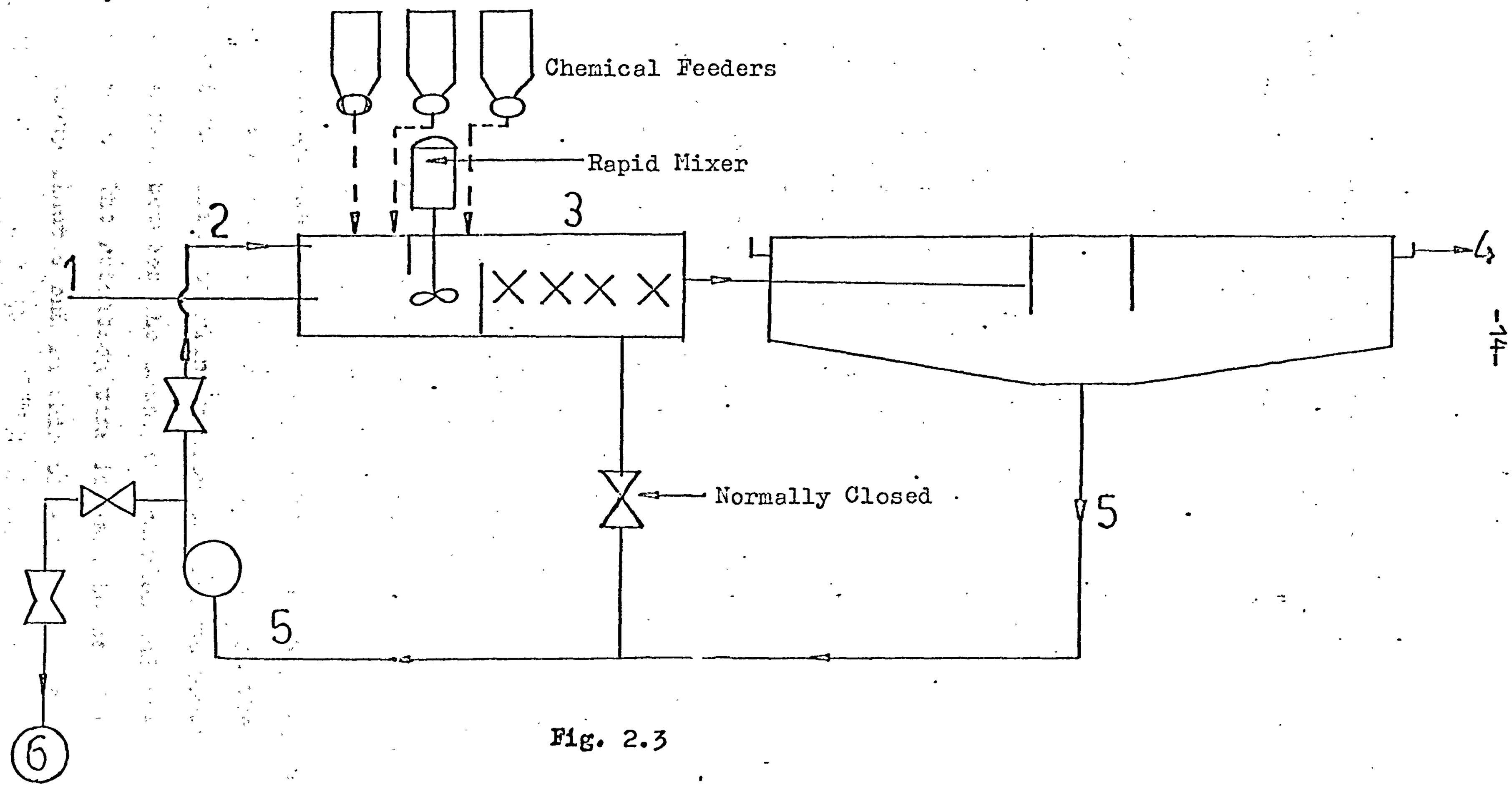

Fig. 2.3

Schematic Profile Sludge Recirculation Systems

lime-softening process. They went furthermore to conclude that recycling of sludge is more effective than crystal seeding probably as a result of increased growth opportunities provided by recycle.

2.3.3 Catalyst Method

In 1936 Zentner was the first who applied the principle of seeding a saturated solution to promote crystal growth to accelerate the lime-softening reaction in Czechoslovakia, by bringing water treated with softening reagents into contact with solid crystallisation nuclei in granule form on which the precipitated hardness would actually accumulate or grow.

In the Zentner process (fig. 2.4), the water treated with lime is passed upwardly through a fluidized bed of marble or sand granules, at a rate of flow not exceeding the rate of sedimentation of the precipitated calcium carbonate but high enough to maintain the nuclei in contact agitation. The precipitates of $CaCO_3$ accumulate as skin formations or accretations on these granules instead of as relatively fine suspensions and the water leaving the top of the bed is relatively clear.

This tangential introduction imparts an upward spiral motion to the stream of water as it rises through the vessel and the spiral swirling motion ensures thorough and uniform contact between the catalyst granules and the treated water. The retention time is said to be of the order of 10-15 minutes and in this time the bulk of the

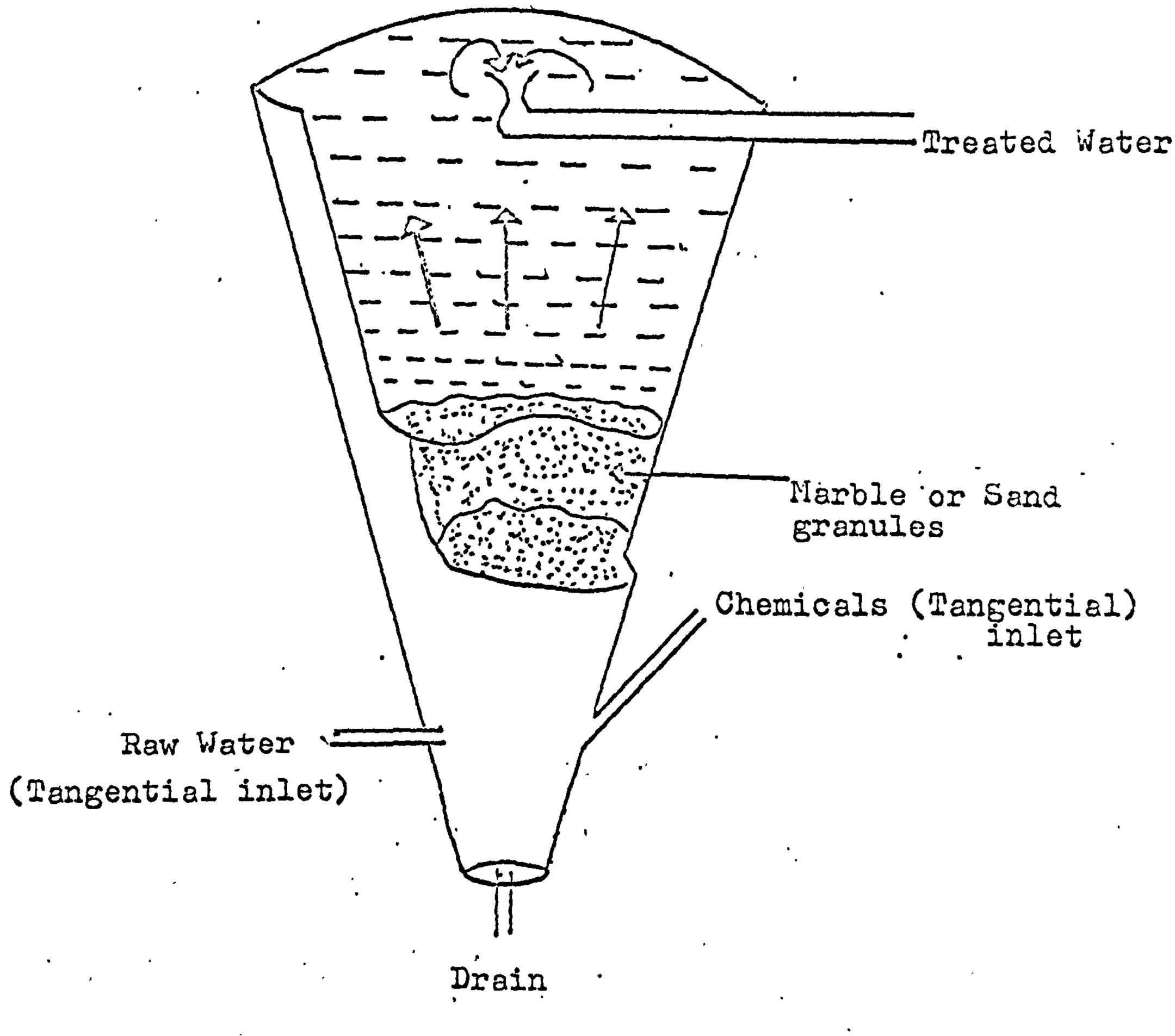

Fig. 2.4

Schematic Profile Of Catalyst Softening

precipitated $CaCO_3$ is said to be taken up and held firmly by the catalyst granules.

2.4 The Calcium Carbonate Solubility Equilibrium

For a basic understanding of the state of completeness of the lime-softening reaction at any stage, it is necessary to apply the law of mass action to derive an equation for the $CaCO_3$ solubility equilibrium.

The precipitation of calcium carbonate from an aqueous solution is completed by the equilibrium relations. Being the salt of a weak acid, the carbonate ion forms an equilibrium with the acid. Therefore, some of the carbonate that would ordinarily be available for precipitation is converted to bicarbonate. This equilibrium, along with the ionization of water and the dissociation of calcium carbonate are all interrelated.

Langelier[28] studied the tendency of lime-softened waters to deposit $CaCO_3$ films on the internal surfaces of water pipes and the effect of these films as protection against corrosion. In water works practice $CaCO_3$ may deposit from natural oxygen-containing waters, if the product of the concentration of the calcium ions and the carbonate ions present in the water exceeds the "solubility product constant" or the "activity product" of the salt in question. If water is deficient in either of these ions, so that the activity product is not attained, a $CaCO_3$ film will not be formed and any existing film will be dissolved. Many surface waters are of this type, and in general, are

known to be corrosive. In such waters, a sufficient increase in either or both of the calcium and carbonate ions is all that is needed to attain saturation. Any alkali added to hard water will convert bicarbonate ions into carbonate ions. The addition of lime, however, has the advantage of increasing both the calcium and the carbonate ions simultaneously. The degree of saturation of the treated water determines, therefore, how far the reaction given by the equation

$$Ca(HCO_3)_2 + Ca(OH)_2 \longrightarrow 2\ CaCO_3 + 2\ H_2O$$

has gone to completion.

2.4.1 Solubility of Calcium Carbonate

The solubility of a sparingly soluble salt such as $CaCO_3$ is not only a function of temperature[29] but also a function of the concentrations of all ions in solution[30]. The proper solubility is determined from the solubility product, K_{sp}. The following treatment can be found in most physical chemistry texts such as Adamson[31].

The dissociation of calcium carbonate is described by

$$CaCO_3 \rightleftharpoons Ca^{++} + CO_3^{''}$$

The solubility product constant is

$$K_{sp} = {}^{a}Ca^{++}\ {}^{a}CO_3^{''} = \gamma Ca^{++}\ \gamma CO_3^{''}\ [Ca^{++}]\ [CO_3^{''}] \ldots 2.1$$

where a = is the activity

γ = is the activity coefficient

and $[\ ]$ = moler concentrations

It is convenient to define a corrected solubility product, K'_{sp}, as

$$K'_{sp} = \frac{K_{sp}}{\gamma Ca^{++}\ \gamma CO''_3} = [Ca^{++}]\cdot[CO''_3] \quad \ldots\ldots\ldots\ldots 2.2$$

The activity concept assumes complete dissociation of salts in dilute solution. The activity coefficient provides a correction for deviations from ideality. Hence, at infinite dilution, i.e. ideal conditions, $\gamma_x = 1$. The x refers to the ion of interest. At any other condition, γ_x has some other value.

According to the Debye-Hükel theory[32], the activity coefficient of an ion in dilute solution may be calculated from:

$$\log\ \gamma_x = -0.509\, V_x^2\ \ \sqrt{\mu}/(1 + A) \quad \ldots\ldots\ldots\ldots 2.3$$

where V_x = is the valences of x

μ = is the ionic strength of the solution

and A = is constant dependent on the ionic diameter which in water works practice is assumed to be 1.

The ionic strength of a solution is defined as one half the summation of the molal concentration, M, of each ion in solution multiplied by the square of its ionic charge, V.

$$\mu = \Sigma \tfrac{1}{2}\, M_x\, V_x^2 + M_y\, V_y^2 + M_z\, V_z^2 + \quad \ldots\ldots\ldots\ldots 2.4$$

In general, the simplified expression (2.3) for natural water of less than 500 p.p.m. mineral content, Langelier[33] reports, ionic strength can be calculated from (2.5)

$$\mu = 0.000025 \times (\text{Total mineral content}) \quad \ldots\ 2.5$$

Larson and Buswell[34] state that the form of K_{sp} that

most nearly fits the experimental data is given by

$$PK'_{sp} = PK_{sp} - 4\sqrt{\mu}/(1 + 3.9\sqrt{\mu}) \quad \ldots\ldots\ldots \quad 2.6$$

where P is an operator such that $P[\ ] = -\log[\ ]$.

In summary, if the molar solubility is desired and K_{sp}, μ, and $[CO''_3]$ are known, then simply find K'_{sp} from equation (2.6) and solve for $[Ca^{++}]$ in equation (2.2).

2.4.2 Ionization of Water and Carbonic Acid

The dissociation constants for water and carbonic acid are defined similarly to the solubility product of calcium carbonate[35].

The dissociation of water is described by the following equilibrium

$$H_2O \rightleftharpoons H^+ + OH^-$$

The dissociation constant, K_w, is defined by

$$K_w = a_{H^+}\, a_{OH^-} = \gamma_{H^+}\, \gamma_{OH^-}\, [H^+][OH^-] \quad \ldots\ldots \quad 2.7$$

and the corrected dissociation constant is

$$K'_w = \frac{K_w}{\gamma_{H^+}\, \gamma_{OH^-}} = [H^+]\cdot[OH^-] \quad \ldots\ldots\ldots\ldots \quad 2.8$$

where the a and the γ are defined as before.

Since the γ can be determined from the ionic strength μ, the corrected dissociation constant, K'_w, is calculated from the following expression

$$pK'_w = pK_w - \frac{\sqrt{\mu}}{1 + 1.4\sqrt{\mu}} \quad \ldots\ldots\ldots\ldots\ldots\ldots \quad 2.9$$

The equilibrium between the carbonate and bicarbonate ions is shown by

$$HCO_3^- \rightleftharpoons H^+ + CO''_3$$

The above equilibrium is the second dissociation step

of carbonic acid, H_2CO_3. The second dissociation constant, K_2, is defined by

$$K_2 = \frac{a_{H^+} \; a_{CO_3''}}{a_{HCO_3^-}} = \frac{\gamma_{H^+} \; \gamma_{CO_3''} [H^+][CO_3'']}{\gamma_{HCO_3'} \; [HCO_3']} \quad \ldots\ldots \; 2.10$$

and the corrected dissociation constant is

$$K_2' = \frac{K_2 \; \gamma_{HCO_3'}}{\gamma_{H^+} \; \gamma_{CO_3''}} = \frac{[H^+] \; [CO_3'']}{[HCO_3^-]} \quad \ldots\ldots\ldots\ldots \; 2.11$$

K_2', the corrected dissociation constant, is calculated from

$$pK_2' = pK_2 - \frac{2\sqrt{\mu}}{1 + 1.4\sqrt{\mu}} \quad \ldots\ldots\ldots\ldots\ldots\ldots \; 2.12$$

2.4.3 Alkalinity

The alkalinity of a water, defined as the capacity for reacting with hydrogen ions to a pH corresponding to stoichiometric formation of carbonic acid (or CO_2 and water), is usually determined by the presence of bicarbonate, HCO_3^-, carbonate, CO_3'', and hydroxyl, OH^-, ions; occasionally phosphate and silicate ions may contribute significantly to the alkalinity. Partial alkalinity or phenolphthalein alkalinity (p value), is a measure of alkaline hydroxides and carbonates when a sample of water is titrated with acid using phenolphthalein as indicator. Total alkalinity or methyl orange alkalinity (m value) is a measure of alkaline carbonate and bicarbonate when the same sample of water is titrated with acid using methyl orange as indicator in consecutive step.

Through the years there has been much discussion as to

what control variable should be used to operate a water softening plant efficiently. In the past pH was the main control variable for optimum operation of a water softening plant. Later it was discovered that for a given operating temperature, optimum operation occurs at a specific combination of alkalinity and pH[36].

It seems logical that a water softening plant should be run at a condition where calcium carbonate has minimum solubility. In waters, such as used in this research, the alkalinity was primarily due to the carbonate, bicarbonate, and the hydroxyl ions.

The total alkalinity, T, as calcium carbomate is defined by the equation[35],

$$[H^+] + \frac{T}{50000} = [HCO_3'] + 2[CO_3''] + [O\bar{H}] \quad \ldots\ldots \quad 2.13$$

where the 50000 arises from converting mg/l to equivalents /l. Equation (2.13) can also be written in units of mg/l as calcium carbonate.

$$H + T = HCO_3 + CO_3 + OH \quad \ldots\ldots\ldots\ldots\ldots\ldots \quad 2.14$$

Alkalinity is normally determined by titrating a sample with a strong acid[37]. Phenolphthalein indicator is used to determine the first endpoint of the titration. This endpoint corresponds closely to the point where all the carbonate has been converted to bicarbonate and the hydroxyl ions have been neutralised. The phenolphthalein alkalinity can be determined from this titration or if the carbonate and the hydroxyl ion concentrations are known it can be calculated from the following defining equation

$$P = [CO_3''] /2 + [O\bar{H}] \quad \ldots\ldots\ldots\ldots\ldots\ldots \quad 2.15$$

The second end point, where all the alkalinity has been neutralised, is determined by titrating until the methyl orange indicator (or some other equivalent indicator) changes colour. This is referred to as the total alkalinity, T.

In this research the phenolphthalein alkalinity (the $CO_3^{=}$ alkalinity) is calculated from equations suggested by Langmuir[11], from knowing pH and $[Ca^{++}]$ will be shown later.

2.4.3.1 Computation of the Three Forms of Alkalinity

Langelier[33] in 1936 derived the necessary equations for alkalinity calculations. The three basic equilibrium equations are:

$$CaCO_3 \rightleftharpoons Ca^{++} + CO_3''$$
$$H_2O \rightleftharpoons H^+ + OH^-$$
$$HCO_3 \rightleftharpoons H^+ + CO_3''$$

As discussed in (2.4.1) the corrected dissociation constants are defined as

$$K'_{sp} = [Ca^{++}][CO_3^{=}] \quad \ldots\ldots\ldots\ldots\ldots\ldots 2.2$$
$$K'_w = [H^+][OH^-] \quad \ldots\ldots\ldots\ldots\ldots\ldots 2.8$$
$$K'_2 = [H^+][CO_3^{=}]/[HCO_3^-] \quad \ldots\ldots\ldots\ldots\ldots\ldots 2.11$$

By solving equation (2.13) and equation (2.11) for $[CO_3^{=}]$ and equating them results in

$$\frac{K'_2\,[HCO_3^-]}{[H^+]} = \frac{T/50000 - [HCO_3^-] - [OH^-] + [H^+]}{2} \quad \ldots\ldots 2.16$$

solving equation (2.16) for HCO_3 we obtain

$$[HCO_3^-] = \frac{T/50000 + [H^+] - K_w'/[H^+]}{1 + 2K_2'/[H^+]} \quad \ldots\ldots\ldots\ldots 2.17$$

substituting the solution for $[HCO_3^-]$ into equation (2.11) and solving for $[CO_3^{=}]$ one finds:

$$[CO_3^{=}] = \frac{T/50000 + [H^+] - K_w'/[H^+]}{2\,(1 + [H^+]/2K_2')} \quad \ldots\ldots\ldots\ldots 2.18$$

And by substituting equation (2.18) in to equation (2.2) one can calculate the calcium concentration.

$$[Ca^{++}] = \frac{K_{sp}'}{[CO_3^{=}]} = \frac{2K_{sp}'\,(1 + [H^+]/2K_2')}{T/50000 + [H^+] - K_w'/[H^+]} \quad \ldots\ldots 2.19$$

To find the three forms of alkalinity in the water softening industry is to measure total alkalinity, T, pH, temperature, and dissolved solids. With temperature and dissolved solids known, one can obtain the proper ionization constant[28].

To calculate and determine the ionization constants which are needed to solve this set of equations are rather difficult. Standard methods[37] provide a numographic solution for quick calculation.

2.4.3.2 Importance of Alkalinity in Water Softening

For many years, the results of alkalinity have been used in the control of lime-water softening plants. When lime is added to hard water, the carbonate immediately sets up an equilibrium with the water. The following conditions

apply,,

$$H_2O \rightleftharpoons H^+ + OH^-$$

$$HCO_3^- \rightleftharpoons H^+ + CO_3^{=}$$

The calcium to be removed by precipitation as calcium carbonate is also in equilibrium with the carbonate ion.

$$Ca\ CO_3 \rightleftharpoons Ca^{++} + CO_3^{=}$$

Optimum operation of a lime-water softening process for calcium removal occurs when the carbonate ion concentration is maximum (minimum calcium carbonate solubility). It was reported[36,38,39] that maximum carbonate occurs when the total alkalinity is twice the phenolphthalein alkalinity (2p = T).

2.4.3.3 Saturation Index

The saturation index, Is, is the algebraic difference between the actual pH (measured experimentally) and the calculated pH (pHs)

$$Is = pH - pHs \quad \ldots\ldots\ldots\ldots\ldots\ldots\ldots\ldots\ 2.20$$

It is evident that if pH equals pHs (i.e. Is is zero), equilibrium exists and there will be absence of scale formation and minimised corrosion of metals. When pH $>$ pHs (i.e. Is is positive) there is a condition of supersaturation of calcium carbonate with respect to alkalinity and scale tends to be deposited. When pH $<$ pHs (i.e. Is is negative), equilibrium is unbalanced in the opposite direction, scale tends to dissolve, and corrosion of metals will tend to occur.

Applying these principles to water softening reactions

using lime, the positive value of Is indicates the state of completeness of the overall reaction, the higher the value of Is, the less complete the reaction, i.e. the greater the degree of supersaturation of calcium carbonate in solution. Theoretically, when Is = 0, the reaction is complete and equilibrium will have been attained.

Larson and Buswell[34] show the pHs may be calculated from equation (2.19) by converting K'_{sp} and K'_2 to K_{sp} and K_2 respectively and combining the corrections for salinity.

The saturation index (Is) may be calculated as follows:-

$$Is = pH + \log[Ca^{++}] + \log[T] - \log \frac{K_{sp}}{K_2} - 9.30 - \frac{2.5\sqrt{\mu}}{1+5.3\sqrt{\mu}+5.5\,\mu} \quad (2.21)$$

where pH = is the actual pH measured experimentally.

9.30 = is the salinity correction.

T = is the alkalinity expressed in p.p.m. as $CaCO_3$.

Ca^{++} = is the calcium concentration expressed in p.p.m.

2.4.3.4 Salinity Corrections

The two ionization constants, K_{sp} and K_2, (see equations 2.2 and 2.11) are apparent constants and are applicable only in solutions of the same total mineral content and at a given temperature. It is proposed to apply to these and other constants, corrections for salinity and temperature according to the most recent work available.

In respect of the second ionization constant, K_2', Harned and Sholes[40] have provided the most authentic values whereby pK_2' is calculated from the equation

$$pK_2' = pK_2 - \frac{2\sqrt{\mu}}{1 + 1.4\sqrt{\mu}} \quad \ldots\ldots\ldots\ldots\ldots\ldots 2.12$$

Similarly the ionization constant for water, K_w', (see equation 2.8) which has been substantiated by Harned and his co-workers[41,42], the equation for pK_w' is given by:-

$$pK_w' = pK_w - \frac{\sqrt{\mu}}{1 + 1.4\sqrt{\mu}} \quad \ldots\ldots\ldots\ldots\ldots\ldots 2.9$$

Larson and Buswell[34] have recalculated the value previously reported for the solubility product for $CaCO_3$, K_{sp}', and they state that the equation for pK_{sp}', is most nearly approximated by:-

$$pK_{sp}' = pK_s - \frac{4\sqrt{\mu}}{1 + 3.9\sqrt{\mu}} \quad \ldots\ldots\ldots\ldots\ldots\ldots 2.6$$

Using data published on temperature variation for K_1, K_2', as well as for K_w', Larson and Buswell[34], calculated the temperature variation for K_{sp}' from 0°C-80°C. Their values for the ionization constants corrected for temperature (with certain extrapolated values) are given in Table 2.1.

TABLE 2.1

Values for K_1', K_2', K_w', and K_{sp}'. (Larson and Buswell).

t°C	$K_w' \times 10^{14}$	$K_1' \times 10^7$	$K_2' \times 10^{11}$	$K_{sp}' \times 10^9$
0	0.115	2.61	2.36	9.50
10	0.298	3.34	3.24	7.07
20	0.681	4.05	4.20	5.25
25	1.008	4.31	4.69	4.55
30	1.460	4.52	5.13	4.03
40	2.916	(4.85)	6.03	(3.06)
50	5.469	(5.05)	6.73	(2.37)
60	9.637	(5.08)	(7.20)	(1.83)
70		(5.00)	(7.51)	(1.38)
80		(4.84)	(7.55)	(1.06)

CHAPTER THREE

Reduction of Suspended Solids in Natural Water by Sedimentation

3.1 Introduction.

Practically all surface waters contain impurities varying in size from a few Angstroms for soluble substances to many microns for suspended materials. Permanent turbidity is most often associated with the presence of small quantities of clay and other minerals, together with some organic matter, all in colloidal suspension. Colour, on the other hand, is frequently due to complex organic compounds, probably of the type collectively known as humic substances[43].

The designation of waters as clear, turbid, or highly turbid, is but arbitrary and indefinite, just as are the terms soft, hard and very hard. The term highly turbid, however, quite generally brings to mind a water like that of the "Tigris River" with a turbidity of at least 1000 p.p.m.

The removal of particulate impurities is accomplished in two steps. The first of these is deposition of coarse particles by sedimentation followed by the second step, clarification of water by filtration.

3.2 Types of Sedimentation

Particles settle from suspension in different ways, depending upon their concentration and the relative tendency of the particles to cohere. Fitch[44] has described four different manners of sedimentation

represented paragenetically in fig. 3.1. The left-hand side of the diagram represents particles with little tendency to cohere, the right side those for which interparticle cohesion is strong.

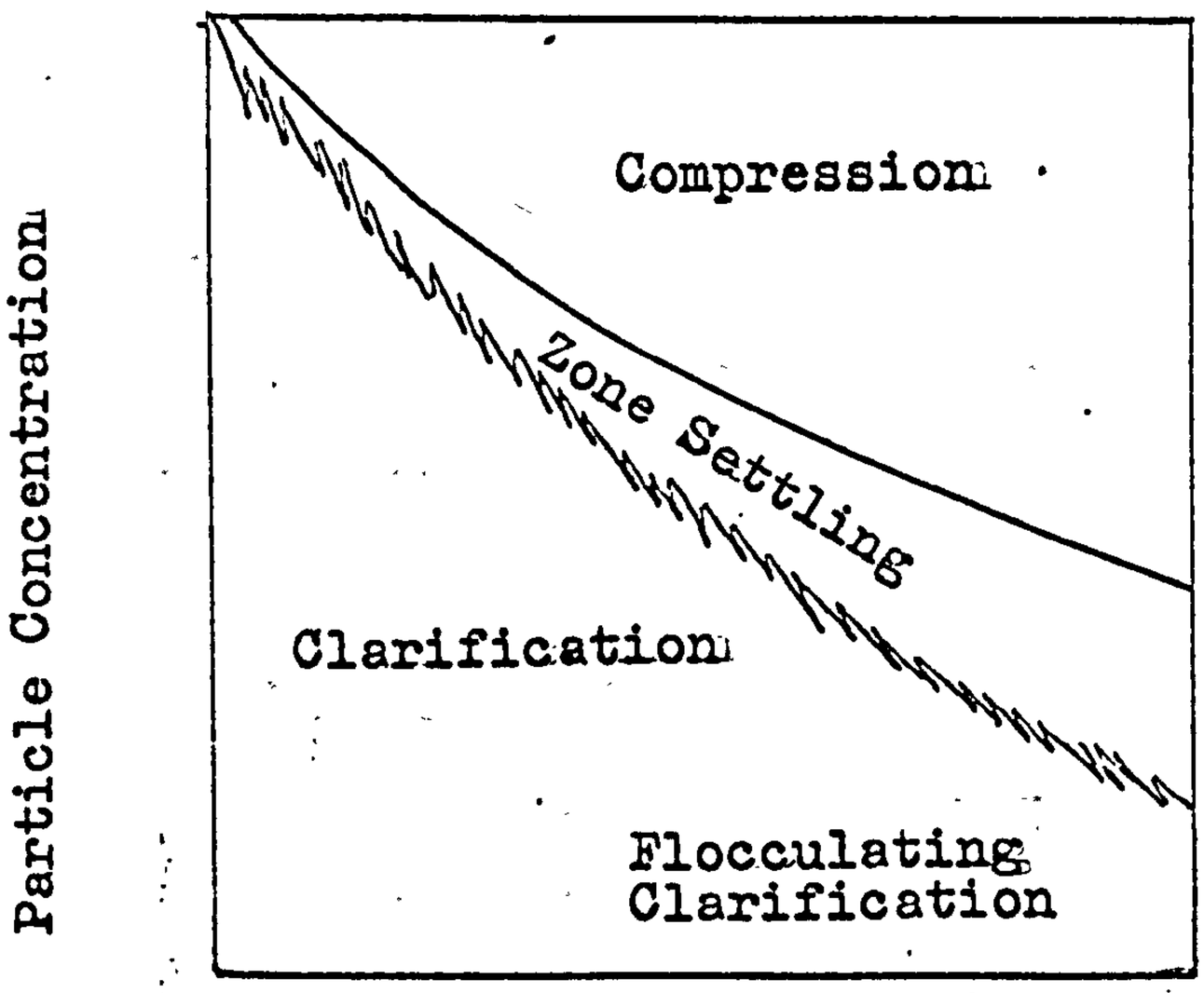

Figure 3.1: Paragenesis Diagram

In dilute suspension the type of sedimentation is called clarification. The sedimentation of a particle is not affected by the presence of other particles and is a function only of the properties of the fluid and the characteristics of the particle. If the particles cohere, they form floccules which settle at an ever increasing rate as they grow. If they do not cohere, each particle sediments downward at its own characteristic rate. Thus in this regime there are two different types of settling: particulate and flocculating clarification.

In the zone settling regime, particles have sedimentation rates that are independent of particle size, i.e. a distinct interface or line will exist between the sedimenting particles and supernatant liquid.

The compression zone occurs when the settling particles accumulate at the bottom of the sedimentation basin. Each layer of this zone is able to provide mechanical support for layers above. Settling of any layer is then slowed by mechanical support propagated up from the bottom of the sedimentation basin.

3.2.1 Effect of Particle Size

According to Stokes law (see equation 6.2) the sedimentation rate of a particle in a fluid is proportional to the square of its diameter. Under the effect of gravity large particles settle out readily but the small particles settle out over a period of time from a few hours to a few days. Some very small particles may never settle out, because their rate of diffusion due to Brownian motion is significantly greater than their sedimentation velocity.

Obviously in a water treatment plant it is not practicle to wait for a very fine suspension to sediment out and when handling large volumes it is too expensive to centrifuge the suspension. Aggregation of the particles to larger assemblies is required. This will be discussed later.

3.2.2 Camp-Hazen Theory

Camp and Hazen have developed relationships to describe the operation of a clarifier. They have suggested that the overflow rate is related to the depth of the basin and detention time as follows:

$$V_o = \frac{\text{basin depth}}{\text{detention time}} = \frac{H}{V/Q} = \frac{H}{(A \times H)/Q} = \frac{Q}{A} \quad \ldots 3.1$$

where V_o = is the overflow rate, m/hr.

H = depth of clarification zone (measured in direction of gravity force vector).

V = volume of clarification zone.

Q = volume of overflow per unit time, m^3/hr.

A = is the surface area of the basin.

The overflow rate has the dimensions of velocity. For a transverse flow basis this equation means that a particle will be removed by sedimentation if it has a sufficient sedimentation velocity v_t to fall through the height of the basin H during its residence time in the basin V/Q. For an upflow clarifier a similar argument will show that particles can only be removed if their sedimentation velocity v_t exceeds the overflow velocity V_o. Degremont[26] suggests that, V_o, should be from 0.5 to 1 m/hr for the clarification of drinking water, and from 1 to 2 m/hr for softening by chemical means and for settling of sewerage.

However, because many of the impurities of surface waters are too small, for gravitational settling alone to be an effective removal process and yet the quantity of suspended solid would overload a filter, the aggregation

of these particles into large, more readily settleable aggregates is of great importance in the purification process.

The words coagulation and flocculation have been used interchangeably in colloid chemistry to describe the aggregation process. In the technological context they are differentiated but the usage differs with the technology considered. La Mer[45] proposed that coagulation be used to describe the destabilisation of colloidal dispersions by adding ions which cause a reduction in the mutually repulsive electrical double layer forces present at the solid liquid interface, whereas flocculation be the aggregation of colloidal suspensions by the action of high molecular weight polymers soluble in the continuous phase by means other than charge reduction. In certain situations both phenomena do occur together but the general usefulness of their differentiation has led to its widespread acceptance in flocculation literature, although not in colloid science in general.

In civil and municipal engineering a different convention exists. Coagulation is seen as the chemical destabilising process brought about by the addition of some reagent to the colloidal system which makes it possible for the particles to adhere and form flocs, whilst flocculation is the hydrodynamic process in which these collisions are brought about. This convention is convenient in water treatment plant, where coagulation and flocculation commonly occur in separate reactors. In

water treatment polymeric flocculants are usually used in combination with coagulant salts, in which context they are known as coagulant aids.

3.2.3 Particle Aggregation

In an unaggregated system, only the larger or dense particles settle at a useful rate, while the fines remain in suspension for a long period of time. If the system is aggregated, the aggregates of fine particles will settle with the larger ones.

Figure (3.2) illustrates the relation between the settling velocity and particle diameter. The settling rate of the particles depends on their size and on their effective density. The different portions of the curve in Figure (3.2) correspond to different settling regimes that occur with different Reynolds number.

3.3 Destabilisation of Suspension

In a fine suspension particles are in continuous Brownian[46] and will experience collisions. A stable suspension is one in which the particles do not cohere on collision but remain dispersed indefinitely whereas in an unstable suspension they cohere to form aggregates that may in time become large enough to sediment or float if they have a different density to the liquid.

3.3.1 The D.L.V.O. Theory

Derjaguin and London[47] and Verwey and Overbeek[48],

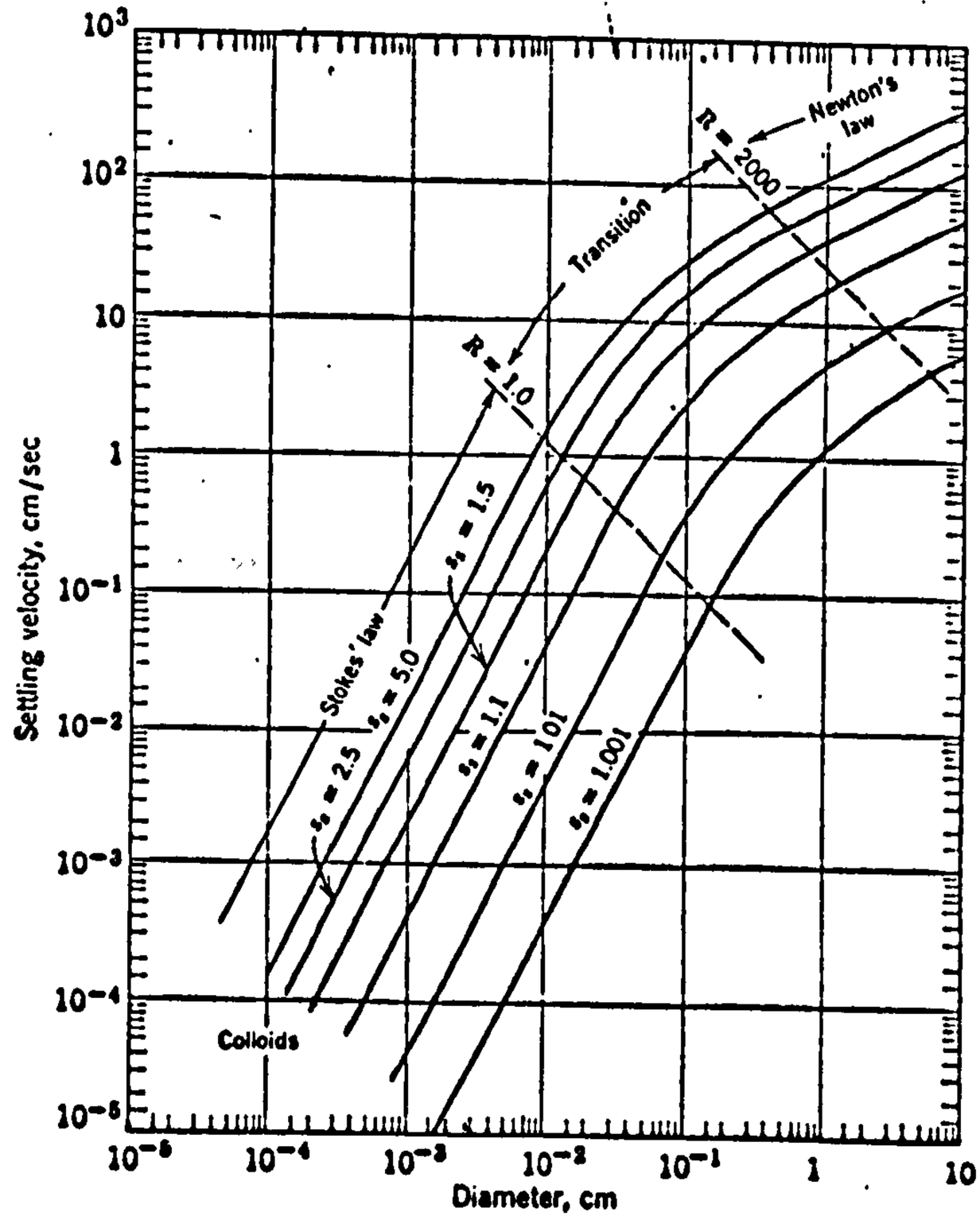

Fig. 3.2

Settling and rising velocities of discrete spherical particles in quiescent water at 10°C.
(Taken from Fair, Geyer and Okun[35]).

showed how to calculate the relative magnitudes of the Van der Waals forces and repulsive forces arising from the double layer overlap as charged particles approach each other. The total potential energy of the system is given by the sum of the attractive and repulsive forces (fig. 3.7). When the repulsive forces predominate over the forces of attraction, the suspension will be stable and the particles exist as single entities. For aggregation to occur the repulsive forces must be sufficiently reduced by charge neutralisation for the particles to approach each other to a distance where Van der Waals forces of attraction predominate.

It is difficult to verify directly the D.L.V.O. or any other theory of colloid stability by macroscopic experiments because the forces involved are so weak compared with the other forces experienced by the system. However, most colloid chemists agree that the D.L.V.O. theory and its subsequent modifications, to take account of hydrodynamic effects and the action of protective colloids, provide a sound basis for understanding colloid stability behaviour.

3.3.2 London Attractive Forces[49]

For two spheres of equal radius with a distance r between their centres, in a vacuum, the attractive forces between the particles has been given by Hamaker[50] as

$$V_A = -\frac{A}{6}\left[\frac{2a^2}{r^2-4a^2} + \frac{2a^2}{r^2} + \ln\frac{r^2-4a^2}{r^2}\right] \ldots\ldots 3.2$$

where A = is the Hamaker constant (generally between 10^{-20} and 10^{-19} J) which depends upon the nature of the material in question particularly the number of atoms per millilitre and the polarizability.

Although widely used the Hamaker approach is being replaced by the more general but difficult to use theory of Lifshitz. The relevant theories are reviewed by Visser[51].

3.3.3 The Electrical Double Layer

A potential difference usually exists at the solid-liquid interface in an electrolyte solution, this potential being due to the presence of one or more of the following:-

(a) Unequal distribution of constituent ions.

(b) Ionization of surface groups.

(c) Isomorphous substitution.

(d) Specific adsorption of ions.

(e) Dipole orientation.

A schematic representation of the structure of the electrical double layer is shown in fig. 3.3.

Due to the presence of this surface potential, ions of opposite charge, the counter ions, will be attracted towards the surface giving rise to a high counter ion concentration adjacent to the surface decaying with increasing distance until the solution equilibrium concentrations are attained.

The first quantitative treatment of this double layer

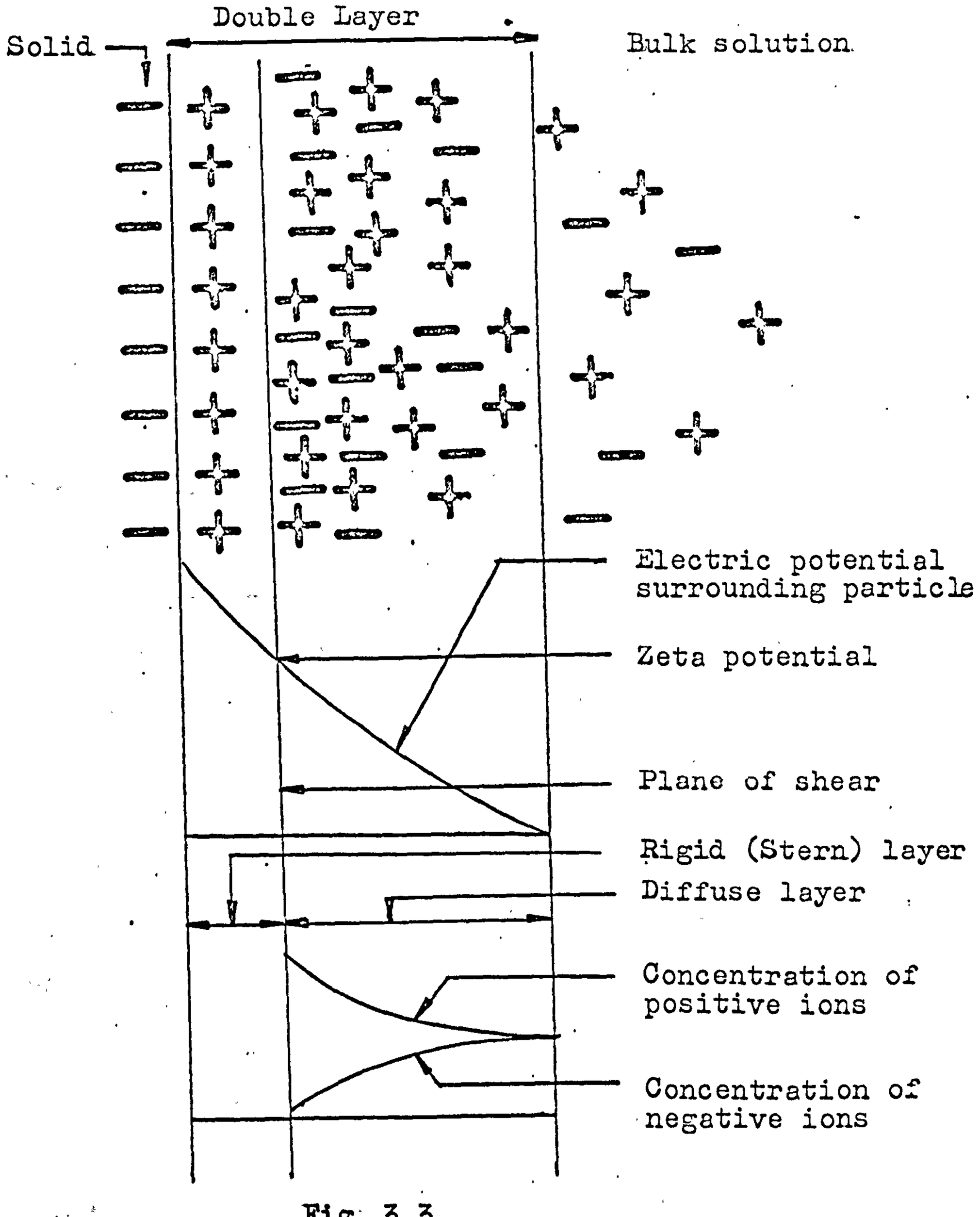

Fig. 3.3

The Electrical Double Layer

was by Gouy[52] and by Chapman[53] who solved the equation for the decay of potential with distance, $\psi(X)$, for a diffuse layer of point charges. For low values of $Ze\psi_o/kT$ where Z = is the counter ion valence.

e = the unit electron charge.

ψ_o = the surface potential.

k = Boltzmanns constant.

and T = the absolute temperature.

their solution reduces for symmetrical electrolytes, i.e. $Z^+ = Z^-$ reduces to $\Psi = \psi_o e^{-Xx}$ 3.3

where $$X^2 = \frac{2e^2 \sum n_{ii} Z_i^2}{\varepsilon kT}$$

where n_i is the number concentration of ions of type i and ε the permitivity of the electrolyte solution.

Figure 3.4 shows $\Psi(X)$ curves for ions of different Z at the same concentrations and figure 3.5 similar curves for the same ion at different concentrations.

This theory has been found deficient and was improved semi-empiracally by Stern. Stern[54] imagined that the double layer was divided into two parts, or in compact layer of ions and an outer diffuse layer obeying the Gouy and Chapman equations. In this theory it is imagined that flow of the liquid relative to the surface will occur at some 'slipping plane' which is close to or at the junction of these layers. Further it is often assumed, although the evidence is weak[55], that the electrical potential at this slipping plane is identical to the ζ potential determined in electrokinetic experiments.

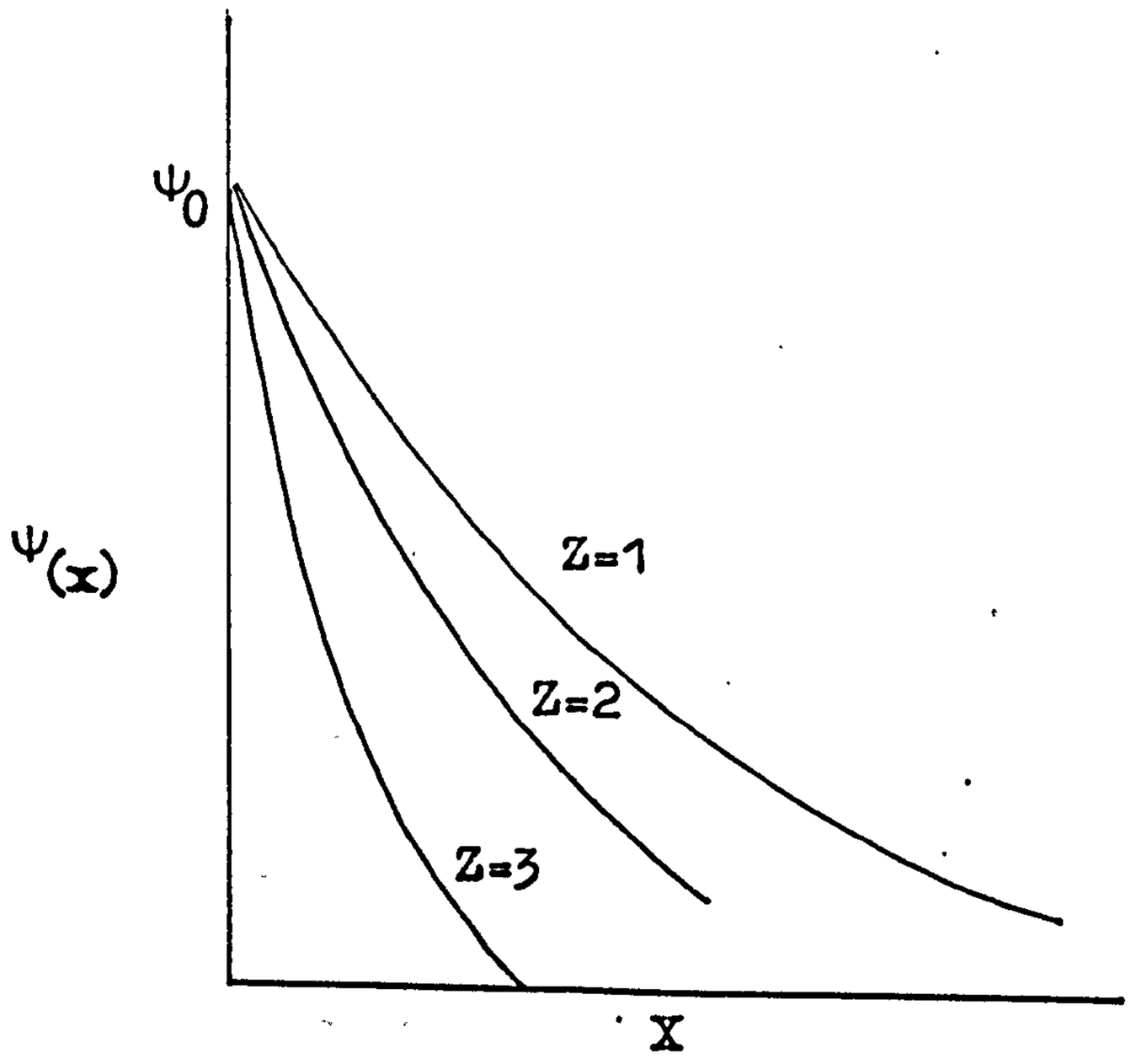

Figure 3.4

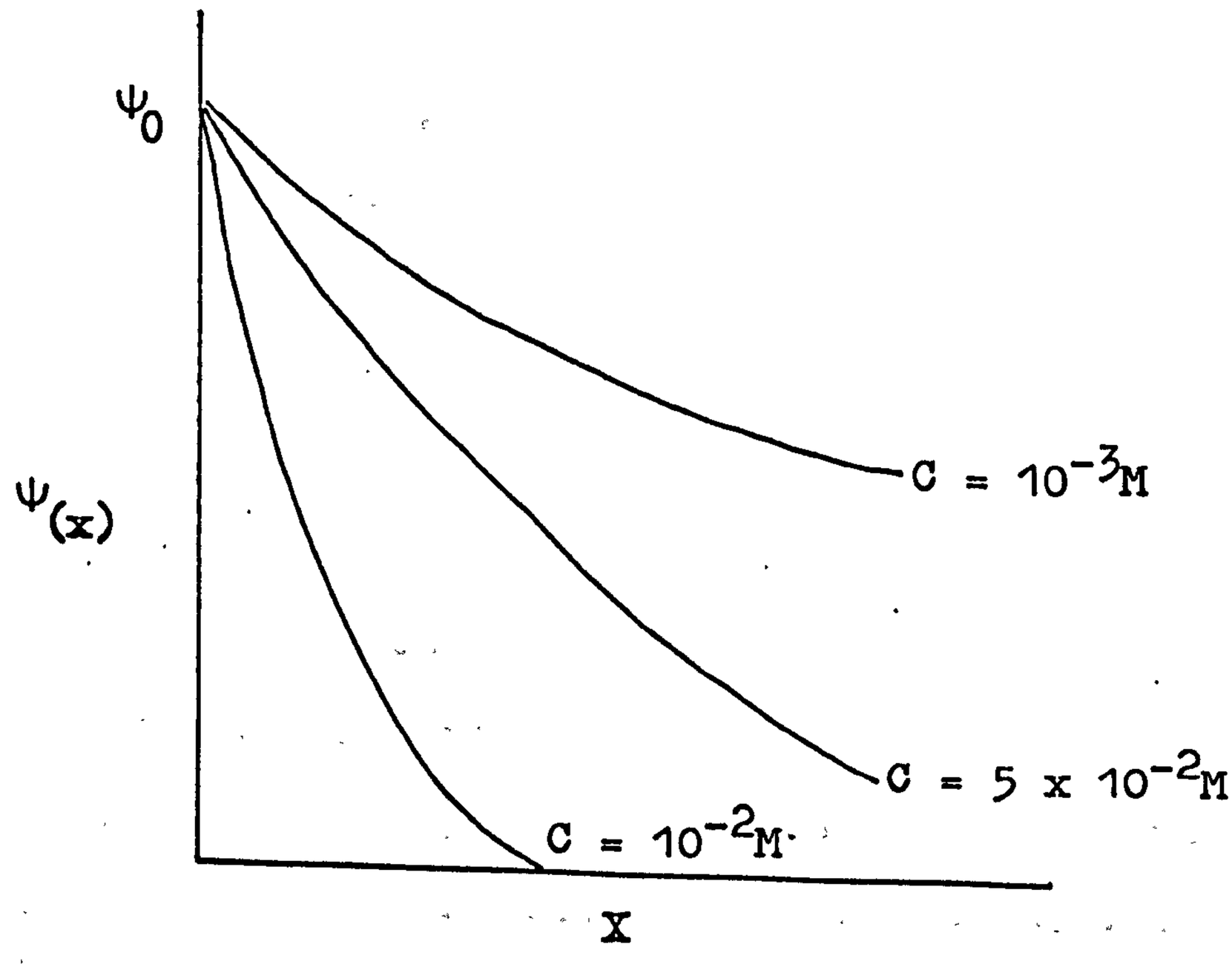

Figure 3.5

Typical potential distributions for the Stern model are shown in figure 3.6.

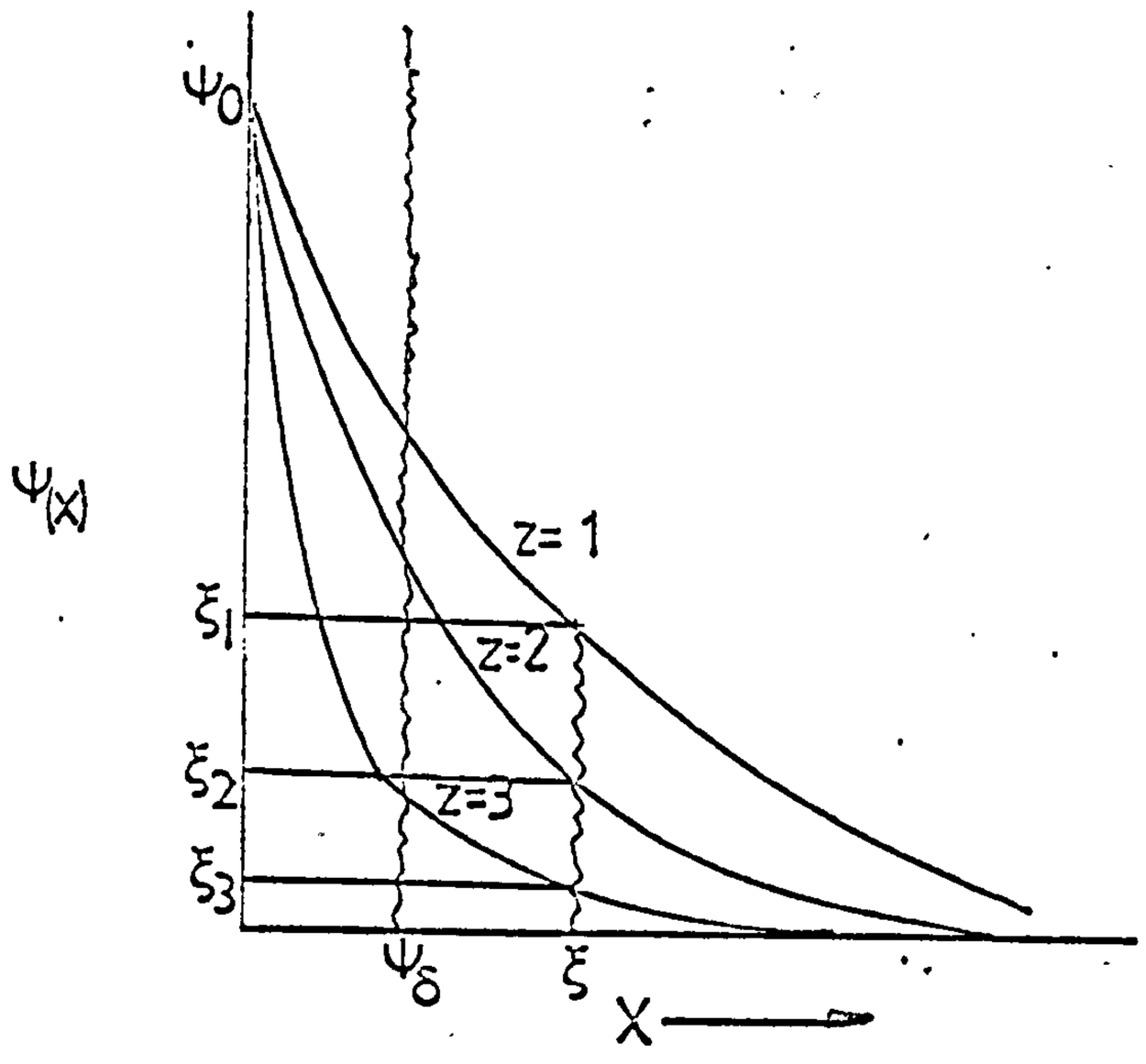

Figure 3.6

The problem of calculating particle interactions from double layer data is complex and discussed in detail by Gregory[55]. A widely used expression[49] for the repulsive potential energy between two spheres of radius a is:

$$V_R = \tfrac{1}{2} \Sigma\ a\psi_\delta^2\ \ln\left[1 + \exp\ (-XH)\right] \ldots\ldots\ldots\ 3.4$$

where H = is the surface-surface distance between the spheres.

ψ_δ = the Stern potential,

and all other terms as above.

ψ_δ is not easily accessible and commonly approximated to by ζ , a valid assumption at low potentials.

3.3.4 The Total Energy of Interaction

The total energy of interaction V_T is obtained by summation of the attraction and repulsion energies:-

$$V_T = V_A + V_R \quad \ldots\ldots\ldots\ldots\ldots\ldots\ldots\ldots \quad 3.5$$

Combination of equations 3.4 and 3.2 enables potential energy curves to be calculated for the interaction between two spherical particles of equal size. The form of the curve, as illustrated in figure 3.7, depends on the particle size and, more particularly, on Ka.

The repulsion energy V_R is an exponential function of the distance with a range of the order of the thickness of the double layer, and the Van der Waals attraction V_A decreases as an inverse power of the distance. In consequence of the dissimilar behaviour of the two forces with distance between the particles, the attractive force predominates at small and large separations; within the intermediate range of distances repulsion may be predominant, but this is dependent upon the specific values of attraction and repulsion.

When the energy maximum V_{max} is large compared with the thermal energy KT of the particles, the system should be stable. When the secondary minimum is also larger than KT, it should give rise to a loose, easily reversible form of flocculation. When V_{max} is large and the secondary minimum small or non-existant the suspension will be stable and will not flocculate. When V_{max} is small, or their is no barrier at all, the suspension will strongly flocculate.

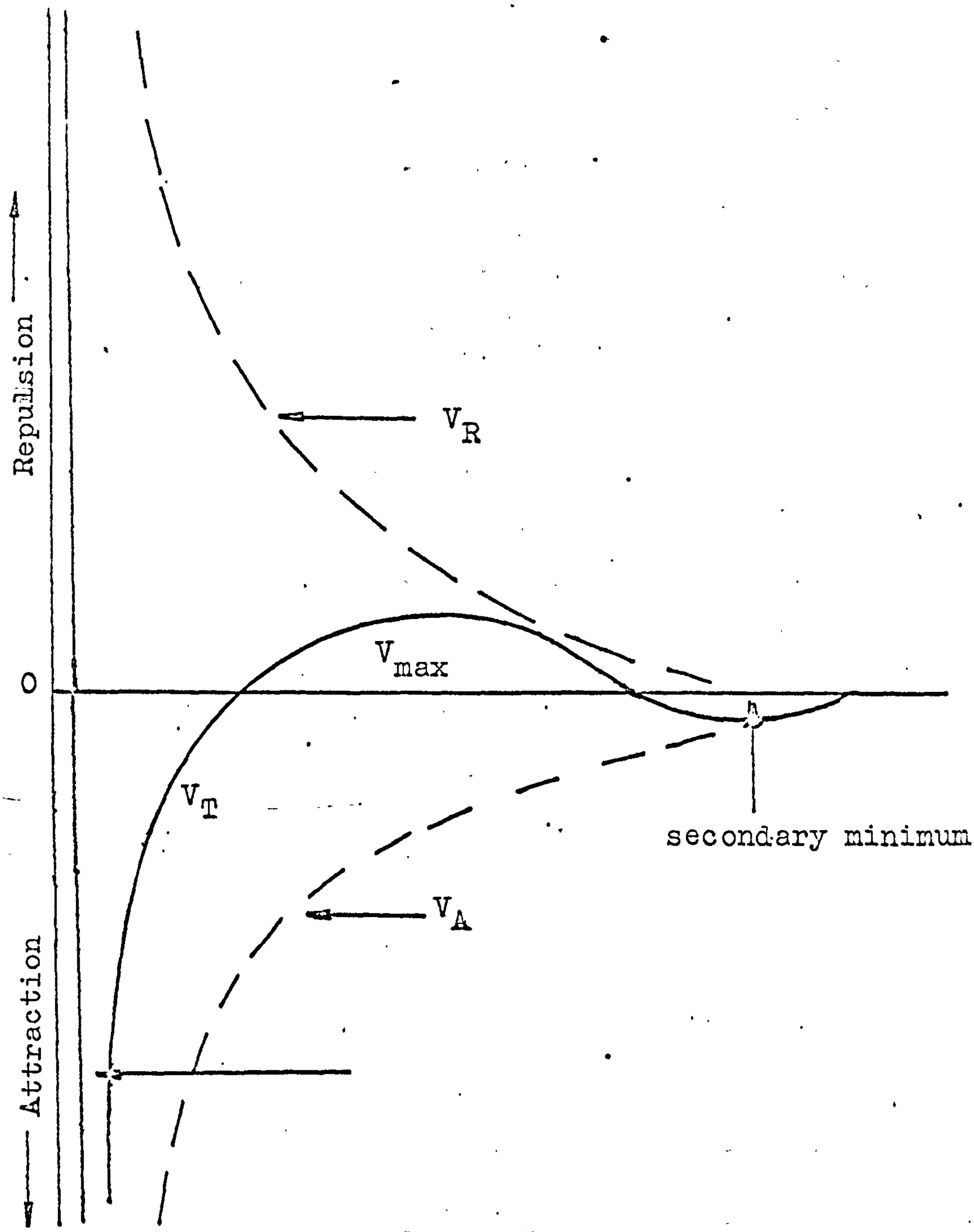

Fig. 3.7

Combination of electrical repulsion (V_R) and Van der Waals attraction (V_A) to give a total interaction curve (V_T).

Figure 3.6 shows how the Stern and ζ potentials vary with counter ion valence; the greater Z the lower the potential and hence the lower the contribution of V_R to V_T. This is consistent with observation and the empirical Schulze-Hardy Rule[56,57]. Practical destabilising counter ions are divalent such as Fe^{++}, Ca^{++}, Mg^{++} and trivalent ions such as Fe^{+++} and Al^{+++}.

3.4 Kinetics of Flocculation

Flocculation kinetics may be conveniently considered in relation to two distinctly physical mechanisms. In the first, (perikinetic flocculation) contacts produced by thermal motion (or Brownian motion) are the principal agents which cause the close approach or collision of colloidal particles. In the second (orthokinetic flocculation) the approach results principally from relative fluid motion.

3.4.1 Perikinetic Flocculation

For particles to come into contact, they must be able to overcome the energy barrier, V_{max}, which determines the stability of the dispersion (see fig. 3.7). If the barrier is reduced to zero there would be nothing to prevent contact of the particles, and flocculation would occur at a rate governed by the collision frequency of the particles.

For bonding to occur the repulsive forces between the particles and between the particles and the polymer must

be sufficiently reduced to enable the particles and polymer to approach each other to a point where bonding forces can predominate. These repulsive forces may be reduced by charge neutralisation, either by flocculating a charged suspension with a polyelectrolyte of opposite charge or by the addition of a suitable inorganic electrolyte.

The rate of particle removal by perikinetic flocculation was first calculated by von Smoluchowski who showed that the rate for particles not experiencing any force until contact occurred was

$$-\frac{dN^o}{dt} = \frac{-4 \alpha KT N^{o2}}{3\eta} \quad \ldots\ldots\ldots\ldots\ldots\ldots 3.6$$

where N^o = is the number of primary particles at time, t.

α = is a collision efficiency factor,

and η = fluid viscosity.

From this equation it can be seen that the rate is second order with respect to concentration and independent of particle size.

Integration of (3.6) with boundary conditions

$$N^o = N_o^o \text{ at } t = 0$$

$$N^o = \frac{N_o^o}{(1+4\alpha KTN_o^o/3\eta)t} \quad \ldots\ldots\ldots\ldots\ldots\ldots 3.7$$

and defining $t_{\frac{1}{2}} = 3\eta / 4\alpha KTN_o^o$ $\ldots\ldots\ldots\ldots\ldots\ldots 3.8$

we obtain $N^o = \frac{N_o^o}{1+(t/t_{\frac{1}{2}})}$ $\ldots\ldots\ldots\ldots\ldots\ldots 3.9$

$t_{\frac{1}{2}}$ being the time required to reduce the number of

particles present to a half of the initial number. For water at 25°C this gives

$$t_{\frac{1}{2}} = \frac{1.6 \times 10^{17}}{\alpha N_o^o} \quad \text{..... 3.10}$$

where N_o^o = is the particle concentration per m^3.

and $t_{\frac{1}{2}}$ = is the half life time.

For example, the particle concentration in water containing 10^{10} bacteria per m^3 takes 200 days to be reduced to half its initial value, assuming $\alpha = 1$.

The effect of viscosity and temperature on destabilisation of colloidal particles is very apparent. The higher the viscosity and the lower the temperature of the liquid, the lower is the rate of flocculation.

In water works it is a well-known fact that effective flocculation and the rate of floc formation are greatly influenced by the temperature of the water. As the temperature is lowered,, the dosage for flocculation must be increased to insure properly formed floc. Powell[58] has presented curves illustrating increased chemical requirements at temperature below 10°C.

The temperature affects the degree of hydration of the colloidal particles aswell, the higher the temperature the less would be the hydration. This is perhaps the reason why floc in cold water is less tough than that in warm water. The lower the temperature, the greater the hydration of the floc and the more voluminous and breakable is the floc. A more hydrated floc is perhaps of lower

specific gravity and therefore settles more slowly. Hydration will be further discussed in (3.4.3) below.

3.4.2 Orthokinetic Flocculation

It has long been observed that agitation promotes the aggregation of colloidal particles. This is due to the velocity gradients which are induced in the liquid causing relative motion of the particles which are present. When contacts between particles are caused by fluid motion the process is termed Orthokinetic flocculation[57].

The basic rate equation for orthokinetic flocculation[59]

$$-\frac{dN^o}{dt} = \frac{-2\alpha G d^3 N^{o2}}{3} \quad \text{..... 3.11}$$

where d = is the particle diameter.

and G = the velocity or shear gradient in the fluid.

It can be seen that this rate is very sensitive to particle size. At $G = 10S^{-1}$, a typical working value, the ortho/perikinetic flocculation rates are about equal for 1 μm particle whereas the ratio is 10^{-3} for a 0.1 μm particle. Hence stirring at rates that will not cause significant floc attraction say $G \leq 100S^{-1}$, is not a significant mechanism for flocs less than 1 μm diameter. For smaller particles the restrictions imposed by perikinetic and orthokinetic theory must be overcome in other ways.

3.4.3 Effect of Salts

When salts of metals like aluminium or iron are added

to water the polyvalent cations Al^{+3} and Fe^{+3} reduce the Zeta potential (see section 3.3.3) and facilitate coagulation. Stumm and Morgan[60] emphasized that the effects of ferric and aluminium salts upon coagulation are not brought about by the simple aquo-metal ions themselves, $Fe(OH)_6^{+3}$ and $Al(H_2O)_6^{+3}$, but by their hydrolysis products. The addition of an Fe^{+3} or Al^{+3} salt to water in concentration less than the solubility limit of the metal hydroxide leads to the formation of soluble monomeric, dimeric, and small polymeric hydroxo-metal complexes, in addition to the free aquo-metal ion:-

$$Fe(H_2O)_6^{+3} + H_2O \longrightarrow Fe(H_2O)_5(OH)^{+2} + H_3O^+$$

$$Al(H_2O)_6^{+3} + H_2O \longrightarrow Al(H_2O)_5(OH)^{+2} + H_3O^+$$

$$Al^{+3} + H_2O \longrightarrow Al(OH_4)^- + 4H^+$$

$$Fe(OH)^{2+} + H_2O \longrightarrow Fe(OH)_2^+ + H^+$$

$$2Fe^{+3} + 2H_2O \longrightarrow Fe(OH)_2^{4+} + 2H^+$$

their relative concentrations depend on pH and ionic concentration (see figure 3.8). The complex ions formed may be regarded as an ion exchange medium capable of adsorbing anionic species. As the complexes grow they will eventually precipitate and form particles which enhance the coagulation rate. The number of particles formed will depend on local concentration and velocity gradients, hence the significance of the very early mixing-stage in coagulant addition.

With polyaluminium chloride, Cl^- is built into the hydrolysed floc which has therefore a lower anion exchange capacity. This is consistent with its observed behaviour

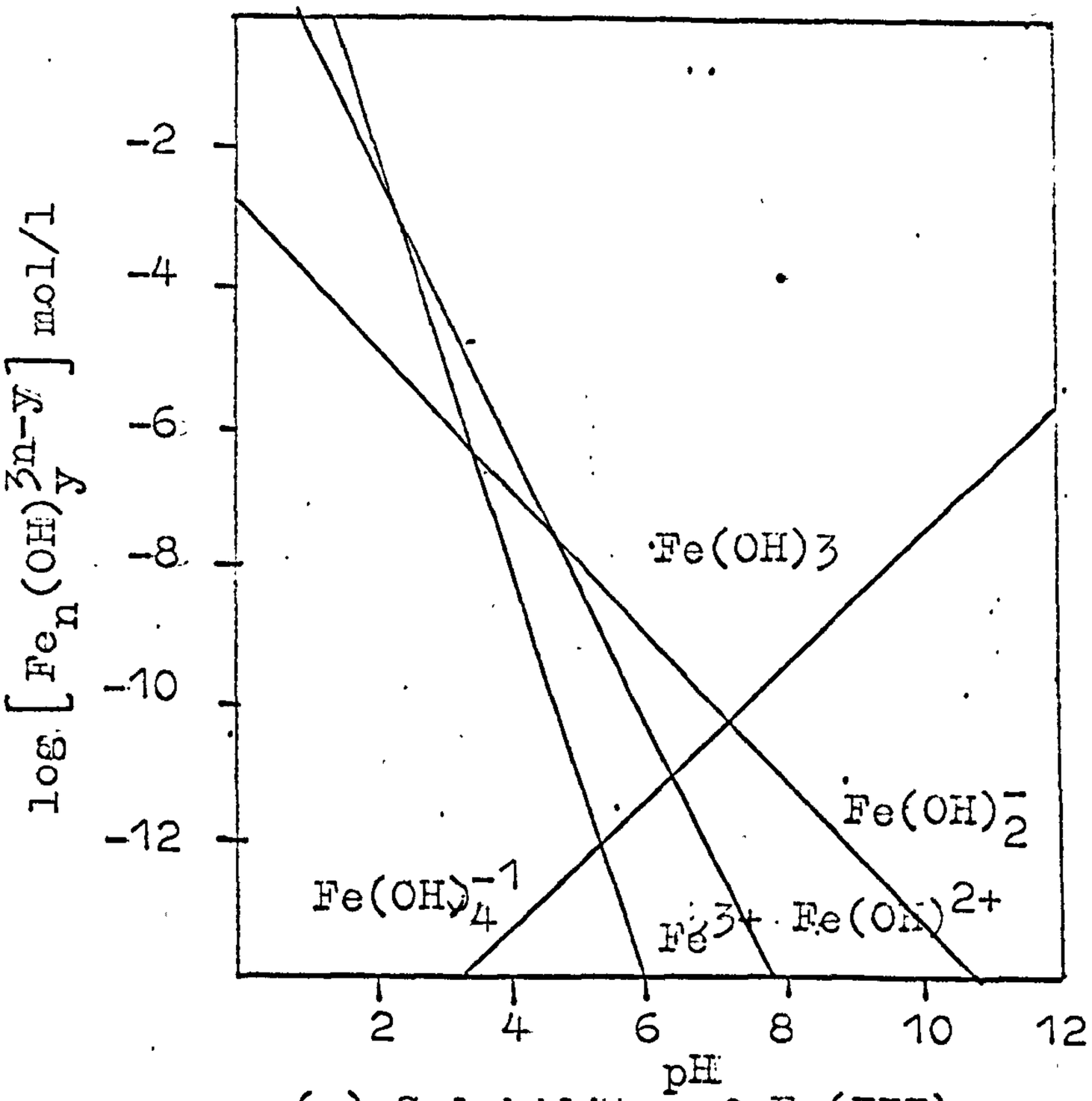

(a) Solubility of Fe(III)

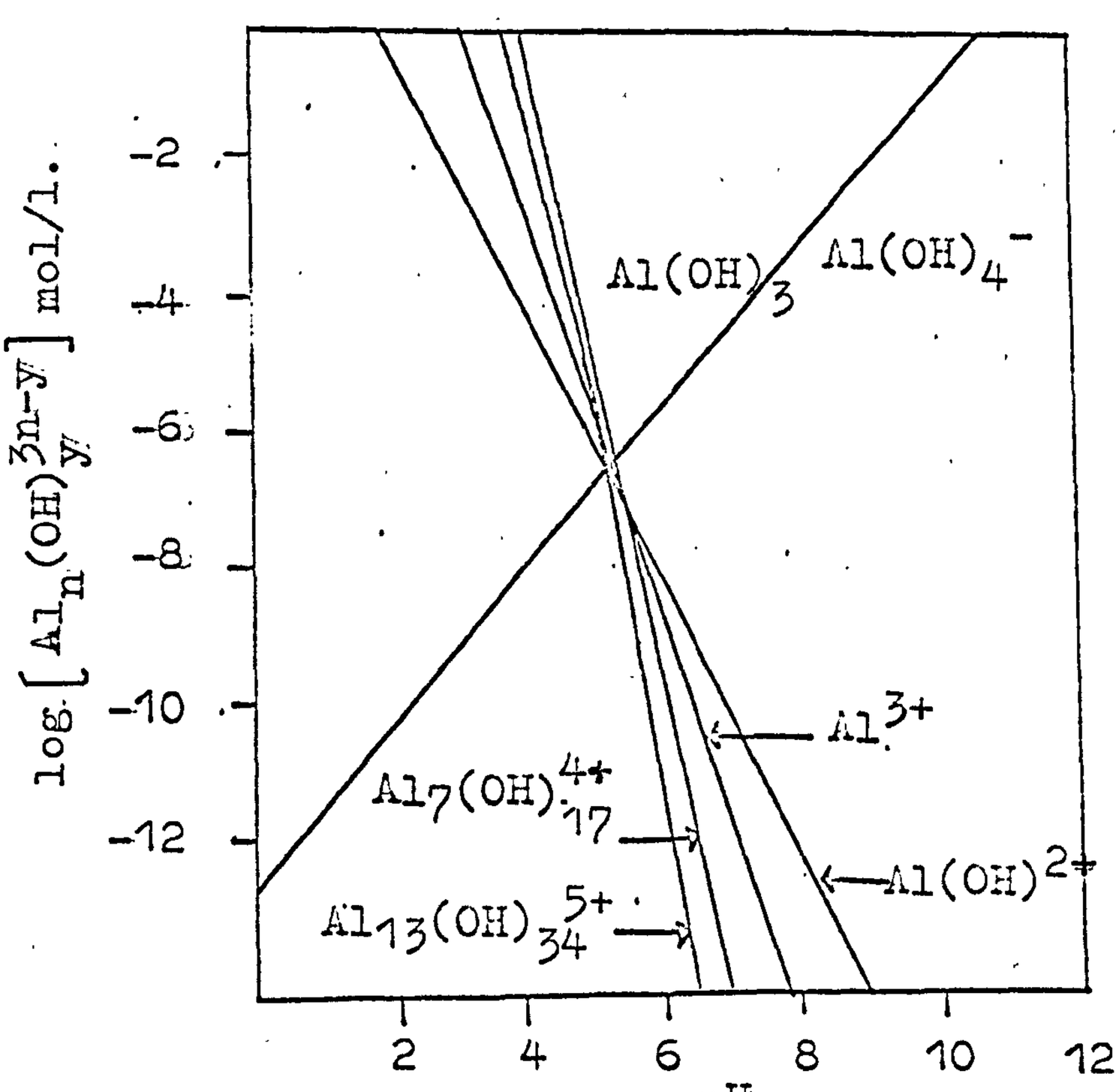

(b) Solubility of Al(III)

Fig.(3.8): Equilibrium composition of solutions in contact with freshly precipitated $Al(OH)_3$ and $Fe(OH)_3$.

as a coagulant, being capable of coagulating particles effectively but not so effective in the removal of colour causing humic acid.

Aggregation of colloids by polymers produced from Al^{+3} and Fe^{+3} salts is primary influenced by three factors; colloid concentration, pH, and coagulant dosage.

Packham[61] confirmed by electrophoretic studies that colloidal particles were removed by enmeshment in the coagulant hydrolysis products. The colloidal particles themselves can serve as nuclei for the formation of the precipitate, so that the rate of precipitation increases with increasing concentration of the colloidal particles to be removed. Stumm and O'Melia[62] have indicated that for polymeric coagulation, the surface area concentration of the colloidal particles in suspension is more value than the weight concentration.

In the pH range below the zero point of charge (Zpc) of the metal hydroxide precipitate, positively charged hydroxo-metal polymers will prevail. Adsorption of these positive polymers can coagulate negatively charged colloids by charge neutralisation. In solutions more alkaline than the (Zpc), anionic hydroxo-complexes will predominate. Ultimately insoluble polymeric complexes of indefinite size are formed; these are referred to usually as the insoluble metal hydroxides. In cases where anionic inorganic polymers are effective coagulants, they may function by adsorption and bridge formation.

The chemical dosage which is required depends upon

how coagulation is achieved[59]. Coagulation by adsorption generally requires a lower coagulant dosage; the required dosage increases with increasing colloid concentration. On the other hand, Hahn and Stumm[63], Stumm and O'Melia[62], demonstrated that restabilisation may occur due to coagulant overdosing.

3.5 Polymer Flocculation

Water-soluble polyelectrolytes, natural and more increasingly synthetic, are being used in water treatment to enhance the sedimentation of flocs. Polymers for this purpose have to reach specified toxicity standards imposed by the appropriate national authorities. The main requirement is that the monomer concentration be less than a stated value because it is the monomer which is toxic and because at correct dose levels there should be no free polymer in the filtrated water.

Packham[64] discussed the use of primary polymeric flocculants. Because colour removal depends upon the removal of humic materials containing carboxylic acid groups, it might be expected that only cationic polyelectrolytes would be effective and experience bears this out. On experiments with three natural waters, the cationic polyelectrolytes were in general less successful than alum both with respect to colour and turbidity removal although in some cases the differences were minimal. Packham[64] attributed the poor clarification performance of the polyelectrolyte as being due to the small number of

particles present and the consequent low flocculation rate. Also the dosage was quite critical, a moderate overdose leading to marked deterioration in performance. It is unlikely that such close dosage control is within the capability of present water installations.

Beardsley[65] discussed the advantages of primary polymeric flocculants, he concludes that they:-

(1) Provide an alternative method to treat difficult waters.

(2) Prevent soluble aluminium carry-through into the distribution system and subsequent fouling due to post precipitation.

(3) Prevent need for extensive pH adjustment.

(4) Prevent carry over of light floc.

(5) Reduce sludge volume.

(6) Provide a sludge more suitable for land filling.

(7) Reduce the amount of soluble anions added with coagulant.

(8) Provide an overall improvement in process quality and/or economics.

Yadev[66] has studied the effect of polyelectrolyte coagulant aids on the removal of alum flocs in sludge blanket clarifier. It was found that the stability of the blanket was increased and the filtrate quality improved, particularly when raw water conditions were poor and variable.

3.5.1 Polymer Types

Natural high molecular weight polymers such as starches, gelatine, and gums have been used for centuries for clarifying potable water. Synthetic polymers have largely displaced natural materials over the last 20 years because of their improved performance, consistency and resistance to biodegradation. These polymers are made almost exclusively by free radical polymerisation, which results in a wide range of the molecular weight in the product. Copolymers are made by direct copolymerisation of mixed monomers, or by subsequent modification of a homopolymer, both processes leading to random copolymers.

Of the polymers listed, polyacrylamides and their derivatives are most widely used in practical applications and have also been quite popular as experimental materials.

Acrylamide is non-ionic and its structure is,

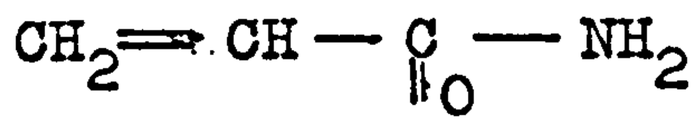

From the monomer a non-ionic polyacrylamide may be obtained by polymerisation. The structure of the polymer is,

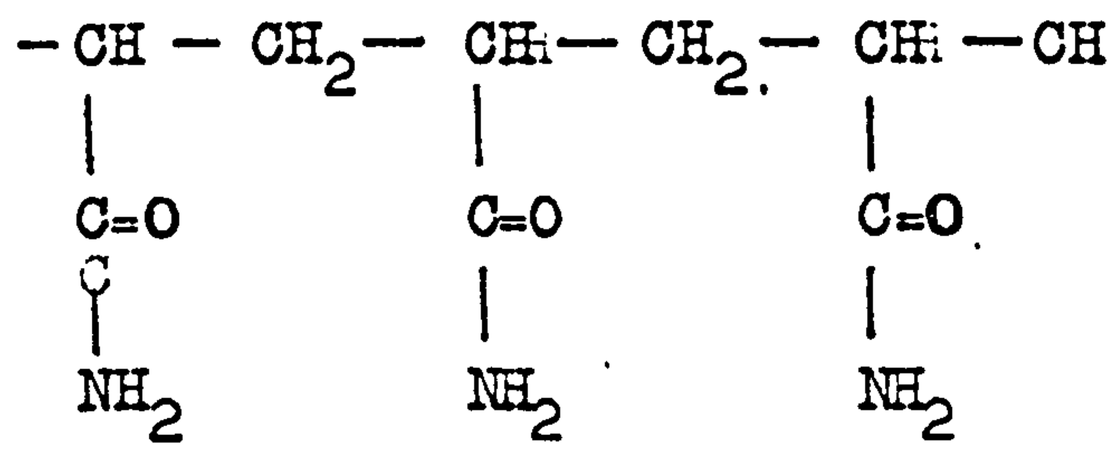

Anionic polyacrylamide may be prepared by the controlled hydrolysis of the monomer, which convert some of the sites to carboxylic groups containing a net negative charge. The structure of the polymer is,

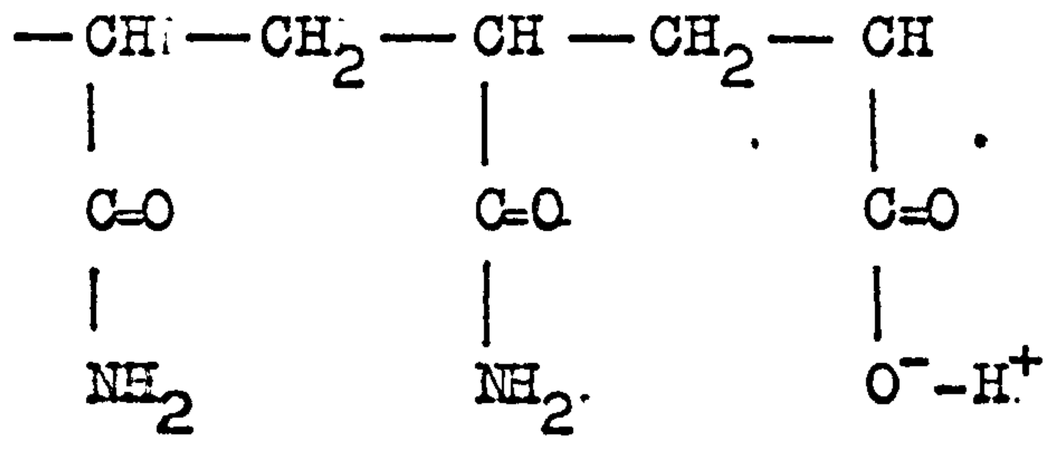

Anionic acrylamide type polymers may also be prepared by the copolymerisation of acrylamide and acrylic acid.

Cationic polyacrylamide may be prepared by the copolymerisation of acrylamide and quaternary ammonium compounds. The structure of the polymer is,

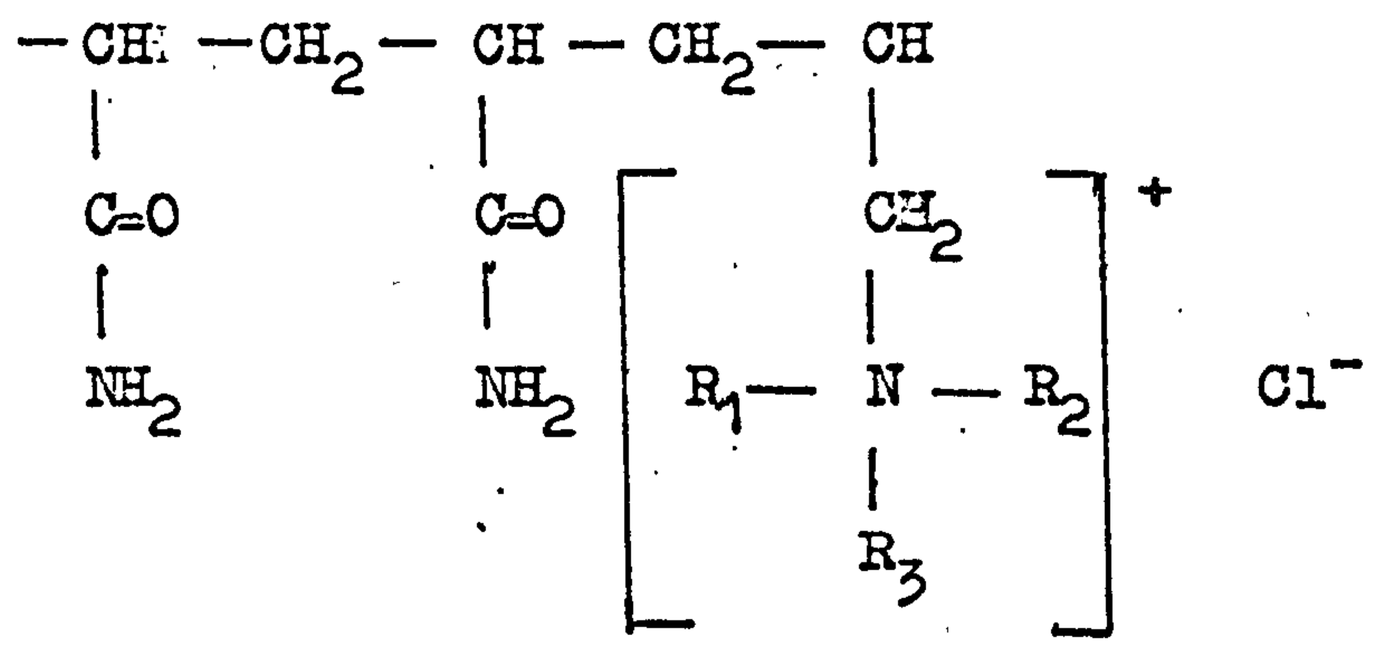

Synthetic organic flocculants are usually supplied as powders which may be anything from free flowing and granular to fine and dusty. For very small users they may be obtained as solutions, but viscosities of solution of polyacrylamides are so high even at low concentration (i.e. 1%) that this is not economic. Powdered polyacrylamides are not easy to get into true solution and it is very easy for considerable quantities of solid to remain in an undissolved gel state.

3.5.2 Bridging Theory

Basically there are two main mechanisms of particle-polymer interaction. The first is one of charge

neutralisation where slurries or dispersions are flocculated by oppositely charged polymers. However, negatively charged particles can also be flocculated by negative polyelectrolytes and even particles that posses considerable charge can be flocculated by non-ionic polymers. These effects imply that in these cases another mechanism must be operative. This leads to the next mechanism - that of Bridging.

The bridging concept of long loops extruding from one particle and interconnecting with another to form polymer bridges was first put forward by Ruehrwein and Ward[67]. The bridging theory proposes that the polymer molecules are adsorbed onto more than one particle hence holding them together. A bridging flocculation reaction may be broken down in several elementary processes:-

(1) Dispersion of the flocculant solution in the liquid phase of the suspension.

(2) Diffusion of the flocculant to the solid-liquid interface.

(3) Adsorption of the flocculant at the solid-liquid interface.

(4) Collision of particles bearing adsorbed polymer with another particle.

(5) Adsorption of polymer onto second particle to form a polymer "bridge".

(6) Subsequent collisions and hence bridge formation to form the final floc.

Evidence for bridging mechanism lies in the ability of

polymers to flocculate particles bearing the same charge[68]. If, however, the electrical double layer repulsion is too strong the particles may not approach close enough for bridging to occur. In these situations flocculation may be facilitated by addition of ions to reduce the Zeta potential. Where conditions are likely to change with respect to pH, non-ionic polymers may be advantageous although in general they are not as effective flocculants as are charged species.

3.5.3 Operating Variables

In the water treatment process, flocs resulting from the combination of a flocculant and a suspension have different physical characteristics which depend on a variety of factors, the more important are:-

(1) Amount and duration of mixing.

(2) Flocculant dosage.

(3) Concentration of the suspended matter.

(4) The pH of the system.

In the presence of a velocity gradient flocs will experience forces which will cause them to disrupt, this disruption being reversible with coagula but irreversible with polymerically bridged flocs. These differences are important in comparing the behaviour of these two mechanisms in process applications. In general coagula are small, weak and reversible whilst flocs are larger, stronger but irreversible. The size of the flocs formed is important as the objective of most effluent treatment

plants is to produce a floc of size and density such that the majority of particles will settle out, and the remainder will be removed by filtration.

Linke and Booth[69] show there is an optimum dosage for producing the required result, e.g. floc size, cake permeability, minimum residual turbidity. This optimum concentration is believed to occur when half the available adsorption sites are occupied by polymer segments. With higher concentrations the degree of flocculation may be greatly reduced, there being evidence to suggest that primary particles and flocs become sterically stabilised resulting in inhibition of the bridging mechanism. Whereas, at lower flocculant dosages the changes for bridge formations is lessened and so smaller flocs are formed.

In situations where the solids content is low, the coagulation rate may be enhanced, by using a coagulating salt which produces hydrolysis products at the operating pH. O'Melia[70] has summarised these conditions. An alternative procedure discussed by Packham[64] is the addition of a fine inert solid,, e.g. a montmorrilonite clay. One disadvantage of the use of hydrolysing salts and inert additives, is the amount of sludge produced, but there may be no alternative to this in some situations.

In a suspension, the pH of the solution determines the surface charge on the particle. For some materials at high pH the surface is highly negative, the particles cannot approach each other very closely, polymer bridging occurs less frequently, and larger proportion of the

polymer becomes attached to single particles and hence they are more difficult to flocculate. The properties of the polymer itself may also depend on solution pH. A polymer with high charge density e.g. a polymer bearing cationic groups in acid solution, will tend to adopt an extended configuration, whilst the same polymer under base conditions, where the charge groups are neutralised, will become randomly coiled.

3.6 Flocculator Design

Many water works have used water treatment process for many years consisting of the following compartments:-

(1) Mixing of flocculant with water.

(2) Flocculator.

(3) Settling basin.

(4) Filtration.

Figure 3.9 illustrates the general flow sheet of the MISHRAK water treatment plant. There have been a large number of different designs suggested for these components of such water treatment plants. Nearly every company and every engineer concerned with water treatment plant has proposed and developed a special device for the mixing, the floc formation and the following separation compartment.

The design of flocculating vessels has received most attention in water treatment process plant design, because the primary particles as precipitated are of sub-micron dimensions and agglomeration to about 1 micron must occur by thermal motion, as the rate of perikinetic flocculation

Figure 3.9.

Mishrak Water Treatment Plant

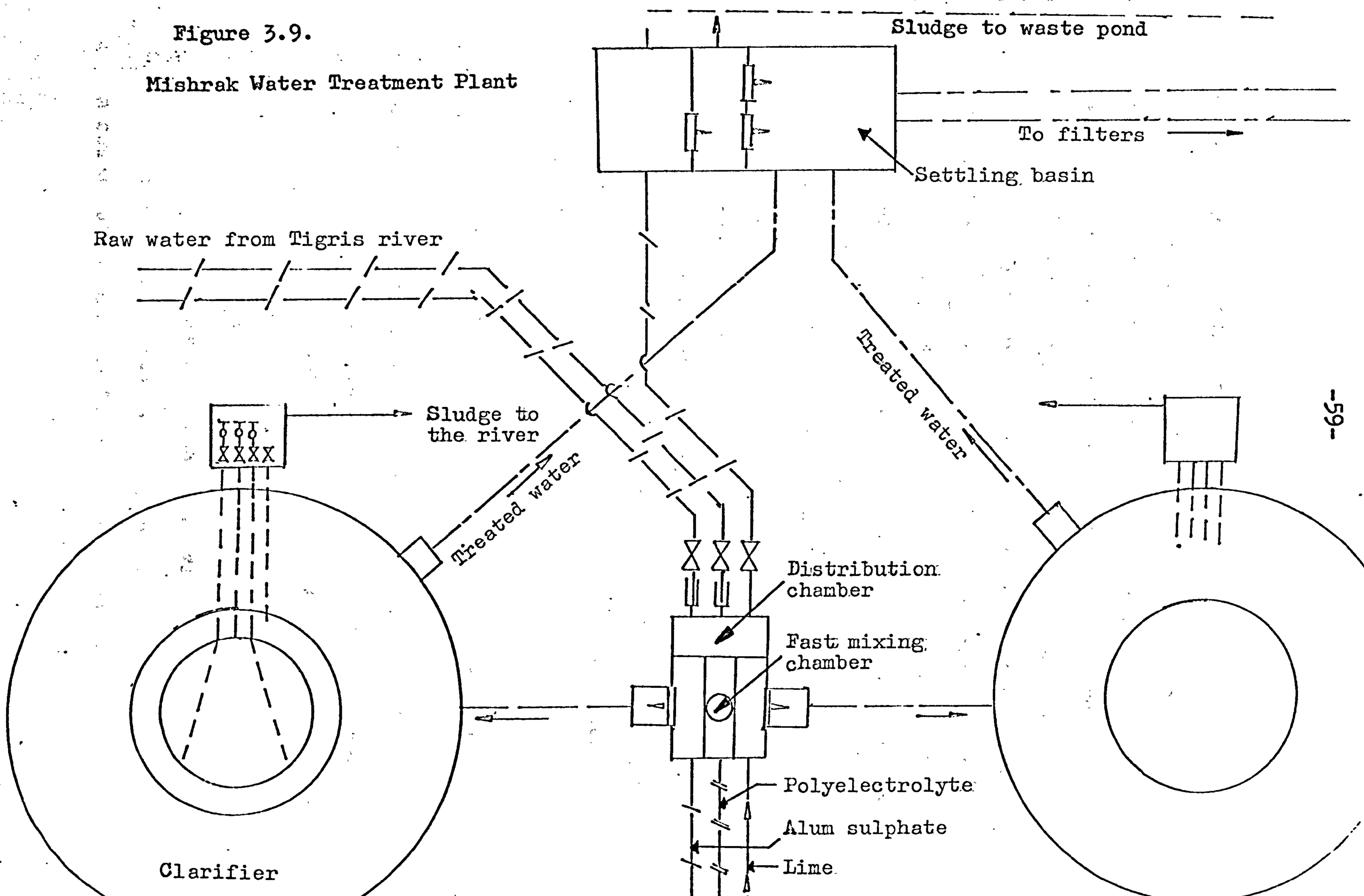

is unacceptably slow. In the presence of a velocity gradient, i.e. a shear, orthokinetic flocculation occurs and is equal in rate to perikinetic flocculation for particles of diameter 0.1 microns at a shear rate 10,000 sec^{-1} and 10 microns diameter at a shear rate 0.01 sec^{-1}. In water treatment, mean velocity gradients of 10-100 sec^{-1} are common[59]. It is in order to overcome the rate limitation imposed by equations (3.6) and (3.11) that hydrolysing precipitating salts or inert solids are added as described in (3.4.3) above.

The simplest type of flocculating process is to add the coagulating or flocculating reagent to the suspension in flash mixer (figure 3.10), and then slowly stir the mixture in a tank with a rotating paddle to enhance orthokinetic flocculation (figure 2.2). The mean velocity gradient for laminar flow was given by Camp and Stein[71] depends upon the power which is dissipated within the water,

$$\bar{G} = \left(\frac{\bar{P}}{V\mu}\right)^{\frac{1}{2}} \quad \text{..... 3.12}$$

where $\bar{G}$ = is the mean velocity gradient, sec^{-1}.

$\bar{P}$ = is the power input to the fluid (determined by measuring the torque on a paddle stirrer shaft).

V = is the tank volume.

μ = is the absolute fluid viscosity.

In baffled flocculator relying on hydraulic mixing as a source of power, the following equations are based on

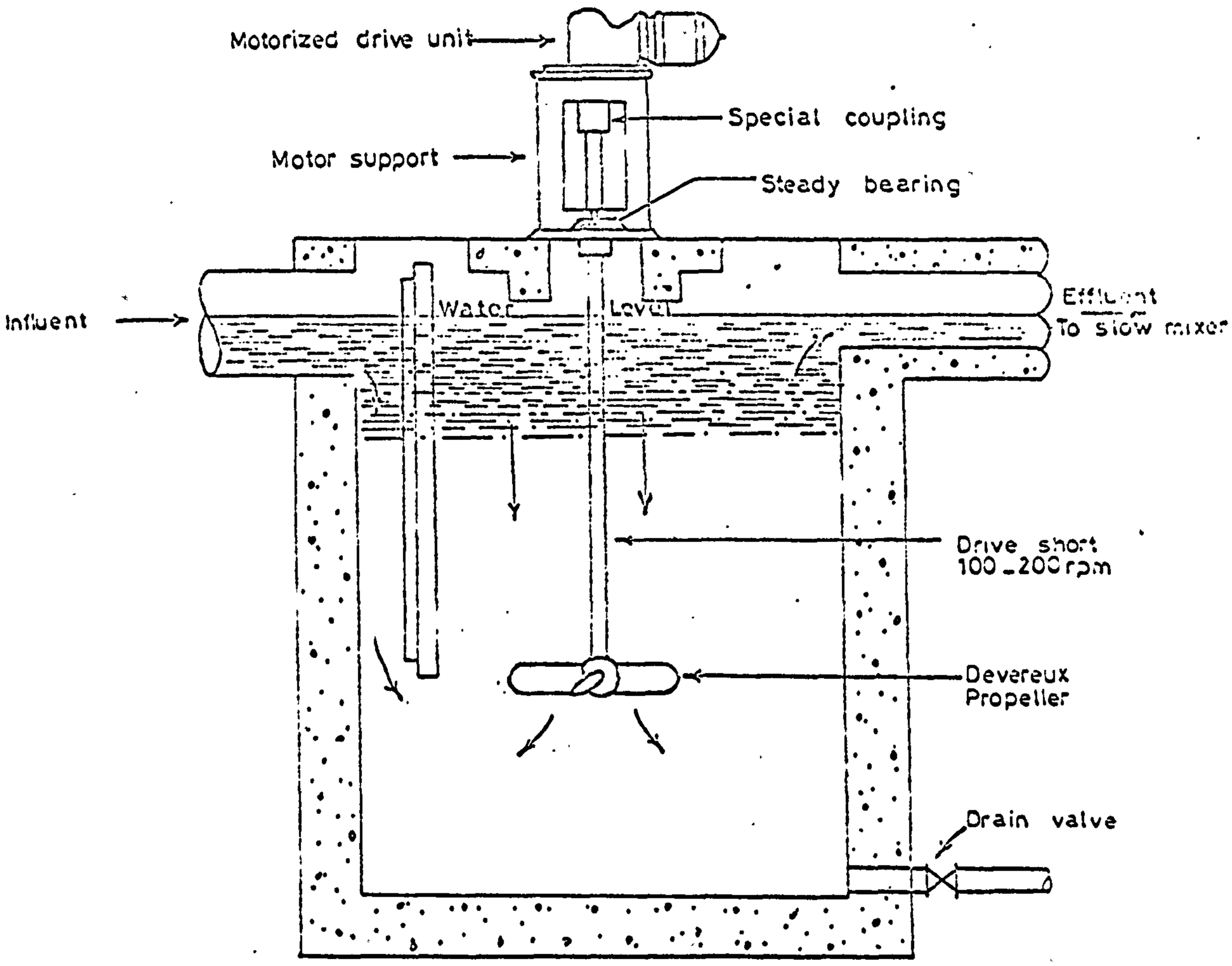

Figure 3.10

Flash Mixer

the work of Camp[72]

$$\bar{G} = \left(\frac{gh_f}{\alpha \bar{t}}\right)^{\frac{1}{2}} \quad \ldots\ldots\ldots\ldots\ldots\ldots\ldots\ldots\ldots\ldots \quad 3.13$$

where g = is the gravitational constant.

h_f = is the hydraulic head loss in the flocculator.

α = is the fluid kinematic viscosity.

$\bar{t}$ = is the mean detention time.

Interparticle contacts are frequently achieved by mechanically stirring the water with rotary paddles, therefore:-

$$\bar{G} = \left(\frac{C_D \, A \, P_L \, V_r^{\,3}}{2\mu V}\right)^{\frac{1}{2}} \quad \ldots\ldots\ldots\ldots\ldots\ldots\ldots\ldots \quad 3.14$$

where A = is the cross sectional paddle area perpendicular to its direction of motion.

C_D = is the drag coefficient which depends upon paddle shape and flow conditions.

P_L = is the fluid density.

V_r = is the relative velocity of the paddle with respect to the fluid. Considerable difficulties are encountered to determine V_r; in most designs its values in the range of $0.5 \leqslant V_r \leqslant 0.75$.

Combining the velocity gradient, $\bar{G}$, and the mean detention time, $\bar{t}$, the following may be obtained:-

$$\bar{G}\,\bar{t} = \left(\frac{PV\mu'}{Q}\right)^{\frac{1}{2}} \quad \ldots\ldots\ldots\ldots\ldots\ldots\ldots\ldots\ldots\ldots \quad 3.15$$

where Q = is the flow rate.

$\bar{G}\bar{t}$ = is known as the Camp number which represents the ratio of power induced to flow to displacement induced flow.

The normal design range for $\bar{G}\bar{t}$ is 10^4-10^5.

An example of a flocculator-clarifier is shown in figure 2.2.a, which has a central feed chamber, equipped with paddle or propeller stirrer. Apart from orthokinetic flocculation another way of enhancing the particle rate is to increase the particle concentration by retaining some formed sludge in the flocculator and/or clarifier. This may be done by recirculating the sludge (see figure 2.3) as in an Acentrifloc clarifier or by maintaining the sludge as a fluidised bed as in the sludge blanket clarifier. In the sludge blanket clarifier both mixing and flocculation occur (figure 2.2.b, and 3.11). The particles rise at a decreasing velocity through the conical or wedge shaped tank and experience orthokinetic flocculation with a stable sludge blanket maintained at a constant level. More recent designs use a rectangular tank.

The use of sedimentation basin for the removal of suspended solids prior to filtration is by no means universal in water treatment plants. The sedimentation basin is designed (figure 3.12) to receive the water from the flocculator and to retain it a sufficient time to permit the sedimentation of the proper amount of floc. Therefore, the hydraulic feature of a settling basin, such as short-circuiting, turbulence, density current, inlet

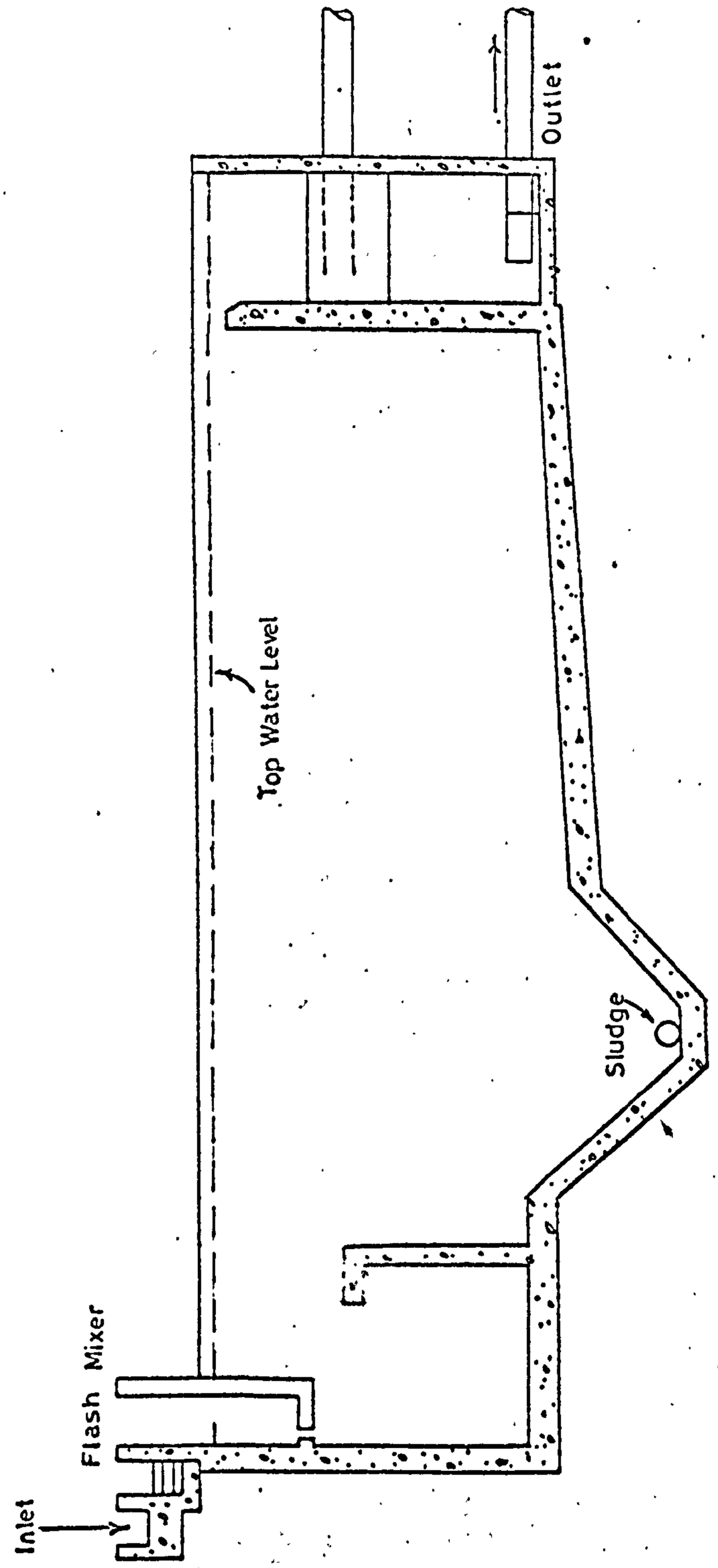

Figure 3.11

Sludge Blanket Clarifier

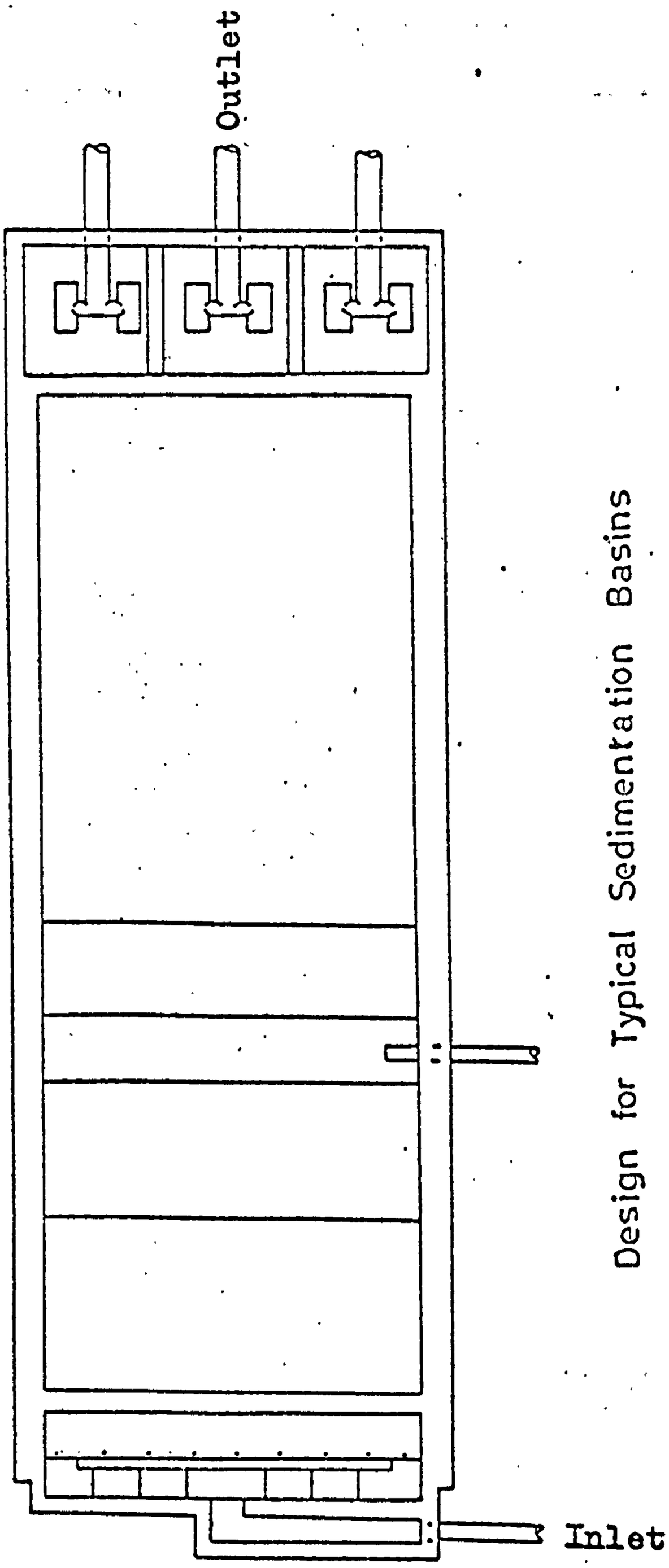

Figure 3.12 Design for Typical Sedimentation Basins

and outlet conditions, and sludge withdrawal means affect solid-liquid separation and, therefore, the performance of the basin.

CHAPTER FOUR

Crystallisation of Calcium Carbonate

4.1 Introduction

Precipitation is a chemical process widely used in analytical and industrial chemistry. In the purification and separation of mixtures of compounds, the relative solubilities of the components is one of the factors that has to be considered. Rapid precipitation - such as those taking place in qualitative analysis - favours the formation of non-stable states. The final form of the solid is therefore not immediately produced, but is preceded by succession of non-stable forms.

The formation of a precipitate from a solution takes place in two steps. In the first, small 'centres' of the solid phase first become distinct at various points in the solution phase, separated by many molecular spacings. In the second step these centres then propagate at the expense of the concentration in solution. Thus precipitation takes place only at the interface between solid centres and solution. These processes are known as nucleation and growth,, nucleation being the birth of the centres.

The phenomena associated with the precipitation process are complex and the understanding of the mechanism of precipitation is not at all clear. The total rate of the precipitation process is determined by two factors; the rate of nucleation, J, of centres of the solid phase, and their rate of growth after nucleation. Both of these

factors must be known in order to establish an interpretation of the experimental data on precipitation rates.

4.2 Supersaturation

The supersaturation created in a given system is the major factor that controls the crystallisation process.

Three most commonly adopted supersaturation expressions[73] are: the supersaturation ratio, S, the concentration driving force, Δc, and the absolute supersaturation, σ, they are defined by:-

$$S = C/C^* \quad \ldots\ldots 4.1$$

$$\Delta c = C - C^* \quad \ldots\ldots 4.2$$

$$\sigma = (C - C^*)/C^* = S - 1 \quad \ldots\ldots 4.3$$

where C = is the concentration.

and C^* = is the saturation concentration.

The supersaturation ratio, S, is usually used[74] in nucleation studies because the rate of homogeneous nucleation, J, given by equation (4.16) has a supersaturation ratio term in it. For growth rate kinetics, the concentration driving force, Δc, has been used very widely, but the absolute supersaturation, σ, is sometimes preferred as it is a dimensionless quantity.

In analytical chemistry, concentrations are normally expressed on a molar basis, e.g. mole/litre solution, because most solutions are prepared on a volume basis.

4.3 Nucleation Mechanisms

With any degree of certainty the true mechanism and natural laws of nucleation and growth are still relatively not clear. The nucleation process, which determines the size and size distribution of crystalline precipitate, is one of great importance in analytical procedures since it governs the nature and purity of the resulting precipitate.

However, the two steps, nucleation and growth, were considered to be independent of each other; nucleation being the more difficult to control. The distinction between the two processes appeared reasonable on simple grounds given by the Arrhenius equation[75] which shows the variation of rate constant with temperature:-

$$K = K_o\, e^{-E/RT} \qquad \text{..... 4.4}$$

where K = is the reaction rate constant.

K_o = is the collision frequency factor (or pre-exponential factor).

E = is the activation energy (or barrier to the reaction).

R = is the gas constant.

and T = is the absolute temperature.

The probability that a molecule will posses energy in excess of an amount E per mole, at the temperature T, is related to the familiar Boltzmann factor $e^{-E/RT}$. If the energy is restricted to translational energy in two components for a single molecule, or in one component for each of two molecules, making a total of two "square terms",

then the fraction of molecules having energy in excess of E is actually equal to $e^{-E/RT}$. It is evident that the larger the value of E the smaller will be the factor $e^{-E/RT}$, and since for many reactions the frequency factor does not vary greatly, it is the energy of activation which often determines whether a reaction is fast or slow at a given temperature.

The relationship between the reaction velocity constant, K, and thermodynamic quantities of free energy, enthalpy and entropy can be written in terms of the activation complex theory[75] as:-

$$K = \frac{RT}{NH} e^{+\Delta s^*/R} \; e^{-\Delta H^*/RT} \qquad \ldots\ldots\ldots\ldots\ldots 4.5$$

where N = is Avogadro's number.

H = is Plank's constant.

Δs^* = is the entropy of the activation process.

and ΔH^* = is the enthalpy of the process.

The value of the enthalpy ΔH^* (the heat effect of crystallisation) is the same order of magnitude for both the nucleation and growth processes. But the entropy Δs^*, (or the orientation function as it is sometimes called) involved in creating the initial nucleus must be considered greater than the entropy change consequence or the extension of an already ordered state.

4.3.1 The Concept of Metastability

Wilhelm Ostwald[76], through a possible influence of Gibbs theoretical thermodynamic work on stability and

metastability zones, first introduced the term 'labile' (unstable) and 'metastable' supersaturation. He proposed that a supersaturated solution will not form a new phase spontaneously unless the supersaturation exceeded certain limits. The term 'metastable' describes a solution which is supercooled insufficiently to cause spontaneous nucleation. The occurence of crystallisation on further cooling was considered due to the solution entering the 'labile' state. Gibbs[77] showed that there was a gradual change from the stable to the 'labile' state. Ostwald further pointed out that many unknown factors would alter the metastable limit as he recognised that crystals could be formed long before reaching the metastable state.

A schematic representation of these conditions is shown in figure 4.1.

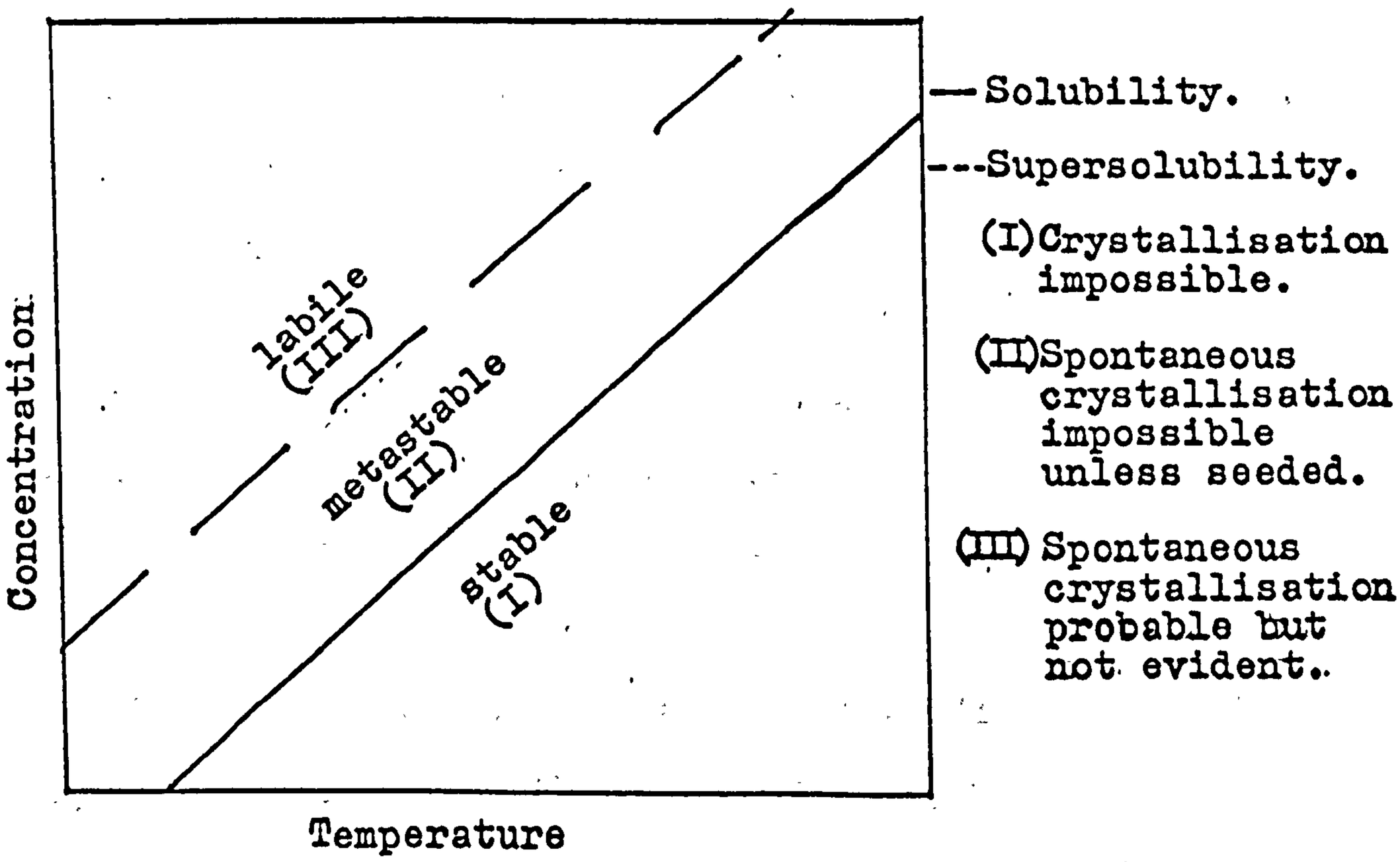

Figure 4.1: Solubility-Temperature Diagram.

Later Miers[78] and his co-worker[79] confirmed Ostwald's concept by following the change in refractive index of solutions as they were cooled. They plotted a number of solubility-temperature diagrams as shown diagrammatically above. A temperature well below the saturation temperature was finally reached when a marked decrease in refractive index occurred accompanied by a large shower of crystals. They realised that the rate of cooling, rate of agitation and previous history of the solution had an effect on the supersolubility curve.

The concept of metastability has been subjected to extensive criticism. Some investigators are in favour and others are against. de Coppet[80], for example,, opposed Ostwald's supersolubility relationship as he observed a time-lag between the onset of supersaturation and spontaneous nucleation. His main objection was the fixing of the supersolubility curve, though he agreed that the crystallisation tendency decreases as the solubility curve is approached, in fact, Ostwald himself appreciated the limitation of his concept by recognising that crystals could be formed long before the metastable limit for the prevailing temperature and pressure had been reached. He attributed this to be due to the unknown and controlled factor.

Nyvlt[81], in his review on crystallisation in chemical engineering suggested that in order to produce good quality coarse crystals in a discontinuous cooling crystalliser cooling must be controlled so that the supersaturation

should not exceed the limits of the metastable zone during the whole operation, thus avoiding the formation of an excess of crystal nuclei. Palmer and Batchelor[82] showed that a mixture of normal paraffins in an oil can be cooled down beyond the solubility curve without crystallisation of solid oil which is known as wax. Granqvist and Buhrman[83] concluded, that for the production of ultrafine metal particles by evaporation, A 15 Cr, fcc Fe, and fcc CO all represent good examples of the phenomenological Ostwald rule which states that in the course of going from a non-equilibrium to a final equilibrium state, the system will pass stepwise through states of intermediate stability.

4.3.2 Particle Size and Solubility

The Gibbs-Thomson equation (4.6) has been used to relate the size of a crystal nucleus to the degree of supersaturation in a solution assuming that solute/solution behaviour is analagous to liquid/vapour behaviour.

$$\ln (Pr/P_\infty) = 2\,MY/RT\rho_c r \quad \ldots\ldots\ldots\ldots\ldots\ldots 4.6$$

where Pr and P_∞ = are the vapour pressure over a liquid droplet of radius r and over a flat surface respectively.

M = is the molecular weight.

Y = is the surface energy.

R = is the gas constant.

T = is the temperature (°K)

and ρ_c = is the density of the droplet.

Ostwald[84] and Freundlich[85] adopted equation (4.6)

to show that the solubility of a crystal increases as the size of a crystal decreases. If Cr and C∞ are the concentration of solutions in equilibrium with a small crystal of size r and size infinity respectively, then:-

$$\ln (Cr/C\infty) = 2M\gamma/RT\rho_c r \quad \ldots\ldots\ldots\ldots\ldots\ldots 4.7$$

but the supersaturation ratio $s = Cr/C\infty$

therefore $\ln(s) = 2M\gamma/RT\rho_c r$ 4.8

equation (4.8) Known as the Ostwald-Freundlich equation. A similar equation was developed by Jones[86]..

Direct verification of Ostwald-Freundlich equation is difficult due to the nature and magnitude of the quantities involved. Im addition, most systems show a wide range of particle size rather than a uniform one. However, the Ostwald-Freundlich equation does not take into account possible ionic dissociation of the solid in solution, and a correction for this factor was introduced by Dundon and Mack[87]. They found the solubility of $BaSO_4$ increased by 90% with decreasing size of $BaSO_4$ crystals. Hulett[88] found a similar increase (80%) by grinding the crystals to sizes of about 0.1 μm. Knapp[89] has modified the equation to allow for the effect of any charge on the particles, and of the dielectric constant of the medium on the solubility of the solid.

Kolthoff[90] has calculated (using equation 4.8) the solubility of minute $BaSO_4$ crystals 0.14 μm in diameter is about 930 times the normal solubility product. Small nuclei of $BaSO_4$ may therefore be expected to remain in solution until a considerable degree of supersaturation

is attained.

4.3.3 Homogeneous Nucleation

Homogeneous nucleation is a spontaneous generation of nuclei which occurs at some high supersaturation level in a solution that is void of all foreign particulate matter such as dust, seed crystals, etc. This is the type of nucleation the thermodynamic theory is based on. Homogeneous nucleatiom occurs when a cluster of molecules have reached the ΔG crit.

Homogeneous nucleation is extremely irreproducible and Fischer[91] goes so far as to suggest that it can never be achieved, because it is virtually impossible to achieve a solution with less than 10^3 foreign bodies per cubic centimetre[73] which might act as nucleation catalysts.

The first successful attempt to study homogeneous nucleation was made by Vonnegut[92], who dispersed a liquid system in to a large number of discrete droplets, exceeding the number of hetero nuclei present. Even if we consider spontaneous crystallisation to occur by homogeneous nucleation and growth, there is still the problem as to whether nucleation has ceased before growth commences or whether both take place concurrently. Collins and Leinweber[93] and Turnbull[94] both favour consecutive processes with nucleation occuring in an initial burst, followed by subsequent growth. Other workers believe that nucleation and crystal growth occur simultaneously and Johnson and O'Rourke[95] derived equations for the two

processes in the crystallisation of Barium sulphate.

Mullin and Ang[74] found the nucleation of Nickel Ammonium Sulphate appeared to be homogeneous for supersaturations S >1.8 and heterogeneous for S <1.3. Katz and Virkler[96] measured the critical supersaturations required for the homogeneous nucleation of 12 different substances, they were found to be in good agreement with the predictions of the classical theory of nucleation (Volmer, Becker, Döring).

4.3.3.1 Free Energy of Formation of Nucleus

Most probably the formation of a solid phase by precipitation from solution, usually takes place in three steps:-

(1) The interaction between ions or molecules leads to the formation of a cluster.

$X + X \rightleftharpoons X_2$

$X_2 + X \rightleftharpoons X_3$ (Cluster)

$X_{j-1} + X \rightleftharpoons X_j$ (Cluster of critical size (embryo))

$X_j + X \rightleftharpoons X_{j+1}$ nucleus

(2) Subsequently, material is deposited on the nuclei.

$X_j + X \rightleftharpoons$ crystal growth

(3) Large crystals may eventually be formed from fine crystallite by a process called ripening.

The formation of a solid particle within a homogeneous fluid requires a certaim quantity of energy to create the new surface. The total quantity of work, W, required to

form a stable nucleus is equal to the sum of the work required to form the surface, Ws, and the work required to form the bulk of the particle, Wv .

$$W = Ws - Wv \quad \ldots\ldots\ldots\ldots\ldots\ldots\ldots\ldots \quad 4.9$$

The following derivation for the work required, W, or free energy of formation, ΔG, to form a spherical particle was first deduced by Gibbs[77]. The work required to create the new phase is thus $4\pi r^2\gamma$, whilst that to create the volume of the particle is $4\pi r^3\Delta P/3$, where r is the radius of the droplet particle, γ is the surface energy of the particle per unit area and ΔP is the pressure difference between the vapour phase and the interior of the liquid droplet. Furthermore, ΔP , is given by the expression $2\gamma/r$.

Thus equation (4.9) becomes:-

$$W = 4\pi r^2\gamma - (4\pi r^3/3) \times 2\gamma r$$

$$\Delta G = W = 4\pi r^2\gamma/3 \quad \ldots\ldots\ldots\ldots\ldots\ldots\ldots \quad 4.10$$

The energy required to form a particle is thus one third that required to form the surface.

The Gibbs-Thomson equation (4.6) gives the relationship between the vapour pressure of a liquid droplet and its size. Similarly the Ostwald-Freundlich equation of (4.8) can be used in the case of a solid particle,

$$\ln s = 2M\gamma/RT\rho_c r \quad \ldots\ldots\ldots\ldots\ldots\ldots\ldots \quad 4.8$$

and

$$r = 2M\gamma/RT\rho_c \ln s \quad \ldots\ldots\ldots\ldots\ldots\ldots\ldots \quad 4.11$$

combining equations (4.10) and (4.11)

$$W = \Delta G = 16\pi\gamma^3M^2/3R^2T^2\rho_c^2 (\ln s)^2 \quad \ldots\ldots\ldots \quad 4.12$$

In the case of a cube, the factor $16\pi/3$ in equation (4.12)

is replaced by the factor 32.

This equation shows that the energy barrier that any nucleation process has to overcome depends on the supersaturation, S, the surface energy, γ , and the temperature, T. However, equation (4.12) also suggests that any supersaturated solutions can nucleate spontaneously because there is some finite work requirement associated with the process it is merely a question of supplying the required amount of energy to the system.

Equation (4.12) has been subjected to many criticisms. For example,, the effect of particle size on surface energy is neglected. Pound and La Mer[97], using the nucleation data of Volmer and Flood[98] predicted an increase in surface energy with particle size.. Kirkwood and Buff[99] have predicted statistically a decrease in surface energy with particle size whilst Tolman[100] and Rastogi and Bassi[101] arrived at the same conclusion thermodynamically.

4.3.3.2 Kinetics of Homogeneous Nucleation

As we have seen already (equation 4.12), in order to become a nucleus a cluster must acquire (by growing to a critical size) a critical free energy ΔG in excess of that of single molecules. This critical free energy acts on a thermodynamic barrier to the process of nucleation.

The classical theories of homogeneous nucleation were developed on this basis. These have been reviewed by Dunning[102],, Farkas[103], Vam Hook[104], Mullin[73], Strickland-Constable[105], and Stevenson[106].

The relationship between ΔG, the free energy required to form a nucleus, and the frequency of formation critical nuclei by spontaneous fluctuation[107] was put forward by Volmer and Weber[108], this frequency is proportioned to $\exp^{(-\Delta G/KT)}$. The free energy of formation of a nucleus plays a role similar to that of activation energy in conventional chemical kinetics but, while the latter activation energy is essentially constant in magnitude, in contrast, the frequency of formation of critical nuclei changes markedly with the supersaturation (see equation 4.12)

Christiansen[109-111], using a very rapid flow technique for mixing various aqueous systems, considered the stepwise mechanism for nucleus formation (see 4.3.3.1). He derived the following expression for the nucleation rate.

$$\frac{dN}{dt} = K C_o^n \quad \ldots\ldots\ldots\ldots\ldots\ldots\ldots\ldots\ldots\ldots\ldots\ldots\ldots\ldots\ldots\ldots 4.13$$

where N = number of nuclei.

C_o = initial concentration.

and K and n = are constants, the latter being the number of ions required to form the critical nucleus.

The assumptions made in the derivation of this equation were:-

(1) all reactions leading to X_j can be treated as steady state processes. Christiansen found an indication in available experimental data that the steady state for nucleation is reached

instantaneously[112].

(2) the supersaturation is large enough so that the dissociation of the nucleus does not take place, and that monomer addition to the nucleus is a relatively rapid reaction.

Szilard[113] and Farkas[103] arrived at a kinetic mechanism of homogeneous nucleation which has formed the basis for subsequent development in the theory by Becker and Döring[114], Zeldovich[115], Frenkel[116], and Bradley[117].

The Becker and Doring treatment has since been known as 'the classical nucleation theory'.

In the formation of a nucleus, work must be done to create a new surface but energy is also released as the bulk of the nucleus is formed. If this process is to occur spontaneously the net energy change must be negative, i.e. there is a minimum size, 'critical size' (rc) for a stable nucleus corresponding to a maximum in the free energy of formation. Once formed, these stable nuclei are capable of growing until the final equilibrium of the system is attained. The critical size of nucleus is given by:-

$$rc = 2\gamma V/KT\ (\ln s) \quad \ldots\ldots\ldots\ldots\ldots\ldots\ldots\ldots\ 4.14$$

where γ = is the surface energy of the droplet (or particle)..

V = molal volume = $\frac{M}{\rho}$.

and K = is Boltzmann's constant = $\frac{R}{N}$.

The rate of nucleation, J, the number of nuclei formed per unit time per unit volume, can be expressed in the form

of Arrhenius equation:-

$$J = A \exp(-\Delta G/KT) \quad \ldots\ldots\ldots\ldots\ldots\ldots\ldots \quad 4.15$$

where ΔG = is the overall free energy of the particle (corresponding to the work of nucleation, W, in equation (4.12)).

and A = is a constant (pre-exponential factor).

On substituting ΔG from equation (4.12) the final form of the equation is:-

$$J = A \exp\left(-\frac{16\pi \gamma^3 M^2 N}{3R^3T^3\rho_c^2 (\ln s)^2}\right) \quad \ldots\ldots\ldots\ldots \quad 4.16$$

If J is plotted on a function of supersaturation, a curve like that in figure 4.2 is produced. It can be seen that there is in essence a critical supersaturation, S*, below which nucleation is very slow and above which nucleation is extremely fast.

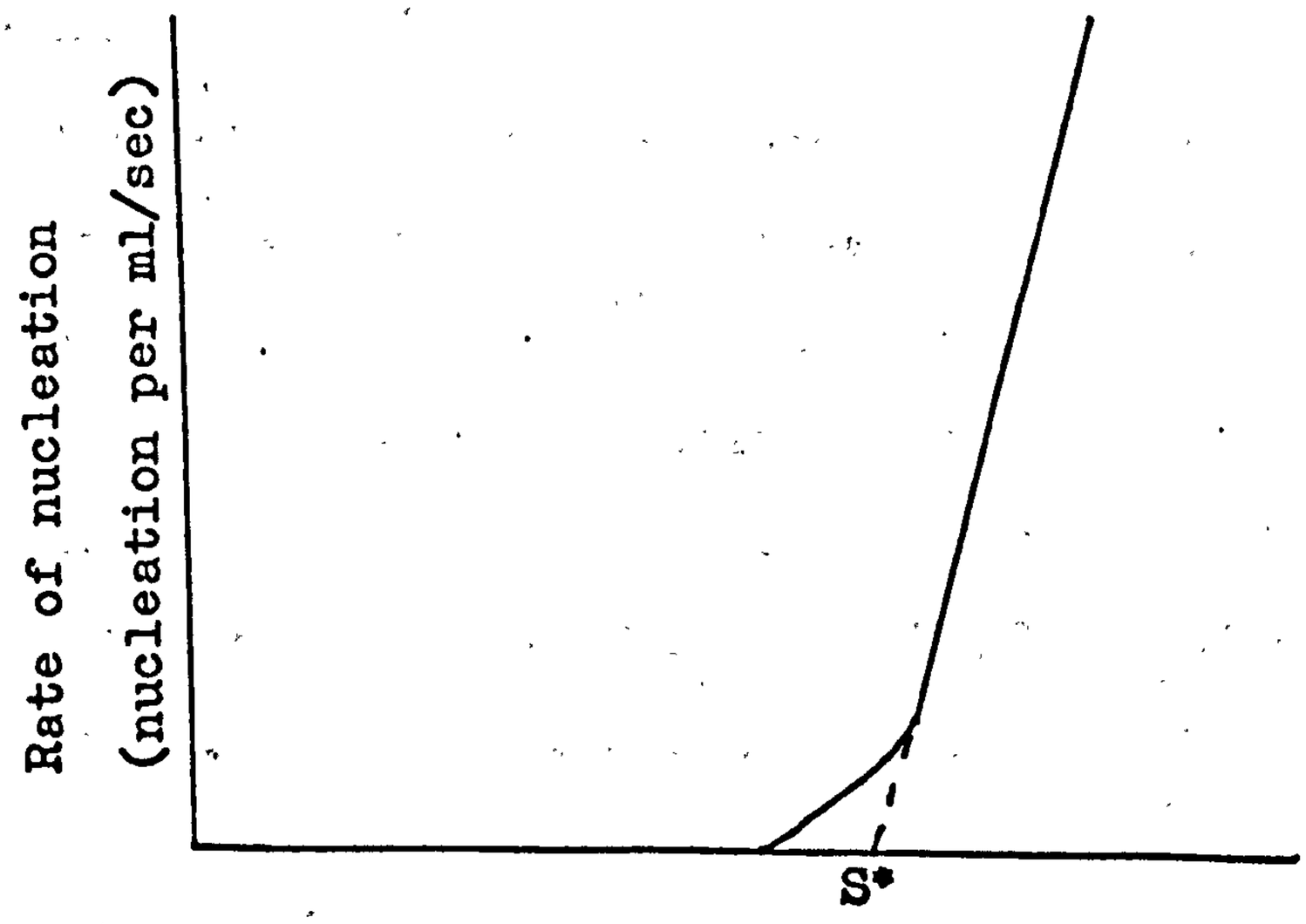

Figure 4.2: The relation between the homogeneous nucleation rate, J, (nuclei per ml/sec) and the degree of supersaturation.
(S = actual concentration/solubility).

Turnbull and Fischer[118] adapted the classical treatment of Becker and Döring for nucleation in condensed systems (i.e. melts and solutions). The following rate equation is obtained:-

$$J = \frac{n_1 KT}{h} \exp\left(-(\Delta Gd + \Delta G)/KT\right) \quad \ldots\ldots\ldots 4.17$$

where n_1 = is the number of molecules per unit volume of condensed system.

h = is plank constant.

ΔGd = is the free energy of activation for the short range diffusion of molecules moving a fraction of an atomic distance across an interface to join the lattice.

Similar expressions have also been obtained by Becker[119] and Bransom etal[120].

The value of the pre-exponential factor for melts has been shown by Turnbull and Vonnegut[121] to be 10^{30} $cm^{-3}sec^{-1}$. Newkirk and Turnbull[122] suggested that this value which holds for melts can similarly be applied to ionic salts nucleating from solution. However, Melia and Moffitt[123] in nucleation studies of aqueous NH_4Cl, NH_4Br, and KNO_3 solutions found that the pre-exponential factor, A, was very small, in the range of 10 to 10^4 cm^{-3} sec^{-1} compared with 10^{30} cm^{-3} sec^{-1} for melts.

Whilst good agreement between theoretical and experimental values of the pre-exponential factor, A, exists for nucleation of liquids from the vapour and

nucleation of solids from the melts, no such agreement can be found in the case of nucleation from solutions.

Discrepancies between the theoretical and experimental value of A have been found by Dunning etal[124,125] for the nucleation of cyclonite from aqueous nitric acid and aqueous acetone solutions, and for the nucleation of sucrose from aqueous solutions. Dunning et al attributed the low values of the pre-exponential factor to the large decrease in entropy which accompanies the activation of the molecules for interfacial transfer. Melia and Moffitt[123] suggested that heterogeneous nucleation rather than homogeneous nucleation was occuring in the cases they studied.

In studies of crystalloluminescence in aqueous NaCl solutions, Garten and Head[126,127] found a value of 10^{25}-10^{30} cm^{-3} sec^{-1} for the pre-exponential factor, which is in close agreement with theory. They suggested that the nucleation processes studied[123,124] previously were due to heterogeneous nucleation as the supersaturation used were too low for homogeneous. They suggested if sufficiently high supersaturation were used (e.g. a supersaturation of 14 for aqueous NaCl solution), homogeneous nucleation could occur. This view was supported by experimental evidence from Nielsen[128] in his studies of nucleation of $BaSO_4$ (up to s = 4000). He found a sudden burst of new particles is produced at supersaturation (s >630), this point represents the true critical supersaturation for the onset of homogeneous

nucleation. Nielsen[128] found the pre-exponential factor, A, ranging from 10^{18}-10^{22} cm^{-3} sec^{-1}, which is in close agreement with theory.

4.4 Heterogeneous Nucleation

In practice homogeneous nucleation is tedious, if not difficult, to study as trace amounts of soluble materials are always present. Kuznetsov[129] distinguishes four types of particles which can act as crystallisation centres:-

(1) Particles of the crystallising substance (seeds).

(2) Particles of substances isomorphous with the crystallising substance and forming solid solutions with it.

(3) Particles forming regular intergrowths with the crystallising substance.

(4) Particles of substances which adsorb molecules of the crystallising substance.

Even if all the insoluble materials could be eliminated, the walls of the containing vessel would still present a second phase to which the supersaturation phase would be exposed.

Collins and Leinweber[93] observed that the supersaturation ratio at which Barium Sulphate precipitated spontaneously was strongly dependent upon the purity of the reagents. A maximum supersaturation of 32 was obtained upon purification of the reagents by filtrations. When no attempt was made to remove the impurities the value was 19. They conclude that the nucleation process in their

experiments is probably heterogeneous.

O'Rourke and Johnson[112] observed that the number of particles of barium sulphate precipitated after mixing of the Ba^{++} and $SO_4^{''}$ solutions, they found that freshly prepared Ba^{++} solutions give finer precipitate of $BaSO_4$ than aged solutions. On ageing these sparingly soluble impurity particles may dissolve.

The formation of nuclei in the presence of various solid particles and solid surfaces is easier since the change in the free energy necessary for the formation of a new phase in heterogeneous (ΔG^-) systems is smaller than in the formation of nuclei in homogeneous solution (ΔG),

$$\Delta G^- = \emptyset \, \Delta G \quad \ldots\ldots\ldots\ldots\ldots\ldots\ldots\ldots \quad 4.18$$

where $\emptyset$ = is a factor less than unity.

According to Volmer[130] the factor $\emptyset$ in equation (4.18) is given by the following expression:-

$$\emptyset = \frac{(2 + \cos\alpha)(1 + \cos\alpha)^2}{4} \quad \ldots\ldots\ldots\ldots\ldots \quad 4.19$$

where α = is the angle of contact between the new phase and the impurity particle.

For low contact angle (small α), the factor $\emptyset$ is small and thus a lower ΔG^- will result favouring heterogeneous nucleation.

It is difficult to prove whether all nucleation in precipitate reactions is heterogeneous. Definitive studies of the heterogeneous nucleation of solids from liquids requires conditions which are not easily achieved experimentally.

4.5 Secondary Nucleation

The phenomenon of nucleation in the vicinity of crystals in a supersaturated system will be referred to as "secondary" nucleation to distinguish the phenomenon from heterogeneous nucleation (4.4) which is induced by foreign particles.

The mechanism of secondary nucleation is still a subject of much speculation, but nevertheless, it is of great importance industrially and much more work has to be done to resolve the various mechanisms by which it occurs. A system of suspended heterodisperse particles can undergo two different types of secondary nucleation, both of which are spontaneous in that they lower the total energy of the system by lowering the interfacial free energy. This is achieved by decreasing the total precipitate surface area either by agglomeration and recrystallisation or by Ostwald ripening.

Strickland-Constable and co-workers[105,131,132] suggested that three types of secondary nuclei were present in the systems they studied, mainly $MgSO_4.7H_2O$, KBr, KCl, and Zn-Hg amalgams. Secondary nuclei derived from needles and poly crystals are normally referred to as 'needle breeding' and 'polycrystalline breeding' respectively. Polycrystalline masses are produced much more readily than single crystals and whenever the forces holding parts together are weak 'polycrystalline breeding' may be expected to occur. 'Needle breeding' is of limited occurrence because high supersaturations or a large number

of surface irregularities on the seed crystals are required to produce this type of growth.

The third form of secondary nucleation is called 'collision breeding'. Lal, Mason and Strickland-Constable[132] have shown that this is the most important form of 'breeding' secondary nuclei. The number of secondary nuclei produced was found to be dependent on supersaturation and it is difficult to believe that small differences in supersaturation can alter the extent of mechanical breakage of the seed crystal giving rise to fragments which develop into nuclei.

According to equation (4.8) a higher supersaturation results in lower critical size and hence a greater number of crystallites would survive to form nuclei.

Melia and Moffitt[133] studied the nucleation of KCl and showed that the rate of secondary nucleation increased with supersaturation and agitation. These results were in variance with those of other workers[131,132,134], in that they showed that the secondary nucleation rate was independent of the number of seeds.

4.6 Induction Period and Critical Supersaturation

The 'induction period' or incubation period[135] or latent period[136,137,138,94,139,140], τ, which is the period of time between the preparation of the supersaturated solution and the occurrence of visible turbidity or the first measureable decrease in concentration of the solute when nucleation occurs was observed as far back as 1872 by

de Coppet[141].

The duration of induction period depends on the degree of supersaturation of solution, the nature of the solute and the solvent, the vigour of stirring of the solution, and the presence of impurities. Studies of the induction period are interesting not only from the point of view of practical information on the crystallisation process but also because they can yield information about the crystallisation mechanism, the nature of the various stages of crystallisation process, and about some of the physical properties of crystalline substances.

The induction period has been observed in quiescent solution[125,142,143] and melts[144] as well as in seeded solutions[115,144,145]. It has been shown[146] that such delays (or time-lag) in nucleation may be anticipated on the basis of the time required for attainment of steady state conditions.

The induction period may be written as the sum of three time parameters:-

$$\tau = ti + tn + tg \quad \ldots\ldots\ldots\ldots\ldots\ldots\ldots \quad 4.20$$

where ti = is the 'relaxation time' is the time required to attain the steady state of embryo distribution.

tn = the time required for the formation of a stable nucleus.

and tg = the time required for the nucleus to grow to detectable dimensions.

Dunning and Shipman[125] suggested that the relaxation

time, ti, may be in the region of hours in their work on sucrose. On the other hand Nielsen[147] has shown ti to be small for steady state nucleation theory which is normally assumed that the time for nucleation, tn, far exceeds that for the nuclei to grow to detectable sizes, i.e. $tn \gg tg$. Therefore, the dominant time parameter controlling the magnitude of induction period is tn, the time required for formation of nuclei. Thus $\tau \sim tn$ and thus the rate of nucleation must be directly related to the induction period.

Although the theoretical calculation of induction period is very difficult, various workers have introduced different simplifying assumptions:-

Mullin[74], Van Hook[143] and Dunning[148] have assumed that the rate of nucleation, J, is inversely proportional to the induction period ($J \propto \tau^{-1}$)

Nielsen[149] applied equation (4.16) to calculate the interfacial energy, γ , for various systems studied ($BaSO_4$, $BaCrO_4$, $BaCO_3$, $PbSO_4$, and $PbCrO_4$). Van Hook and Bruno[143] plotted the supersaturation, S, versus the reciprocal of the induction period, τ . The shape of the curves obtained were as represented in the diagram (see figure 4.3). Their results suggest that sucrose solutions have a critical supersaturation at about 1.6, there is a very rapid onset of nucleation above this concentration.

Felbinger and Neels[150] applied equation (4.16) in their investigation of the rate of nucleation of sodium bicarbonate, formed by the carbonisation of ammoniacal solution of sodium chloride, at different temperatures.

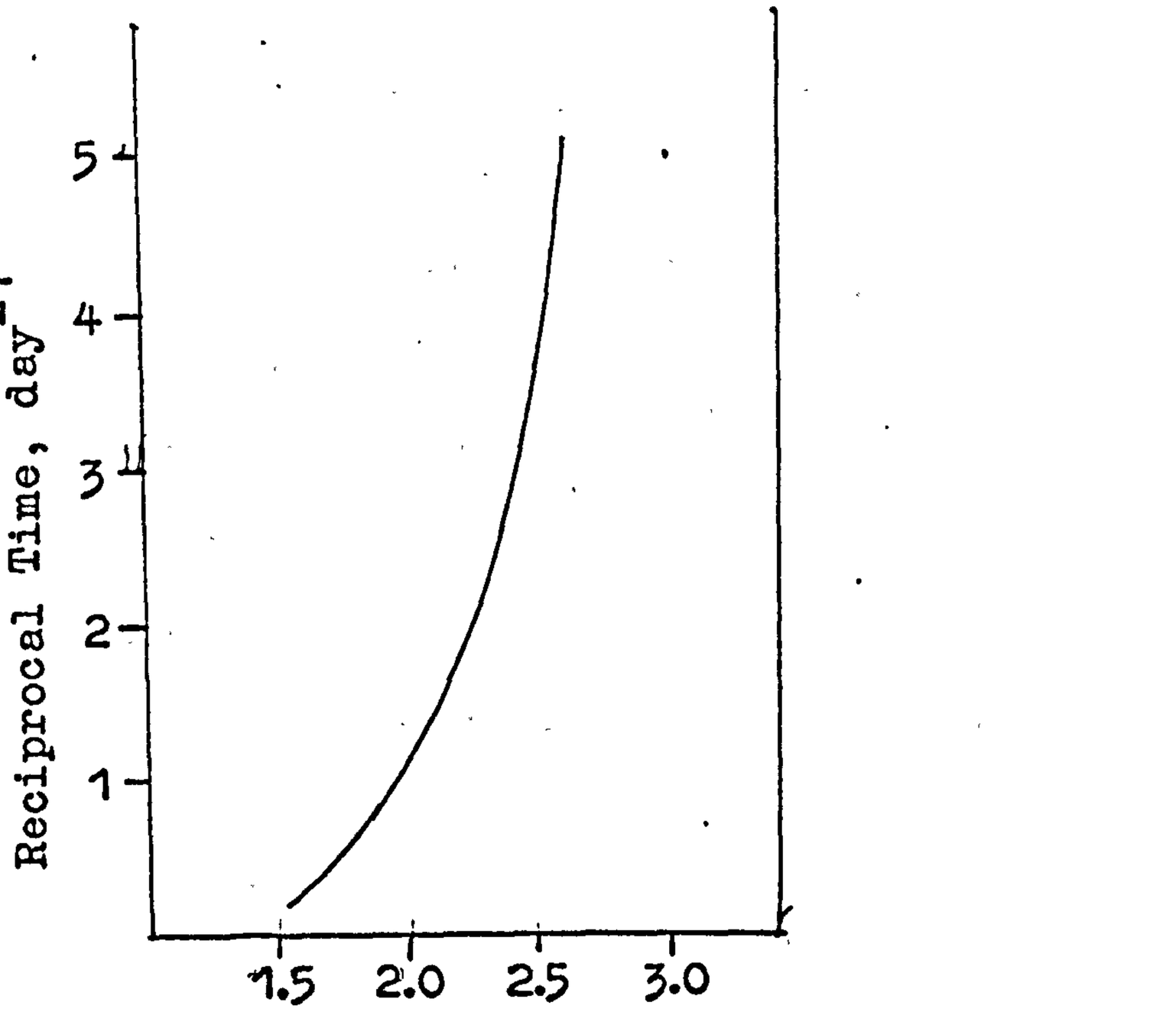

Figure 4.3

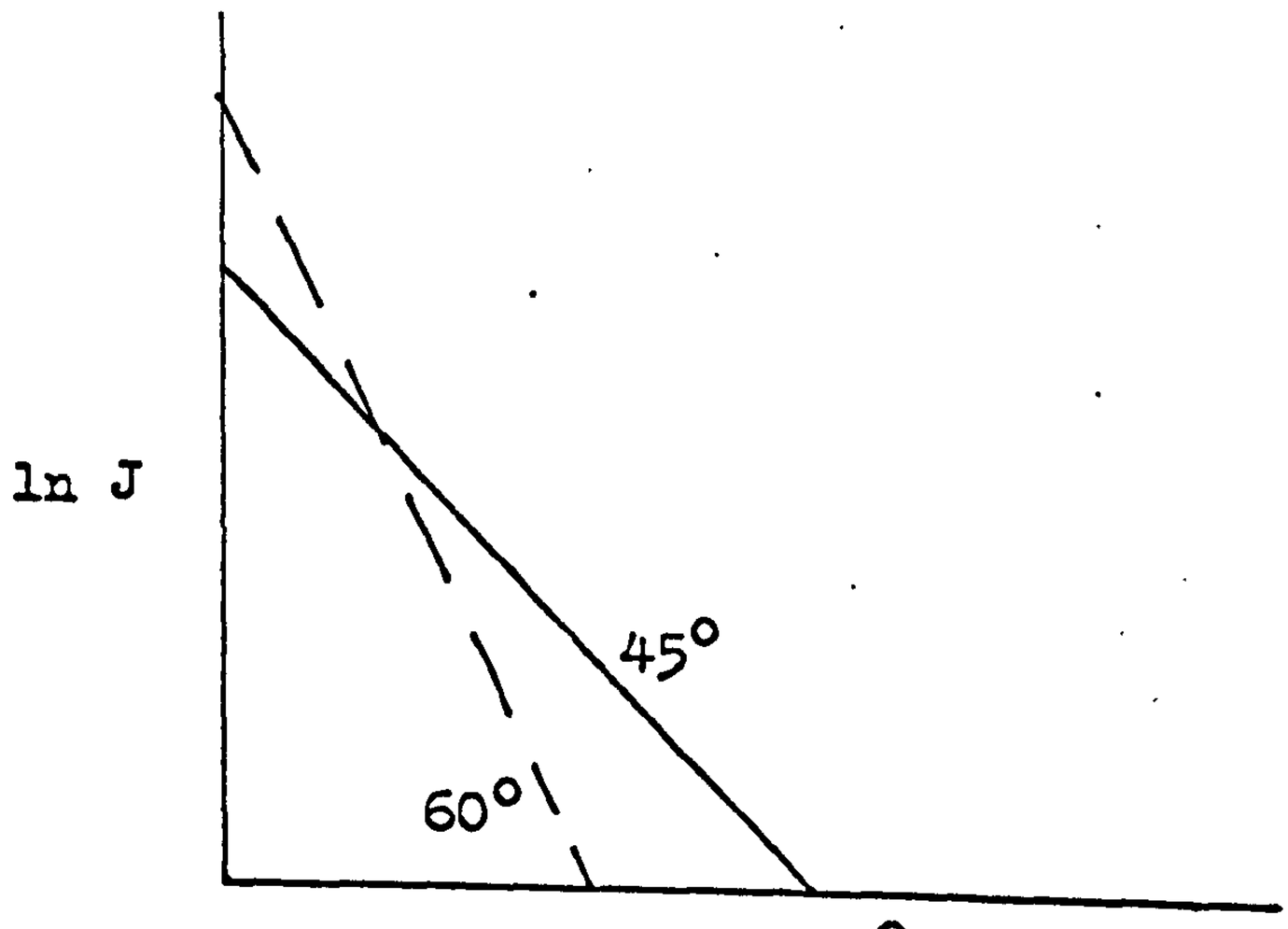

Figure 4.4

$45^{\circ}_{o} = 17 \pm 2$ erg/cm^2

$60^{\circ}_{o} = 11 \pm 2$ erg/cm^2

They plotted their results in the form of ln J versus $1/(\ln s)^2$ (see figure 4.4) and were able to calculate the following values for the interfacial energy from the slopes of the straight lines.

It is important to note that the methods for determining the interfacial energy are:-

(a) Calculation.

(b) Adsorption of gases on solid surface.

(c) Wetting.

Some published values of surface energy of solid substances are given in Table 4.1.

Table 4.1

Some published values of surface energy of solid substances

Substances	$\sigma \times 10^2 Jm^{-2}$	Medium	Technique	Ref.
NaCl	15	air	grinding	151
AgCl	17	water	solubility	152
AgBr	16	water	solubility	153
pbI	13	water	solubility	31
$BaSO_4$	11.6	water	solubility	87
$BaSO_4$	125	water	solubility	31
$CaSO_4$	3.9	air	grinding	151
$CaSO_4$	37	water	solubility	31
CaF_2	14.6	air	grinding	151
CaF_2	250	water	solubility	31
$CaCO_3$	7.8	air	grinding	151
$CaCO_3$	35	air	cleavage	154
$CaCO_3$	23	air	cleavage	154

4.7 Crystal Growth Mechanisms

The production of critical nuclei in the supersaturated solution is followed by subsequent growth of these nuclei into crystallites which will usually continue to grow if the solution is supersaturated.

Several approaches have been made to explain the mechanism and rate of crystal growth. Bircumshaw and Riddiford[155], considered that for the general case of a reaction between a solid and a solution, resulting in soluble products, the overall process may comprise five primary steps:-

(1) Transport of solute molecules to the interface.

(2a) Adsorption of solute at the surface.

(2b) Chemical reaction at the surface.

(2c) Desorption of products from the surface.

(3) Transport of solute from the interface to the bulk of the solution.

Steps 2a, 2b, and 2c represent the interaction between the solid and the solute and can be combined to give an overall interface step, step 2.

Crystallisation will therefore be interface controlled if step 1 is much faster than step 2, and diffusion controlled if step 2 is faster than step 1, and the situation is analogous for dissolution if steps 2 and 3 are compared.

Crystal growth, like nucleation, is also affected by the presence of impurity, Sears[156,157] considered that small molecules tend to be adsorbed at kinks on the growth

steps, monostep coverage being necessary to cause an appreciable reduction in the rate of step motion. Adsorption of impurity at a step should reduce the critical energy for two-dimensional nucleation and result in an increase in the rate of surface nucleation.

The influence of agitation on crystal growth is well known, and can be expressed by the equation[155]:-

$$K = a N^b \quad \ldots\ldots\ldots\ldots\ldots\ldots\ldots\ldots\ldots\ldots\ 4.21$$

where K = is the reaction rate.

N = is a measure of agitation (e.g. r.p.m. of a stirrer).

and a and b = are constants.

The value of b depends on the reaction mechanism, and varies between zero for purely surface mechanisms and a value of unity for diffusional processes; diffusional processes are aided by agitation, whilst surface mechanisms are unaffected.

4.7.1 Surface Energy Theories

Gibbs[77] suggested that the total free energy of a crystal in equilibrium with its surroundings at constant temperature and pressure would be a minimum for a given volume. If the volume free energy per unit volume is constant throughout the crystal, then:-

$$\sum_{i=1}^{n} a_i \gamma_i = \text{minimum} \quad \ldots\ldots\ldots\ldots\ldots\ldots\ 4.22$$

where a_i = is the area of the ith face for a crystal having n faces.

and γ_i = is the surface free energy/unit area of the

ith face.

Accordingly, the shape assumed by crystal growing in a supersaturated medium is that in which the various faces develop in such a manner that the whole crystal has a minimum total surface energy per unit volume.

Curie[158] and Wulff[159] adopted these principles and pointed out that the crystal faces would grow at rates proportional to their respective surface energies. Wulff had also indicated that the rate of growth of a face is inversely proportional to the reticular or lattice density of the respective lattice. Thus faces with low reticular densities would grow faster and eventually disappear.

Because of the lack of experimental evidence to support these surface energy theories, this theory (Gibbs-Curie-Wulff) has not been generally accepted in explaining the mechanism of crystal growth. Furthermore, the theory is unable to explain the dependence of the rate of growth of crystals on supersaturation, agitation and various other factors.

Crystal growth according to this theory is considered to proceed by incorporation of molecules at kinks in a growth step on the crystal surface. Any molecule of the solute on arriving at the crystal surface can be adsorbed on to various sites (see figure 4.5).

A molecule adsorbed on to the surface at A has only one adjacent molecule whilst that adsorbed on to the surface adjacent to another molecule at position B has two adjacent molecules causing it to be more stably adsorbed.

Similarly a molecule adsorbed on to a ledge at C will have two neighbouring molecules but the most stable attachment of an adsorbed molecule is at a kink (position D) where three neighbouring molecules are present or at a surface vacancy (E). Therefore, any molecule adsorbed on to a kink or a surface vacancy will get incorporated in to the lattice causing growth whereas those adsorbed on to the plane surface will have a high tendency to evaporate.

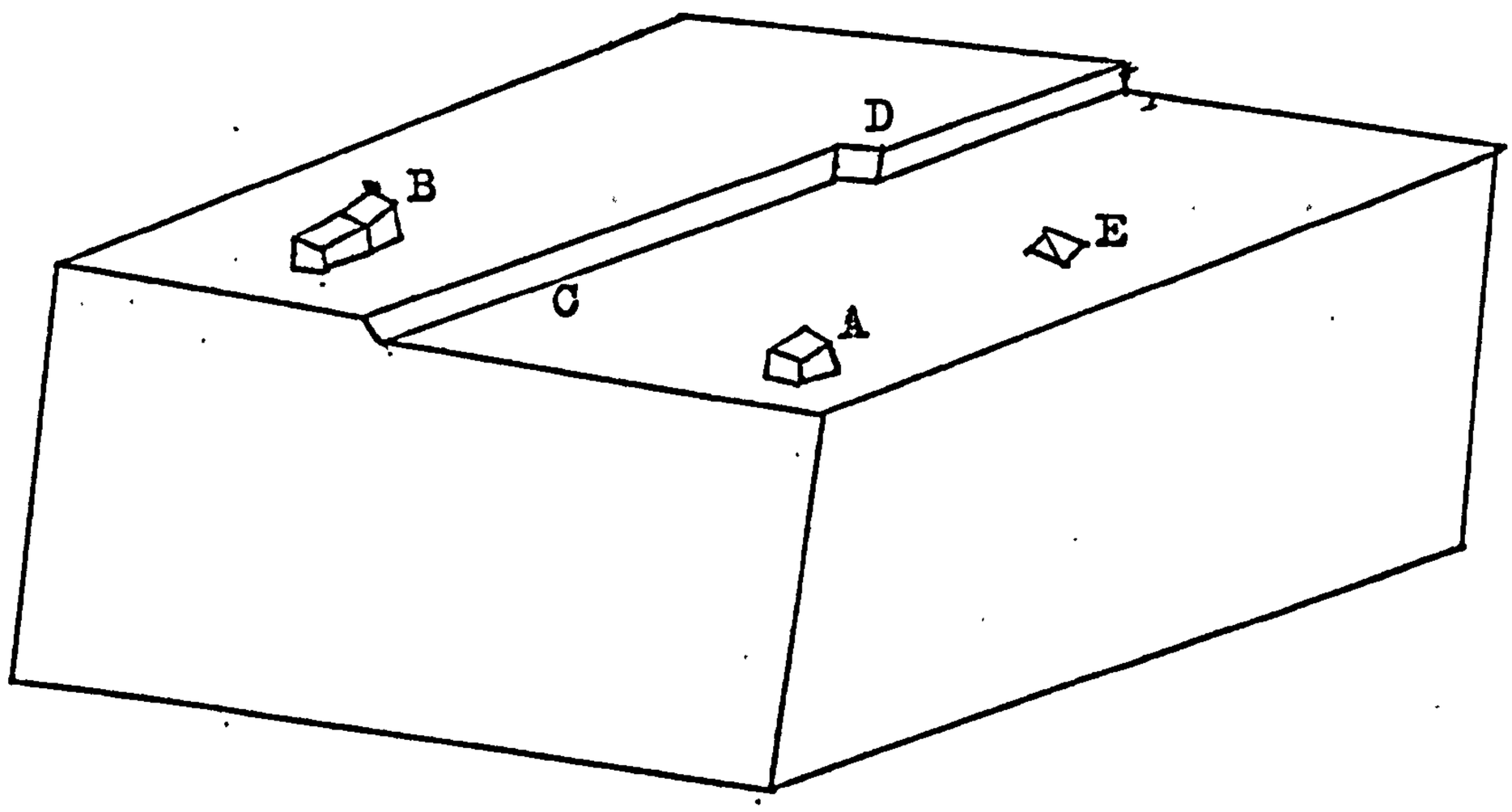

Figure 4.5: Surface Structure of a Crystal.

A = face adsorbed molecules.

B = adjacent pairs of adsorbed molecules.

C = ledge.

D = kink on a ledge.

E = surface vacancies.

Burton and Cabrera[160] postulated that the edge of

growth layers are not smooth but kinks exist along these edges. Marc[161] suggested that growth occurs at a measureable rate by the addition of molecules to the lattice from this adsorbed layer, and that the abstracted molecules are replaced from the surrounding solution.

4.7.2 Diffusion Theories

Noyes and Whitney[162] observed that the rate of dissolution of cylinders of benzoic acid and lead chloride in water could be represented very well by the first order equation:-

$$\frac{dC}{dt} = Kd\ (C^* - C) \quad \ldots\ldots\ldots\ldots\ldots\ldots\ 4.23$$

where C = is the instantaneous concentration at time, t.

C^* = is the solubility.

and Kd = is the reaction rate constant.

This result was later generalised by Nernst[163] in a theory of heterogeneous reactions is now known as 'Noyes-Whitney-Nernst' theory. It was assumed that crystallisation is the direct opposite of dissolution and thus the equation suggested for crystallisation was:-

$$\frac{dC}{dt} = Kd\ (C - C^*) \quad \ldots\ldots\ldots\ldots\ldots\ldots\ 4.24$$

where $\frac{dC}{dt}$ = is the mass growth rate.

Nernst[163] has modified equation (4.24) by introducing, on the right-hand side, the diffusion coefficient of the solute. When the crystal surface of area A is in contact with a solution of volume V at

concentration C, Fick's law gives for the rate of diffusion:-

$$\pm \frac{dC}{dt} = \frac{DA}{V} \frac{dc}{dy}$$

where $\frac{dC}{dy}$ = is the concentration gradient normal to the surface.

and D = is the diffusion coefficient of the solute.

If δ is the length of the diffusion path (thickness of the boundary layer) then the gradient across this interface is $\frac{C - C^*}{\delta}$ thus, the rate of transfer of material in this so-called 'strategic step' is the controlling kinetic factor, i.e. for growth.

$$\frac{dC}{dt} = \frac{DA}{V\delta} (C - C^*) \quad \ldots\ldots\ldots\ldots\ldots\ldots\ldots\ldots 4.25$$

the specific rate constant in the original Noyes-Whitney (4.23) expression is:-

$$Kd = \frac{DA}{V\delta}$$

Marc[161] has demonstrated the inadequacy of the Noyes-Whitney-Nernst theory in his extensive studies on seeded growth of various inorganic systems (K_2SO_4, $K_2Cr_2O_7$, KNO_3, and Alum, etc.), chiefly by means of conductivity changes. Growth was shown to differ from dissolution in the following ways:-

(1) It is relatively much slower and more easily measured.

(2) The velocity of growth is independent of the rate of stirring if this is sufficiently vigorous.

(3) The growth rate is not necessarily unimolecular

with repeat to concentration driving force (e.g. in K_2SO_4, it changes from unimolecular to bimolecular with temperature).

(4) When a supersaturated solution is inoculated with seed crystals, a very rapid addition of material to this base occurs initially after which the normal growth rate is established (i.e. there is a preliminary adsorption followed by incorporation in to the space lattice from this adsorbed layer).

(5) Many substances when adsorbed considerably reduce the rate of growth, yet do not influence the rate of solution.

The Noyes-Whitney-Nernst theory was further modified by Berthoud[164] and Valeton[165]. They have divided the crystallisation process into two stages. The first stage is governed by diffusion and involves the transport of the solute from the solution to the surface. The second stage consists of the deposition of the solute on the surface of a growing crystal and is described by the rate equations for first order reactions. The two stages can be represented by the equations:-

$$\frac{dC}{dt} = Kd\ (C - C_i) \quad \ldots\ldots\ldots\ldots\ldots\ldots\ldots\ldots \quad 4.26$$

$$\frac{dC}{dt} = Kr\ (C_i - C^*) \quad \ldots\ldots\ldots\ldots\ldots\ldots\ldots\ldots \quad 4.27$$

where Kd and Kr = are the mass transfer coefficients by diffusion and surface reaction respectively.

and Ci = is the concentration of the solute near a growing surface.

These two equations are difficult to test as the value of C_i is too difficult to measure. Thus Berthoud[164] eliminated this term by combining the two equations to give:-

$$\frac{dC}{dt} = K_G (C - C^*) \quad \ldots\ldots\ldots\ldots\ldots\ldots\ldots\ldots 4.28$$

where $$K_G = KdKr/(Kd + Kr) \quad \ldots\ldots\ldots\ldots\ldots\ldots\ldots\ldots 4.29$$

Similar equations have been obtained by Valeton[165] and Friedal[166].

The diffusion theory can further be modified by assuming a n-th order surface reaction step, thus:-

$$\frac{dC}{dt} = \acute{K}r (C_i - C^*)^n \quad \ldots\ldots\ldots\ldots\ldots\ldots\ldots\ldots 4.30$$

Combining equations (4.26) and (4.30), C_i could be eliminated to give the following equation:-

$$\frac{dC}{dt} = \acute{K}r \left[(C - C^*) - \frac{dc}{dt}/Kd\right]^n \quad \ldots\ldots\ldots\ldots\ldots\ldots 4.31$$

This equation is not easily solved as $\acute{K}r$ and Kd cannot be measured separately and m is not known. However, assuming that the diffusion steps for both growth and dissolution are the same, then Kd can be obtained by performing dissolution experiments:-

$$\left(\frac{dC}{dt}\right)_D = Kd (C - C^*) \quad \ldots\ldots\ldots\ldots\ldots\ldots\ldots\ldots 4.32$$

Thus $Kd = \left(\frac{dC}{dt}\right)_D / (C - C^*)$ 4.33

Combining equations (4.31) and (4.33), the growth rate equation becomes:-

$$\frac{dC}{dt} = \acute{K}r\ (C - C^*)\ \left(1 - \frac{dc/dt}{(dc/dt)_D}\right)^n \quad \text{..... 4.34}$$

The diffusion theories are limited in application as most recent work[167] has shown that surface reaction step is generally the rate controlling step for crystal growth.

4.8 Measurement of Crystallisation Kinetics

In the earlier sections two major stages, nucleation and growth, have been considered for the formation of precipitates. Precipitation studies are complex because no fixed point is reached when one stage replaces another; the different stages overlap to a large degree. Furthermore, within each stage several mechanisms can occur, depending for instance on the crystallisation condition. For example, nucleation could be either homogeneous or heterogeneous.

In the crystallisation process, the desupersaturation rate (change of concentration with time, see figure 4.6) can furnish a considerable amount of information.

- part (ab) refers to the induction period when the concentration of the solution remains virtually constant.
- part (bc) refers to the stage when most of the

precipitate is formed at the expense of the solution concentration.

- finally, (cd) refers to slow crystal growth, together with recrystallisation when larger crystals grow at the expense of the smaller ones (Ostwald ripening) (equation 4.7). The induction period (part ab) is easily observed at low supersaturations but it contracts and virtually disappears at very high supersaturation.

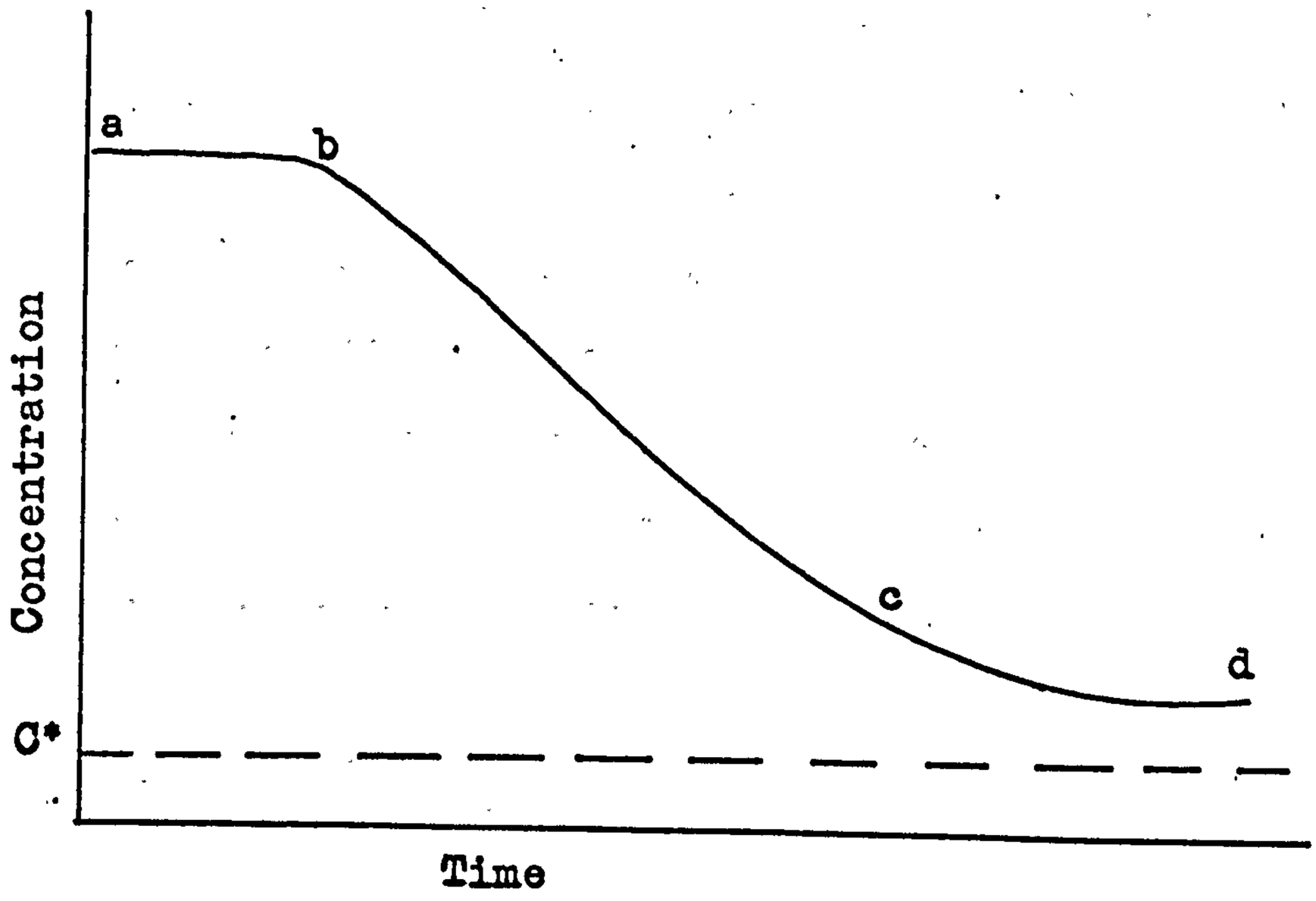

Figure 4.6

In general, the rate of growth of crystals in solution is a function of two variables; the crystal surface area and the concentration of solute. The rate of mass deposition, therefore, can be represented by:-

$$\frac{dm}{dt} \propto A\,(C - C^*)^n \quad \ldots\ldots\ldots\ldots\ldots\ldots\ldots\ldots\ldots\ldots 4.35$$

where A = is the surface area of the crystal.

m = is the mass of solid deposited in time t.

C = is the solute concentration in the bulk of the solution.

C* = is the equilibrium saturated concentration.

and n = order of the crystallisation process.

The driving force for mass transfer, ΔC, is the overall supersaturation $(C - C^*)$.

Bircumshaw and Riddiford[155], Berthoud[164] and Valeton[165] suggested that the deposition of solute on a crystal surface involves two consecutive steps, viz., a diffusion process, whereby solute molecules are transported from the bulk of the fluid phase to the solid surface followed by a 'first order' surface reaction process when the solute molecules arrange themselves in to the crystal surface. These two steps can be represented by:-

$$\frac{dm}{dt} = Kd\ A\ (C - C_i) \quad \text{(diffusion)} \quad \ldots\ldots\ldots 4.36$$

and

$$\frac{dm}{dt} = Kr\ A\ (C_i - C^*) \quad \text{(surface reaction)} \quad \ldots 4.37$$

where Kd = is a coefficient of mass transfer by diffusion.

Kr = is a rate constant for the surface reaction.

and C_i = is the solute concentration in the solution at the crystallisation interface $(C > C_i > C^*)$.

In practice, equations (4.36) and (4.37) are not so simple to apply (see 4.7.2), therefore, the general equation for crystallisation (or mass deposition rate) based on this overall driving force is:-

$$\frac{dm}{dt} = K_G A (C - C^*) \quad \ldots\ldots\ldots\ldots\ldots\ldots\ldots\ldots \quad 4.38$$

where K_G = is an overall mass transfer coefficient, i.e.,

$$\frac{1}{K_G} = \frac{1}{Kd} + \frac{1}{Kr} \quad \ldots\ldots\ldots\ldots\ldots\ldots\ldots\ldots \quad 4.39$$

It is important to note that assumption of first-order surface reaction (equation 4.37) is questionable. There is plenty of evidence that many inorganic salts, crystallising from aqueous solution, do not correspond to first-order reaction. Orders of growth in the range of n = 1.5 to 2 have been reported. The generalised form of equation (4.38) may, thus, be used to correlate crystal growth measurements:-

$$\frac{dm}{dt} = K_G A (C - C^*)^n \quad \ldots\ldots\ldots\ldots\ldots\ldots\ldots\ldots \quad 4.40$$

If Rg is the growth rate (mass deposited per unit time per unit surface area), then:-

$$Rg = K_G \ \Delta C \quad \ldots\ldots\ldots\ldots\ldots\ldots\ldots\ldots\ldots\ldots \quad 4.41$$

where $\Delta C = C - C^*$

The overall mass transfer coefficient, K_G, depends on many parameters. For example, when a crystal is growing in a supersaturated solution under constant concentration

driving force, ΔC, the rate of mass transfer for a diffusion controlled system, Kd, may depend on the following variables:-

(1) The relative velocity between the solid surface and the solution, U.

(2) The viscosity of the solution, η .

(3) The diffusivity of the solute molecules in the liquid, D.

(4) The density of the solution, ρ .

(5) A chosen length or diameter of the crystal, d.

Therefore, few values of K_G are reported in the literature.

4.8.1 Measurement of the Time Dependence of the Concentration of Solution

In a precipitation process the concentration of the solution decreases as the process proceeds. This continuous change can normally be followed in several ways:-

Williams and Ruehrwein[4] in studying the effect of polyelectrolytes on the precipitation of calcium carbonate, used a light scattering photometer to follow the change in the turbidity of the solution as precipitation occured.

Reddy and Nancollas[167] measured the growth rate of calcium carbonate with calcite seed crystals by continuously measuring the change in calcium and hydrogen concentration by using 45Ca radioactive tracer with liquid scintillation and atomic absorption spectroscopy. Marshall and Nancollas[168] studied the crystal growth of dicalcium

phosphate dihydrate in a similar manner.

Bujac and Mullin[169] measured the growth rate of ammonium alum in a fluidised bed crystalliser, while the change in solution concentration is measured continuously with a recording density meter.

Davies and Jones[170] studied the precipitation of silver chloride, the precipitation being followed by continuous measuring the electrical conductivity of the solution. Campbell and Nancollas[171] used the same method in measuring the growth rate of strontium sulphate.

Other less common methods in thermometric methods[172] which are suitable only with materials having a high heat of crystallisation.

4.8.2 The Size Distribution of Precipitate

In industrial production it is not possible, as a rule, to ensure strict uniformity of condition throughout a crystalliser. As a result, and also because of the formation of new nuclei in the course of crystallisation process, one obtains in general a product consisting of a mixture of crystals of varying sizes. To characterise this product, one employs the size distribution. Various methods of obtaining the size distribution of crystals are available ranging from sieving, microscopy, coulter counter to adsorption; all of which are discussed in detail by Allen[173].

The results of a size analysis can be represented graphically in several ways. For crystalliser materials a

method proposed by Power[174] for the sugar industry and modified by Mullin[175] is the arithmetic-probability graph paper (one scale divided into equal intervals, the other marked off according to the probability integral).

The cumulative oversize or undersize (expressed as percentage), are plotted on the probability scale (e.g. 0.1 to 99.9). The only condition required for this method is that the data between 10% and 90% must lie on a straight line. If the crystalline product satisfies this straight line relation, routine analysis of the crystalline material is greatly simplified. The size distribution is represented in terms of two numbers only - the median size (50% of the material is larger than or smaller than the mean aperture size), MS, and a statistical quantity, the coefficient of variation, CV, expressed as a percentage given by:-

$$CV = \frac{100\ (a_{84\%} - a_{16\%})}{2MS} \qquad \ldots\ldots\ldots\ldots\ldots\ldots\ 4.42$$

where a = is the sieve aperture (corresponding to 84% and 16% of the cumulative weight on the probability plot). This quantity indicates the extent of the size spread of the product with respect to the median size. The higher the values of CV the greater the spread.

For example, a size distribution expressed as MS/CV = 300/35 means that 50% by weight of the material pass through 300 μm aperture, and the standard deviation X100 divided by the mean aperture = 35%.

4.8.3 Crystal Population Balance

The population balance approach for studying the kinetics of crystallisation have been published for many systems[176-178]. The use of a continuous, mixed suspension, mixed product removal (CMSMPR) crystalliser was considered because it is very similar to the real process and it lends itself to analysis by the population balance theory. A schematic representation of a CMSMPR crystalliser is shown in figure 4.7.

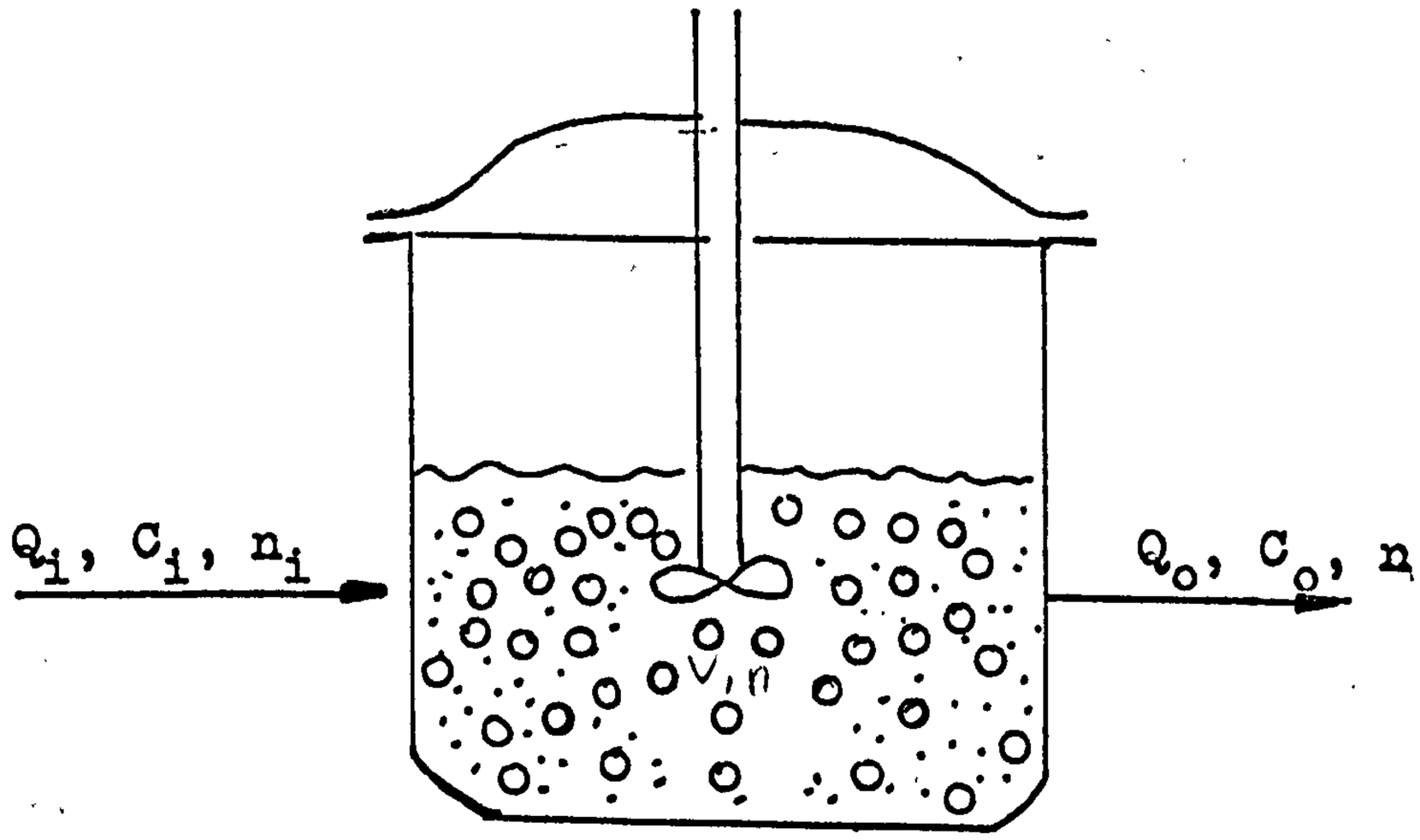

Figure 4.7: A Schematic Representation of CMSMPR Crystalliser.

The following conditions are assumed in CMSMPR crystalliser[179]:-

(1) Well mixing to minimise the tendency toward agglomeration.

(2) No attribution of the crystals.

(3) No crystals in feed.

(4) Steady state.

The population density, n, is defined by:-

$$\lim_{\Delta L \to 0} \frac{\Delta N}{\Delta L} = \frac{dN}{dL} = n \qquad \ldots\ldots\ldots\ldots\ldots\ldots\ldots\ldots 4.43$$

Where N is the number of crystals in the size range ΔL (L_1 to L_2) per unit volume of system (see figure 4.8).

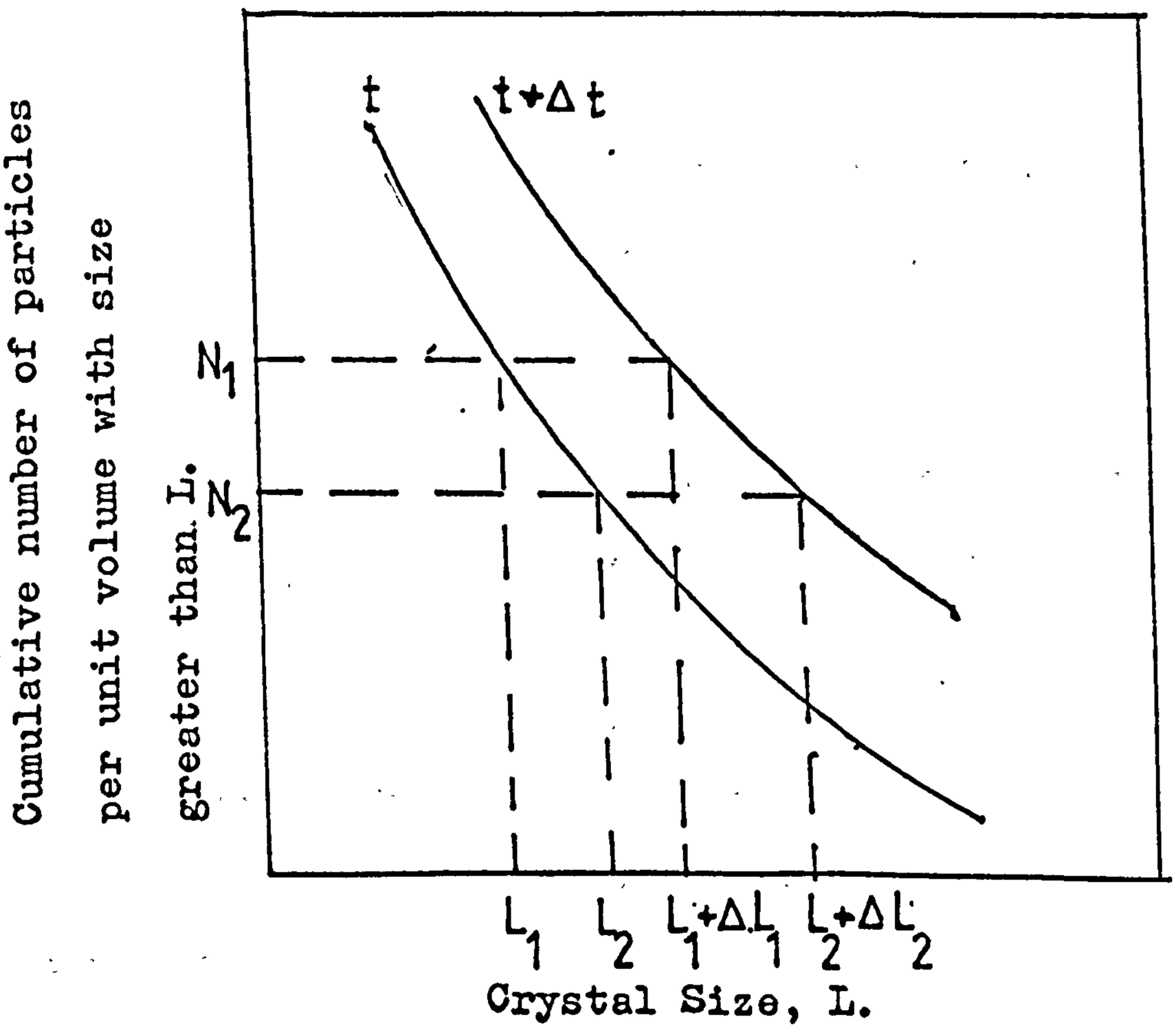

Figure 4.8: Determination of Growth Rate

The number of crystals in the range L_1 to L_2 is thus given by:-

$$\Delta N = \int_{L_1}^{L_2} n \, dL$$

A population balance for the CMSMPR crystalliser shown in figure 4.7 in a system volume, V, for an arbitrary size range, L_1 to L_2 and time interval, Δt, is:-

$$n_1 \, VG_1 \, \Delta t = n_2 \, VG_2 \, \Delta t + Q\acute{n} \, \Delta L \, \Delta t \quad \ldots\ldots \quad 4.44$$

where Q = volumetric feed and discharge rate.

Q_i and Q_o = is the volumetric feed and discharge flow rate respectively.

C_i = feed concentration of solute.

C_o = concentration of solute in crystalliser and discharge.

G = is the linear growth rate (dL/dt).

n = is the population density (numbers per unit length per unit volume).

$\acute{n}$ = is the average population density.

The input term represents the number of crystals growing in to the arbitrary size range over the time interval. The first output term represents the number of crystals growing out of the size range. The second output term represents the number of crystals in the size range when removed from the crystalliser. Equation (4.44) can be written as:-

$$\frac{V \, (G_2 n_2 - G_1 n_1)}{\Delta L} + Q\acute{n} = 0 \quad \ldots\ldots\ldots\ldots\ldots \quad 4.45$$

and in the limit, $\Delta L \rightarrow 0$.

$$V \frac{d(nG)}{dL} \times Qn = 0 \quad \ldots\ldots\ldots\ldots\ldots\ldots\ldots\ldots \quad 4.46$$

Letting $V/Q = Td$, the drawn time and assuming that growth is independent of size, McCabe's ΔL law, then,

$$\frac{dn}{dL} + \frac{n}{GTd} = 0 \quad \ldots\ldots\ldots\ldots\ldots\ldots\ldots\ldots \quad 4.47$$

Integration of equation (4.47), letting n^o denote the population density of zero-size particles (the nuclei population density), gives,

$$n = n^o \exp(-L/GTd) \quad \ldots\ldots\ldots\ldots\ldots\ldots \quad 4.48$$

Equation (4.48) is the fundamental relationship between L and n characterising the CSD (crystal size distribution). A plot of log n versus L gives a straight line with an intercept at L = 0 equal to n^o and a slope of $-1/GTd$.

Equations (4.47) and (4.48) are applicable to CMSMPR crystallisers so long as the holding time Td is the mean residence time of the crystals in suspension. In the case of mixed product removal, this is true if $Td = V/Q_o$,

where, V = is the crystalliser volume.

Q_o = is the slurry withdrawal rate.

Therefore, under the assumptions made earlier[179], if an experiment is carried out at a given residence time, Td, the crystal growth rate, G, and the nuclei density, n^o, can be determined from measurement of population density,

n, as a function of size, L.

4.9 Object of Present Work

The object of the present work is to carry out a precipitation crystallisation study of $CaCO_3$ using calcium bicarbonate and calcium hydroxide as the working substances. The reason for the choice of this system is discussed in Chapter Two (Reduction of Dissolved Solids).

It is obvious from the above literature survey that impurities in crystallisation processes sometimes modify the shape of crystals and/or retard nucleation and crystal growth. On the other hand, for many years it has been known that in practice it is possible to accelerate the softening reactions and to approach equilibrium by bringing the saturated solution in to contact with the solid phase 'seeding'. It was, therefore, decided to carry out a precipitation study where both nucleation and growth could be investigated together to try to elucidate the effects of polyelectrolyte flocculants on the cold-lime softening itself.

CHAPTER FIVE

Effect of Impurities on Calcium Carbonate Precipitation

5.1 Introduction

For many years, it has been known that impurities in crystallisation processes sometimes modify the shapes of crystals and/or retard nucleation and crystal growth, and a considerable literature exists. This review is restricted almost entirely to calcium carbonate. Much of the experimental work directed at an understanding of these effects, however, has been qualitative in nature, and the emphasis has been on crystal habit modification. Much work on inhibition and habit modification has been concerned with the deposition of minerals. Further, in most cases, the additives studied have been naturally occurring organic acids, humic and stearic acid[3,180,181], low molecular weight species such as dyestuffs[182], surface-active agents[183,184], or highly-charged ions[185,186]. More recently, there has been an increasing interest in polymers as impurities[74,4,187,188], partly because of their increasing use in water treatment processes. Natural materials such as alginates[189], agar, tannin, and gelatin[190] and synthetic organic polymers are also used as scale inhibitors, in which role they modify the rate of production or deposition of scale onto surfaces.

Williams and Ruehrwein's work with calcium carbonate and low M.W. sodium polymethacrylate[4] (degree of polymerisation around 6000), observed that the 'time-lag' before precipitation commences is prolonged, that the rate

of precipitation is decreased and that the $CaCO_3$ crystals are also distorted. They found the size of the $CaCO_3$ crystals first decreased and then increased with increasing polyelectrolyte concentration. The increase in size was explained as a consequence of polymer molecules adsorbing onto more than one small crystal, thus flocculating the suspension into large, disordered aggregates. No explanation was offered for the initial decrease in particle size.

Reddy[2], in his most recent study, has shown that several ions inhibit calcium carbonate formation at concentrations occurring in conventional waste water. Their ability to inhibit calcium carbonate formation is as follows:- sodium metaphosphate $>$ sodium dihydrogen phosphate $\approx$ stearic acid $\approx$ magnesium chloride $\approx$ nucleic acid $\approx$ humic acid $\gg$ strontium chloride $\simeq$ phosphatidylinositol $\simeq$ albumin.

Other work with phosphate impurities on $CaCO_3$ precipitation has been reported by Reitemeier and Buehrer[191]. Raistrick[192] showed that the polyphosphate ion forms an almost perfect geometrical fit onto the calcium lattice. Miura[193] was able to correlate the degree of inhibition caused by various phosphate species, on calcium carbonate, with the amount of adsorption on the crystal.

Kitano and Hood[194] have studied the effects of various organic impurities on polymorphic crystal formation of calcium carbonate, they found:-

(1) Glycylglycine, glylogen, malate, pyruvate, inhibited the rate of calcium carbonate formation because of very strong complex formation with calcium ions.

(2) Glycoprotein, glutamate, glycine, lactate, serine, and succinate, affected the rate of calcium carbonate formation moderately but had a fairly strong influence on the crystal type of $CaCO_3$.

(3) Alanine, dextrose, galactose, had little influence on the rate and crystal type of $CaCO_3$.

(4) The rate of calcium carbonate formation decreased and the influence of organic material on the crystal type of calcium carbonate increased with an increase in the concentration of organic material in solution.

Smith and Alexander[187] studied the effect of a wide variety of polymeric additives on crystallisation of calcium sulphate from aqueous solution. They concluded that anionic polyelectrolytes were the most active inhibitors, polyacrylamide had little effect, and polycationic additives had no effect at all. No explanations were offered to explain these differences in behaviour. Liu and Nancollas[188] observed the inhibiting influence of various additives upon the rate of growth of calcium sulphate seed crystals. McCartney and Alexander[195] studied the effects of a large number of additives on the crystallisation of calcium sulphate in order to characterise the most active inhibitors. It was found that polymers

containing carboxyl groups, such as alginic acid, carboxymethylcellulose, polyacrylic acid and polymethacrylic acid were particularly effective. It was noted that polymethacrylic acid showed much less activity than polyacrylic acid at the same concentration, and also that the pH of the crystallisation solution affected the retarding power of the additives.

Miura and co-workers[196] observed habit modification and inhibition caused by various phosphate species with strontium sulphate. Their paper reports a study of the pH dependence on the effect of sodium tripolyphosphate on strontium sulphate crystallisation. The polyphosphate was much less effective at low pH value.

Mullin and Ang[74] came to the conclusion that the presence of trace quantities of the long-chain organic polymer polyacrylamide supressed nucleation considerably, for both seeded and unseeded nickel ammonium sulphate systems. The order of nucleation is relatively unaffected but the nucleation rate constant is greatly reduced.

5.2 Types of Inhibition Mechanism

In spite of the availability of extensive experimental data, the mechanism of the influence of impurities on the crystallisation processes is often not clear. There are many views on the nature of this mechanism. Some investigators are of the opinion that the influence of impurities is due to considerable changes in the composition and properties of a solution[197]. It is postulated that

in the presence of impurities complexes are formed and these complexes decompose to form crystals. Another group of investigators[129] attributes crystal inhibition by impurities to the surfactant effect, which alters the specific surface energy of crystal faces by adsorption. A third group suggests that the influence of impurities is due to their selective adsorption on crystal faces[198,199]. A fourth group of researchers assumes that an impurity affects crystallisation processes when its structure is related in a certain way with the structure of the crystallising substance[200]. It has also been suggested that the influence of impurities is due to the different solubilities of the impurity and the crystallising substance[201].

5.2.1 Ion-Pair Formation

Ion-Pair formation is often responsible for a decrease in solution supersaturation when the concentration of the added ion is sufficiently high to form a stable complex with one of the precipitating ions.

Reddy[2] came to the conclusion that phosphate and glycerophosphate ions form moderately stable ion pairs with calcium ion, while magnesium ions form somewhat weaker complexes with carbonate and bicarbonate ions in solution. He was able to calculate the extent of such ion-pair formation and correlate it with the relatively greater inhibiting effect on calcium rather than magnesium carbonate precipitation.

Other work with polyphosphates[202] and phosphonic acid[203] and humic acid[2] impurities on calcium carbonate precipitation has been reported. In these experiments an abrupt change in crystal growth rate occured over a narrow range of additive concentration. This type of crystal growth inhibition is similar to that described by Sears[204], i.e. ion-pair formation is a significant kinetic factor.

5.2.2 Specific Surface Energy Changes

Gibbs' theory[77] of perfect crystal growth was contradicted by Volmer and Schultze[205] who discovered a number of systems in which there was no critical supersaturation. They demonstrated that if the mobility of the molecules is high, then the rate of crystal growth will be determined by both the rate which the molecules impinge upon the surface of the growing crystal and by the number of nuclei which are capable of continued growth (i.e. critical size nuclei). They suggested that there was, at the surface, a mobile 'adsorbed' layer in thermodynamic equilibrium with the crystal surface. This adsorbed layer caused some roughness of the surface and consequently resulted in the possibility of crystal growth without surface nucleation.

Smith and Alexander[187] postulated that adsorbed polymer molecules acted as immobile impurities on the crystal surface of calcium sulphate, reducing the step velocity and therefore the crystal growth rate.

5.2.3 Adsorption on Specific Sites

The influence of impurities upon the crystallisation velocity of supercooled melts was studied by Freundlich[206] who applied Marc's adsorbed layer concept. He postulated that the adsorbed molecules impeded growth by preferentially occupying specific lattice sites.

McCartney and Alexander[195] studied the effects of a large number of additives on the crystallisation of calcium sulphate in order to characterise the most active inhibitors, and to elucidate the mechanism of their action. They correlated the order of inhibition with the degree of dissociation of polyacrylic acid. The crystal habit was modified by the additives, adsorption occurring most strongly on the (III) faces of the crystals. Kuntze[207] has made similar conclusions, after studying the effects of various protein hydrolysates on their synthetic analogues of the crystallisation of calcium sulphate. Liu and Nancollas[188] interpreted the effect of added gelatin upon the rate constant for crystal growth in terms of its adsorption, following the Langmuir isotherm at the available crystal growth sites.

5.2.4 Ionic Effect

Raistrick[192], in his paper on the influence of polyphosphate ion on crystal growth of calcium carbonate, suggested that growth was stopped because the polyelectrolyte ion, is adsorbing onto those faces of a growing crystallite which were composed of calcium ions,

lowered the electrostatic potential for the adsorption of another layer, since each phosphate group is capable of replacing one carbonate group. In this way, the nucleus was prevented from attaining critical size, and dissociated into its component ions.

5.3 Adsorption of Organic Substances at the $CaCO_3$ Surface

Concentrations of dissolved organic substances in natural waters usually range from 0.1 to 10 mg/litre. The organic substances found include compounds such as amino acids, polysaccharides, amino sugars, fatty acids, organic phosphorus compounds and aromatic compounds containing -OH and -COOH functional groups. Dissolved organic compounds interact with calcium carbonate surfaces to form organo-carbonate associations, as coating or as molecular layers.

When synthetic polymers are used in water treatment to destabilise suspensions they are normally added at a concentration below that required to form a saturated monolayer hence at these dosages all of the polymeric solute will be removed from solution by adsorption. Because of the nature of polyelectrolyte adsorption (see 5.3.1) it is reasonable to assume that the more strongly adsorbed high molecular weight components of the polymer will adsorb more rapidly, assuming no diffusion rate effects, but if all is adsorbed these selective effects will not be apparent. In commercial grade polyacrylamide type flocculants there is normally a residue of up to a few percent non-polymerised monomer which is assumed not to

adsorb. Doses of polymer in excess of the monolayer capacity resulting in an equilibrium concentration in solution are associated with a deterioration in flocculant performance.

Chave and Suess[208] attributed the lack of equilibrium between calcite and sea water to organo-carbonate association which blocks any new nucleation of $CaCO_3$ precipitate. Suess[209] showed organo-carbonate association affects the $CaCO_3$ equilibrium in solution by physically isolating the calcite surface and by reducing the surface energy of the solid. Otsuki and Wetzel[3] showed the adsorption of humic substances on calcium carbonate.

Adsorption data is most commonly presented as an isotherm which is a representation of the amount of adsorbate adsorbed per unit mass a per unit area of adsorbent as a function of the equilibrium adsorbate concentration at a constant temperature. Isotherms are conveniently expressed graphically. Many types of isotherm based on experimental observation and theoretical argument have been proposed[210]. The simplest theoretical isotherm is that of Langmuir[211] in which it was assumed that:-

(a) the adsorbate molecules adsorb on specific sites on the adsorbent,

(b) that each site only adsorbs one molecule of adsorbent, and

(c) that there is no lateral interaction between adsorbed molecules.

The second assumption implies that only one layer of

adsorbent may accumulate on the surface, i.e. it is a monolayer model.

Langmuir assumed a dynamic equilibrium between those molecules on the surface and those in the bulk phase. For a gas the number of molecules striking unit area in unit time is given by kinetic theory as:-

$$U = \frac{P}{(2\pi mKT)^{\frac{1}{2}}} \quad \ldots\ldots\ldots\ldots\ldots\ldots\ldots\ldots \quad 5.1$$

where U = is the number of molecules.

P = is the vapour pressure.

m = is the mass of molecules.

K = is the Boltzman constant.

T = is the absolute temperature.

Molecules striking occupied sites are immediately reflected in accordance with assumption (b). Those striking unoccupied sites have a probability α of being retained. α is known as the accommodation coefficient. Hence the rate of adsorption of molecules per unit area is:-

$$\alpha U(1 - \theta) \quad \ldots\ldots\ldots\ldots\ldots\ldots\ldots\ldots \quad 5.2$$

where θ is the fraction of sites occupied. The rate of desorption from the surface is given by:-

$$V\theta$$

where V is the desorption rate from a completely covered surface.

At equilibrium

$$\alpha U(1 - \theta) = V\theta \quad \ldots\ldots\ldots\ldots\ldots\ldots\ldots\ldots \quad 5.3$$

and if $b = \frac{\alpha}{V(2\pi mKT)^{\frac{1}{2}}}$ 5.4

then $bP = \frac{\theta}{1-\theta}$ or $\theta = \frac{bP}{1+bP}$ 5.5

This may be represented graphically by figure 5.1. The plateau represents the existence of a complete monolayer.

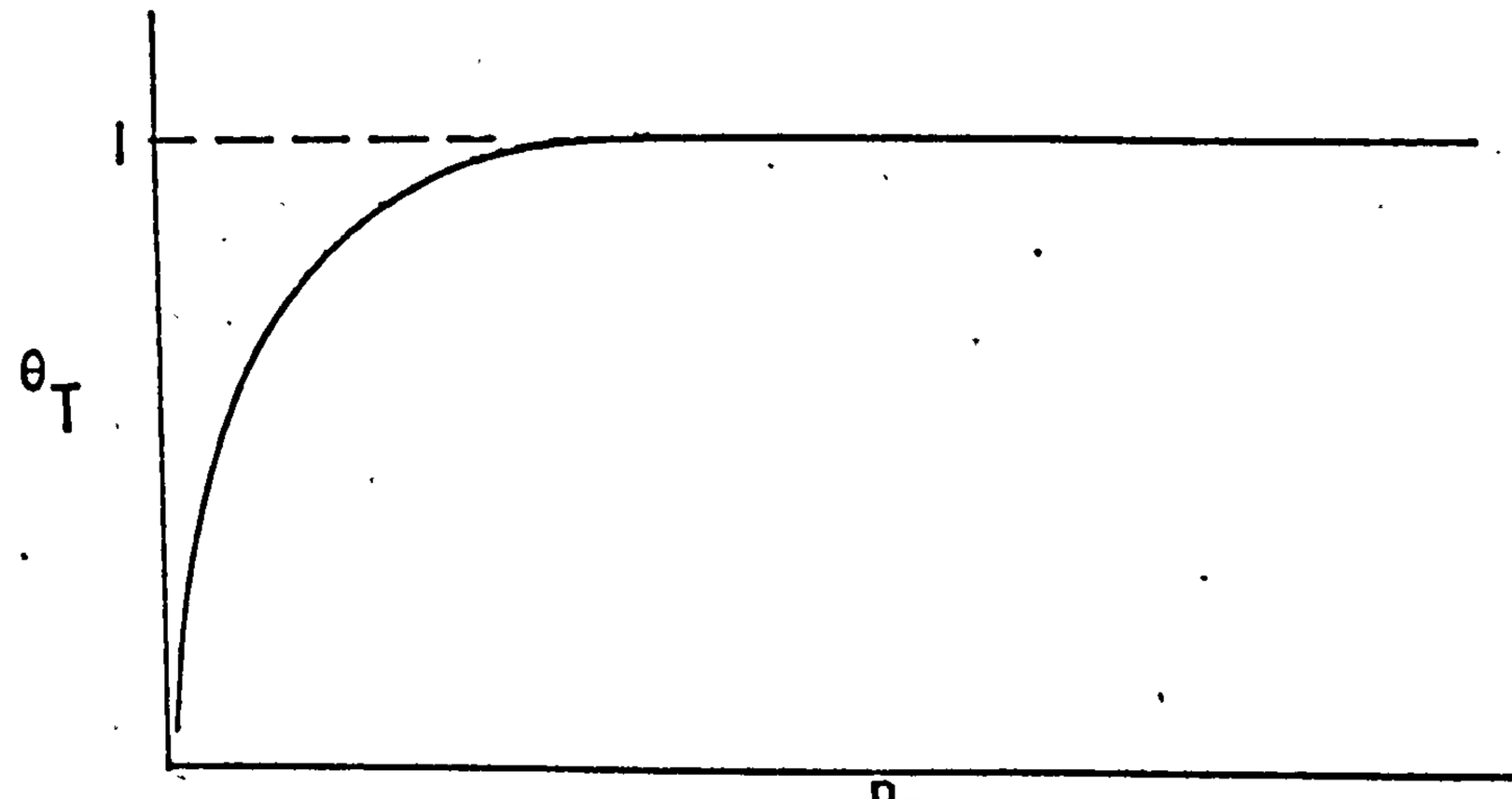

Figure 5.1

Some adsorption phenomena exhibit isotherms corresponding to multilayer adsorption. This is usual with the low temperature adsorption gases in which the bonding forces of adsorbent to adsorbate are of the same order as those associated with Van der Waals forces and liquid condensation. This is commonly referred to as physical adsorption. When the adsorption forces are stronger, e.g. the adsorption of ions at charged sites, the phenomenon is termed chemisorption and the Langmuir isotherm is common in such systems.

5.3.1 Adsorption of High Molecular Weight Polymers

High molecular flocculants are, ideally, linear

polymers carrying many sites capable of adsorption. Typical is an anionic polyacrylamide which has the general formula:-

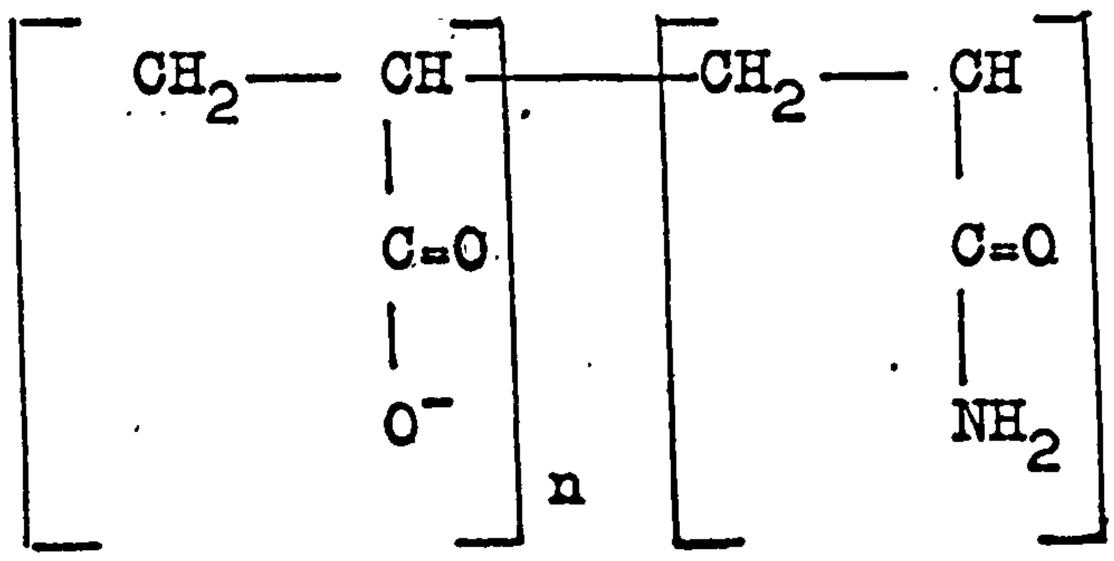

Where the ratio of n to m groups is typically 5%-35% and where m + n = 5000-100,000. Such polymers are known to give a Langmuir type adsorption isotherm(210) although the rise to the plateau is very steep and occurs at lower concentrations than would be expected for Langmuir.

Much work has been done on the theory of polymer adsorption and although the properties of highly charged polyelectrolytes are too difficult to treat comprehensively it is reasonable to expect that these materials would exhibit the same general behaviour as uncharged polymers with allowance being made for specific effects due to their charge.

As a rule of thumb, almost any polymer adsorbs on any surface. Because of the many points of attachment to the surface, therefore, only a low bonding energy per segment suffices to render the affinity of several segments together so high that their adsorption is virtually irreversible and monolayer giving an isotherm similar to that of Langmuir.

The theories, in general, predict that when a high

molecular weight soluble polymer is at equilibrium adsorption it is present in the form of loops, trains and tails (see figure 5.2).

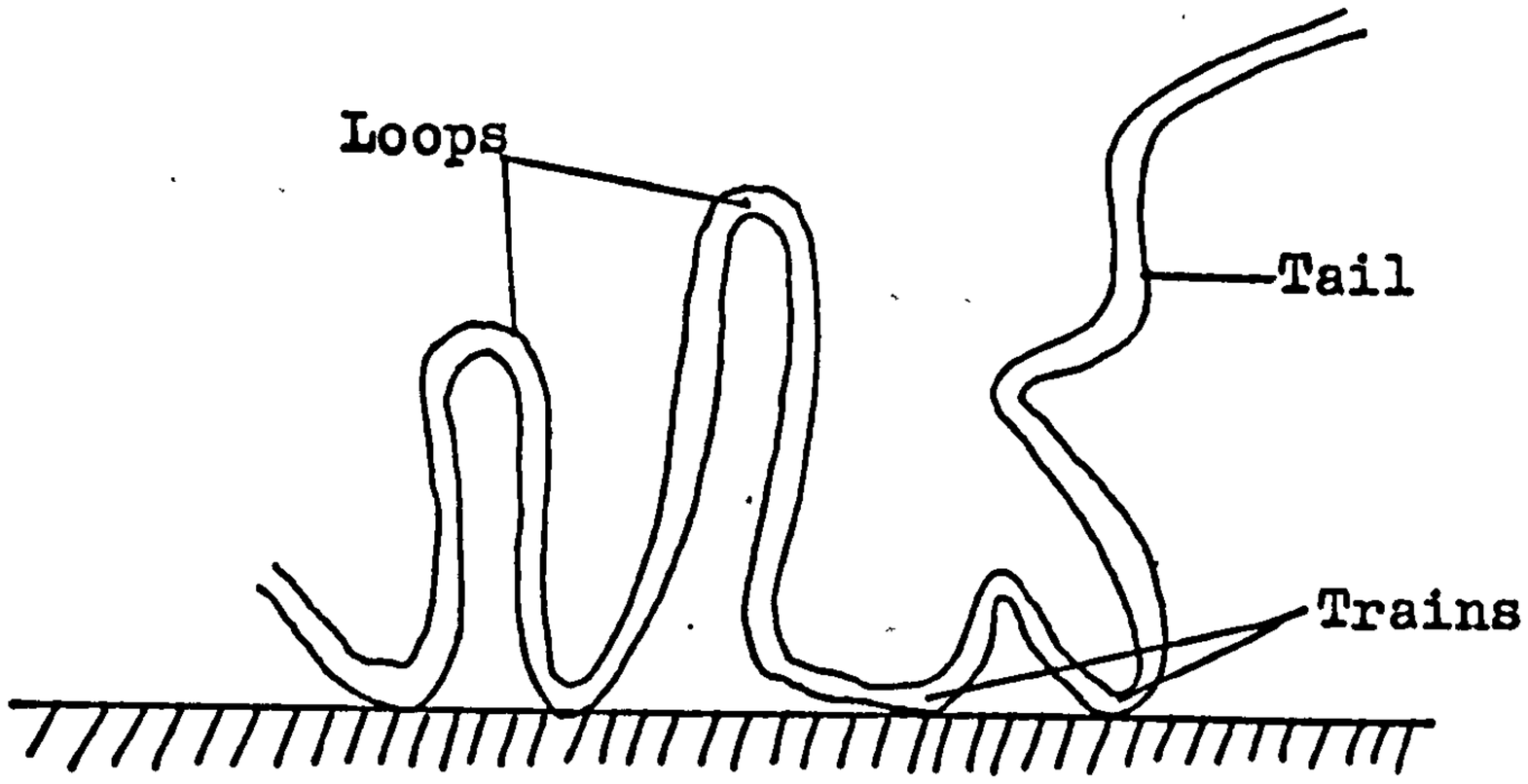

The distribution of adsorbed polymer segments over trains, loops and tails.

Figure 5.2

A train is a series of polymer segments lying adsorbed at the surface, a loop is a series of polymer segments projected from the surface into the solution from between two chains and a tail is a length of segments with one free end projecting into the solvent. As each linear molecule has only two tails some workers believe that the effect of tails on the properties of high molecular weight polymers with many segments is insignificant. It is, however, possible that tails might be significant in bridging flocculation at a non-equilibrium stage in adsorption[212].

The theories of adsorption differ in their prediction of the proportion of loops, tails and trains, in the prediction of the segment density with distance from the surface and in the effects of segment-segment, segment-

solvent, segment-surface and solvent-surface interaction.

Although it has been in some aspects superseded, the theory of Silberberg[213-215] is typical of this work and attempts a very comprehensive treatment of the problem. The conclusions[213] of this theory include that:-

(a) at low molecular weights the adsorption in mass per unit area increases with molecular weight to a limiting value beyond which it becomes M.W. independent,

(b) the fraction of segments forming chains is about 0.5,

(c) that although the adsorption energy of each segment may be low, the overall energy for all segments adsorbed is high and the probability of a large number of segments desorbing simultaneously spontaneously is very low. Hence desorption is practically very difficult.

(d) that the adsorption isotherm for a polymer is of the Langmuir type although the arguments used in deriving the classical Langmuir equation cannot be used in this case.

5.3.2 Interaction of Humic Substances With $CaCO_3$

Humic substances producing colour in water are of vegetable origin and are mainly derived from the water-soluble and peptisable constituents of soil humus and peat. Humic substances are dark-coloured, acidic, predominantly aromatic, hydrophilic, chemically complex, polyelectrolyte-

like materials that range in molecular weight from a few hundred to many thousand.

Oden[216] was the first to classify the humic substances into the following three main fractions:-

(1) Humic acid, HA, which is soluble in dilute alkali but is precipitated on acidification of the alkaline extract.

(2) Fulvic acid, FA, which is that humic fraction which remains in solution when the alkaline extract is acidified, i.e. it is soluble in both dilute alkali and acid.

(3) Humin, which is that humic fraction that cannot be extracted from the soil or sediment by dilute base or acid.

Schnitzer and Khan[217] proposed that the three humic fractions are similar, but they differ in molecular weight. Molecular weights of up to 50,000 have been reported for humic acid[43], with equivalent weights in the range of 150-400. Very little data has been published on fulvic acids, although they are frequently assumed to have lower molecular weights.

The chemical nature of humic substances has been discussed by Packham[218]. Their complete structure, if, indeed, such a structure may be said to exist, is a mystery. They are composed mainly of carbon, hydrogen and oxygen. Black[219] believed that they are aromatic, polyhydroxy, methoxy, carboxylic acids. Schnitzer and Khan[217] proposed that humic substances are phenolic and

benzencarboxylic acids joined by hydrogen bonding to form large molecular structures.

The physical nature of the humic substances is of much greater interest at this time. Packham[218] has measured the optical density for humic and fulvic fractions from seven different waters expressed as optical density/cm light path per unit concentration of humic substance. He concluded that the optical density of humic acid solutions is approximately double that of fulvic acid solutions at 300m μm and three to six times greater at 450m μm.

Humic substances are capable of interacting with metal ions, metal oxides, metal hydroxides and more complex minerals to form metal-organic associations of widely differing chemical and biological stabilities and characteristics. Interactions between humic substances and metal ions have been described as ion-exchange, surface adsorption, chelation, coagulation and peptisation.

Guy and co-workers[220] indicated that the so-called humic acids, HA, and fulvic acids, FA, are among the most important complexing agents of metal ions in natural waters and interstitial waters of soil and sediments. They proposed that solid humic acids have acidic functional groups at the water-solid interface which can chelate metal ions:-

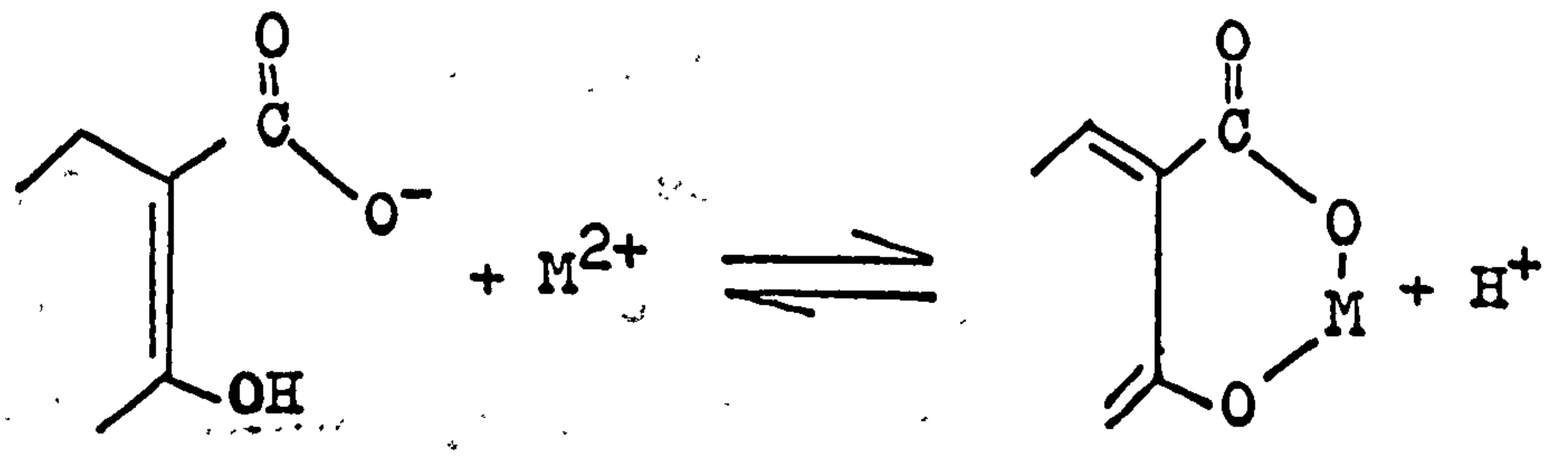

This sorption mechanism is consistent with the following conclusions:-

(1) The amount of metal sorbed would be proportional to the number of available complexing sites leading to a limiting sorption value.

(2) The relative affinity of different metal ions for HA will be a function of the ability of those ions to form metal chelates. The maximum sorption values parallel the order of stability of HA complexes, i.e.,

$Cu^{2+} > Zn^{2+} > Cd^{2+} > Ca^{2+}$

France and Werner[221] were able to measure the complexation properties of HA and FA in natural waters with Cu^{++} and pb^{2+}. Van Dijk[222] also noted that the capacity of HA's to bind metal ions was approximately equal to the number of titratable H^{+}-ions divided by the valency of the interacting metal ions. Schnitzer and Skinner[223] showed that either one acidic CO_2H and one OH phenolic groups or two acidic CO_2H groups reacted simultaneously with metal ions and hydrous oxides. The involvement of CO_2H and phenolic OH groups of humic substances in metal complexing has been confirmed by Van Dijk[222] and Stevenson[224]. Both authors mentioned the formation of mixed complexes.

Because of these reactions HA and FA may markedly modify the chemical properties of metal ions and thus may affect natural processes such as the rate of growth of plants or the accumulation of metal in sediments[225,226]. Numerous investigations by various workers[227] have

demonstrated that lime (and exchangeable Ca^{2+}) retards the decomposition of humic substances because of the formation of soluble Ca-humates.

Otsuki and Wetzel[3] show the adsorption of humic acid by precipitating $CaCO_3$ is not a simple surface phenomenon. They suggested that some of the humic acids were incorporated into crystals during a rapid growth of calcium carbonate nuclei which was supported by the lack of equilibrium of the isotherm between 18 and 41 hours; this could be in the form of organic layers which alternate with $CaCO_3$ layers.

CHAPTER SIX

Materials and Experimental Techniques

6.1 Materials and Solutions

6.1.1 Calcium Carbonate

6.1.1.1 Natural Calcium Carbonate

Natural calcium carbonate is almost entirely calcite. A paper coating grade of ground whiting was obtained from the Queensgate Whiting Company. Akram[228] had previously found the mean diameter of the distribution of this calcium carbonate is 2.3 microns and Riley[229] had shown the specific surface area to be 2.08 m^2/gm.

6.1.1.2 Precipitated Calcium Carbonate

The sample of precipitated $CaCO_3$ (CALOFIL B_1) used was obtained from John and E. Sturge Ltd., Birmingham.

6.1.1.2.1 Particle Size Analysis

The sedimentation velocity of a particle in a fluid is determined by the particle size and shape, the immersed density, the fluid viscosity and the acceleration experienced by the particle. If the particle velocity is such that

$$Re = \rho \frac{dU_t}{\eta} < 0.2 \quad \ldots\ldots\ldots\ldots\ldots\ldots\ldots\ldots \quad 6.1$$

where Re = is Reynolds number.

ρ = is the fluid density.

d = is the particle diameter.

η = viscosity of liquid.

0.2 = is the Laminer and Stokes region where

inertia forces are negligible.

U_t = is the terminal velocity.

The terminal sedimentation velocity for a spherical particle is given by Stoke's equation:-

$$U_t = \frac{g}{18\mu} (P_s - P_L)\, d^2 \quad \ldots\ldots\ldots\ldots\ldots\ldots\ 6.2$$

where g = is the acceleration of gravity.

P_s = is the density of the particle.

This principle may be used to determine particle size if the sedimentation velocity in a gravitational field is insignificant with respect to Brownian diffusion and could give excessively long sedimentation time. It is possible to speed up sedimentation by performing the experiment in a centrifugal field.

Two techniques may be used in sedimentation, the homogeneous method where a homogeneous suspension is centrifuged and the line start technique where all particles start from one radius. In both methods the particle concentration at a set radius is determined as a function of time.

A well proven line start method is that using the Joyce Loebl disc centrifuge[230]. It is a well designed and sophisticated instrument consisting of three parts: the disc centrifuge with sampling equipment, the sample collection unit and the electronic control unit (see figure 6.1).

The centrifuge disc is a rotor, manufactured from

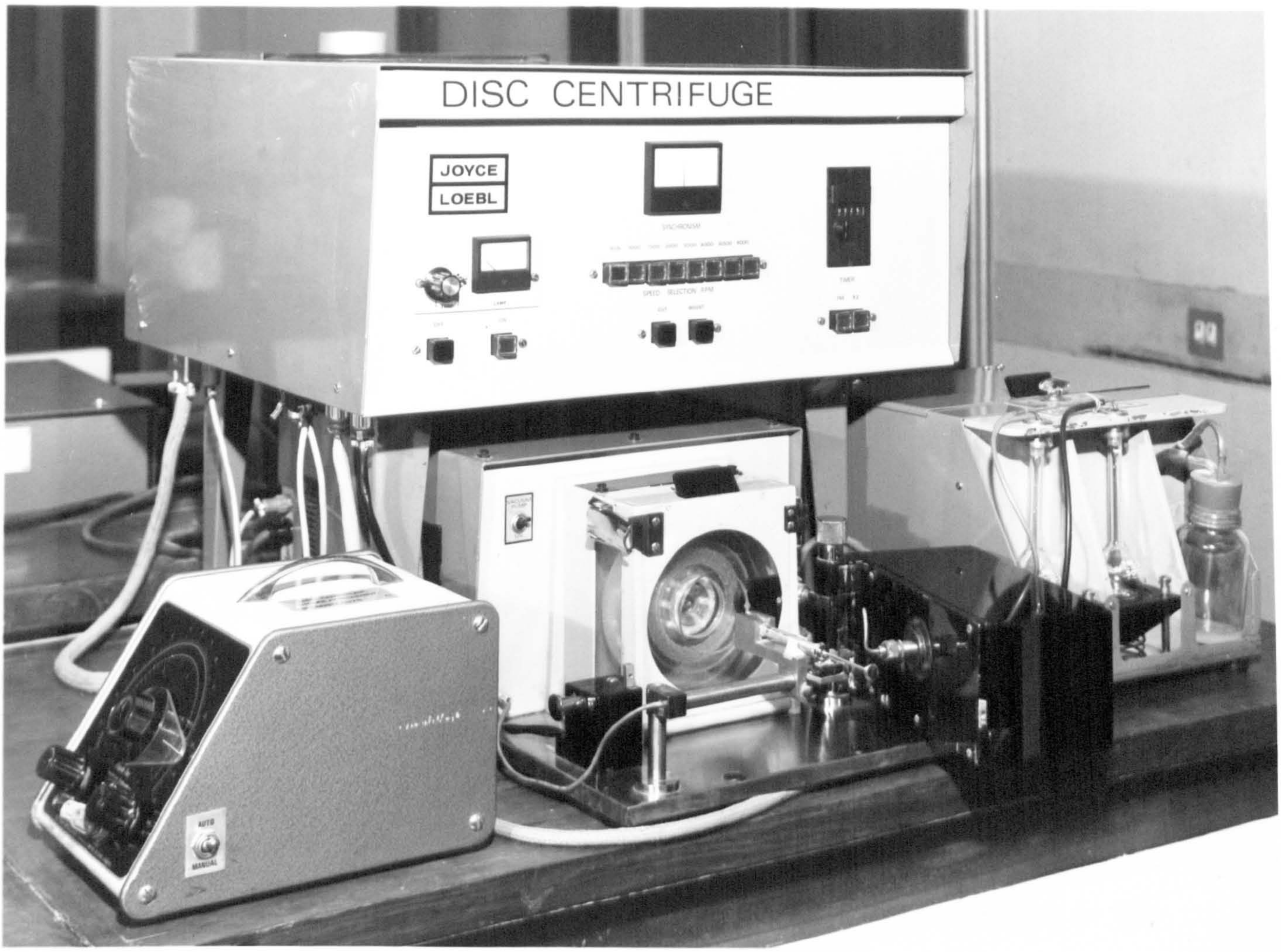

Fig. 6.1

solid perspex, with a cavity 10.2cm in diameter and 0.65cm deep, driven by an electronically stabilised motor at one of a number of speeds in the range 1000-8000 rev/min. The sample collection unit is essentially a vacuum pump which extracts from the rotating disc, by means of a moving small bore metal probe, all suspension lying at radii smaller than the final collection radius. The electronic control unit houses the motor stabilisation servo-mechanism, the sequential switching system and a time which provides for automatic operation after sample injection.

The rotating disc was filled with 40ml of spin fluid (40% w/w glycerol). One ml of the sample suspension (1% w/w calcium carbonate dispersed with Nonidet p40 as a wetting agent) was injected by a syringe on to the back face of the disc. At the pre-set time the undersize fraction was removed from the rotating disc by suction through the probe as it rotates through 360° inside the disc analogous to inside cutting on a lathe.

Each operation of the centrifuge leads to single point on the cumulative size distribution curve. The undersize fractions collected analysed quantitatively by a simple back titration with 0.01N HCl.

For the precipitated calcium carbonate the distribution obtained (figure 6.2), shows 1.28 microns as top size and that there was 5.26% by weight below 0.1 microns.

The median size (MS) calculated from weight distribution/size curve using equation 6.3, was found to be 0.48 microns, comparing with 0.58 microns obtained from

Figure 6.2

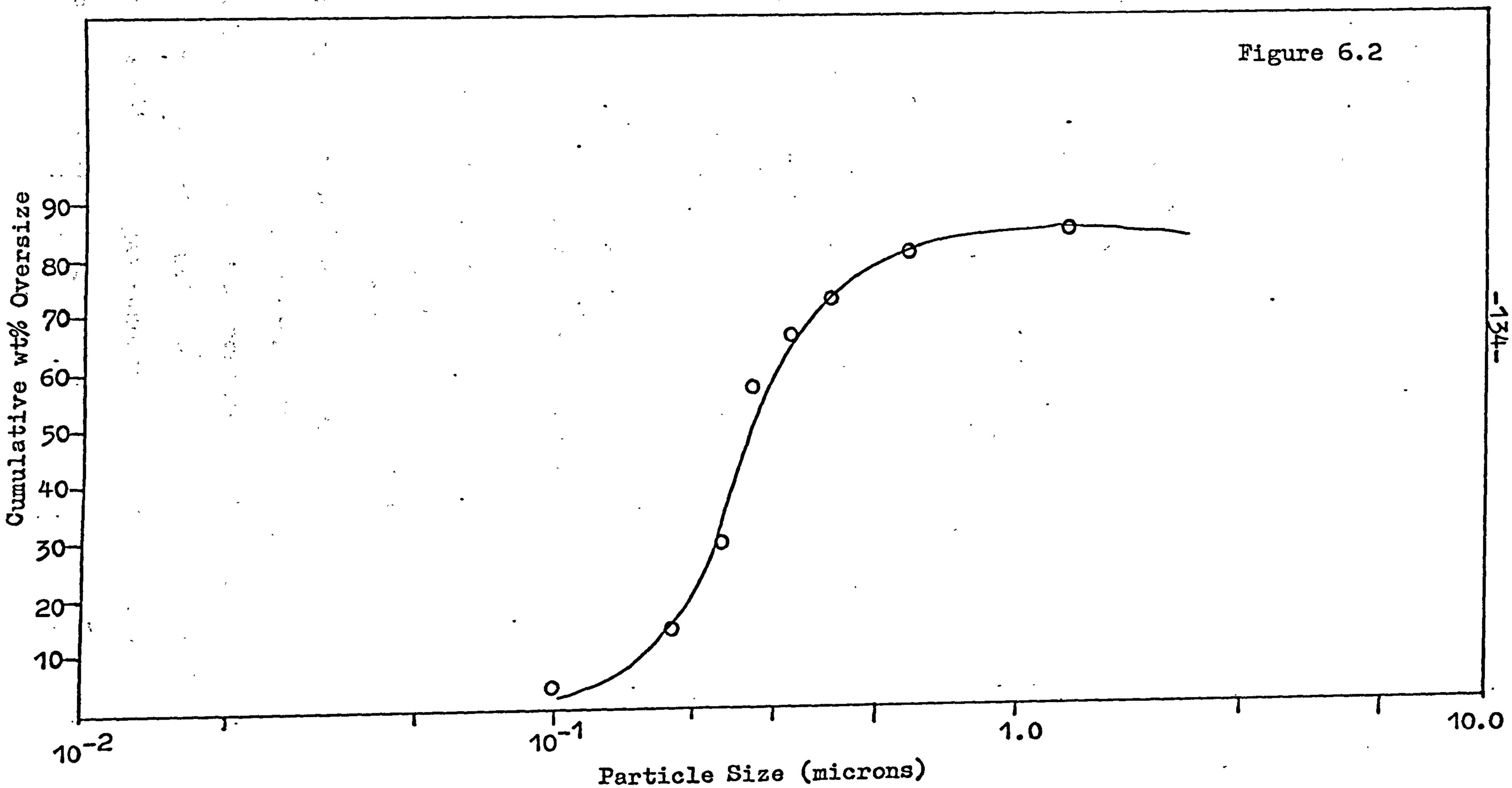
Cumulative wt% Oversize
90
80
70
60
50
40
30
20
10
10^{-2}
10^{-1}
1.0
10.0
Particle Size (microns)

B.E.T. adsorption confirms the validity of the results.

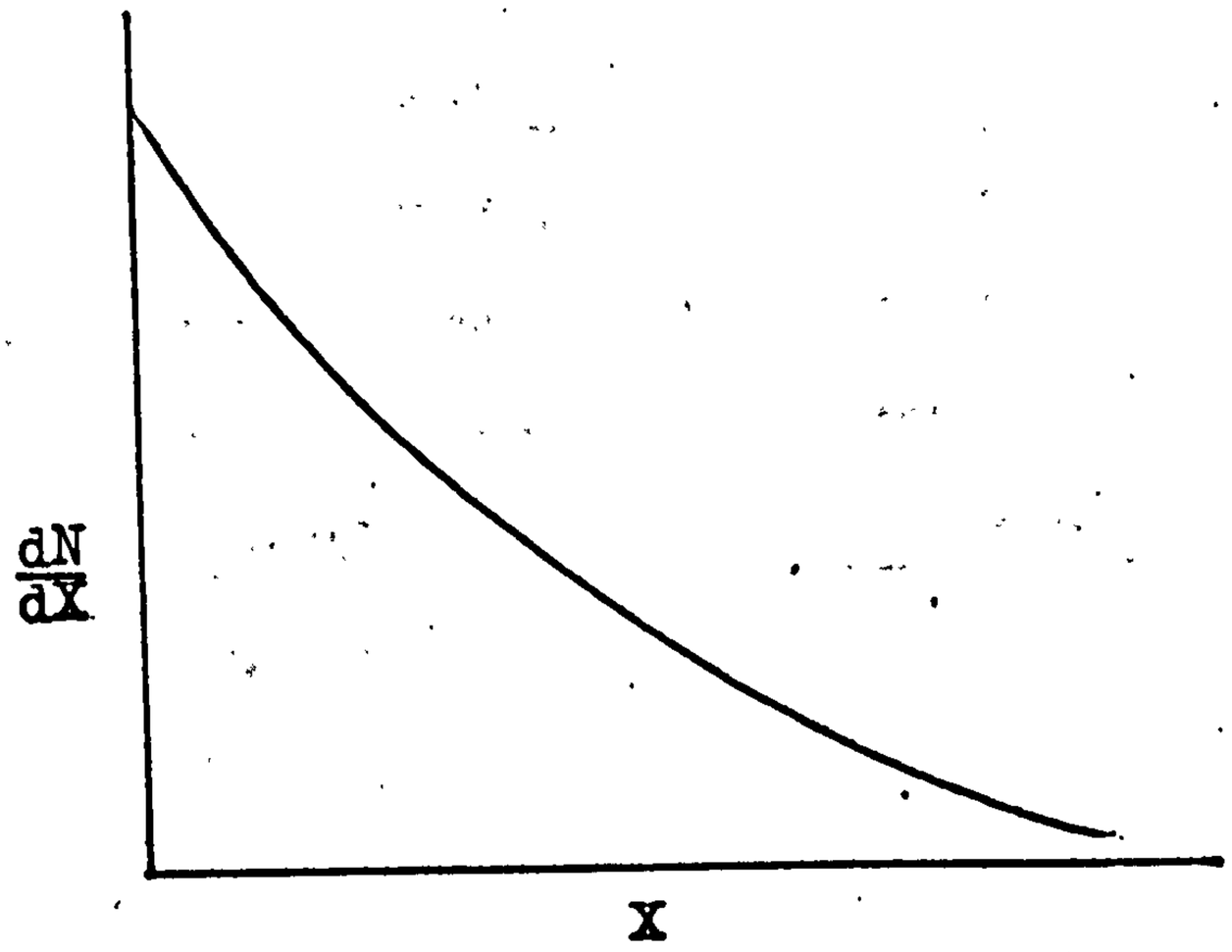

Area under curve = $\Sigma X dN$

First moment of area = $\Sigma X^2 dN$

$$\text{hence generally } X^{-r} = \frac{\Sigma X^{r+1}\, dN}{\Sigma X^{r}\, dN} \quad \ldots\ldots\ldots\ldots\ldots 6.3$$

where r = is the order of dimension, i.e.,

r = 1 diameter or length.

6.1.1.2.2 Surface Area

The surface area of precipitated calcium carbonate was determined using the B.E.T. method[231]. Nitrogen adsorption was measured on a typical volumetric adsorption apparatus designed by Krieger[232] at a temperature of -195°C and atmospheric pressure of 775.4mm Hg.

The data obtained are in the form of pairs of values of the volume of gas adsorbed corrected to S.T.P. (V ml) and the corresponding equilibrium pressure of N_2 above the

nitrogen (P), presented in Table 6.1.

Table 6.1

weight of calcium carbonate = 0.960gm.

Ambient temperature = 23°C.

Ambient pressure, Po = 775.4mm Hg.

P (mm Hg)	X = P/Po	V (ml at S.T.P.)	$XV^{-1}/(1-X)$
9.5	0.1225	0.465	0.300
13.3	0.1715	0.957	0.347
17.2	0.2218	0.706	0.404
20.7	0.2669	0.813	0.448

The nitrogen adsorption isotherm of the calcium carbonate is shown in figure 6.3. The linear plot of X versus $XV^{-1}/(1-X)$ up to X = 0.3 obtained, corresponds to Type II isotherm in the B.E.T. classification.

The surface area calculated from the measurements of the slope and intercept using the B.E.T. theory, was found to be 3.81m^2/gm, assuming that one molecule of nitrogen covers 16.2 x $10^{-20}m^2$. The surface area was checked using Ströhlein Areameter, the surface area determined from four measurements was calculated to be 3.76m^2/gm.

6.1.2 Polymers

The polymers used in this study were cationic, anionic, and non-ionic polyacrylamides. The polymers were supplied by Floerger (A, B and C) and Crossfield Polyelectrolytes (D).

Figure 6.3

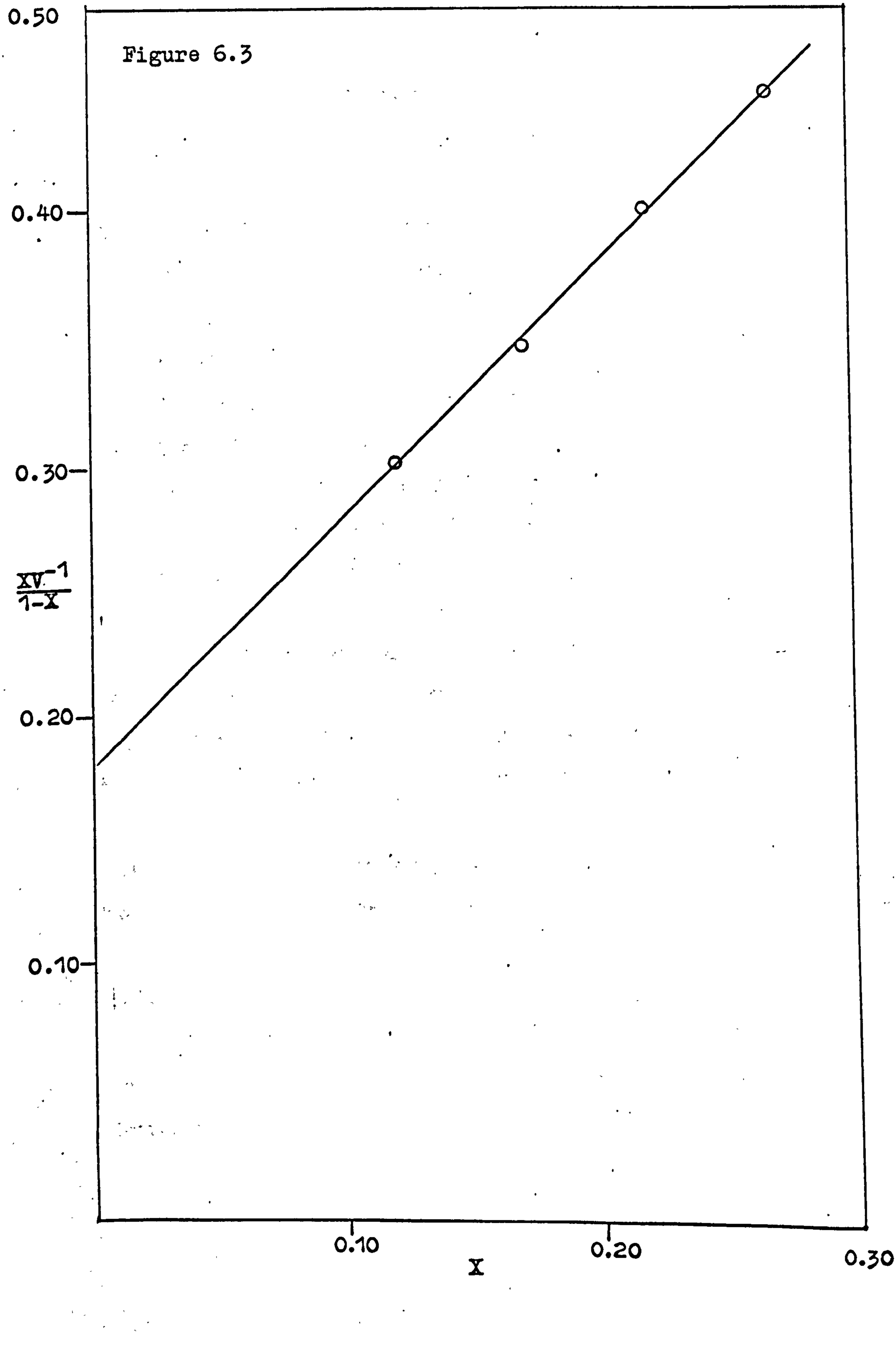

Table 6.2

	Polymer	Ionic Character	Stated Molecular Weight
(A)	FO 115 PD 1200	Cationic (20%)	5×10^6
(B)	FA 60H MAX 6	Anionic (36%)	10×10^6
(C)	FA 20H MAX 2	Nonionic	10×10^6
(D)	FA 200-5	Anionic (84%)	$5\text{-}10 \times 10^6$

The ionic character was determined by titration.

The polyacrylamides used were extremely difficult to dissolve in deionised water. Exactly one gram of the polymer was weighed out (± 0.0002gms) and added slowly in to the vortex of 1000mls of deionised water which was being agitated by a stirrer. Care was taken to ensure that the polymer was not damaged. Once all the polymer had been added the mixture was stirred moderately, a whole day was required to dissolve the polymer. A very viscous solution results. This solution is stored in a refrigerator until used for experiments. Due to the fact that these polymers deteriorate with time when in solution, a given batch was not kept for more than three weeks in this concentrated form.

6.1.3 Dispex N-40

This is a sodium salt of polyacrylic acid manufactured by Allied Colloids Ltd., Bradford, and having the following formula:-

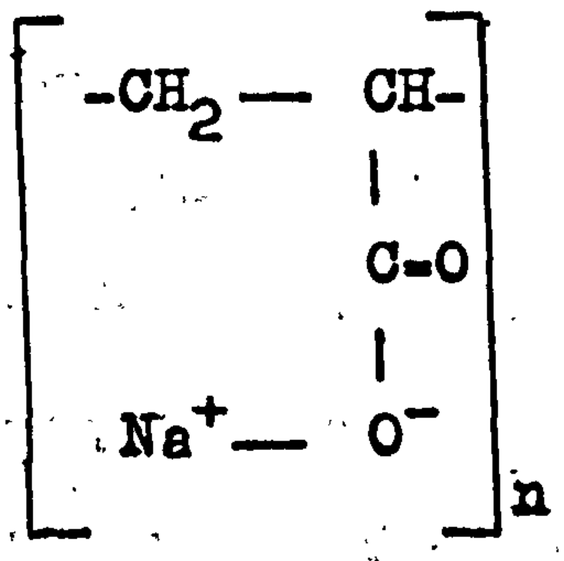

The average molecular weight is 40,000 hence n has an approximate value of 400. 0.1% (w/v) solution was prepared.

6.1.4 Starch

This is soluble starch produced by B.D.H. freshly prepared solution (0.1% w/v) was used. The type of starch is not known.

6.1.5 Aluminium Sulphate

The material used was Aluminium Sulphate $Al_2(SO_4)_3.16H_2O$ containing not less than 98.0% $Al_2(SO_4)_3.16H_2O$. A 0.1% (w/v) solution was prepared.

6.1.6 Humic Substance

This material was kindly provided by Dr. I. Sheiham, Water Research Centre, Medmenham.

Humic substances which produce colour in water[233] are a complex mixture of compounds arising from the chemical and biological degradation of plant and animal residues and from synthetic activities of micro-organisms. The literature on humic substances is vast[227], but despite the fact that they have occupied the attention of many research workers since the early nineteenth century there

are still many uncertainties, not the least being their composition and molecular structure. Important characteristics of humic substances are their ability to interact with metal ions and hydrous oxides forming water-insoluble and water-soluble complexes[234].

The humic substance used was isolated[233] from Thames water by adsorption on strong base anion exchange resin type IRA 904, which is a macroporous resin with a high affinity for organic acids. The humic substance was recovered from the resin by regeneration with sodium chloride. A 0.5% v/v solution of the concentrate corresponded to a colour of 60 Hazen units[235]. Figure 6.4 is a calibration graph prepared using the platinum-cobalt standard described in reference 235.

The humic acid fraction was obtained by reducing the pH of the concentrate to 1 with 1N HCl[233]. The humic acid was then separated by filtration and dissolved in the minimum volume of 5N ammonium hydroxide solution. Complete solution was obtained.

6.1.7 Lime $Ca(OH)_2$

This was a calcined mineral lime kindly supplied by the Mishrak Sulphur Company, Iraq, and having the following composition:-

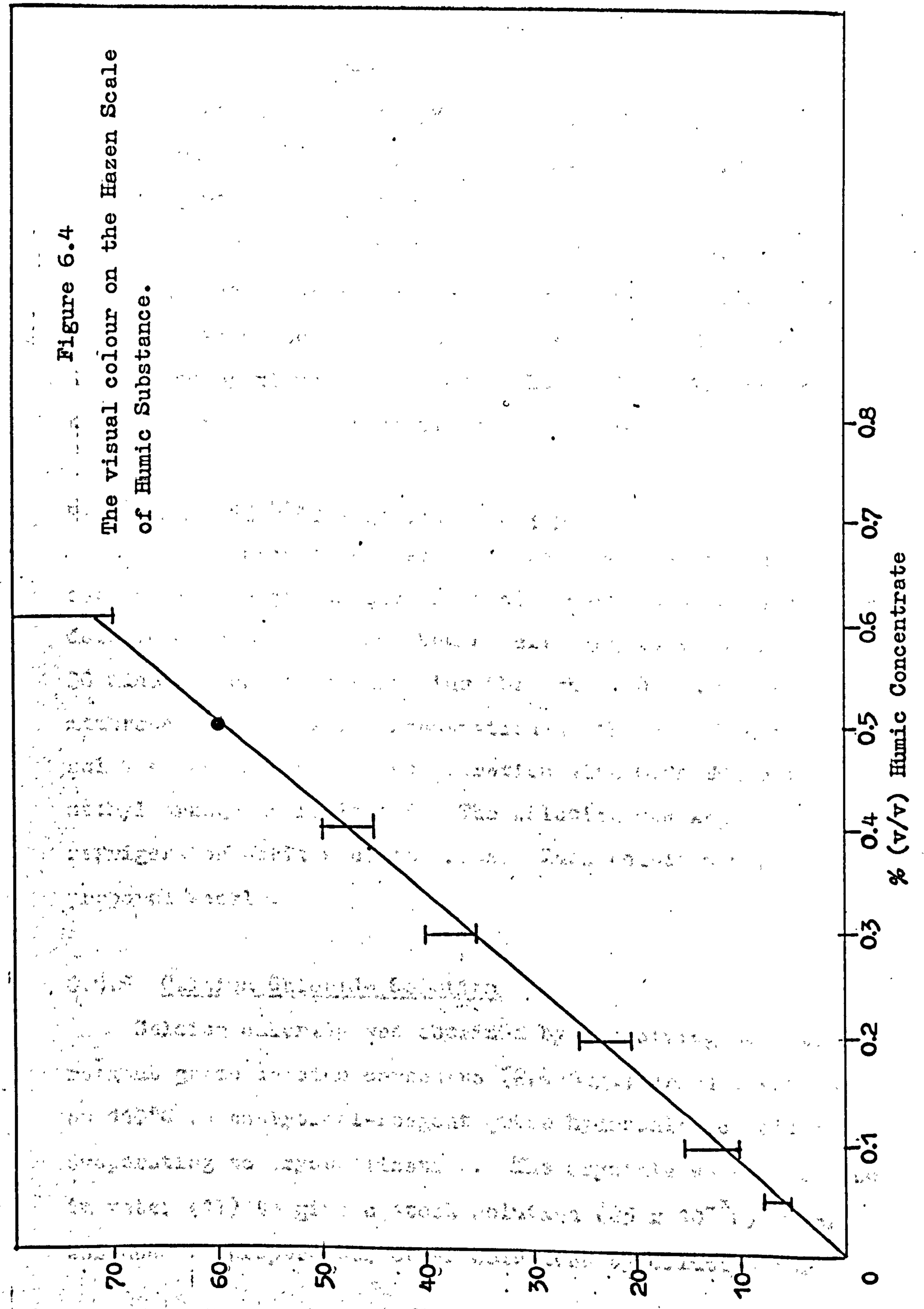

Figure 6.4 The visual colour on the Hazen Scale of Humic Substance.

Table 6.3

$Ca(OH)_2$	96.80%	F_2O_3	0.10%
$CaCO_3$	0.86%	Al_2O_3	0.23%
$CaSO_4$	0.23%	SiO_2	0.47%
$Mg(OH)_2$	0.92%	H_2O	0.39%

Half saturated solutions were prepared by diluting a saturated solution. The concentration of $Ca(OH)_2$ was determined by titration with 0.1N HCl. The solution was kept in a refrigerator until used for runs.

6.1.8 Calcium Bicarbonate, $Ca(HCO_3)_2$

Calcium Bicarbonate solution was prepared by bubbling carbon dioxide gas through a calcium carbonate suspension in deionised water for three hours, allowing it to stand for 30 minutes, and then filtering through an 0.2 microns membrane filter. The concentration of the bicarbonate solution was determined by titration with 0.1N HCl using methyl orange as indicator. The solution was kept in a refrigerator until used for runs. This solution was prepared weekly.

6.1.9 Calcium Chloride Solution

Calcium chloride was obtained by dissolving analytical-reagent grade calcium carbonate (2.4752gm) dried overnight at 110°C in analytical-reagent grade hydrochloric acid and evaporating to crystallisation. The crystals were dissolved in water (1l) to give a stock solution (25×10^{-3}M) which was used to prepare all other solutions by dilution for

calibration of the calcium electrode.

6.1.10 Deionised Water

The deionised water was provided by Ionmiser Model 6C Houseman Hegro. All water used to dilute the reaction mixture to the desired supersaturation was filtered through 0.2 microns millipore membrane filter disc.

6.2 Adsorption Techniques

6.2.1 Adsorption of High Molecular Weight Polymers

Calcium carbonate was dried, overnight, at 110°C and kept in a desiccator until used for measurements.

Samples of calcium carbonate (1.0gm in the case of natural $CaCO_3$ and 0.3gm in the case of precipitated $CaCO_3$) were weighed into stoppered 50ml centrifuge tube. A range of concentrations, the highest being approximately 32×10^{-2} mg/litre, of the polyacrylamide was prepared with deionised water. Aliquots (25ml) of each concentration were added to samples of calcium carbonate. The sealed tubes were subjected to end over end mixing (see figure 6.5) for two hours at 25°C in a thermostat, kept still for about 18 hours and shaken for a further two hours to ensure complete equilibrium. The solid was separated by centrifuging, then a portion of the supernatant liquid was pipetted off and analysed. Equation 6.4 was used to determine the surface excess, Γ the amount adsorbed per m^2.

$$\Gamma = \frac{V.\ \Delta c}{1000\ M.A.}\ mg/m^2 \quad \ldots\ldots\ldots\ldots\ldots\ldots\ 6.4$$

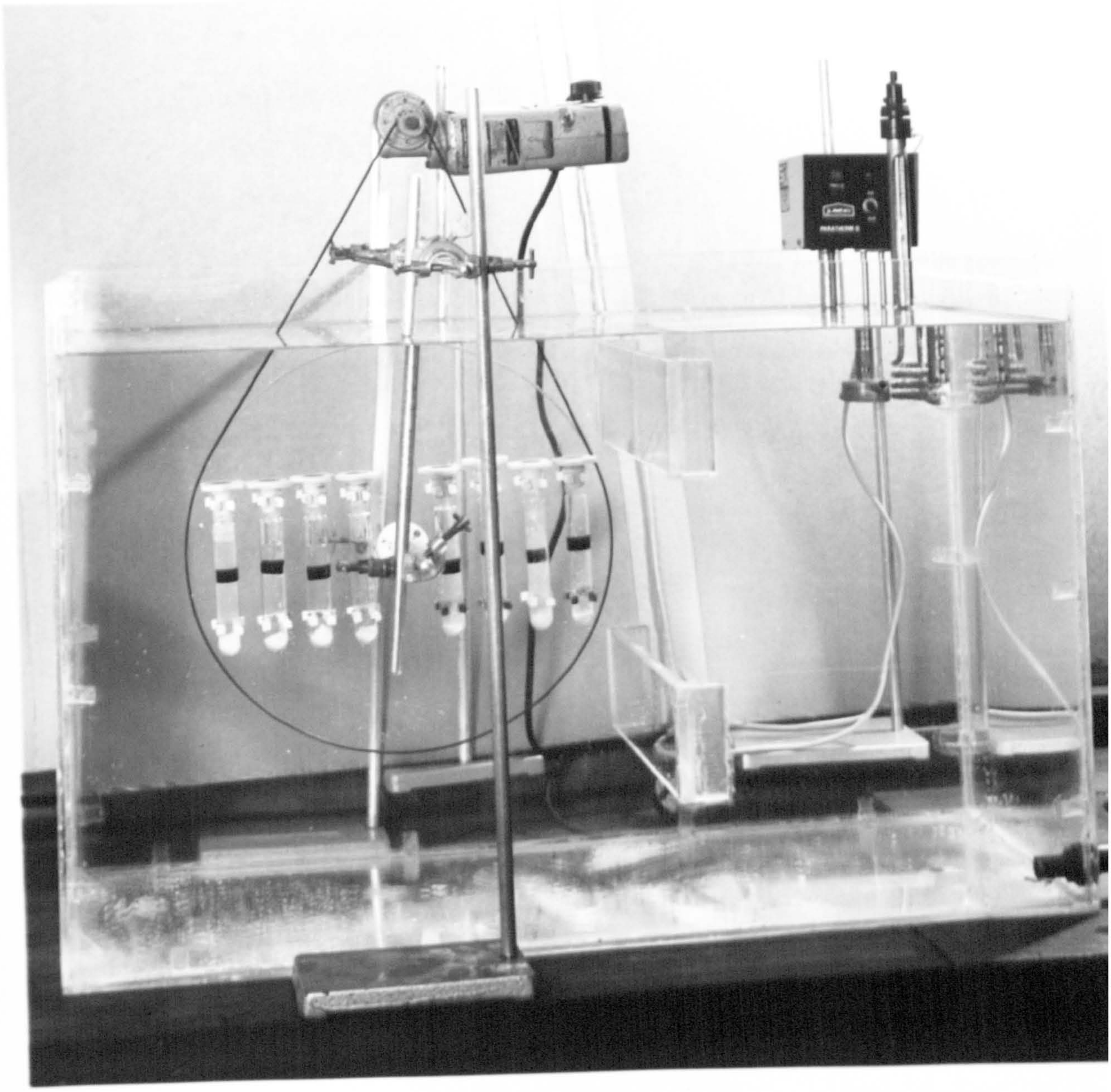

Fig. 6.5

where V = volume of liquid (25ml).

ΔC = concentration change (mg/l).

M = mass of adsorbent (1.0gm and 0.3gm).

A = specific surface area of adsorbent ($2.08m^2/gm$ and $3.81m^2/gm$) for natural and precipitated $CaCO_3$ respectively.

The surface excess, Γ , is plotted against the equilibrium concentration, C_e, of the adsorbate.

Turbidmetric techniques were employed for analysing the supernatant solutions. The Attia and Rubio[236] method was used for determination of cationic and non-ionic polyacrylamide and Crummett and Hummel[237] method for anionic polyacrylamide, as described below.

6.2.1.1 Determination of the Concentration of Solutions of Cationic and Non-ionic Polyacrylamide[236]

A 5ml aliquot of the centrifuged solution was pipetted off into a 50ml volumetric flask already containing 5ml of 0.1% (w/v) Tannic acid and 40ml of 0.1N. NaCl. The flask was shaken for about one minute by inverting end over end, and was then allowed to stand for a period of two hours before measuring the turbidity with the turbidimeter. Calibration curves of turbidity versus polyacrylamide concentration were constructed and are shown in figure 6.6 and 6.7. The turbidities were measured using a Brice-Phoenix light scattering photometer, type PP1. This turbidity is proportional to the scattering ratio which is the ratio of light scattered by a solution at 90° to the

Figure 6.6: Calibration Curve for Cationic Polymer FO 115 PD 1200.

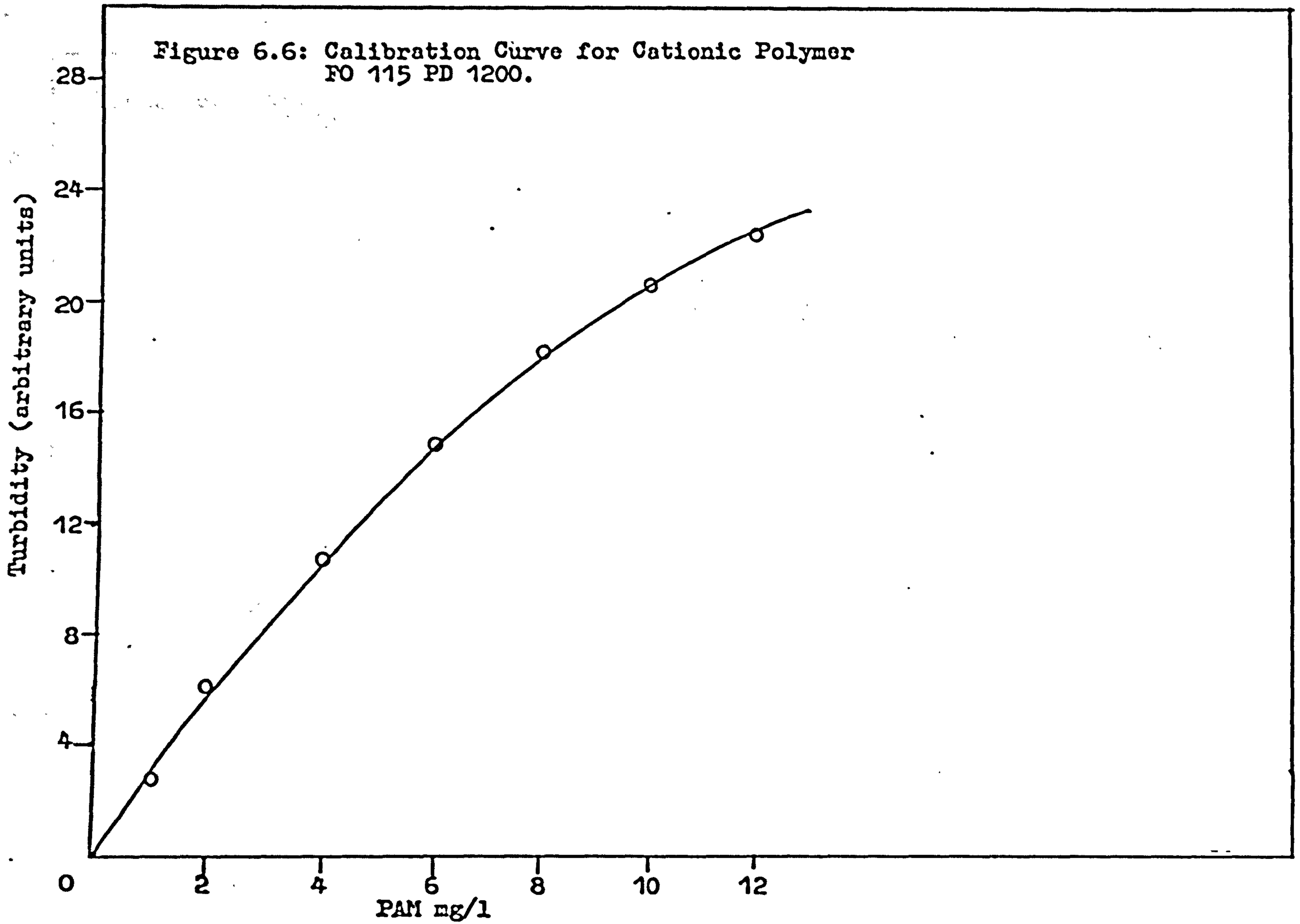

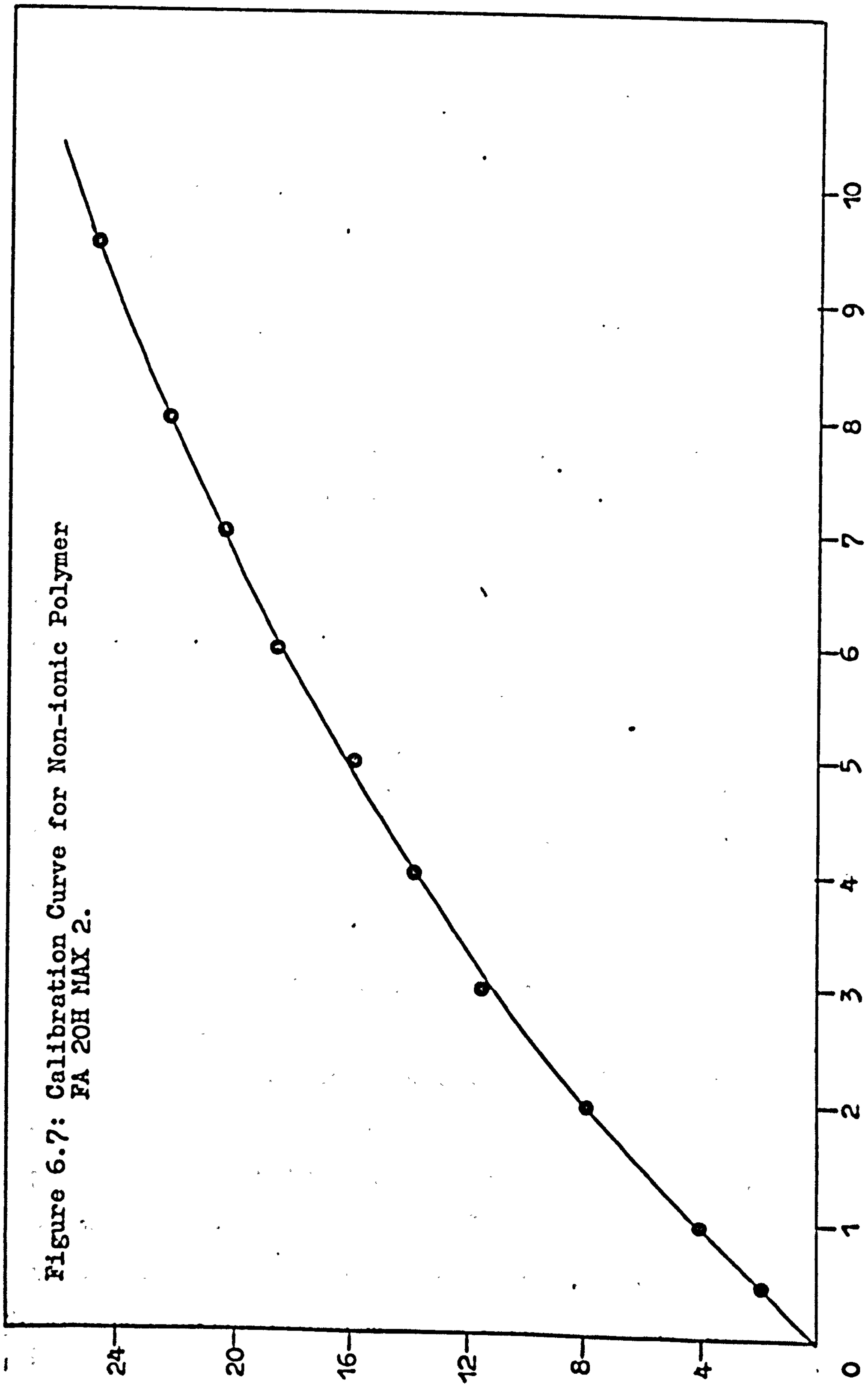

Figure 6.7: Calibration Curve for Non-ionic Polymer FA 20H MAX 2.

light transmitted at 0°.

6.2.1.2 Determination of the Concentration of Solutions of Anionic Polyacrylamide[237]

A 5ml aliquot of the centrifuged solution was pipetted in to a 100ml volumetric flask, diluted with deionised water and one ml of 10% (w/v) NaOH added. The flask was mixed and heated on a steam bath for 30 minutes. The solution was allowed to cool to room temperature and then neutralised with 0.1N HCl using phenolphthalein as indicator. One ml of 3% sodium citrate was then added and the solution was adjusted to 100ml volume with deionised water. The flask was mixed for about one minute by inverting and then one ml of 4% Hyamin (1622) was added and remixed by inverting end over end. The turbidity was measured after exactly 15 minutes. Results were read from a turbidity versus concentration graph (figure 6.8 and 6.9) made from solutions of known strength.

6.2.2 Adsorption of Humic Substances and Humic Acid Fraction

A range of concentrations, 0.1-1.5 v/v per cent of the concentrate, of humic substances and humic acid were prepared. Aliquots (25ml) of each concentration were added to one gm $CaCO_3$, dried at 110°C, and the adsorption technique was followed as described in 6.2.1.

Figure 6.8: Calibration Graph for Anionic Polymer FA 60H MAX 6.

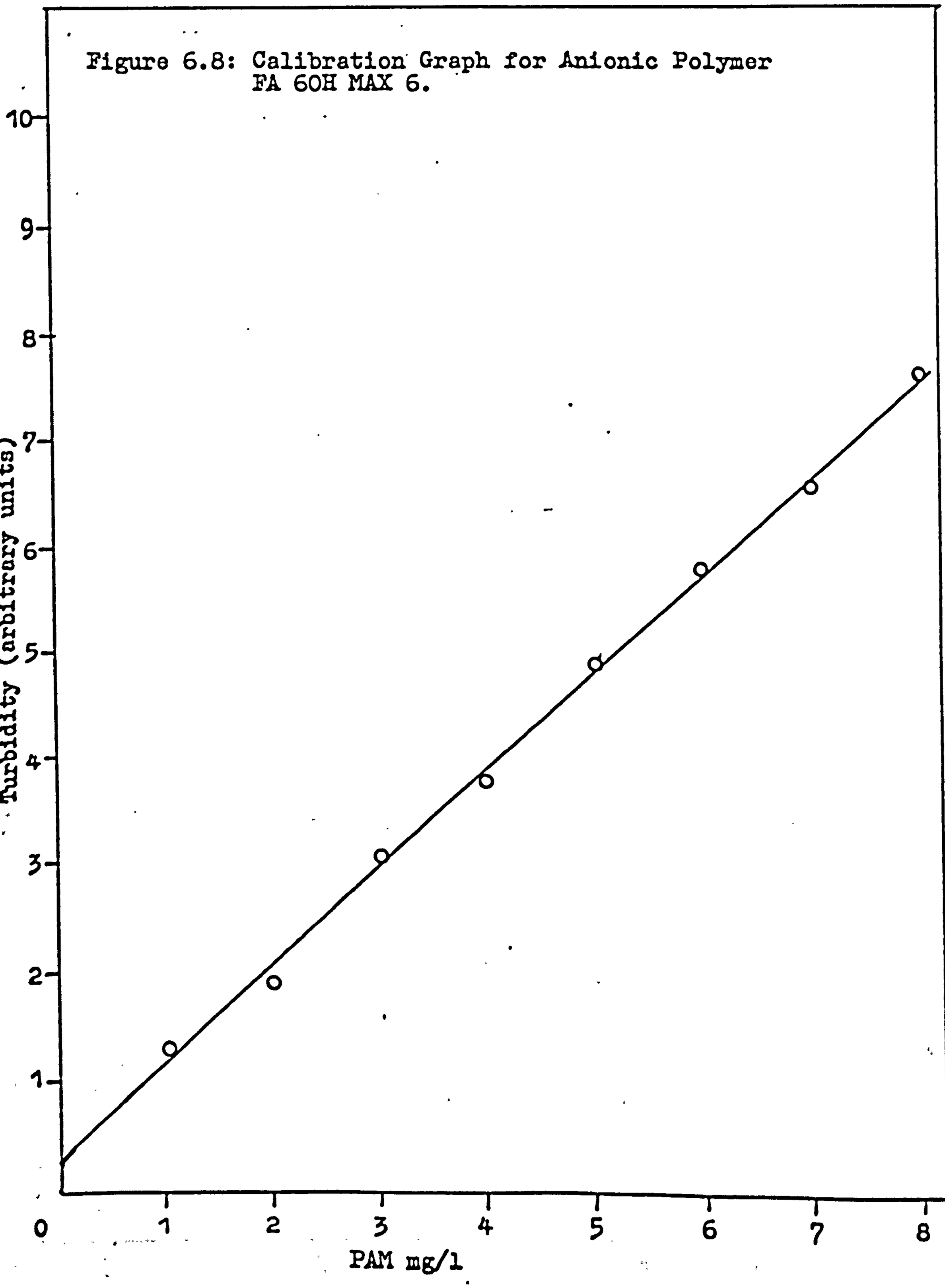

Figure 6.9: Calibration Graph for Anionic Polymer FA. 200-5

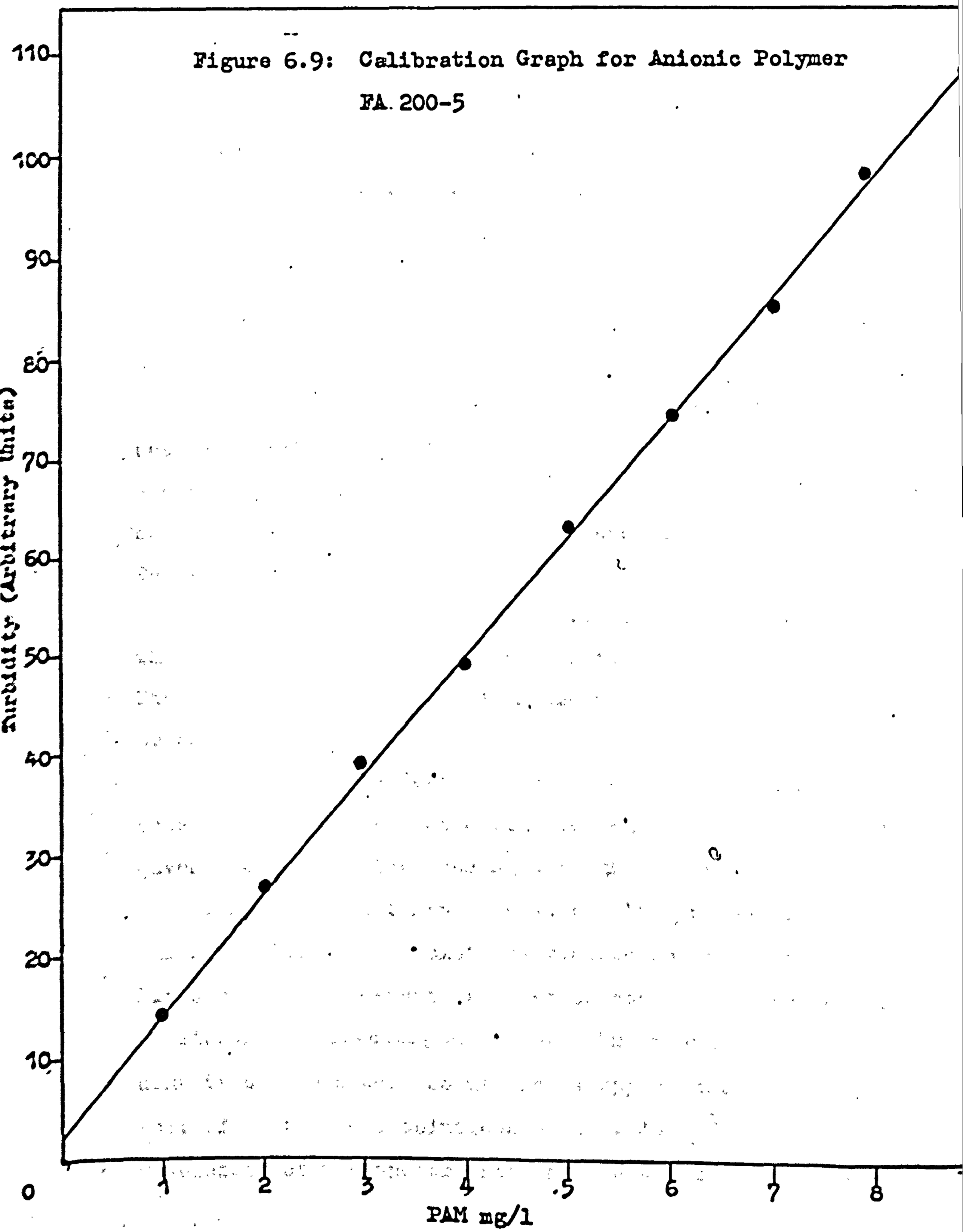

6.2.2.1 Determination of the Concentration Changes of Solutions Containing Humic Substances and Humic Acid

Solutions of humic substances and humic acid have a golden-yellow colour which developes a reddish tinge at high concentrations.

When a ray of monochromatic light of initial intensity Io passes through a solution in a tranparent vessel, some of the light is adsorbed so that the intensity of the transmitted light I is less than Io. The relationship between I and Io depends on the path length of the adsorbing medium, l, and the concentration of the adsorbing solution, C. These factors are related in a law known as Beer-Lambert law[75].

$$\log_{10} (Io/I) = \varepsilon C l \quad \ldots\ldots\ldots\ldots\ldots\ldots \quad 6.5$$

where ε = adsorption coefficient.

The expression $\log_{10} (Io/I)$ is known as the extinction, E, or adsorbence.

If the Beer-Lambert law is obeyed and l is kept constant, then a plot of extinction against concentration gives a straight line passing through the origin.

The spectrophotometer used in this work was a pye unicam SP·500 ultra-violet and visible spectrophotometer. Plots of optical density against concentration are reported as linear for wavelengths below 500m μm and the optical density of humic acid solutions is approximately double that of fulvic acid solutions at 300m μm[233]. The wavelength of the spectrophotometer was set to 300m μm and

calibration graphs for humic substances and humic acid (see figure 6.10) were constructed. Figure 6.11 shows that transmittance of the solutions obeyed the Beer-Lambert law.

An aliquot one ml of the centrifuged solutions of the adsorption experiments were pipetted into one cm cuvette and the transmittances were recorded. The concentrations of these aliquots were determined directly from the calibration graphs. The change in concentration, which corresponds to the amount associated with one gm $CaCO_3$, was then calculated.

6.3 Methods of Assessing Flocculation

The effectiveness of flocculation was determined on $CaCO_3$-polyacrylamide suspension by two most common laboratory methods used to evaluate the optimum concentration of polyacrylamide for flocculation and to prove that flocculation does occur. The reproducibility of the technique used will be discussed in the results section.

6.3.1 Capillary Suction Time (C.S.T.)

This test was invented by Baskerville and Gale[238] for laboratory assessment of the conditioning of sewage sludges.

The principle of this method is that filtration is achieved by the "suction" applied by the capillary action of an adsorbent paper (Whatman's chromatography paper, Grade 71) and the capillary suction time is the time taken by the spreading liquid front to pass between marks of radii of

Figure 6.10

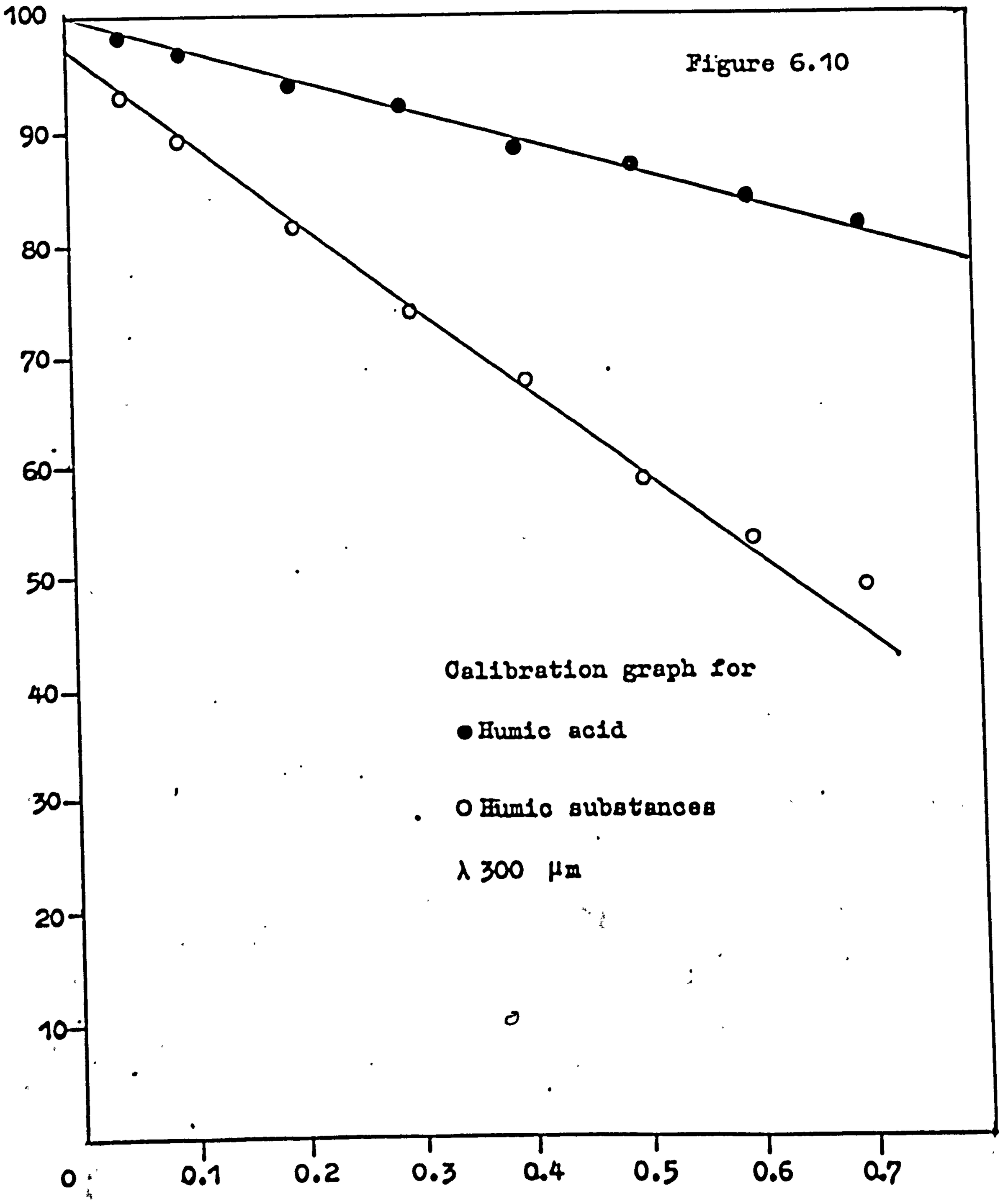
100
90
80
70
60
50
40
30
20
10
Transmittance
0
0.1
0.2
0.3
0.4
0.5
0.6
0.7
% Humic Concentrate
Calibration graph for
● Humic acid
○ Humic substances
λ 300 μm

Figure 6.11

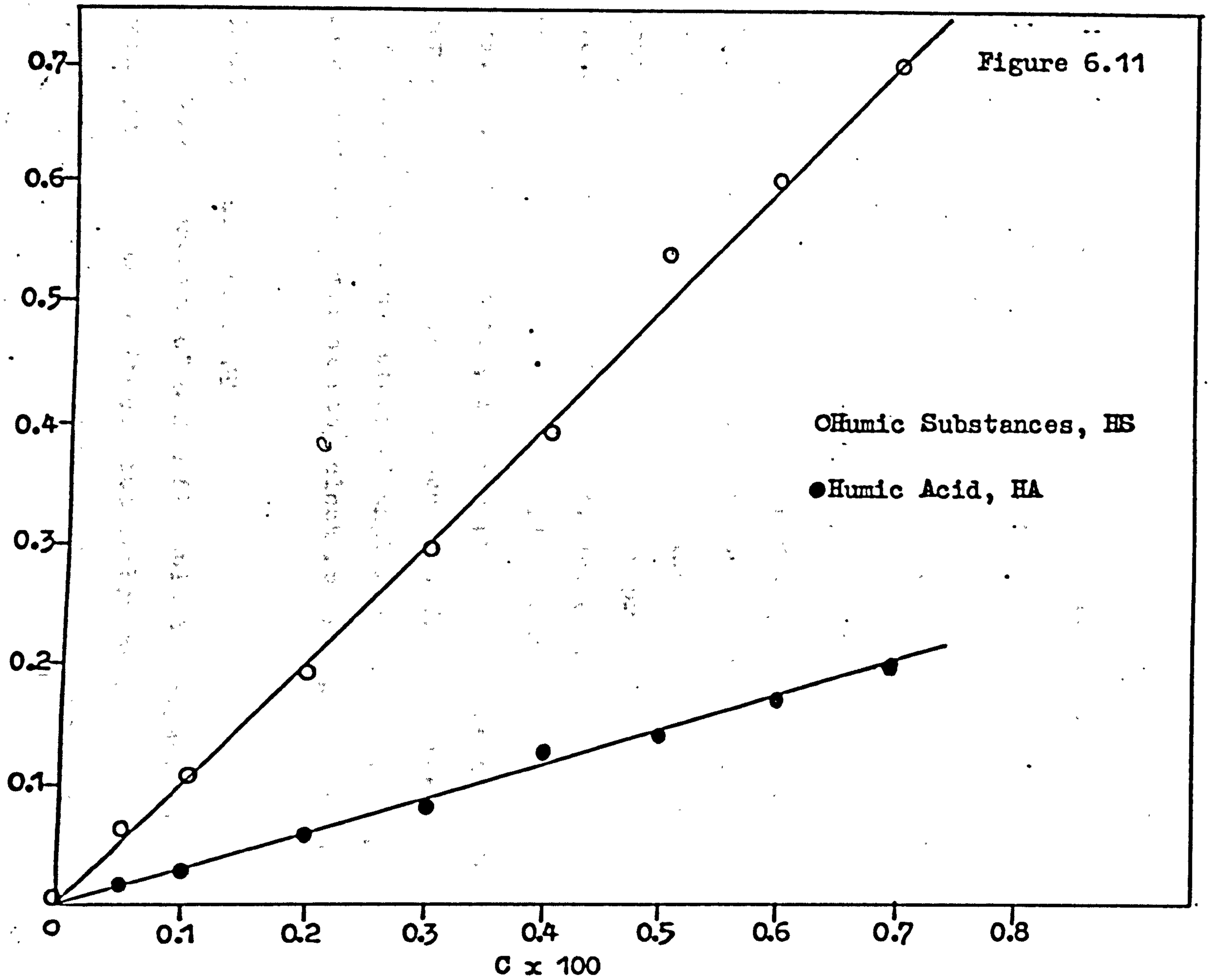

C x 100	$-\log T_{H.S}$	$-\log T_{H.A}$
0.7	0.713	0.198
0.6	0.616	0.174
0.5	0.545	0.139
0.4	0.393	0.128
0.3	0.301	0.083
0.2	0.195	0.062
0.1	0.111	0.030
0.05	0.073	0.020

3.2cm and 4.5cm.

The instrument consists of two separate components, (see figure 6.12) the filtration apparatus and the automatic time recording unit including its start/stop control amplifier. The former is a rectangular piece of adsorbent filter paper measuring 7 by 9 cms, sandwiched between two rectangular pieces of perspex. In the centre of the upper perspex block is a circular hole in which a stainless steel cylinder (1.90cms external diameter, 1.80cms bore and 2.5cms high) loosely fits. This rests on the paper and serves as a sludge reservoir. On the underside of the upper perspex block are two engraved circles of diameters 3.2 and 4.5cms concentric with the reservoir. This upper block stands clear of the paper by standing on five stainless steel supports, 1A, 1B, 2, 3, and 4 in the diagram. 1A and 1B are specially machined probes in line with the first concentric circle and 2 is a similar probe in line with the second concentric circle. Electrical connections are made to these probes through screws which lead to the terminal box. The other two supports are provided to hold the block parallel with the paper. Connections from the terminal box are made to the transistorised amplifier which is coupled to a digital electrical stop clock recording in seconds.

6.3.1.1 <u>C.S.T. Technique</u>

Varying amounts of 0.05% flocculant (polyacrylamides) were added to 50ml of 4% calcium carbonate solution and these were left for ten minutes before another 50ml of

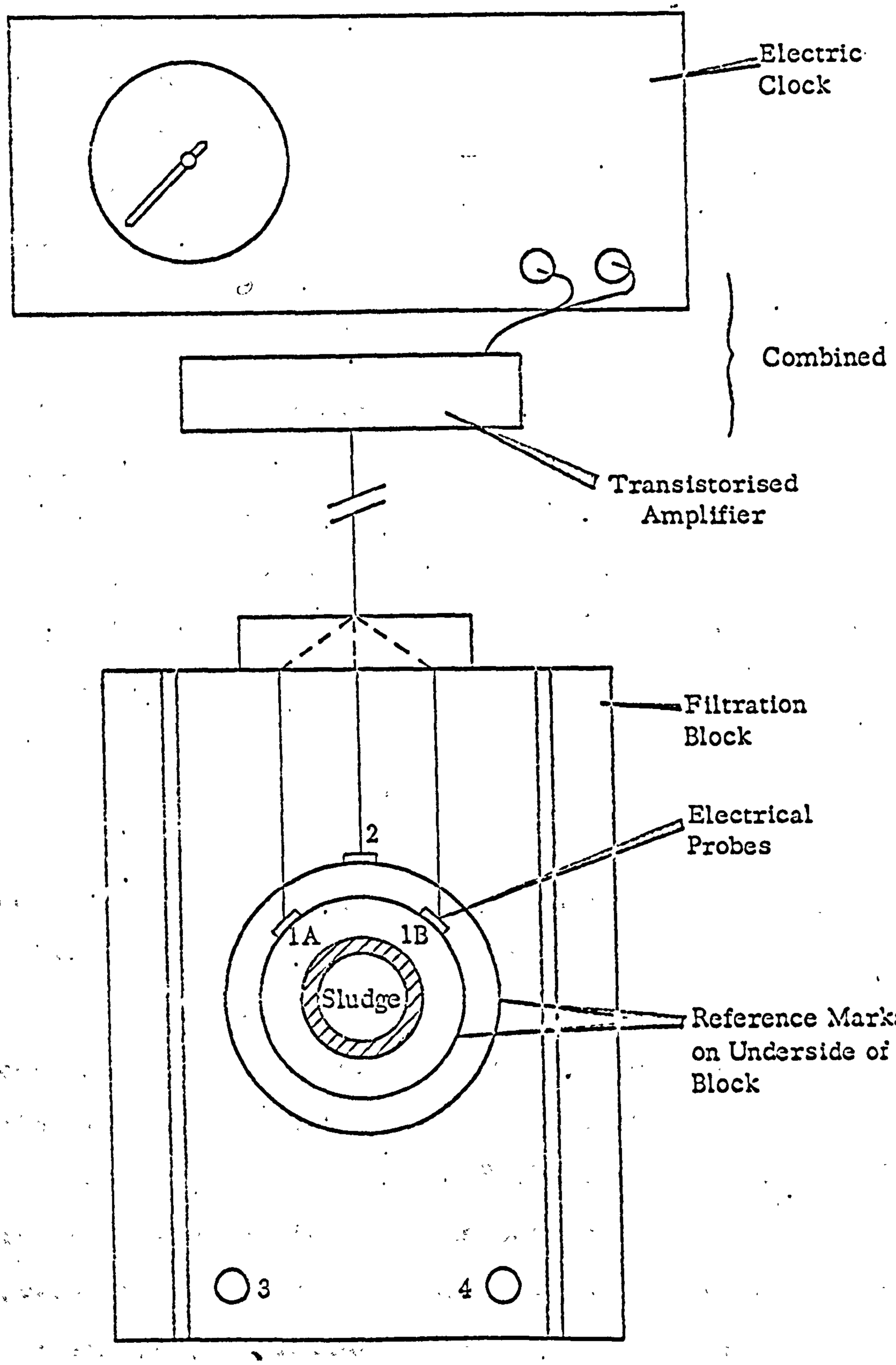
Electric Clock
Combined
Transistorised Amplifier
Filtration Block
Electrical Probes
Reference Marks on Underside of Block
2
1A
1B
Sludge
3
4

Figure 6.12

chalk solution were added. The 100ml solutions, after three inversions, were left to stand for a further five minutes. Following three more inversions, five separate readings on the C.S.T. apparatus were taken. The averages were calculated and a graph of C.S.T. seconds versus polyacrylamide concentration was plotted.

6.3.2 Sedimentation

All sedimentations were carried out in a two litre stoppered measuring cylinder with an internal diameter of 7.5cm. For a two litre suspension the ratio of suspension height to cylinder radius was 5.9 which was in the range 5-9 which Oliver[239] and Kwatra etal[240] have reported to be the best suited for hindered settling experiments.

6.3.2.1 Sedimentation Procedure

A two litre suspension of 4% calcium carbonate was prepared in a stoppered measuring cylinder. The suspension was dispersed by inverting the cylinder several times. The required polyacrylamide concentration was then added to the suspension in the cylinder and the cylinder stoppered and inverted for three times. The sedimentation time to a fixed point was then measured. Following three more inversions, five separate sedimentation times were taken. The averages were calculated and a graph of sedimentation time versus polyacrylamide concentration was drawn.

6.4 Precipitation of Calcium Carbonate

6.4.1 Apparatus

The apparatus is shown in figure 6.13. The precipitation cell consisted of a three litre round-bottom flat flange flask fitted with a five standard neck lid carrying an epoxy-resin coated anchor shape stirring bar (shaft diameter 6.0mm and paddle dimensions are 100mm x 20mm), the stirrer passing through the central neck and is driven by a geared AC motor with a variable speed controller (Heidolph type 50 111). A nitrogen gas lead-in tube was fitted to the centre of the flask and could be effected by the flushing of nitrogen through the cell to remove carbon-dioxide. Calcium electrode model (Phillips IS 561-Ca^{2+}), single junction reference electrode (ORION model 90-01) and glass electrode (model 33 1160 200) were also fitted in to the flask.

The precipitation cell was suspended from a metal frame in a 20 litre water bath with glass sides (Townson and Mercer Ltd., Croydon) E 270, series II. The temperature of the bath was thermostatically controlled to $\pm$ 0.02°C with the aid of a heater and a refrigeration unit. All the experiments were carried out at 25$\pm$ 0.02°C. A high precision thermometer of the range 21-27°C (0.01 division) was used. A lamp was placed at the rear of the bath to illuminate the solution.

6.4.1.1 pH

The pH changes accompanying calcium carbonate

Fig. 6.13

crystallisation were followed using EIL 7030 Model pH meter (±0.1mV) 0.02 pH on 3pH scale, with an EIL combination electrode. The electrode system was calibrated before each experiment with NBS standard buffer solutions, covering the pH range of interest. The decrease in solution pH during crystallisation raises the pCO_2 of the supersaturated solution causing a net loss of CO_2 from the solution.

6.4.1.2 Calcium Specific Electrode

Of the various ways to follow a precipitation process (see 4.8.1), the continuous measuring of the change in calcium ion concentration by using a calcium specific electrode was chosen.

A calcium specific electrode Model (Phillips IS 561-Ca^{++}) was purchased. This type of probe is made by incorporating a liquid ion exchange into a polyvinylchloride matrix (see figure 6.14). Unfortunately, for unknown reasons, this electrode exhibited about half the Nernstian potential, continually drifted and had a very slow response.

An ORION calcium ion electrode model 92-20 was then borrowed from Ratcliffe Power Station. The Orion membrane system is based on a millipore filter diaphragm 0.076mm thick with 'wick' pores (about 0.1 microns in diameter) which are filled by the liquid ion exchanges (Calcium dialkylphosphate). This system exhibited a very good response time (<1 minute) with Nernstian potential of 29 mV/PCa over the range 10^{-2} to 10^{-5}M. However, this electrode was found to be very noisy. The reason for this

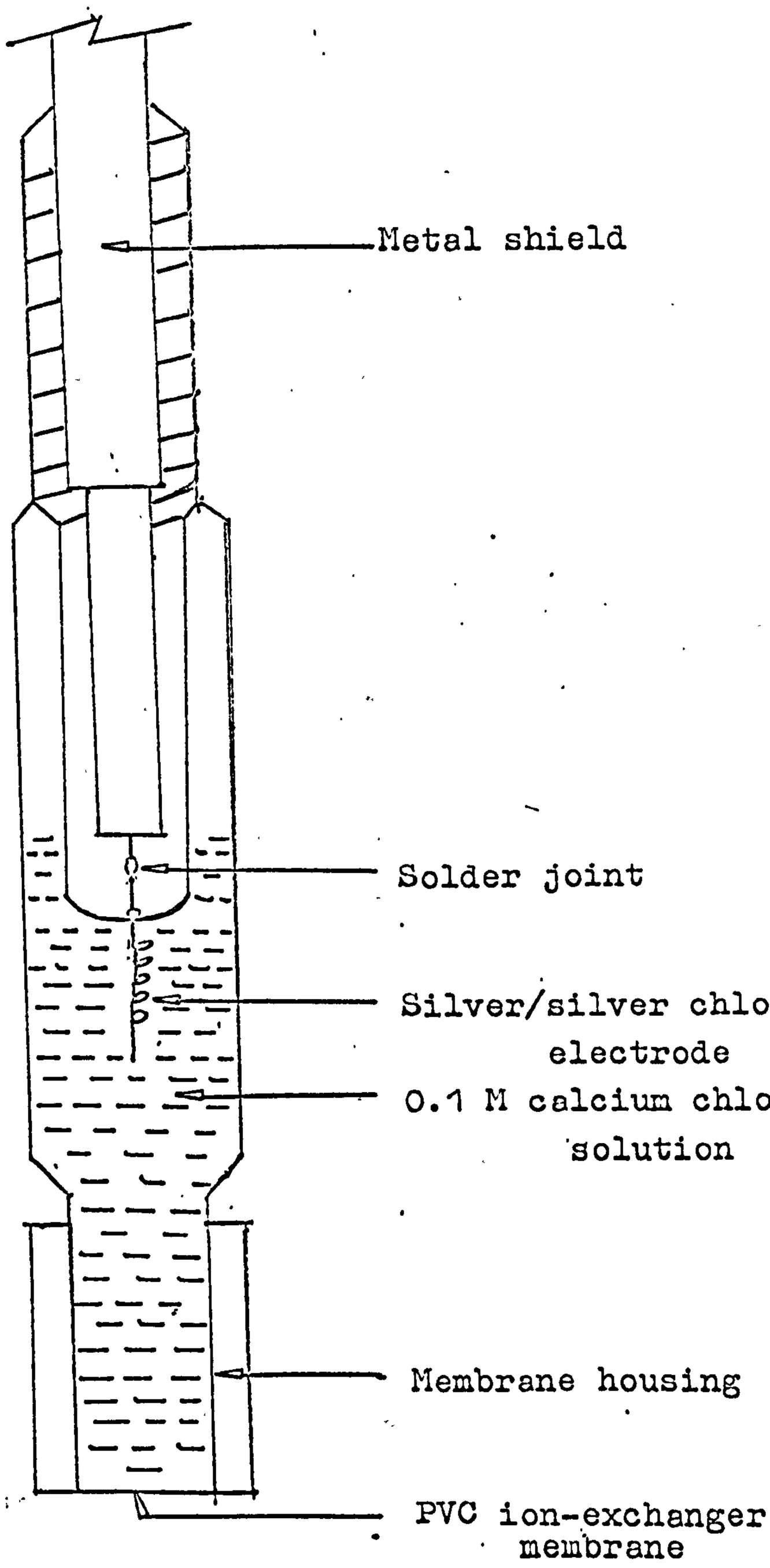

Figure 6.14

The Ca^{++}-Electrode Assembly

noise was most likely the lack of an electrically-screened metal shield as was present in the 561-Ca^{++} electrode.

Therefore, it was recommended[241] to use a home-made membrane. 0.4gm of ion-exchanger solution (Calcium dialkylphosphate) standard Orion 92-20-02 and 0.17gm of PVC[242] were dissolved in about 6ml tetrahydrofurane and poured into a 28mm i.d. glass ring resting on a sheet of plate glass. The ring was covered with a pad of filter paper with a heavy weight on top. The assembly was left for 48 hours to allow slow solvent evaporation. The resulting membrane was about 0.5mm thick. A 6mm disc cut from the membrane was then centred on the 6mm outer diameter membrane packing piece of the Phillips electrode (see figure 6.14). The membranes were tough, resilient and flexible. This system exhibited correct Nernstian potential with a response time of <1 minute in the range of 5-11 pH. The membrane lasted for at least 75 measuring hours.

The home-made membrane electrode and a single junction type reference electrode (Orion 90-01) together with EIL pH meter (Model 7050, ± 0.1mV), were used to follow the change in calcium concentration. The measurements were made on the logarithmic concentration scale. Two standards of calcium chloride solutions were required to set up the instruction scale length.

6.5 Factors Affecting the Choice of Experimental Technique

The apparatus and materials adopted in this study was basically that described earlier in this chapter. In each

run the relevant volumes of calcium bicarbonate and the corresponding stoichiometric amount of calcium hydroxide were pipetted into a three litre round-bottom flask and separating funnel respectively. The amount of water necessary to dilute the reaction mixture to the desired supersaturation was added to the three litre round-bottom flask suspended in the water bath (25.0 $\pm$ 0.02°C). A sample calculation for achieving the level of supersaturation is shown in Appendix 1. To maintain a constant hydrodynamic conditions in the precipitation studies, a constant volume of reaction mixture was used. This volume, $\simeq$ two litre, was sufficient to keep the measuring electrodes immersed in the solution and also to prevent air entrainment at the agitator speed selected for the experiments.

The reactant solutions were first placed in a thermostat bath for two hours to reach the working temperature. The calcium hydroxide solution was poured into the reaction vessel via a tube reaching the centre of the reaction vessel (see figure 6.13) and the stirrer was started (speed was 120 $\pm$ 10 r.p.m.). At the same time the stop watch was started and the calcium concentration and the pH were followed by reading the meters indicating the calcium electrode and glass electrode potentials.

A lamp was placed behind the bath to illuminate the solution so that the visible onset of precipitation might be recorded. Precipitation was allowed to continue until no significant change in calcium ion concentration over at least one hour had been observed. The suspension was taken

out of the bath and filtered through a 0.2 microns membrane filter. The crystals were washed with deionised water and dried in a desiccator. The crystal size distributions were measured by the Coulter Counter technique using a 100 microns orifice tube.

6.6 Determination of Crystal Size Using A Coulter Counter

6.6.1 Coulter Counter Theory

A TA-II Coulter Counter with sampling stand, population accessory and X-Y recorder was used to measure and record the crystal size distributions. The complete set-up is shown in figure 6.15.

The Coulter Counter determines the number and size of particles suspended in an electrically conductive liquid. This is done by forcing the suspension to flow through a small aperture having an immersed electrode on either side.

As a particle passes through the aperture, it changes the resistance between the electrode. This produces a voltage pulse of short duration having a magnitude proportional to particle volume. The series of pulses is then electronically scaled and counted into 16 different size ranges.

The model TA-II allows sampling of a specified volume (0.5, 1.0, 2.0ml), a specified count, or a specified time. The results are displayed in terms of a differential size distribution or a cumulative size distribution based on volume. The user can then record the results on a data sheet or plot them automatically with an X-Y recorder.

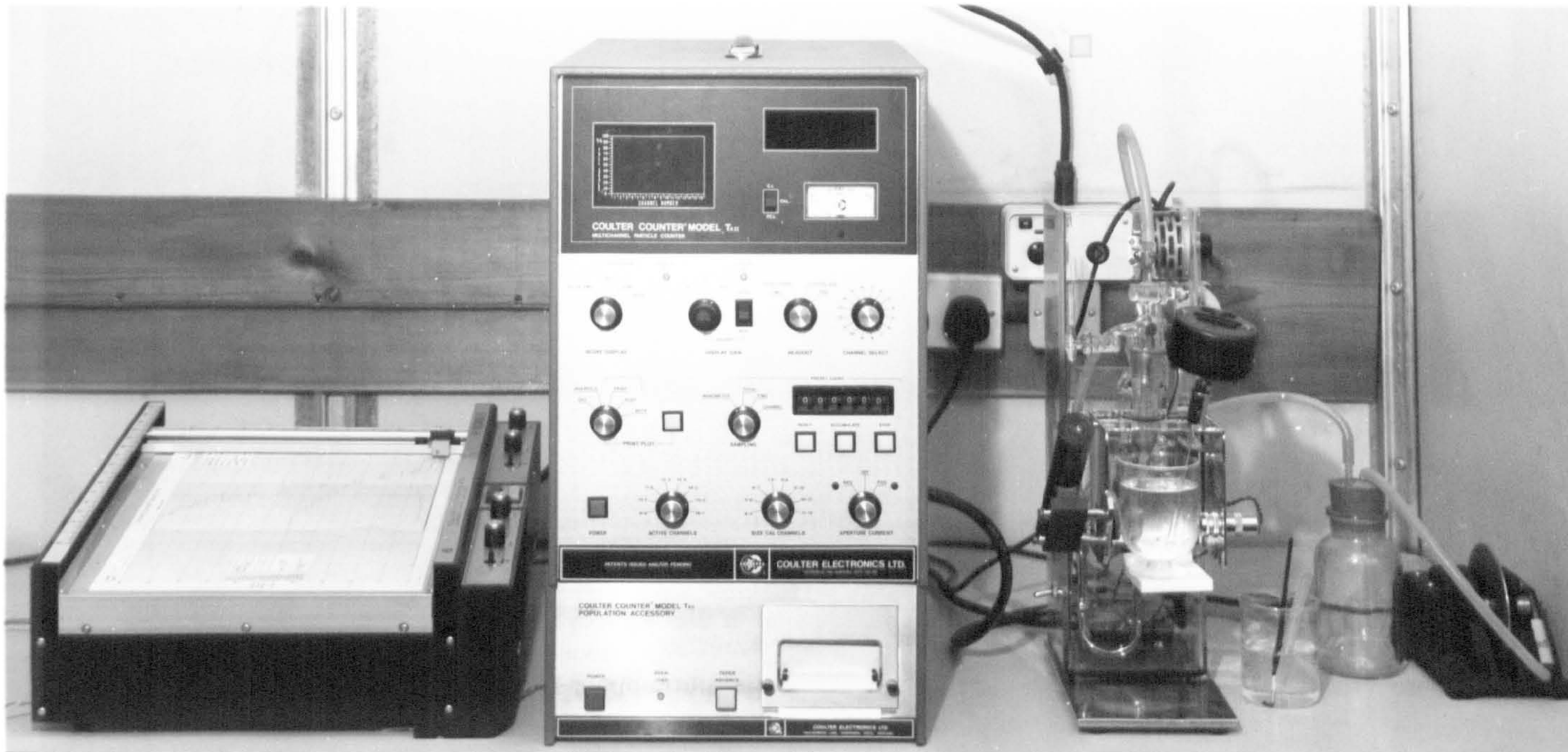
COULTER COUNTER MODEL T₄₃
COULTER ELECTRONICS LTD
COULTER COUNTER MODEL T₄₃
POPULATION ACCESSORY

Fig. 6.15

6.6.2 Choice of Electrolyte

The electrolyte recommended[243] (0.9% NaCl and 4% Trisodium phosphate) cannot be used because of harming effects of polyphosphate on calcium carbonate[191,244]. The best electrolyte and its proper strength was found to be 1% NaCl (w/v) in saturated calcium carbonate solution. Filtration through 0.2 microns membrane filter is the most important outside aspect of the Coulter Counter. It is essential that the background count from the electrolyte be as low as is practicable. A preservative 0.1% (w/v) sodium azide (NaN_3) was added to aqueous electrolytes before filtration to prevent micro-organism growth. Dispex N40 (0.1% w/v) was also added to the electrolytes before filtration to enhance the stabilisation of the particles.

6.6.3 Calibration of the Orifice Tube

A 100 microns aperture tube was used for the analysis. The 100 microns refers to the diameter of the aperture through which the sample is drawn. Any one crystal larger than 100 microns would plug the aperture. The full range of accuracy for the aperture tube is between 2% and 40% of the aperture diameter. Therefore, the best calibration standard to employ is one which falls between 5% and 20% of the aperture diameter. D.V.B. Latex with an average diameter of 8.99 microns was chosen as the calibration standard. The 100 microns aperture tube was calibrated several times with identical results, so the settings obtained were taken to be correct. The calibration

procedure was obtained from the manual[243].

6.6.4 Coulter Counter Sampling

After the crystallisation had started, sampling was begun. A 50ml sample was withdrawn from the crystallisation vessel and immediately diluted with 100ml of the electrolytes solution. The sample from the crystalliser had to be diluted in order to get accurate results. If the sample has too many crystals per ml, it is likely that one will get coincident passage through the aperture. The proper dilution was found that 2:1 dilution was sufficient.

The sample was then placed on the sampling stand of the Coulter Counter. As soon as it was determined that there was not excessive noise, the count was begun. The Coulter Counter model TA-II offers several modes of operation. In the manometer mode a sample of either 0.5, 1.0, or 2.0ml can be drawn. The Coulter Counter will record the volume per cent of each size and the total number of crystals counted. Because counts per unit volume were needed the manometer mode seemed to be the most convenient and accurate. With the 100 microns aperture tube 2ml of sample provided enough counts for reliable statistical results.

CHAPTER SEVEN

Results and Discussion

Characterisation of High Molecular Weight Substances

7.1 Adsorption of Flocculant Polymers

The results of the adsorption experiments of high molecular weight polymers are shown in figure 7.1 and 7.2. The adsorption isotherm results for the cationic and nonionic polymers are of the Langmuir type, consisting of a rapid rise in adsorption followed by a plateau region, the so-called monolayer region such that no more polymer can be adsorbed. A similar type of isotherm was obtained by Akram[228] using Dispex N-40 as adsorbate (see figure 7.3). It can be seen from figure 7.1 and 7.2, if one assumes monolayer coverage and applying equation 6.4, that the surface excesses, Γ , are shown in Table 7.1.

Table 7.1

High Molecular Weight Substances	Surface Excesses, Γ , mg/m^2	
	Natural $CaCO_3$	Precipitated $CaCO_3$
FO 115 PD 1200	1.4	1.5
FA 20H MAX 2	1.5	1.3

There is reasonable agreement between the surface excesses on precipitated and natural calcite for a given adsorbate. During the adsorption experiments it was noted that the natural calcite wetted relatively easily whereas the precipitated material did so much less readily. Care was

Figure 7.1

Adsorption of High Molecular Weight Polymer onto Natural $CaCO_3$

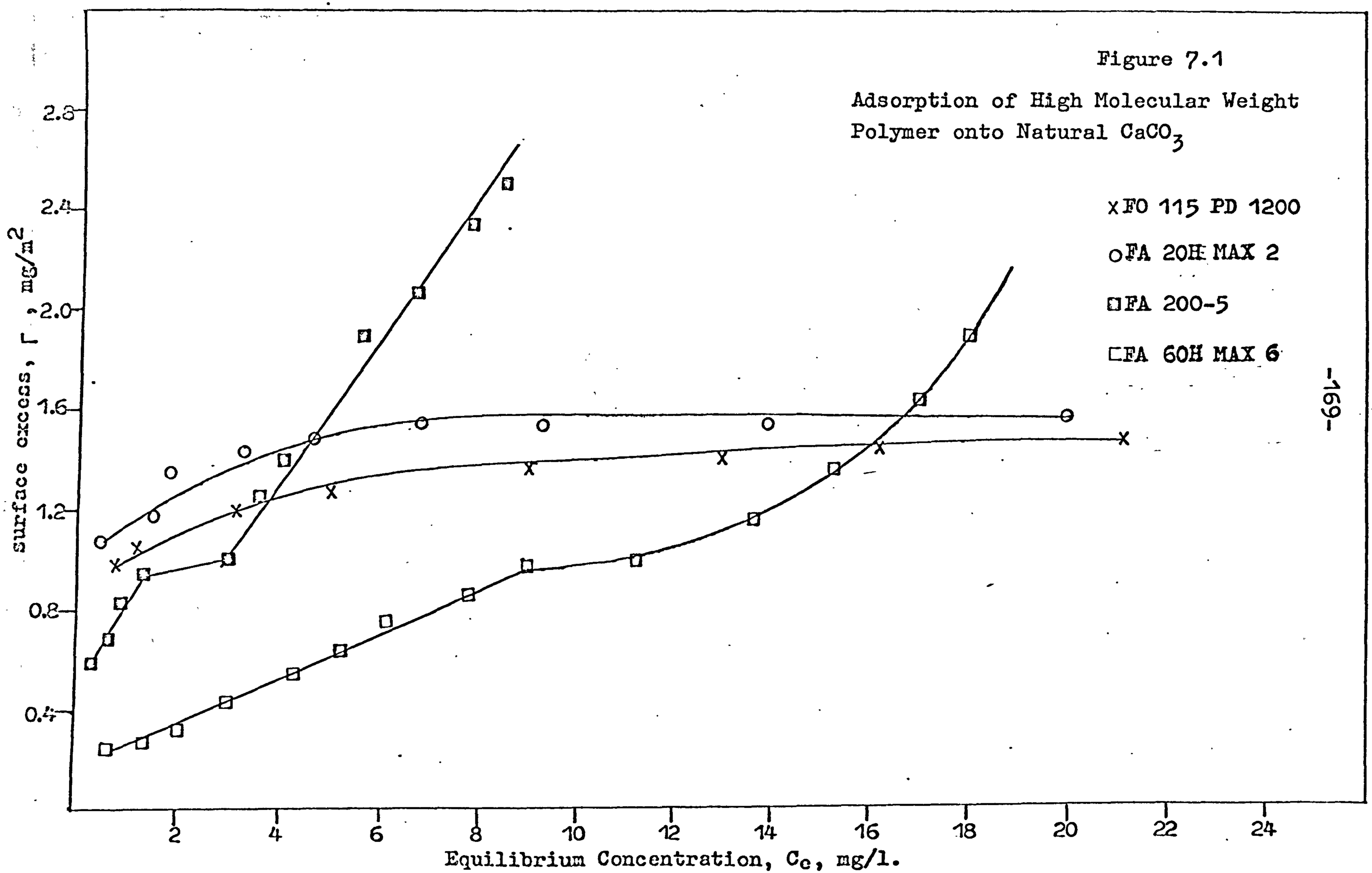

Figure 7.2

Adsorption of High Molecular Weight Polymer onto Precipitated $CaCO_3$

X FO 115 PD 1200

O FA 20H MAX 2

□ FA 60H MAX 6

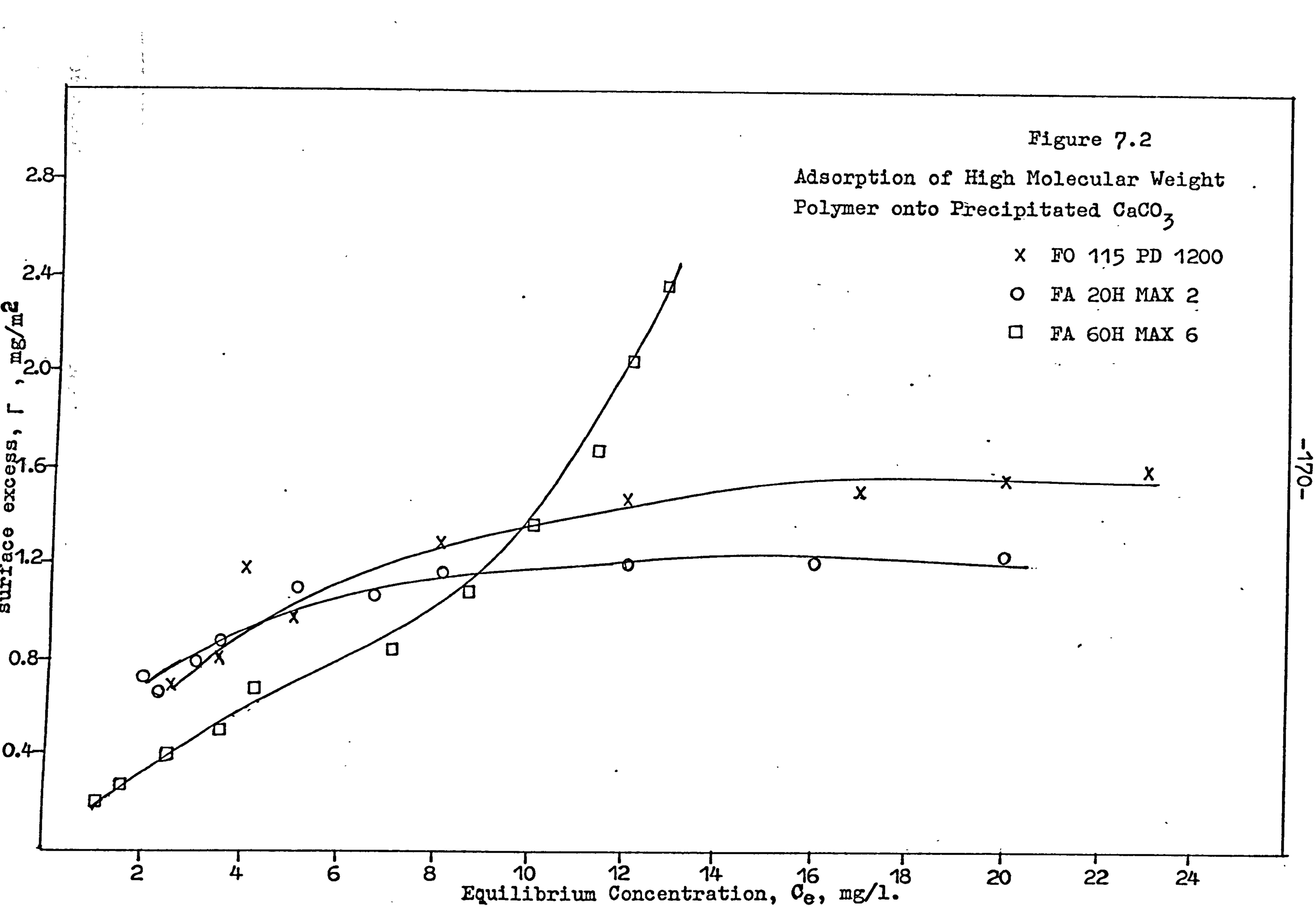

Figure 7.3

Adsorption of Dispex N-40
on Natural $CaCO_3$

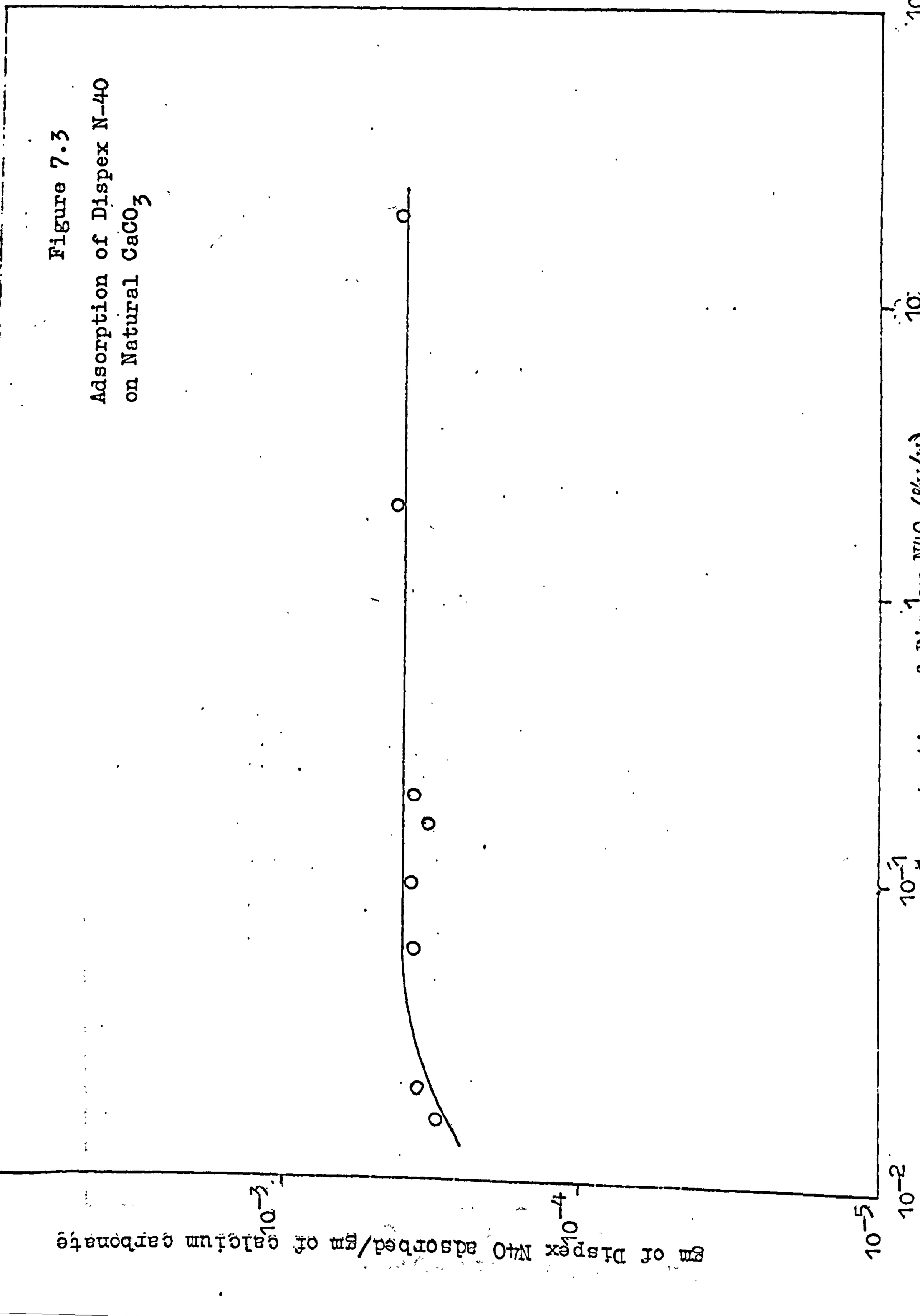

Figure 7.4: Adsorption of Humic Acid on $CaCO_3$

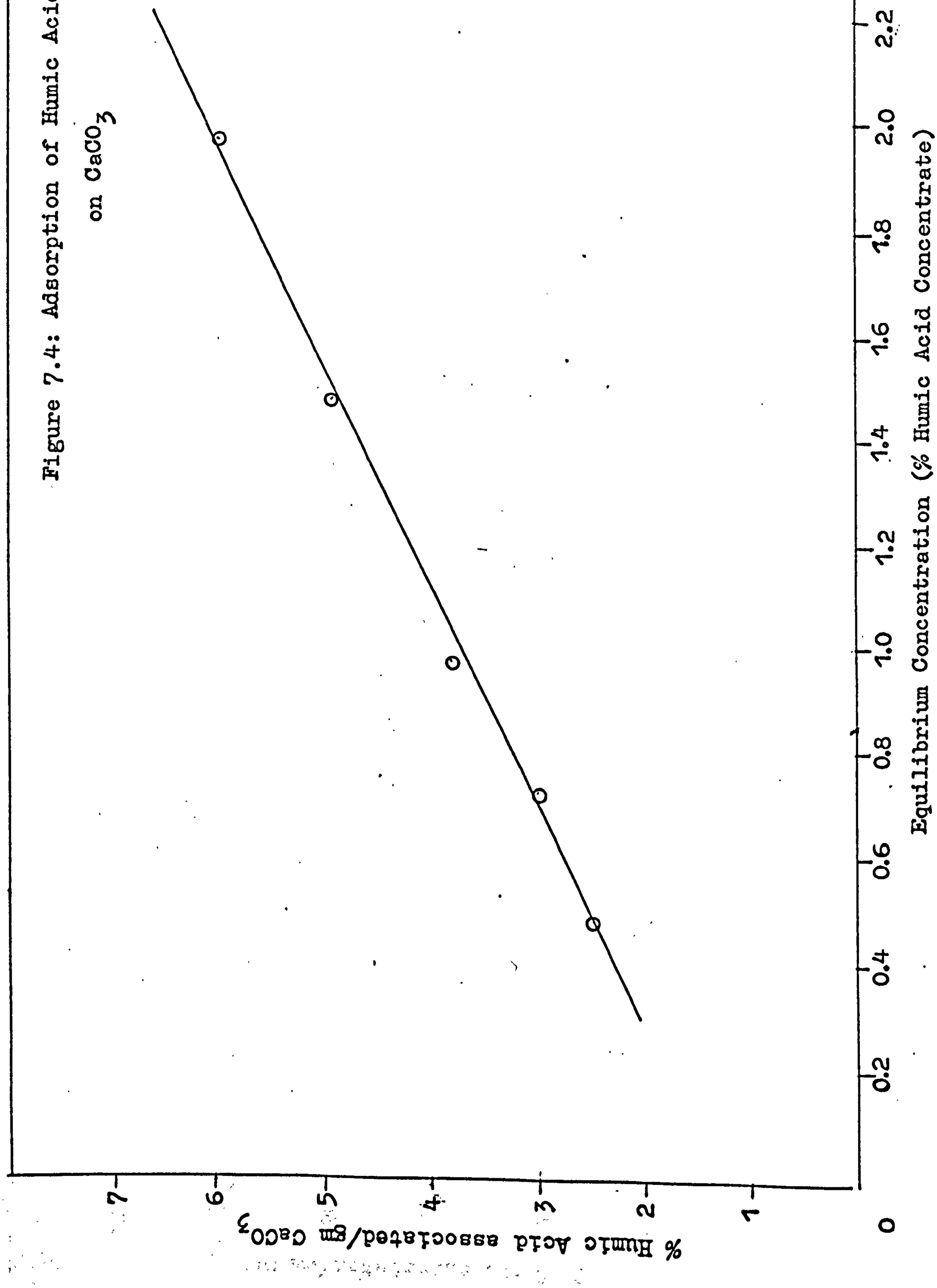

Figure 7.5: Adsorption of Humic Substances on $CaCO_3$

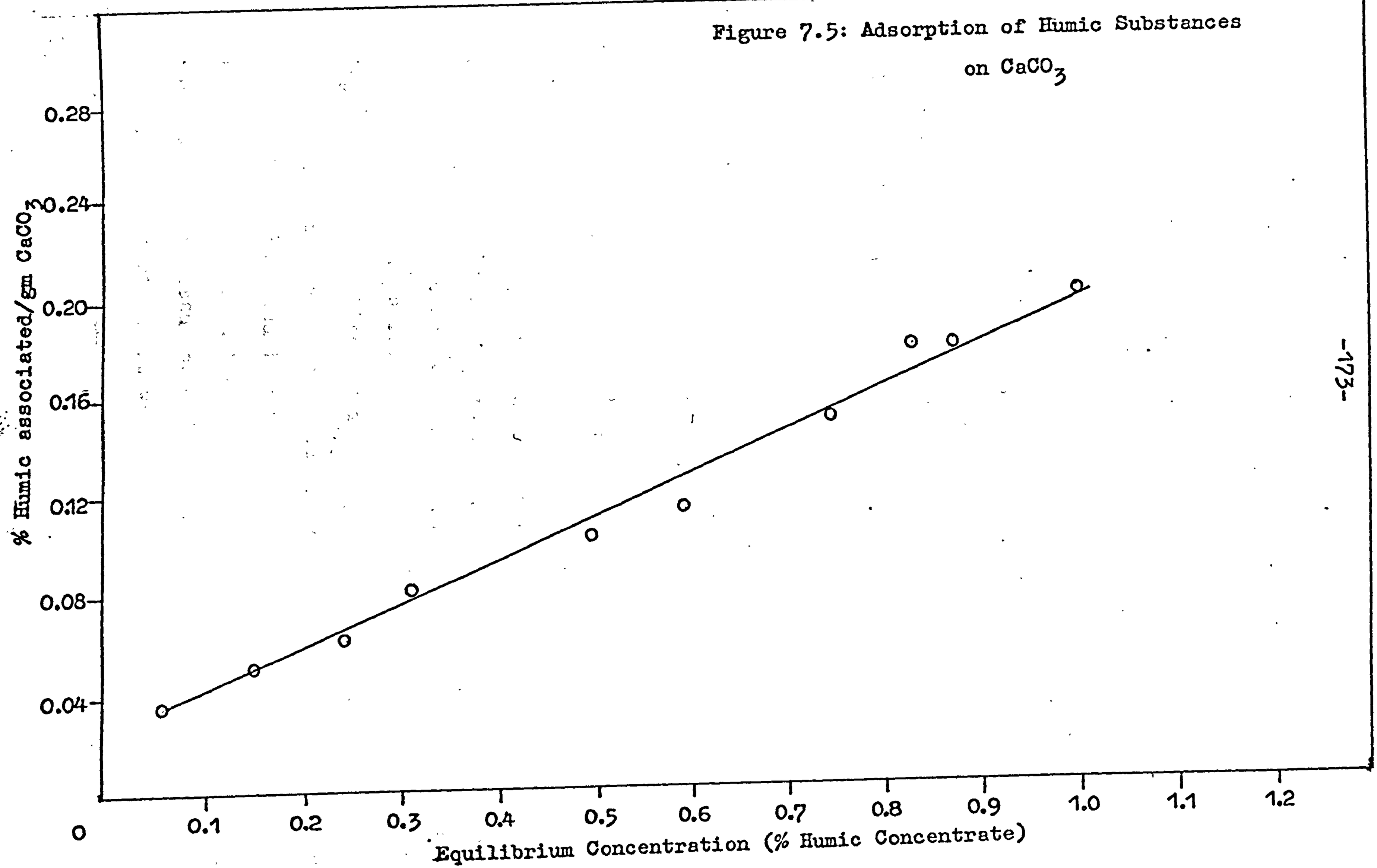

taken to ensure that the precipitated calcite was not surface treated, and was stated by the manufacturers to be calcite. The differences in wetting behaviour cannot be explained on the evidence available.

The surface excesses shown in table 7.1 are typical of those found for many types of high molecular weight polymer. Figures 7.1 to 7.5 also show the isotherms for the anionic and high anionic polyacrylamide materials and humic acid and humic substance (see 6.1.6). These isotherms do not show the plateau associated with a saturated monolayer but continuing adsorption appears to be occurring with increasing solution concentration. This may be due to multilayer adsorption or the formation of insoluble complexes that are removed during centrifugation prior to analysis or to soluble complexes in which the chemical bonding is such that the substances do not respond to the analytical method used. Riley[229] found an isotherm of this type for lauric acid on calcium carbonate and it is well known that calcium laurate is an insoluble soap. The stability of this soap is such that lauric acid would bind the calcium ion in solution equilibrium with the calcite (approximate solubility 6.3×10^{-3} gm/l), causing more ion to dissolve while a new equilibrium was attained.

It had been noted in the adsorption experiments with the anionic flocculant that at concentrations in excess of those where a plateau would be expected, a haze was present in the supernatant liquid which did not centrifuge down. One consequence of this haze was interference with the

turbidmetric method of analysis.

Further experiments were carried out to check on the origin of the non-plateau isotherms. During the humic substance adsorption experiments where analysis was by optical adsorption at 300m μm an increase in adsorption with time was noted (see figure 7.6). If the system had reached adsorptiom equilibrium this would not have been expected. The increase must have been due to either desorption of previously adsorbed material or to the formation of a soluble complex with a greater adsorption coefficient at 300m μm. To check this full ultra violet adsorption spectra were taken at increasing time intervals. As seen in figures 7.7 and 7.8 a hump appears at about 300m μm after 48 hours. The existence of this hump confirms the previous finding and is circumstantial evidence of a change in the nature of the soluble ultra violet adsorbing species present.

Direct addition of Ca^{++} to humic substance and the polyacrylamides was them used to test for complex formation. Calcium chloride solution was added to a solution of the substance to be tested, the Ca^{++} level being monitored with time using the Ca^{++} selective electrode. The results are shown in figures 7.9 and 7.10. For the nonionic PAM Ca^{++} was added in increments to 5×10^{-4}, 8.4×10^{-4}, and 11.5×10^{-4}M. These measured values agree well with the quantities added. It can be seen from the graph that after 30, 60 and 200 minutes respectively, there was no change in measured Ca^{++}. Similarly with the cationic polyacrylamide

Figure 7.6

Optical Adsorption of Humic Substance at 300m μm

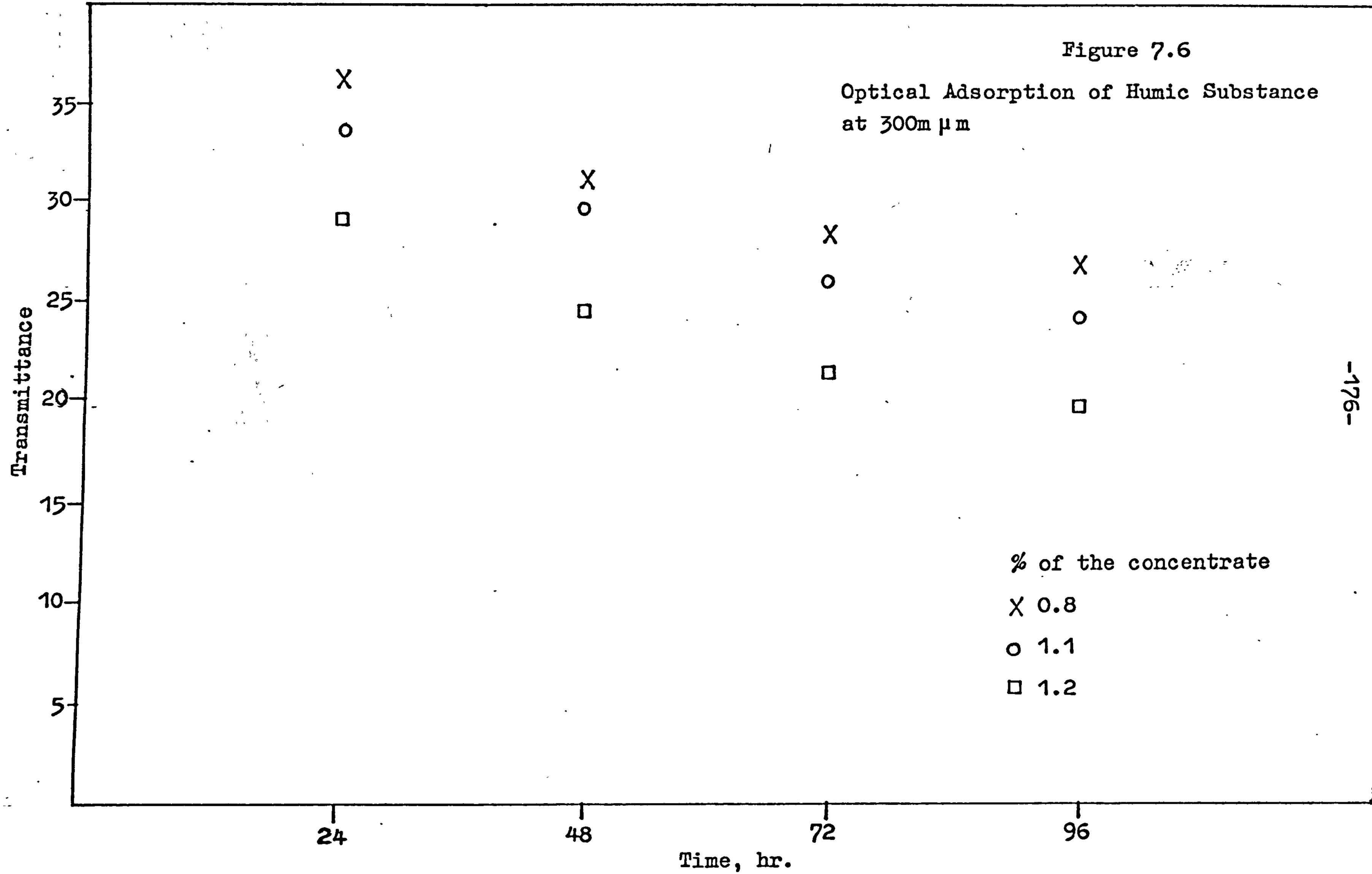

Figure 7.7

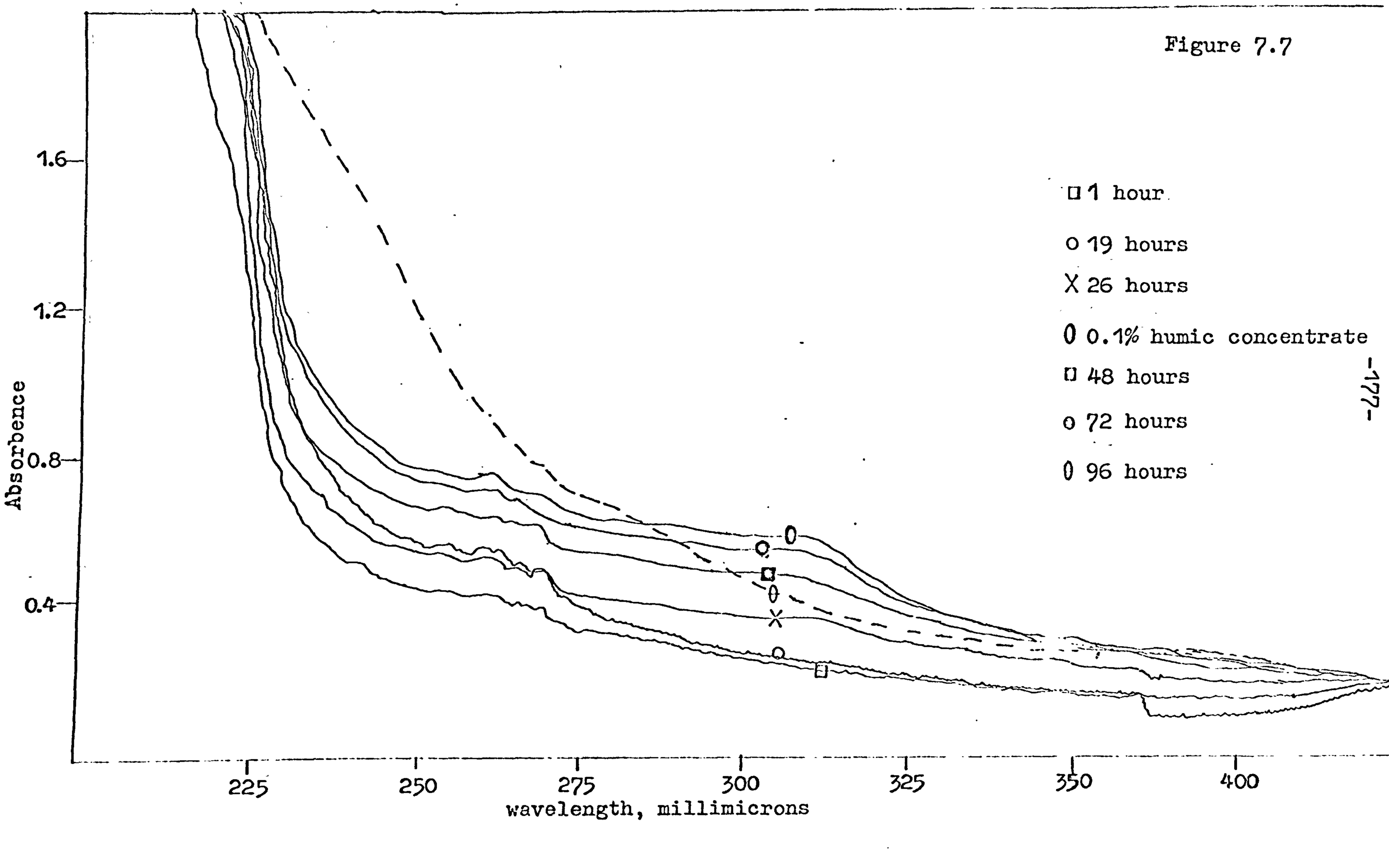
1.6
1.2
0.8
0.4
Absorbence
225
250
275
300
325
350
400
wavelength, millimicrons
□ 1 hour
o 19 hours
X 26 hours
0 0.1% humic concentrate
□ 48 hours
o 72 hours
0 96 hours

Figure 7.8

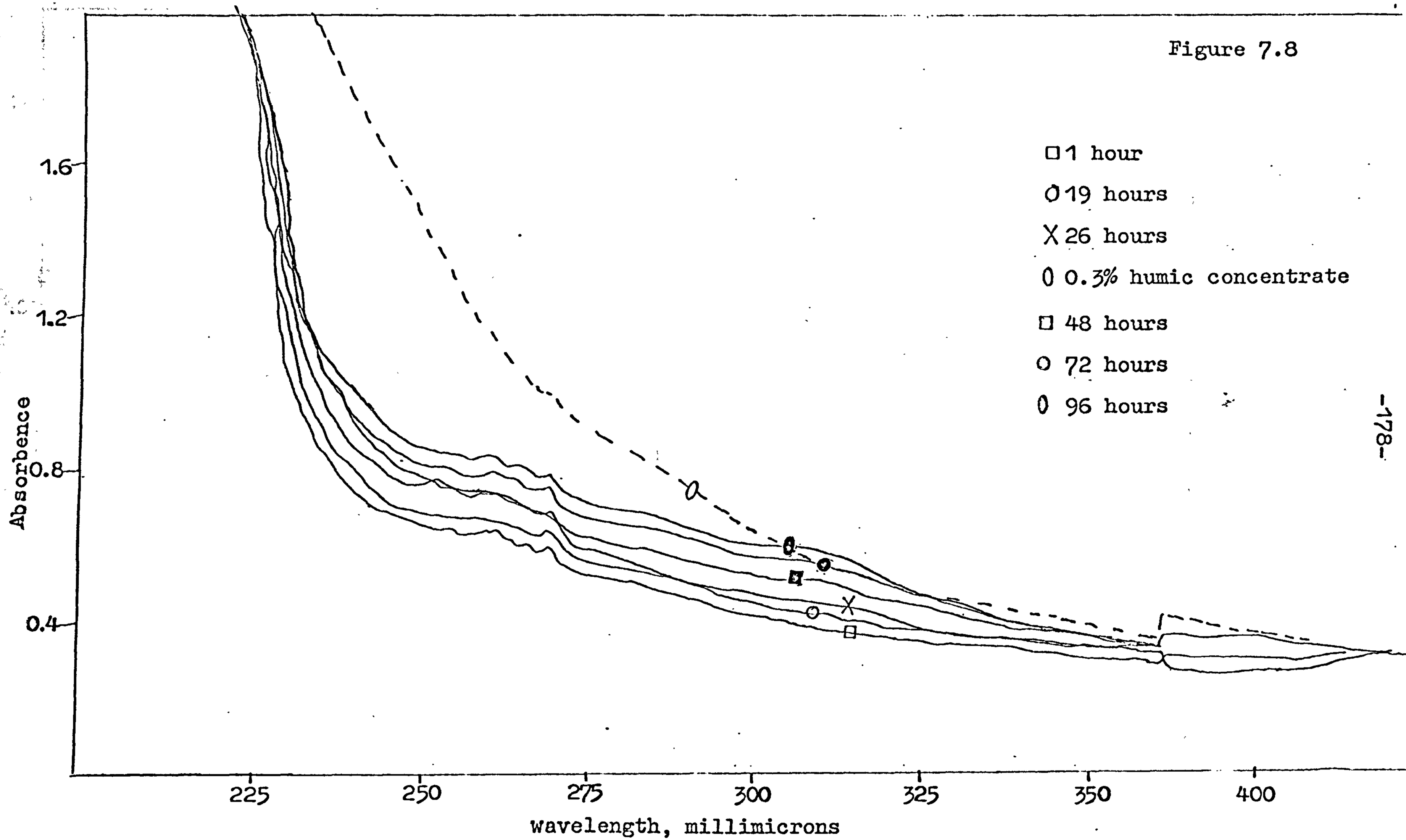
□ 1 hour
O 19 hours
X 26 hours
0 0.3% humic concentrate
□ 48 hours
O 72 hours
0 96 hours
Absorbence
1.6
1.2
0.8
0.4
225
250
275
300
325
350
400
wavelength, millimicrons

Figure 7.9

□ FO 115

■ Dispex N-40

○ Humic Substance

X FA 20HE

$[Ca^{++}] \times 10^4 M$

14 12 10 8 6 4 2 1

30 50 100 200 600 900

Time, min.

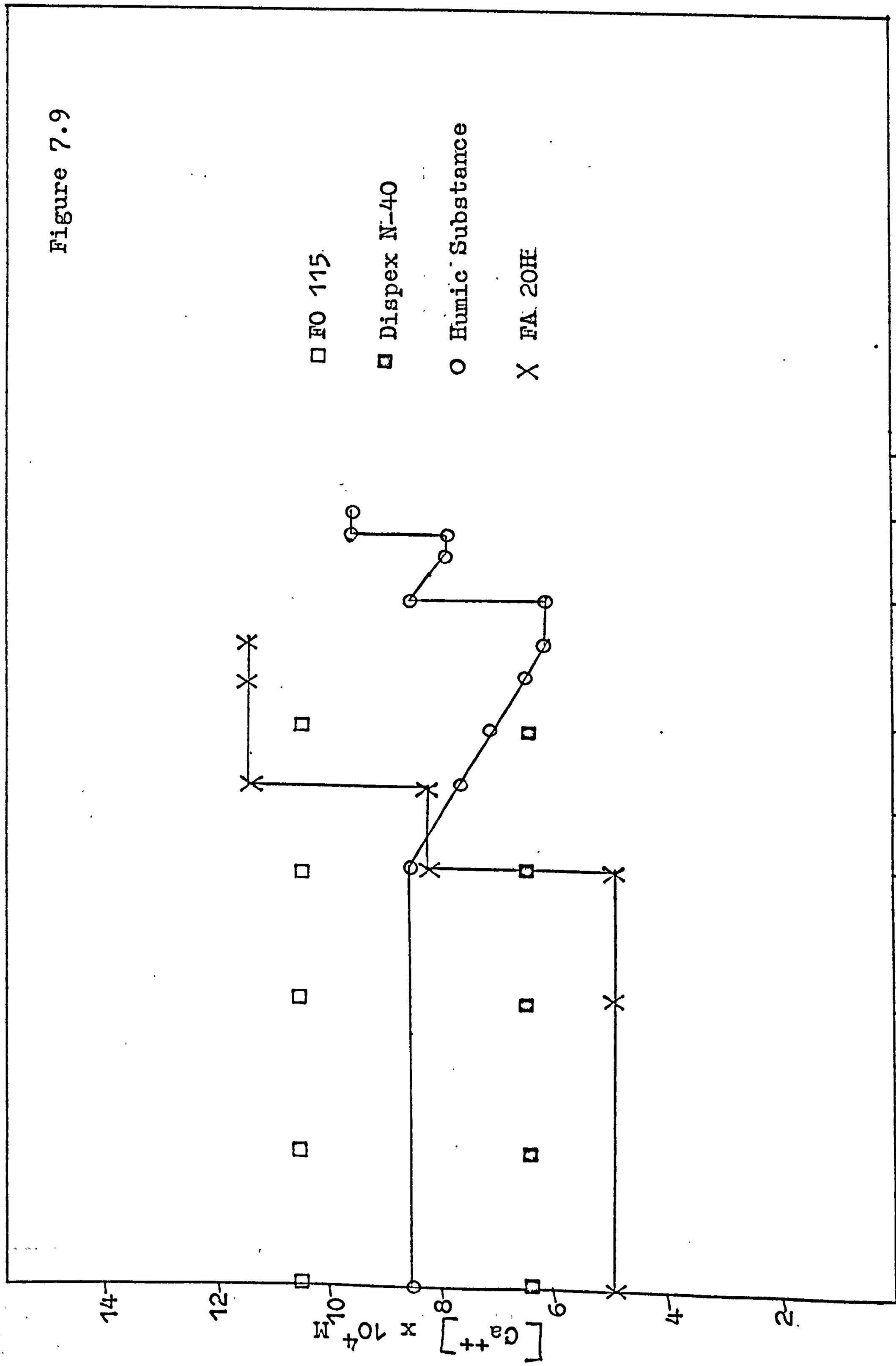
Figure 7.9
□ FO 115
■ Dispex N-40
○ Humic Substance
X FA 20HF
[Ca++] x 10⁴M
14
12
10
8
6
4
2
1
30
50
100
200
600
9000
10
Time, min.

Figure 7.10

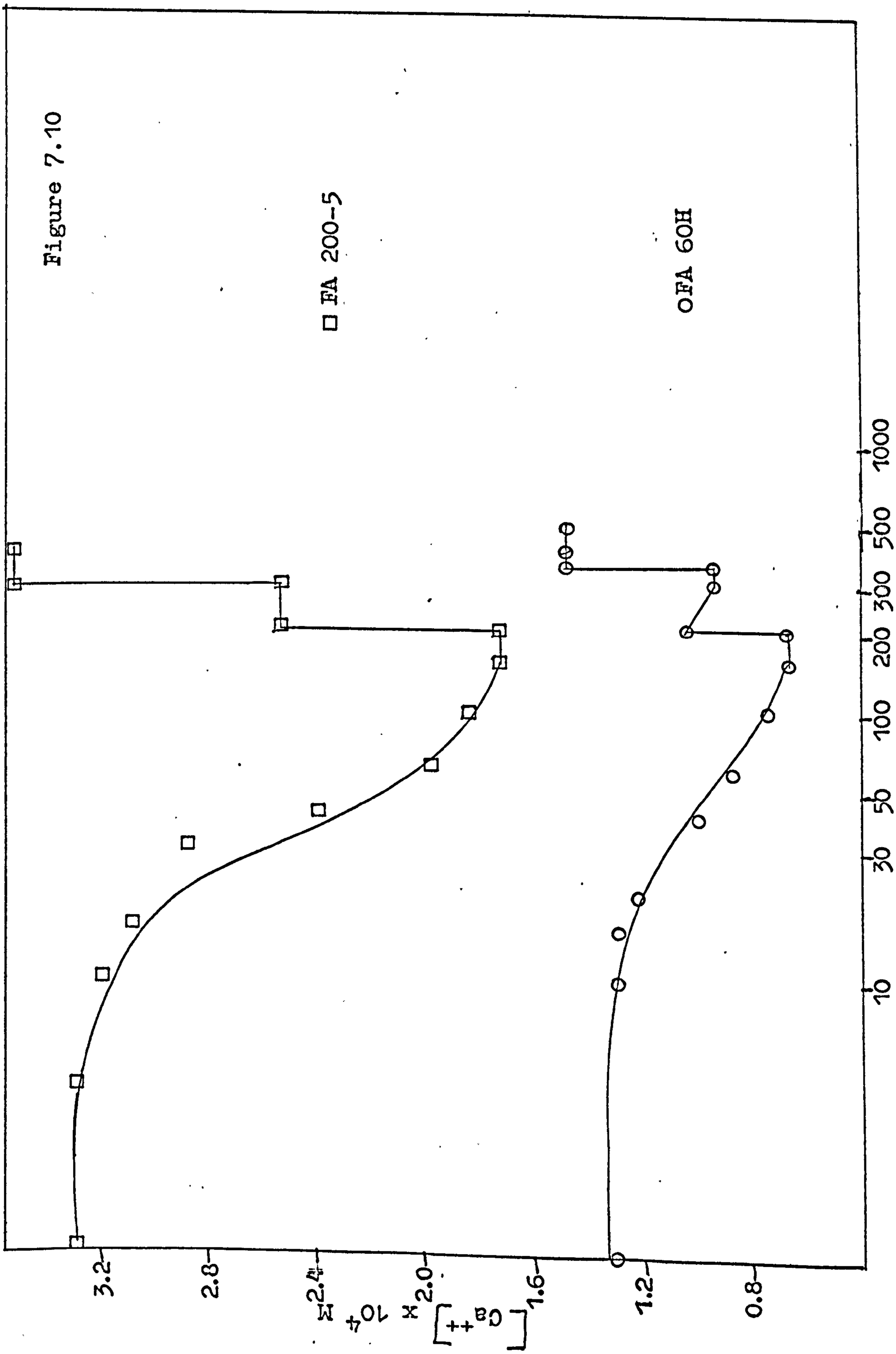
□ FA 200-5
○ FA 60H
Time, min.
10
30
50
100
200
300
500
1000
$[Ca^{++}] \times 10^4$ M
3.2
2.8
2.4
2.0
1.6
1.2
0.8
0

and Dispex N-40 no decrease in Ca^{++} from its original value of 10.4×10^{-4} and 6.5×10^{-4}M was observed over 100 minutes.

With humic substance an initial Ca^{++} of 8.5×10^{-4}M began to decrease after 30 minutes, reaching 6.2×10^{-4}M after about 200 minutes. Further increasing the concentration to 8.5×10^{-4}M it dropped over a further 200 minutes to 8.0×10^{-4}M. There was no further decrease over 100 minutes when the level was raised to 9.5×10^{-4}M.

Similar results are shown in figure 7.10 for the two anionic polyacrylamide flocculants.. They both show a decrease in $[Ca^{++}]$ with time. The amounts of calcium bound for each substance are:-

Anionic PAM FA 60H 1gm ion Ca^{++} per 3.5×10^{2}gm polymer

Anionic PAM FA 200-5 1gm ion Ca^{++} per 1.67×10^{2}gm polymer

Assuming an equivalent weight of 94 for the acrylate group the amounts of Ca^{++} bound correspond to 1gm ion Ca^{++} per 1.34 or 1.49 eqivalents of acid respectively.

No published data on the stability constants of polyacrylamide-Ca^{++} complexes has been found. The nature of the complex is not known. The results show that complexes are not formed when the polymeric species is entirely polyacrylic acid (Dispex N-40, 99% acid groups) but are when the side groups are a mixture of acrylic acid and acrylamide functions. In spite of the Ca^{++}/acid ratio the inability of Dispex N-40 to complex suggests that the complexes are not salts of the Ca^{++}-carboxylic acid type, e.g. Ca^{++} soaps. The lack of an obvious precipitate

Figure 7.11

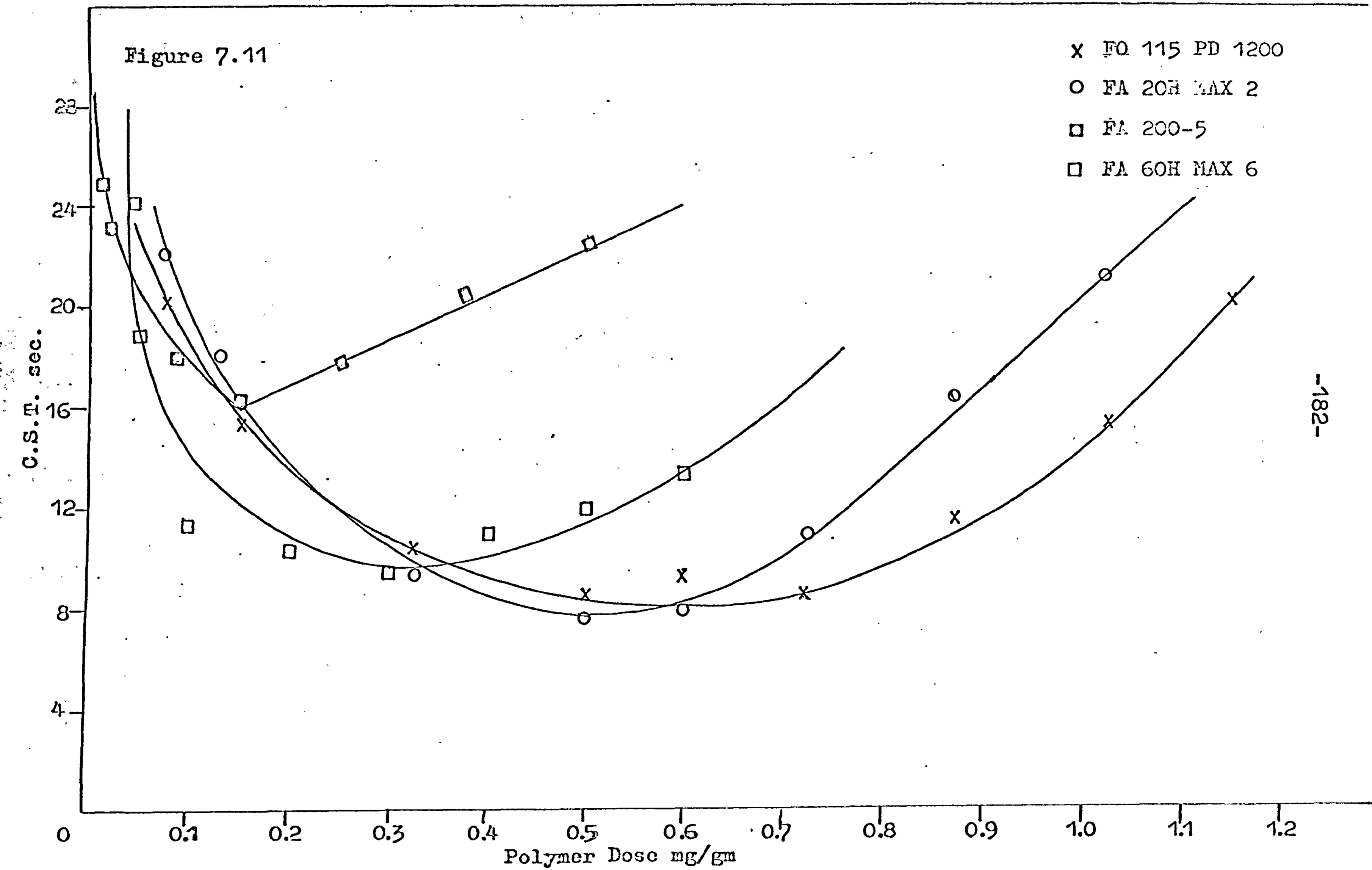
X FO 115 PD 1200
O FA 20H MAX 2
□ FA 200-5
□ FA 60H MAX 6
C.S.F. sec.
24
20
16
12
8
4
0
0.1
0.2
0.3
0.4
0.5
0.6
0.7
0.8
0.9
1.0
1.1
1.2
Polymer Dose mg/gm

Figure 7.12

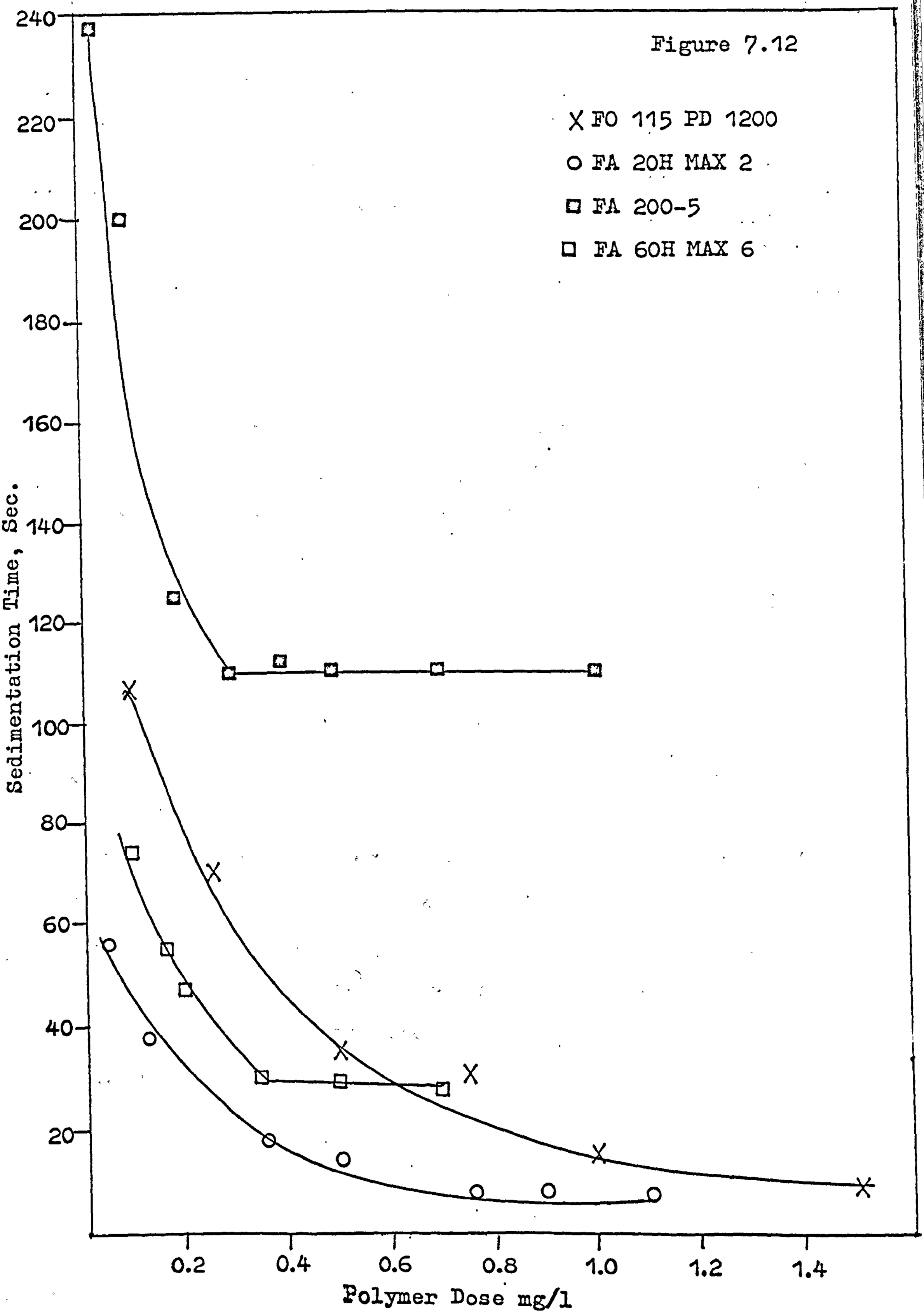
X FO 115 PD 1200
O FA 20H MAX 2
□ FA 200-5
□ FA 60H MAX 6
Sedimentation Time, Sec.
240
220
200
180
160
140
120
100
80
60
40
20
0.2
0.4
0.6
0.8
1.0
1.2
1.4
Polymer Dose mg/l

in the experiments where calcium chloride was added to the polymer solution points to the fact that the complex may be water soluble although a haze that would not centrifuge down was seen in some of the adsorption experiments. No further information as to the nature and structure of these complexes exists although there is little doubt as to their presence.

7.2 Determination of Optimum Flocculant Dose

The optimum amount of each of the polymeric flocculants for the calcium carbonate were determined by studying the sedimentation rates of treated suspensions and their capillary suction times (CST) (see section 6.3.1). CST/ concentration plots are shown in figure 7.11 where it can be seen that a minimum CST exists, although the spread of data makes its exact location difficult for some of the curves. Figure 7.12 shows the time taken for the interface of a 4% w/v suspension to fall 30cm in a 1L graduated cylinder. These curves do not show an optimum dose although both anionics showed increasing residual turbidity when overdosed. In table 7.2 the concentrations corresponding to the CST minimum are shown and compared with the equivalent added concentrations corresponding to the adsorption plateau values.

Table 7.2

	optimum conc. (mg/gm)	plateau conc. (mg/gm)
Cationic FO 115	0.60	0.68
Anionic FA 60H	0.30	0.46^{+}
Anionic FA 200-5	0.15	0.46^{+}
Nonionic FA 20H	0.50	0.59

The plateau values for the cationic and nonionic polyacrylamides were determined using the linearised Langmuir isotherm:-

$$\frac{C}{\Gamma} = \frac{C}{\Gamma m} + \frac{1}{b\,\Gamma m} \quad \ldots\ldots\ldots\ldots\ldots\ldots\ldots\ldots\ 7.1$$

Good straight lines were obtained (see figure 7.13) for the anionic polymers in which no plateau was reached, the figure in table 7.2 was estimated from the apparent shoulder in the isotherms.

Table 7.2 shows the plateau or saturation values to be from 1.2 to 3.1 times the flocculation optimum values. Fleer[245] has said that the ratio should be 2:1, i.e. that optimum flocculation occurs when the surface is half saturated. The present ratios are similar to this prediction allowing for the spread in data and that Fleer's experiments were performed with the very different system silver iodide/polyvinylalcohol. The CST minimum values agree reasonably well with the minimum concentration required to give the maximum sedimentation rate although the curves for the nonionic and cationic polymers are too gradual to permit this point to be identified with any precision.

Figure 7.13

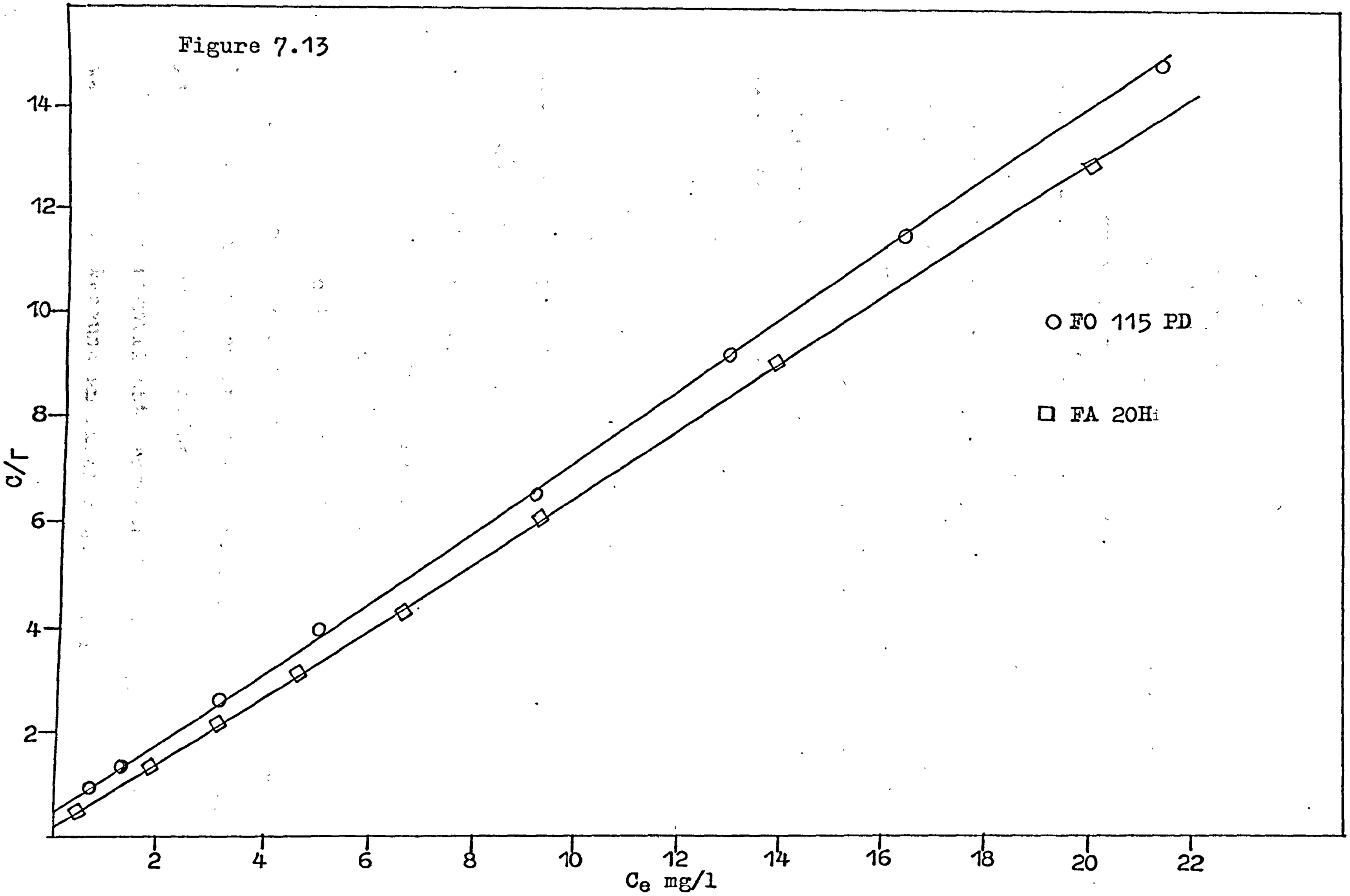

CHAPTER EIGHT

Results and Discussion

Crystallisation of Calcium Carbonate

8.1 Preliminary Experiments on the Precipitation of $CaCO_3$

The first phase of the experimental work was to test the experimental procedure for reproducibility. Experiments were carried out using the technique described in 6.4 at a supersaturation ratio, S_i, of 30. The $[Ca^{++}]$ versus time plots are shown in figure 8.1, from which it can be seen that the reproducibility was poor. It was suspected that this might be due to variations in the concentration of heterogeneous nuclei with solution age and to variations in the initial concentration of calcium bicarbonate and calcium hydroxide prepared as described in 6.1.7 and 6.1.8.

8.1.1 Ageing Effects

Stock solutions of calcium bicarbonate and calcium hydroxide sufficient for about ten runs were prepared thus enabling a whole series of runs at increasing solution age to be carried out. Seven runs at 3, 24, 48, 72, 96, 120 and 144 hours after preparation of the solutions were performed, all of them under otherwise identical experimental conditions as described in 6.5. The calculated initial supersaturation for all runs was kept constant at 30. In all these runs, the induction period, τ, that is the period of time between the preparation of the supersaturated solution and a significant decrease in calcium concentration, was observed. Because an experiment lasted for ten or more

Figure 8.1

S_i = 30

Age of stock solution

X 24 hours

O 48 hours

□ 96 hours

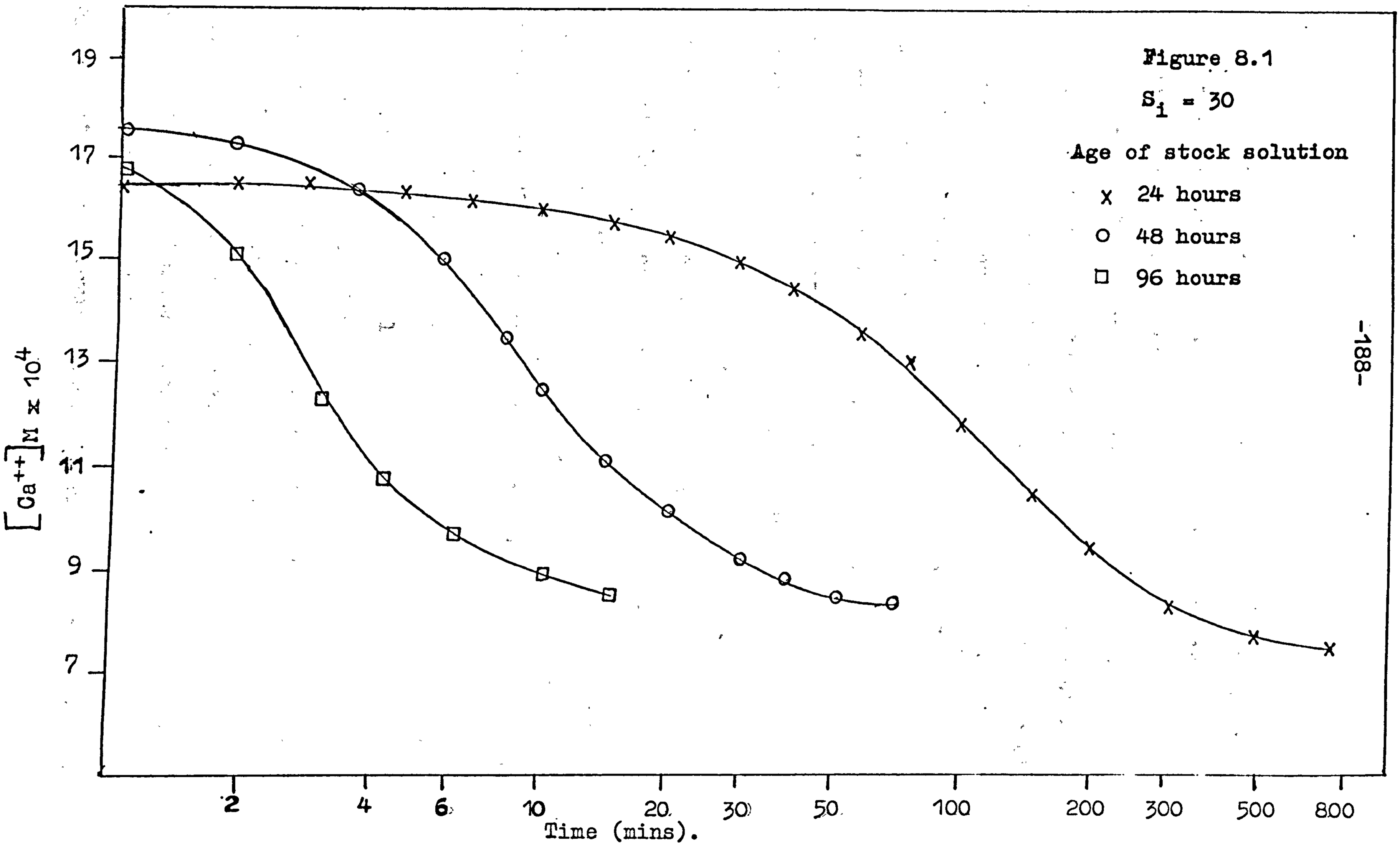

hours but significant changes were possibly occurring in the first few minutes it was decided, for convenience, to represent the data graphically as a $\left[Ca^{++}\right]$ versus log t plot. Figure 8.2 is typical of such a plot. It was noted that on such plots the data points during the precipitation stage fitted a straight line well. If an induction period was present the induction time, τ , was taken as the intercept of this straight line with the initial horizontal line. In figure 8.2 this is shown as point b, ab representing the induction time, τ . The rate of precipitation was expressed in terms of the precipitation half time, $t_{\frac{1}{2}}$, the time taken for $\left[Ca^{++}\right]$ to drop half way from its initial to final value. The results are shown in figure 8.3 and table 8.1. The induction period, τ , decreases with increasing age of the solutions and no induction period was observed when the age of the stock solutions were greater than about 72 hours. The median crystal size, MS, (on completion of the run) increased with age of the solutions and gradually attained a constant value after the solutions had aged for more than 96 hours.

It was thought likely, therefore, that the fluctuations in the precipitation characteristics of calcium carbonate with age of the stock solutions of calcium bicarbonate and calcium hydroxide (prepared as described in sections 6.1.7 and 6.1.8 except dilution to half saturated solutions) were due to calcium carbonate precipitation in the stock lime solution giving crystal nuclei. An attempt to obviate this by saturating and storing all solutions under nitrogen was

Figure 8.2

$S_i = 40$

Calcium Concentration Change During A Desupersaturation Run.

ab = τ

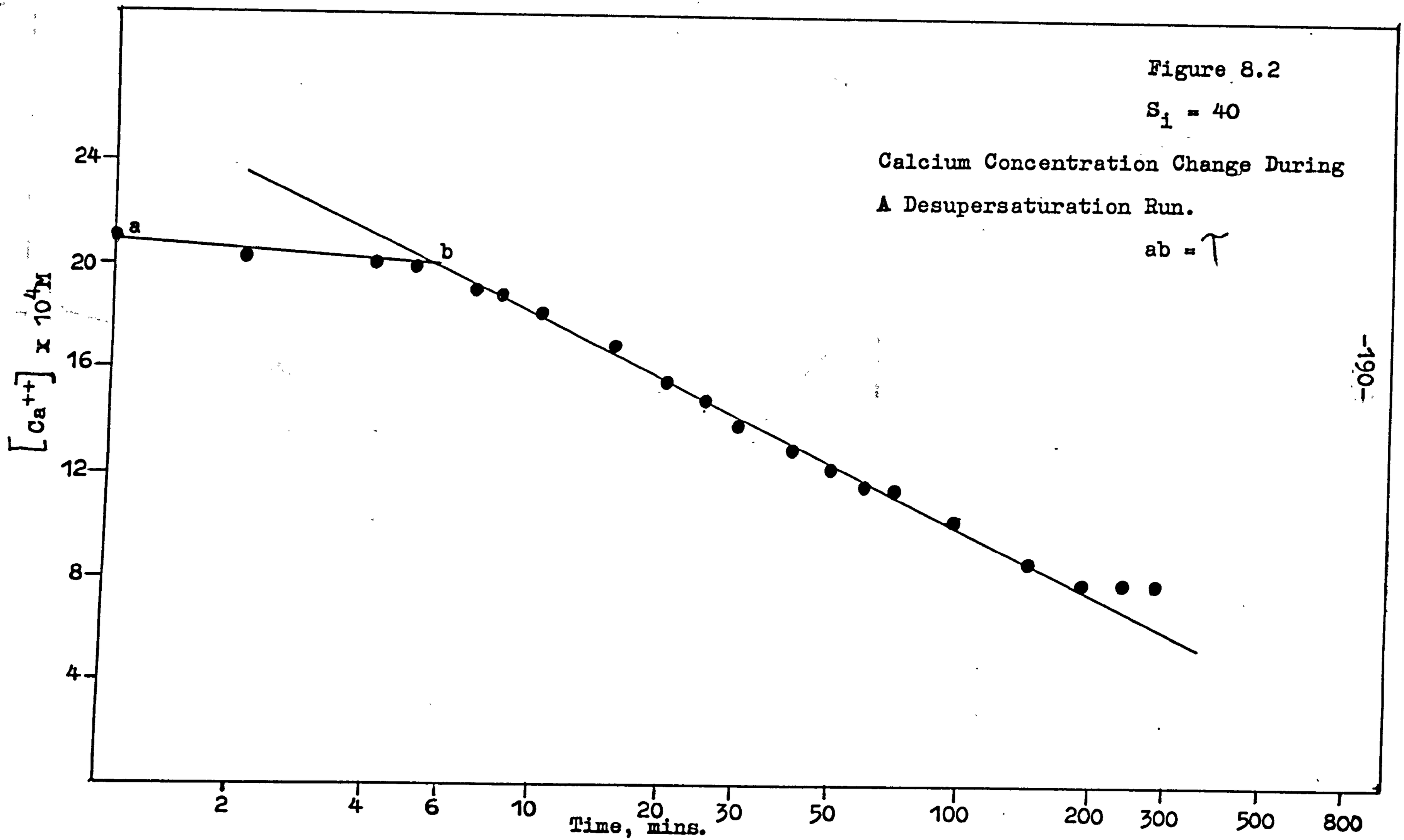

Figure 8.3

Effect of age of reactant solutions.

o Induction Period, τ, mins.

□ Median Crystal Size (Ms) microns.

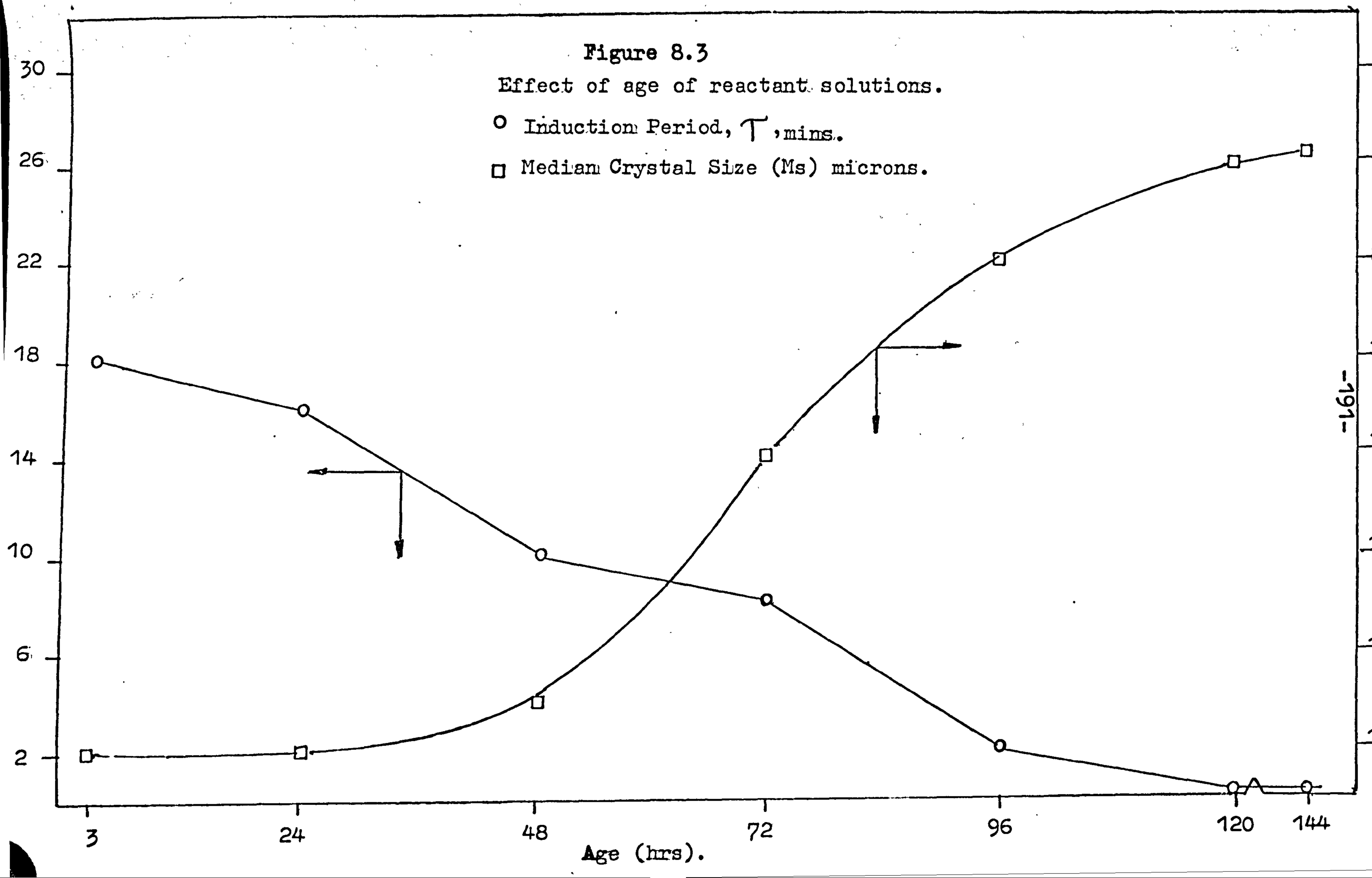

Table 8.1

Effect of Age of Solutions on Desupersaturation of $CaCO_3$

Age, hr.	τ min.	$t_{\frac{1}{2}}$ min.	MS μ m.
3	18	55	15.5
24	16	50	15.5
48	10	28	16.0
72	8	9	18.4
96	2	4	20.5
120	1	3	21.4
144	1	3	21.5

not successful.

Because of this difficulty, an alternative method of preparing supersaturated solution of calcium carbonate was sought. Of the various methods available for the production of supersaturated solutions, the most suitable for calcium carbonate seemed to be the generation of one of the precipitating ions 'in situ'. For example, La Mer and Dinegar[139] used the reaction between persulphate and thiosulphate to produce sulphate ions for the precipitation of barium sulphate. Therefore, calcium hydroxide solution was prepared by mixing equal volumes of 1.35×10^{-2}M NaOH and 6.757×10^{-4}M $CaCl_2$. Two modes of introducing the reactant solutions into the precipitation vessel were used. In the first method, the reactant solutions (NaOH and $CaCl_2$), after being kept in a water-bath at 25 ± 0.02°C were introduced via two separate funnels. In the second method, the relevant volumes of NaOH and corresponding stoichiometric amount of $CaCl_2$ were mixed together and the calcium hydroxide prepared in this method which is stable for several hours when kept in a thermostated bath[246], was introduced into the precipitation vessel through a single funnel. Again, high irreproducibility was observed in the results of these techniques (see figure 8.4). This irreproducibility could be due to the enormous number of air bubbles produced 'in situ' on mixing NaOH and $CaCl_2$ which possibly enhance nucleation. Another difficulty of this technique was sodium ion interference causing inaccuracies in the calcium measurements which could lead

Figure 8.4

S_i = 30

$Ca(OH)_2$ produced 'in situ'

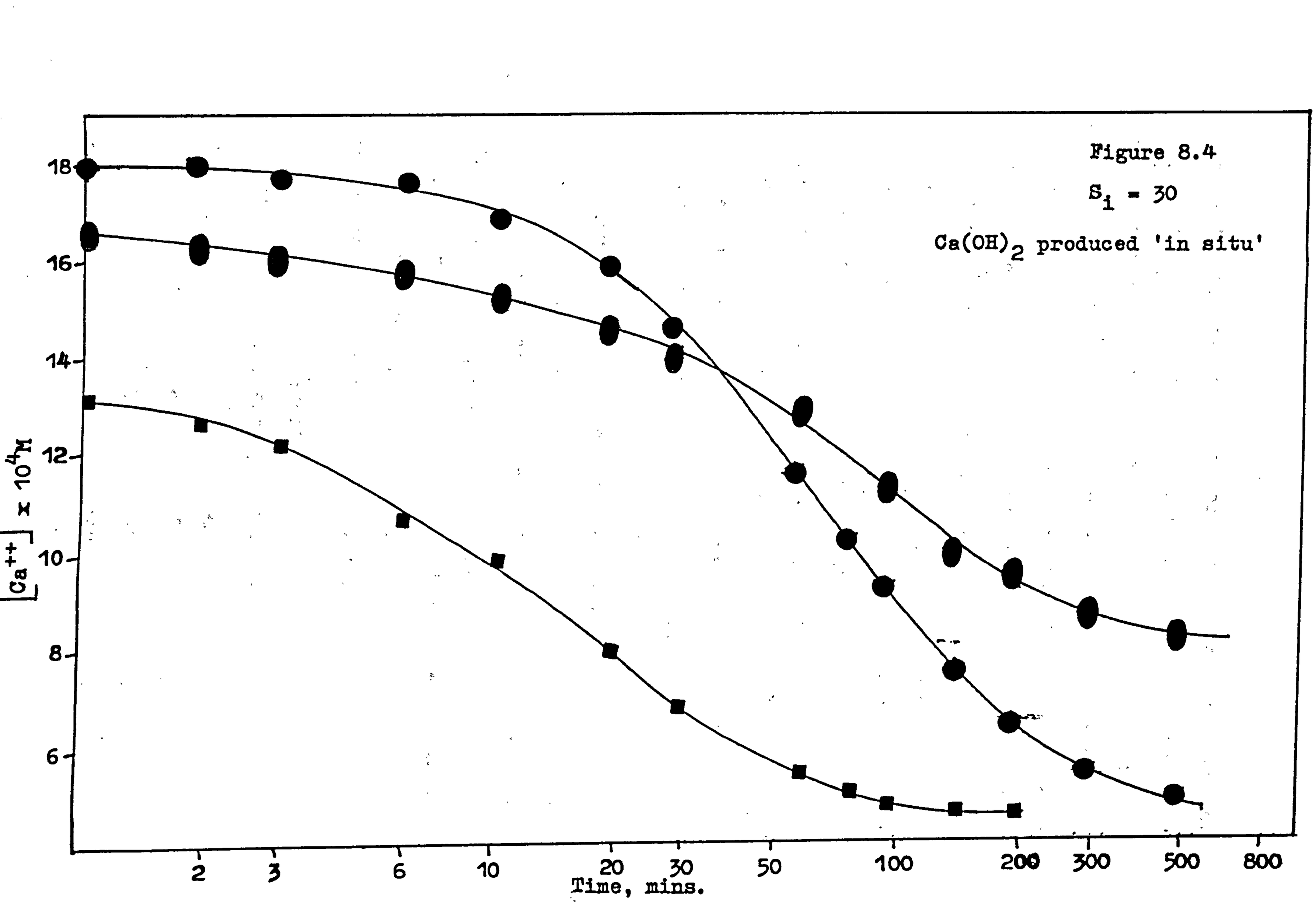

to some difficulty in the interpretation of the results.

In view of the above findings, for all subsequent work on the precipitation of $CaCO_3$, half saturated stock solutions of calcium hydroxide and calcium bicarbonate (prepared as described in sections 6.1.7 and 6.1.8) were kept in a refrigerator until required for runs. Precautions were also taken to control the number of possible nuclei in calcium hydroxide solution by membrane filtration immediately prior to the experiment. Figure 8.5 shows the apparatus used for this purpose. After being kept for three hours in the thermostated bath (25 $\pm$ 0.02°C) the stoichiometric amount of $Ca(OH)_2$ was filtered through a 0.2 microns membrane filter into a separating funnel and then introduced into the precipitation vessel.

Figure 8.6 and Table 8.2 show the results of three consecutive runs performed to check the reproducibility of the results given by the apparatus and techniques in their final form as described above. The initial supersaturation ratio, S_i, of $CaCO_3$ was 20, corresponding to 10.8×10^{-4}M $CaCO_3$. Figure 8.6 shows that the desupersaturation curves for the three runs (a,b,c) were almost parallel and running very close to one another showing a high reproducibility.

Table 8.2

Effect of filtration prior to the experiment

Age	Υ	$t_{\frac{1}{2}}$	MS, μm
3	60	170	24.5
24	50	140	—
72	55	150	—

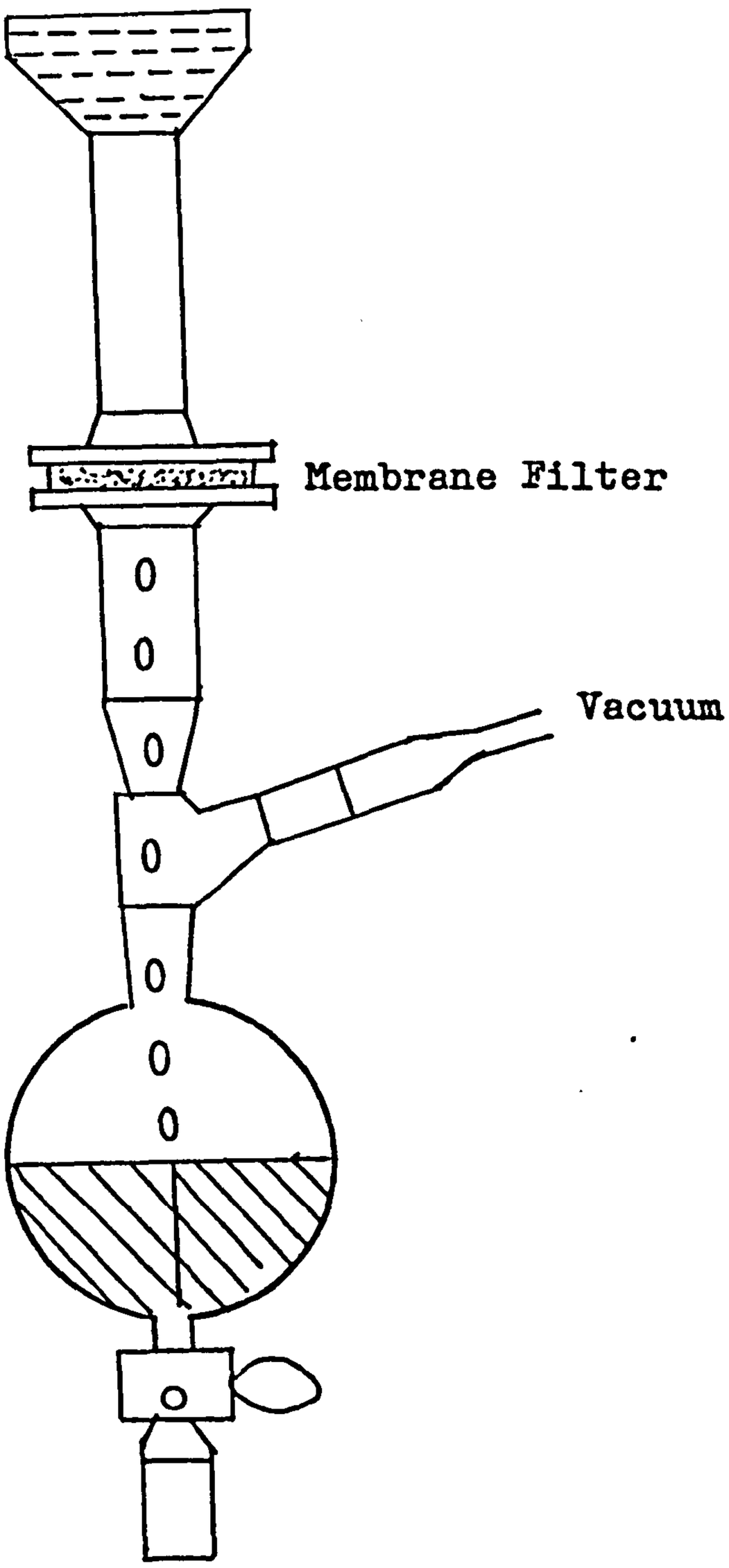

Figure 8.5

Filtration Apparatus Used For The Filtration of $Ca(OH)_2$ Solution.

Figure 8.6

Results of three consecutive runs showing the reproducibility of the Results.

x 3 hours

□ 24 hours

○ 72 hours

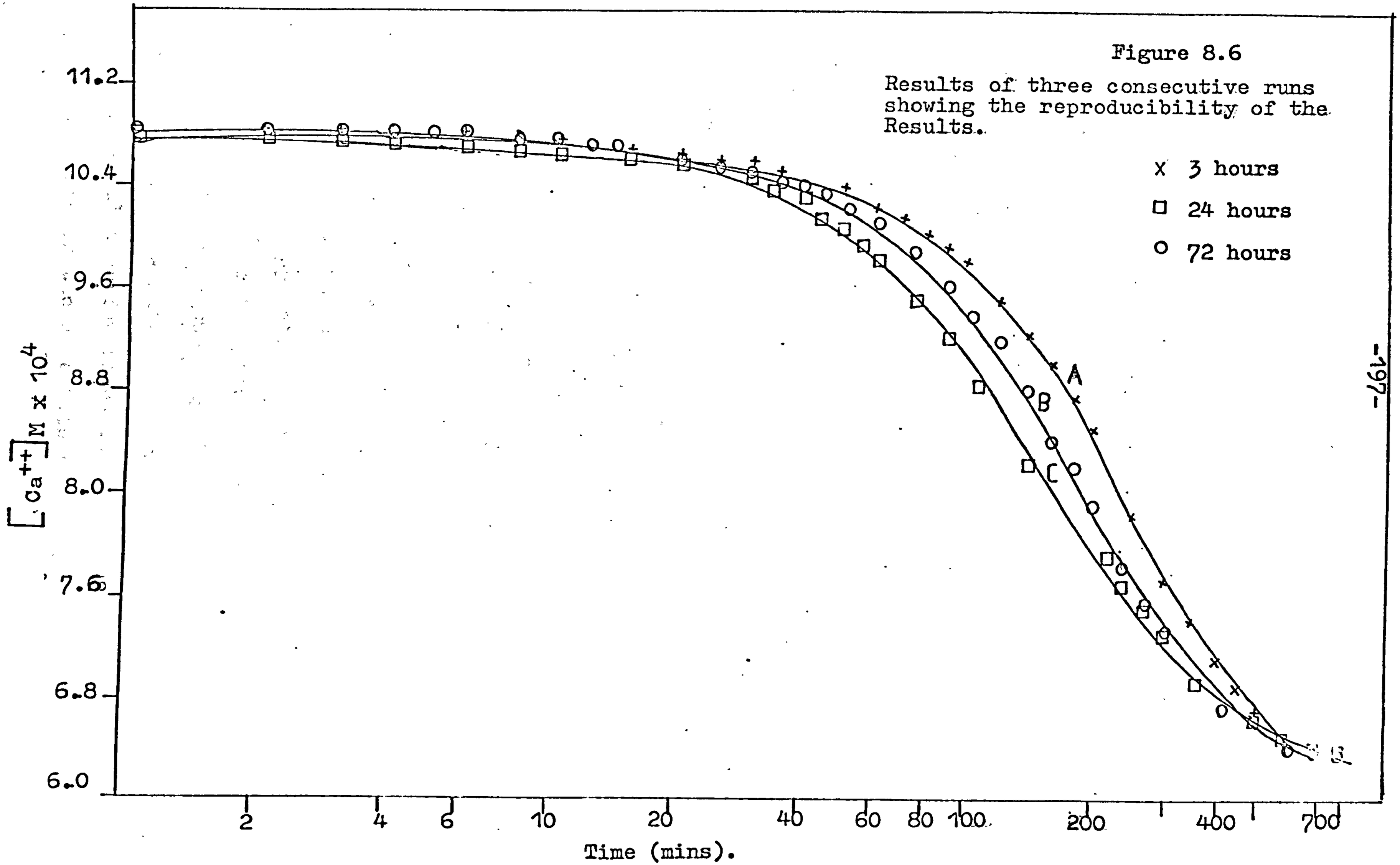

8.1.2 Effect of Agitation

The effect of stirrer speed was investigated over the range of 40-210 r.p.m. The results of this work are shown in figure 8.7. It can be seen that the rate of agitation does not influence the rate of crystallisation, suggesting that the rate controlling process is surface diffusion or surface reaction rate, rather than diffusion through the bulk of the solution (see 4.7). At high speed (210 r.p.m.) the rate of stirring slightly affected the crystallisation, possibly due to air entrained in the solution and acting as nuclei. Entrainment was not noted at lower stirrer speeds.

The rate of stirring was checked with an optical tachometer and maintained constant at 120 r.p.m. This speed was chosen since it keeps the particles well stirred in suspension and avoids air entrainment.

8.2 Desupersaturation of Calcium Carbonate Solutions

8.2.1 In the Absence of Seeds or Additives

An understanding of the effect of seeds or additives on the crystallisation of calcium carbonate first requires knowledge about the crystallisation processes itself. The effect of supersaturation on desupersaturation was performed by the apparatus and techniques in their final form as described in the preceding section.

Typical desupersaturation curves are illustrated in figure 8.6 with low initial supersaturation ratio (S_i = 20). A sample calculation for adjusting the level of supersaturation in the experiments is shown in Appendix 1.

Figure 8.7

Effect of agitation on crystallisation of $CaCO_3$.

0 40 r.p.m.

o 80 r.p.m.

◇ 120 r.p.m.

× 180 r.p.m.

□ 210 r.p.m.

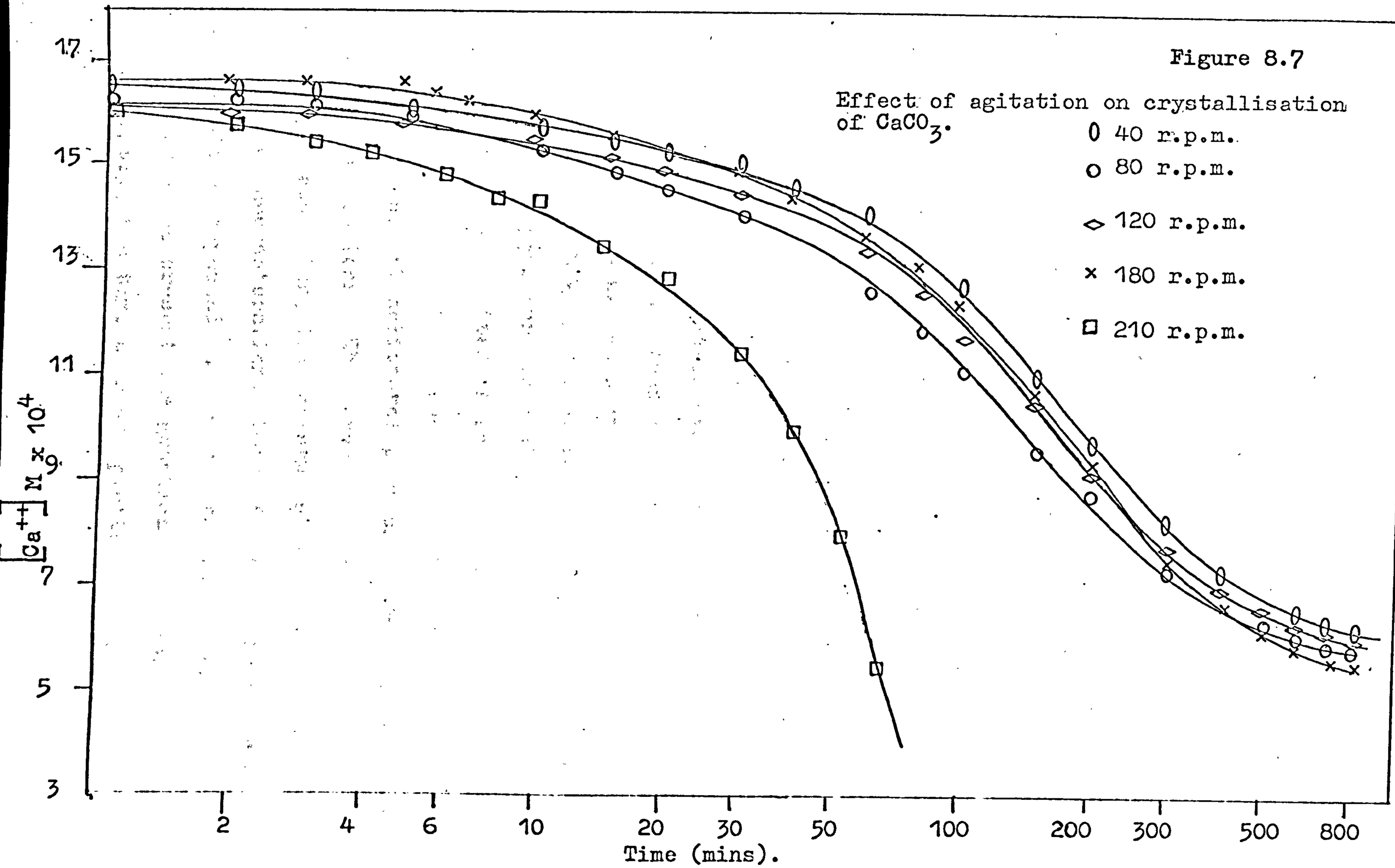

With increasing supersaturation the crystallisation process takes a shorter time to complete, the induction period and the half life time are shorter.

The calcium concentration of the final plateau after all precipitation had appeared to cease, $[Ca^{++}]_\infty$, was noted to be considerably greater than the value calculated from the solubility product at the experimental pH[12]; 6.3×10^{-5}M.

Table 8.3 and figure 8.8 show the results of experiments carried out under the same general conditions as above, but different initial concentrations of calcium carbonate.

An experiment with an initial supersaturation of 10 did not begin to precipitate for at least five hours after mixing the solutions, while experiments using initial supersaturations higher than 40 began to crystallise before the mixing process was complete.

Figure 8.8 shows plots of $[Ca^{++}]$ versus time for runs with initial supersaturations of 15 to 60. The fraction of $[Ca^{++}]$ removed is plotted in reduced form to enable the curves to be compared. It can be seen that the curves are sigmoid, an initial horizontal portion becoming apparent at low supersaturations. The curves also show that the rate of desupersaturation, i.e. crystal growth, increases with increasing supersaturation. Both of these findings are what would be expected in a precipitating system.

In order to present the graphical data more conveniently, the time axis was plotted in logarithmic time

Table 8.3

Induction period, τ, half life time, $t_{\frac{1}{2}}$, and the time to complete, t_{∞}, at different initial supersaturations, S_i, at 25°C for the experiments described in 8.2.1.

S_i	$[Ca^{++}]_o$ x 10^4M	τ min	$t_{\frac{1}{2}}$ min	t_{∞} min	$[Ca^{++}]_{\infty}$ x 10^4M
5	2.7	>5 hr	—	—	—
10	5.4	>5 hr	300	>1000	—
15	8.1	170	280	>1000	—
20	10.8	50	180	400	2.2
30	16.1	16	55	400	8.0
40	21.5	9	20	200	8.5
50	26.8	imm.	4	150	2.2
60	32.2	imm.	1	30	2.4

Figure 8.8

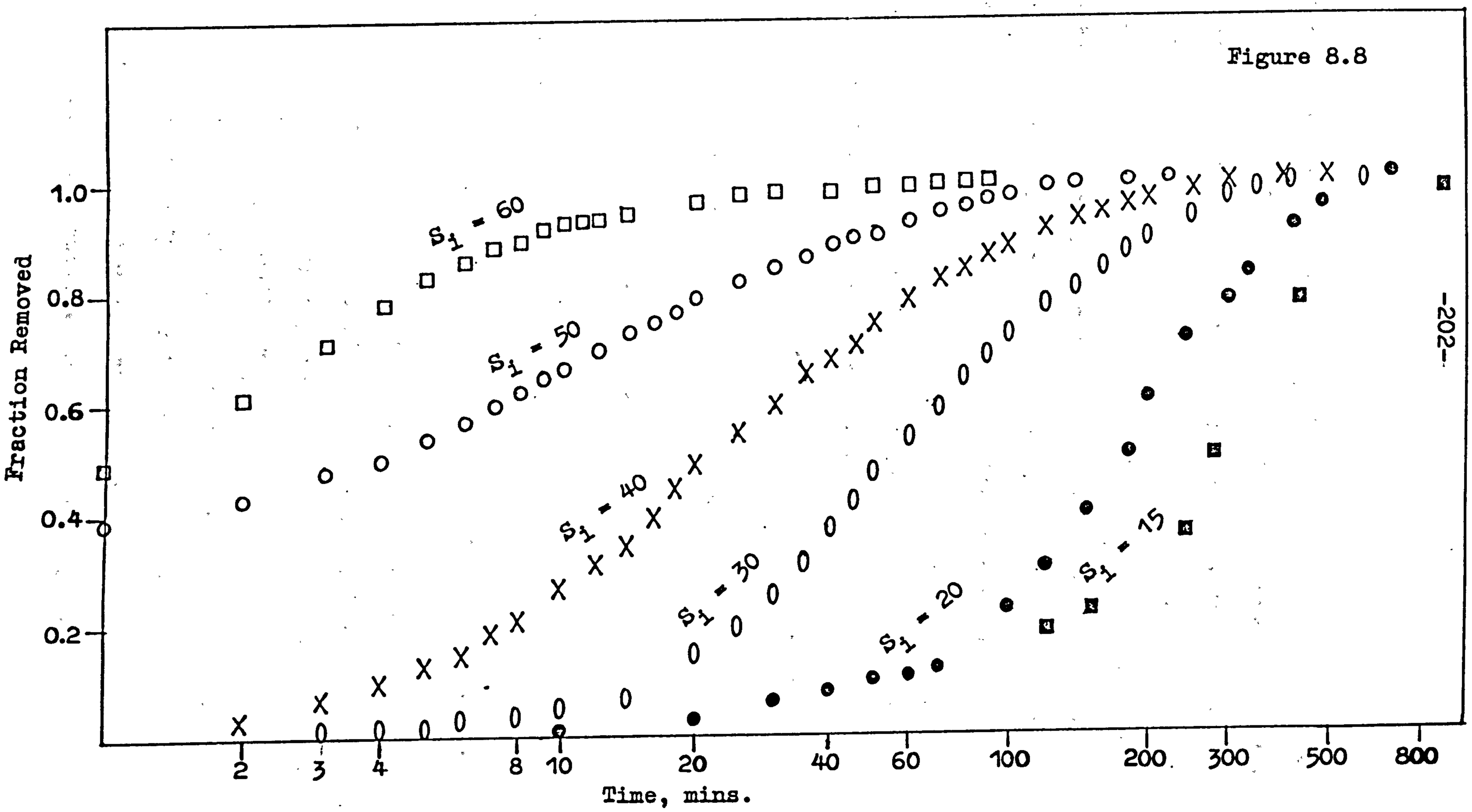
Fraction Lon Removed
1.0
0.8
0.6
0.4
0.2
S_i - 60
S_i - 50
S_i - 40
S_i - 30
S_i - 20
S_i - 15
2
3
4
8
10
20
40
60
100
200
300
500
800
Time, mins.

and the corresponding set of $[Ca^{++}]$ versus log t are shown in figure 8.9. It will be seen that these curves show two or three well defined linear portions. The first horizontal portion present in the lower supersaturation curves represents an induction period in which the rate of crystal growth is undetectable from $[Ca^{++}]$ measurements. There is then a linear falling $[Ca^{++}]$ versus log t line and finally a plateau representing completion of the precipitation reaction.

Reddy[2] has shown that the growth of $CaCO_3$ in seeded systems follows a second order rate law:-

$$\frac{dC}{dt} = -kA_sC^2 \quad \text{..... 8.1}$$

where k = is a second order rate constant.

A_s = the surface area of the seed crystals.

and $C = C_{(t)} - C_{(\infty)}$

where $C_{(t)}$ = is Ca^{++} at time, t.

and $C_{(\infty)}$ = is Ca^{++} at completion of precipitation.

Integrating this expression gives:-

$$\frac{1}{C_{(t)} - C_{(\infty)}} - \frac{1}{C_{(0)} - C_{(\infty)}} = kA_st \quad \text{..... 8.2}$$

and Reddy obtained straight lines for this plot. From their observation of second order kinetics, Nancollas and Reddy[247] very reasonably propose a rate law of the form:-

$$\frac{dC}{dt} = -kA_s[Ca^{++}][CO_3^{=}]$$

Figures 8.10 to 8.13 show similar plots for the data shown above. Figures 8.10 and 8.11 show the curve when the experimental $C_{(\infty)}$ for the actual run was used and figures 8.12 and 8.13 the curve when the theoretical value of $C_{(\infty)}$

Figure 8.9

S_i	
□	40
o	30
0	50
x	60

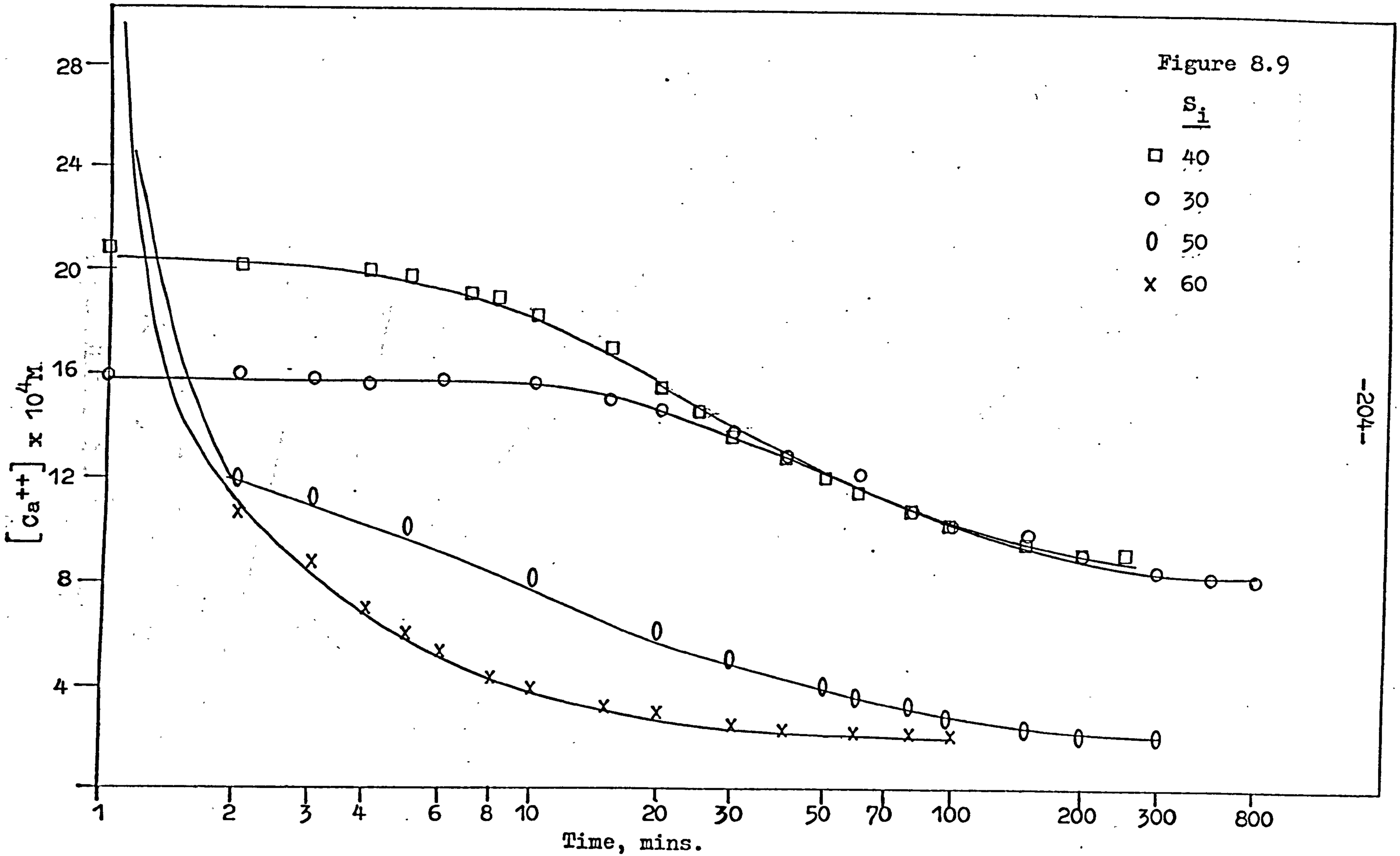

Figure 8.10

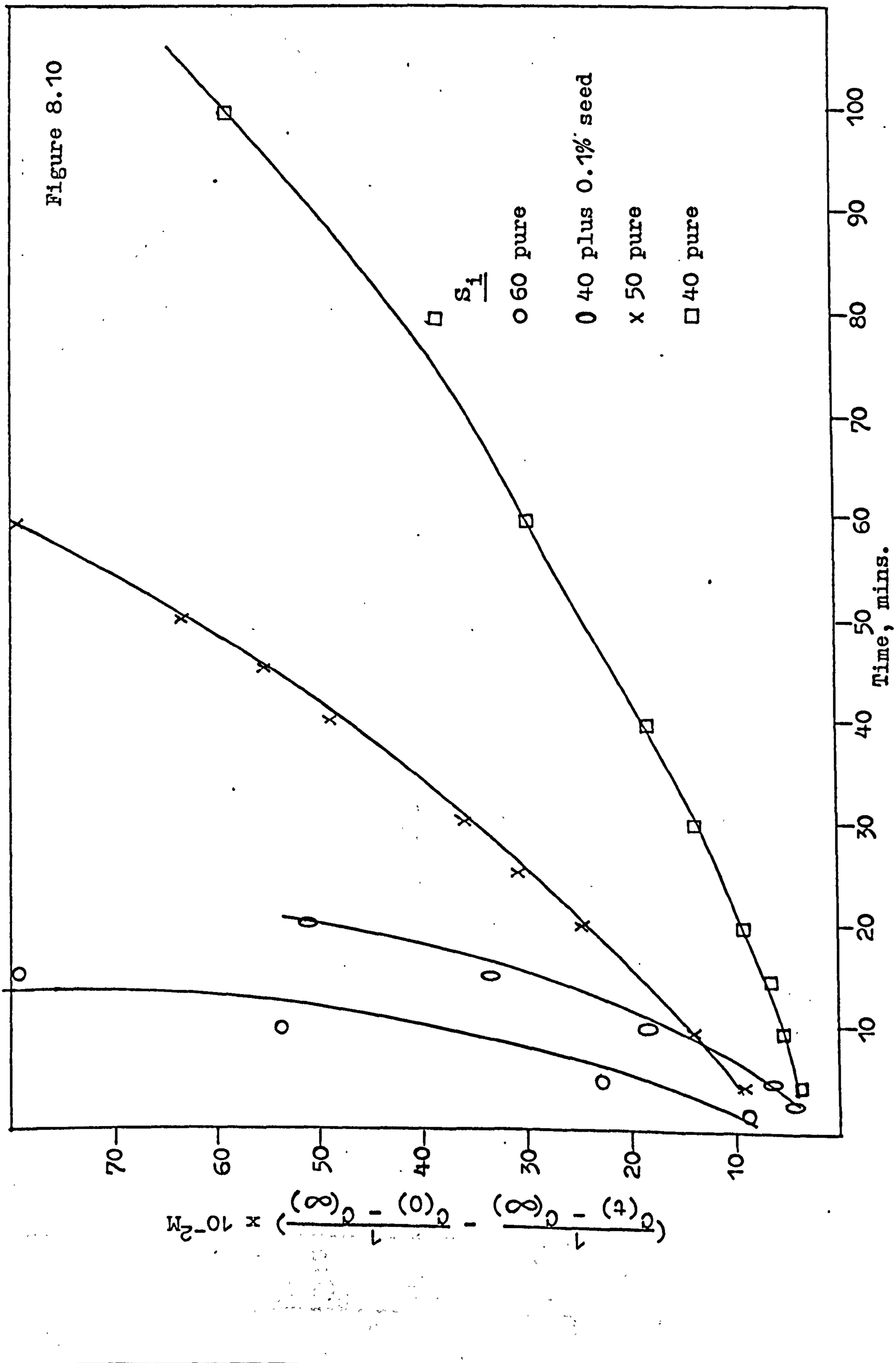
S_1
□ 60 pure
○ 40 plus 0.1% seed
○ 50 pure
× 40 pure
Time, mins.
10
20
30
40
50
60
70
80
90
100
$\frac{1}{D_{(\infty)}} - \frac{1}{D_{(0)}} - \frac{1}{D_{(\infty)}} - \frac{1}{D_{(t)}}) \times 10^{-2}M$

Figure 8.11

S_i

x 30 plus 5 p.p.m. Dispex and 0.1gm seed

0 30 plus 2 p.p.m. Nonionic PAM

□ 30 pure

o 30 plus H.S. (60 Hazen)

$\left(\frac{1}{C(t) - C(\infty)} - \frac{1}{C(0) - C(\infty)}\right) \times 10^{-2}M$

Time, mins.

Figure 8.12

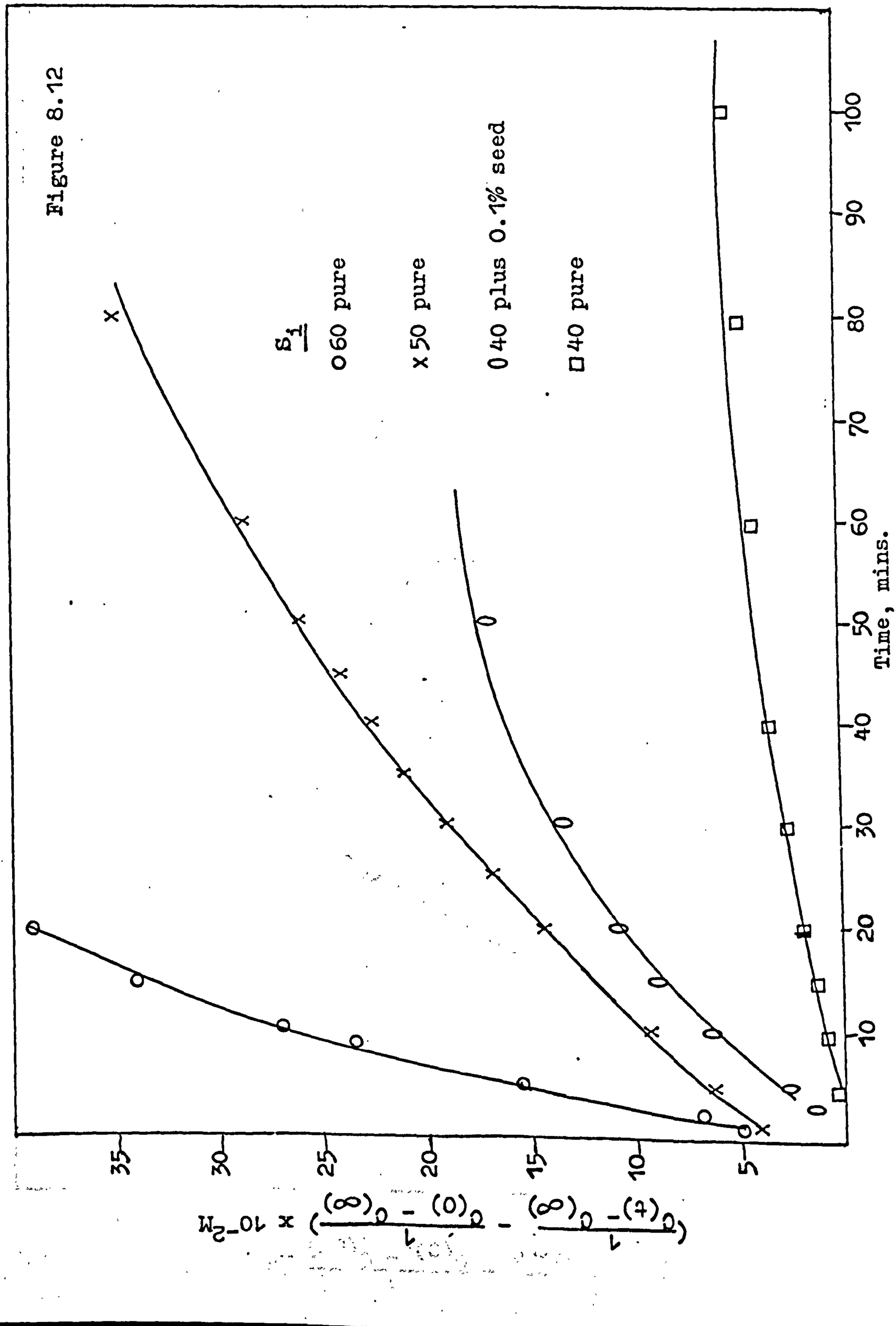
S_1
○ 60 pure
× 50 pure
◊ 40 plus 0.1% seed
□ 40 pure
Time, mins.
$W_2 \times 10^{-2} \times \left(\frac{(\infty)_D - (0)_D}{1} - \frac{(\infty)_D - (7)_D}{1}\right)$

Figure 8.13

$\underline{S_i}$

0 30 plus 2 p.p.m. Nonionic PAM

x 30 plus 5 p.p.m. Dispex and 0.1gm seed

□ 30 pure

o 30 plus H.S. (6 Hazen)

$\frac{1}{(\infty) - c(t)} - \frac{1}{c(\infty) - c(0)}) \times 10^{-2}$M

Time, mins.

was used, calculated from the known solubility product[12] of $CaCO_3$ at the measured solution pH. It will be seen that neither of these procedures gives a good linear plot. This is probably because of the presence of the A_s term in equation 8.1. During crystal growth the crystal area, and hence the growth rate, will increase but by using a relatively coarse seed suspension Reddy is able to ignore this term. Reddy used seed crystal aggregates of about 2 μm diameter corresponding well with a measured specific surface of $1.71 m^2 gm^{-1}$ which, assuming uniform spherical crystals, is equivalent to 1.30 m diameter spheres. Taking the run starting at $[Ca^{++}] = 2.6 \times 10^{-4} M$ from Reddy's figure 2 in which a final concentration of approximately 1.6×10^{-4} was reached and assuming the presence of 100mg/l of seed, as stated in the text, the amount of solid $CaCO_3$ deposited is 10mg/l corresponding to an increase of mean seed crystal size from 2 to 2.06 μm, i.e. an insignificant increase. The runs shown in figures 8.10 to 8.13 are for unseeded experiments in which the crystals would grow from their critical nuclear size to an observed maximum diameter of approximately 37 μm, with a mean diameter of 27 μm, during which there would be a great change in surface area available for growth. Figure 8.14 shows the particle size analysis of the final product from a typical experiment. The log normal size distribution obtained is characteristic of precipitation and crystallisation processes[73].

Figure 8.14

Size Distribution of $CaCO_3$

S_i = 60

Precipitation Time = 60 mins.

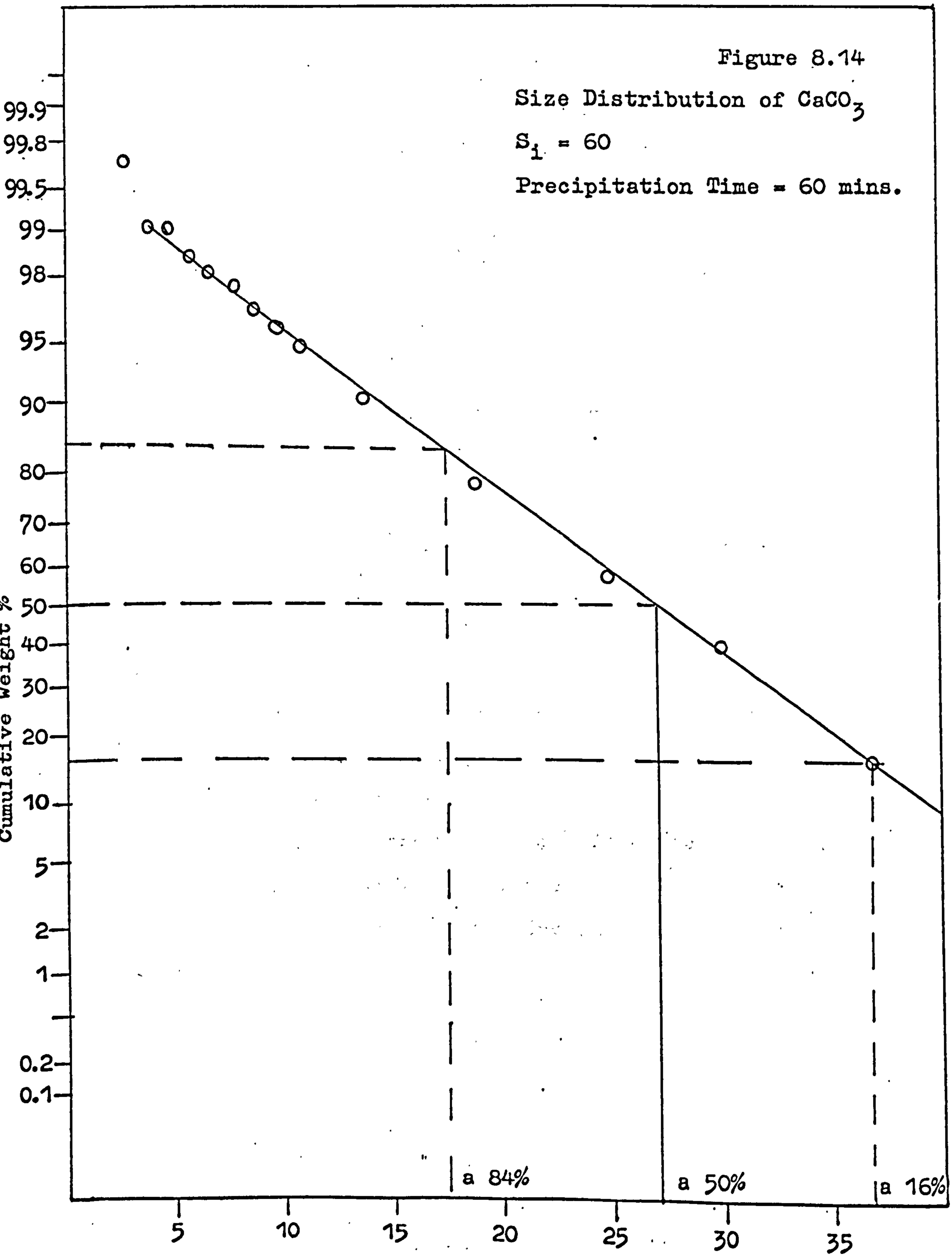

8.2.1.1 Calculation of Data - Reaction Rate Constant

In order to allow for the change in surface area during a run, samples were removed from an experiment at fixed time intervals for particle size analysis by Coulter Counter. The cumulative number versus diameter analyses at 3, 5, 10, and 15 minutes are shown in table 8.4 and are plotted as frequency versus diameter in figure 8.15. This shows the possible presence of a trimodal size distribution, consisting of fine particles of <3 μm diameter, a small peak, not always present, of increasing size with time having a maximum in the range 2 to 7 μm diameter, and a third large peak with its maximum in the range 10 to 16 μm. Using a 100 μm Coulter Orifice it is possible to count particles down to 2 μm diameter at which size the 'finer' peak is still increasing.

From the size distributions shown in figure 8.15 the cumulative mass of the samples removed was calculated. The calculation procedure is given in Appendix 2. From this mass and the known removal of Ca^{++} from the system, the ratio of $CaCO_3$ present in the counted particles to that precipitated was calculated. The results are shown in table 8.5.

Table 8.4

Cumulative Number for Run I at 3, 5, 10, and 15 Residence Time.

Channel Numbers	Diameter μm	Cumulative Number at:- 3 min	5 min	10 min	15 min
3	2	30373	31749	31746	35599
4	2.52	27502	28574	27705	30218
5	3.17	25801	27234	26190	28010
6	4	24587	25847	24854	26323
7	5.04	23587	24688	23657	25019
8	6.35	22770	23178	22692	23979
9	8	22005	21786	20321	23058
10	10.08	3591	20759	18845	22004
11	12.7	142	8188	3061	19975
12	16	33	106	40	15232
13	20.16	18	21	10	139
14	25.4	8	6	5	16
15	32	3	1	2	6

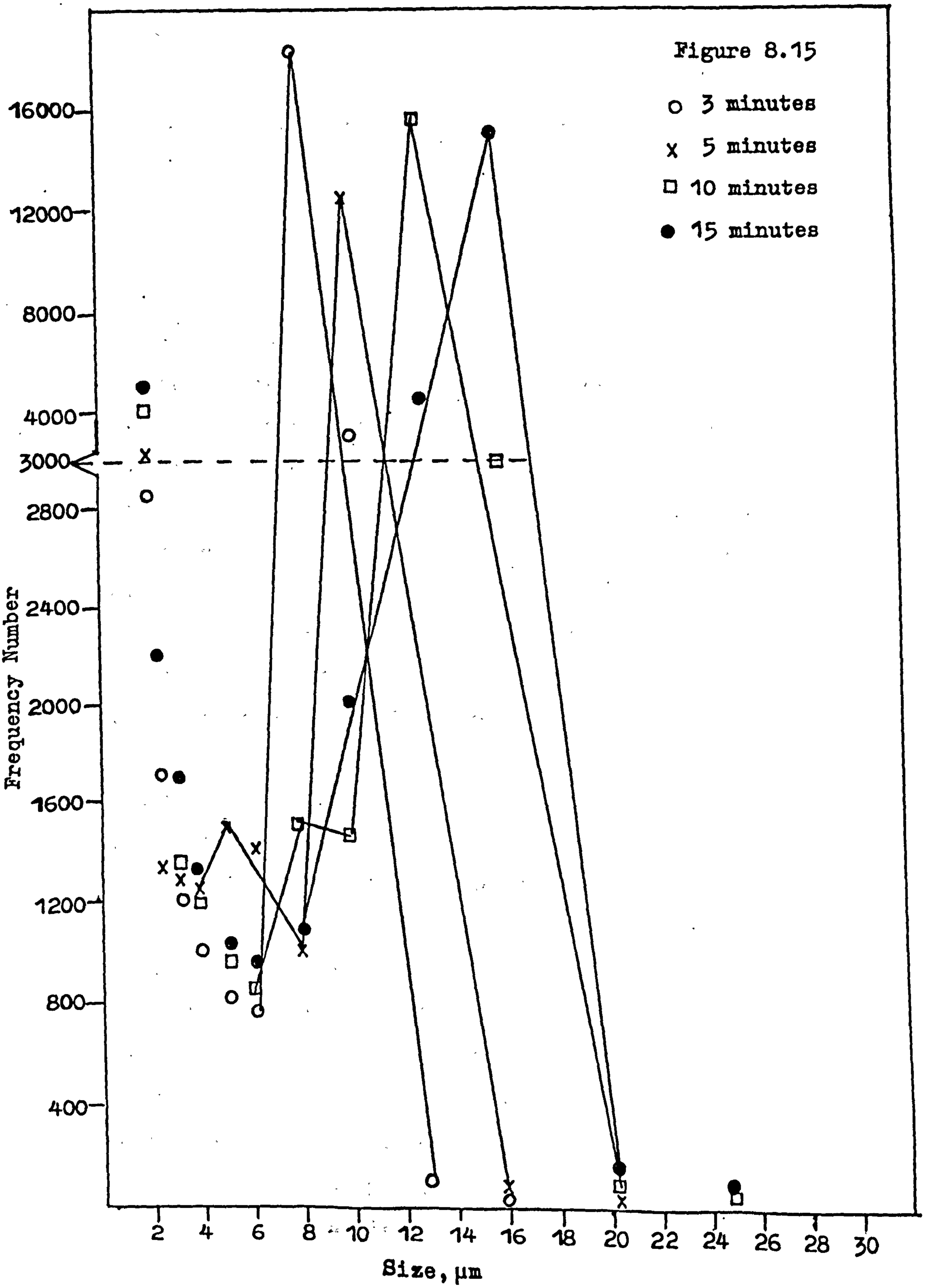
Figure 8.15
o 3 minutes
x 5 minutes
□ 10 minutes
● 15 minutes
Frequency Number
16000
12000
8000
4000
3000
2800
2400
2000
1600
1200
800
400
2
4
6
8
10
12
14
16
18
20
22
24
26
28
30
Size, μm

Table 8.5

Sample Time (minutes)	Mass Particle Yield	Total Particles Counted/100ml
3	18%	4.56×10^6
5	38%	4.76×10^6
10	56%	4.76×10^6
15	85%	5.34×10^6

The frequency/distribution plot (see figure 8.15) shows the existence of a peak going beyond the lower particle size limit of the counting technique. The results point to the existence of many particles <2 μm, this number decreasing with time. This decrease cannot be due to growth because of the relatively small increase in the total particle number with time and it must be concluded that these particles disappear by Ostwald ripening. Crystal growth was seen on the flask wall and stirrer blade. The blade was coated with epoxy resin and the flask was siliconised in an attempt to prevent heterogeneous growth but this was not successful. From the recovery figures quoted above it can be seen that heterogeneous growth is not a major consumer of Ca^{++} from solution, 85% being accounted for at 15 minutes and an analysis of surface deposited $CaCO_3$ at the completion of a run representing a recovery of 76%. As the supersaturation was reduced and the crystal growth period prolonged a greater amount of material was noted to be deposited on surfaces. This was not studied systematically.

The critical nuclear size for crystal growth is given

by the Ostwald-Freundlich equation:-

$$r_{crit} = \frac{2M\sigma}{\rho RT \ln S_i} \quad \ldots\ldots\ldots\ldots\ldots\ldots\ldots\ldots\ 4.8$$

where the terms are as defined previously. To calculate r_{crit} it is necessary to know σ , the surface energy of the solid-liquid interface. Estimates of surface energy vary widely with the measuring technique and experimenter. Some literature values are listed in Table 4.1.

Taking the surface energy as lying between the possible limits of 5.0×10^{-2} and 1.0 Jm^{-2} and for supersaturations in the range 10-60 r_{crit} is found to be within the range 3.6×10^{-10}-1.29×10^{-7}m, i.e. 3.6×10^{-4} to 1.29×10^{-2} µm which is below the lower limit of sensitivity of the particle size analysis method used.

Because the particles being measured were likely to be undergoing growth and dissolution, it was not considered practicable to subject them to the lengthy wet sieving procedure that would have been necessary to extend the measured particle size range downward and in any case 0.5 µm is about the lower limit of the Coulter Counter. In further calculations of the rate of crystal growth only those particles in the large third peak were considered as growing.

Table 8.6 shows, for samples taken at 3, 5, 10 and 15 minutes from run I, the specific surface as calculated from the size distribution of particles over 8 µm diameter, $\left[Ca^{++}\right]$ at the time of sampling and $\frac{d[Ca^{++}]}{dt}$ measured from a

Table 8.6

Sample Time	3 min	5 min	10 min	15 min
A, $m^2 l^{-1}$	0.94×10^{-2}	1.61×10^{-2}	2.16×10^{-2}	2.98×10^{-2}
$[Ca^{++}]$, M	8.5×10^{-4}	7.2×10^{-4}	5.5×10^{-4}	4.8×10^{-4}
$d[Ca^{++}]/dt$, $M.min^{-1}$	0.86×10^{-4}	0.38×10^{-4}	0.26×10^{-4}	0.16×10^{-4}
dCa^{++}/dt, $m^3 min^{-1}$	3.17×10^{-9}	1.40×10^{-9}	0.96×10^{-9}	0.59×10^{-9}
dG/dt, $m.min^{-1}$	3.37×10^{-7}	0.87×10^{-7}	0.44×10^{-7}	0.20×10^{-7}
Ca^{++}_{I}	4.90×10^{-4}	3.60×10^{-4}	1.90×10^{-4}	1.20×10^{-4}
Ca^{++}_{II}	7.87×10^{-4}	5.67×10^{-4}	4.87×10^{-4}	4.20×10^{-4}
log (dG/dt), $m.min^{-1}$	-6.472	-7.060	-7.356	-7.698
log A, $m^2 l^{-1}$	-2.027	-1.793	-1.666	-1.526
log Ca^{++}_{I}, M	-3.310	-3.444	-3.721	-3.921
log Ca^{++}_{II}, M	-3.104	-3.246	-3.312	-3.377
log (dG/dt) - log A	-4.445	-5.267	-5.690	-6.172

$$Ca^{++}_{I} = C_{(t)} - C_{(\infty)}$$

$$Ca^{++}_{II} = C_{(t)} - 6.33 \times 10^{-5}$$

tangent to the $[Ca^{++}]$ versus t graph (see figure 8.16).

Assuming that all particles were the same size and spherical, the linear growth rate at time, t, was calculated from $\frac{-d[Ca^{++}]}{dt}$ and the specific surface calculated from the particle size distribution, taking the density of calcite as 2.71gm cm^{-3}. The calculation procedure is given in Appendix 3. This data was then tested to see if it fitted a growth rate equation of the type:-

$$\frac{dG}{dt} = k\,[\Delta Ca^{++}]^n\,A \qquad \ldots\ldots\ldots\ldots\ldots\ldots\ldots\ 8.3$$

To determine n, the order of reaction with respect to $[\Delta Ca^{++}]$ the equation was expressed in logarithmic form:-

$$(\log \frac{dG}{dt} - \log A) = n \log [\Delta Ca^{++}] + \log k$$

and the data plotted as:-

$$(\log \frac{dG}{dt} - \log A) \text{ versus } \log [\Delta Ca^{++}]$$

The results are shown in figure 8.17. Two forms of $[\Delta Ca^{++}]$ were considered, it having been noted that final experimental values of $[Ca^{++}]$ were significantly greater than those predicted from solubility values. Points I are based on $[\Delta Ca^{++}] = ([Ca^{++}]_{t=t} - [Ca^{++}]_{t=\infty})$ and points II on $[\Delta Ca^{++}] = ([Ca^{++}]_{t=t} - [Ca^{++}]_{theory})$.

The points corresponding to 5, 10 and 15 minutes of set I fall on a reasonably straight line of slope 1.88, the 3 minute point being somewhat off this line. The four points of set II all fall onto a straight line of slope 6.26. Similar plots were made for another set of data and are shown in figure 8.18. In this case both sets of data lie on reasonably straight lines of slopes 2.18 and 15.0 respectively.

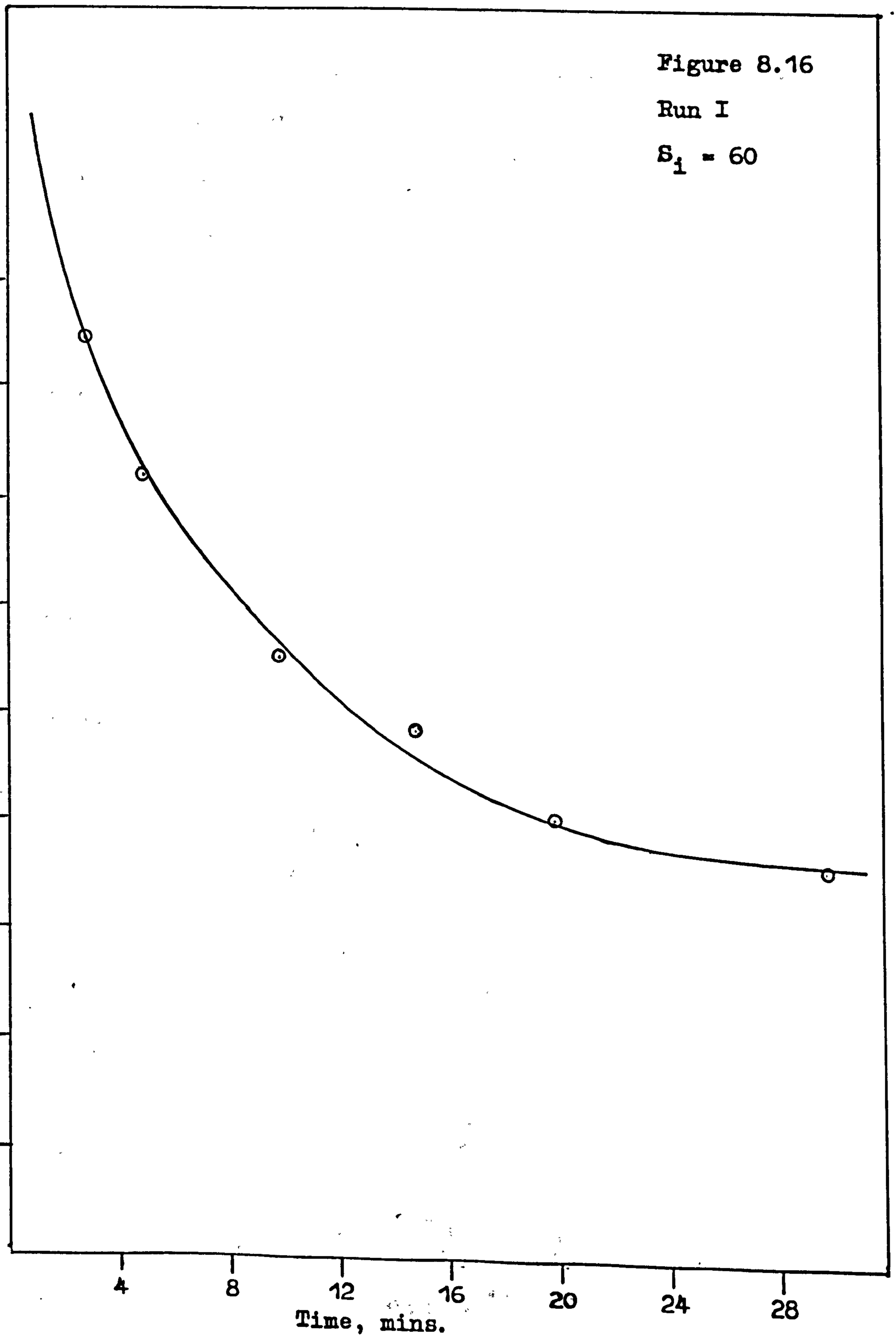

Figure 8.16

Run I

S_i = 60

Figure 8.17

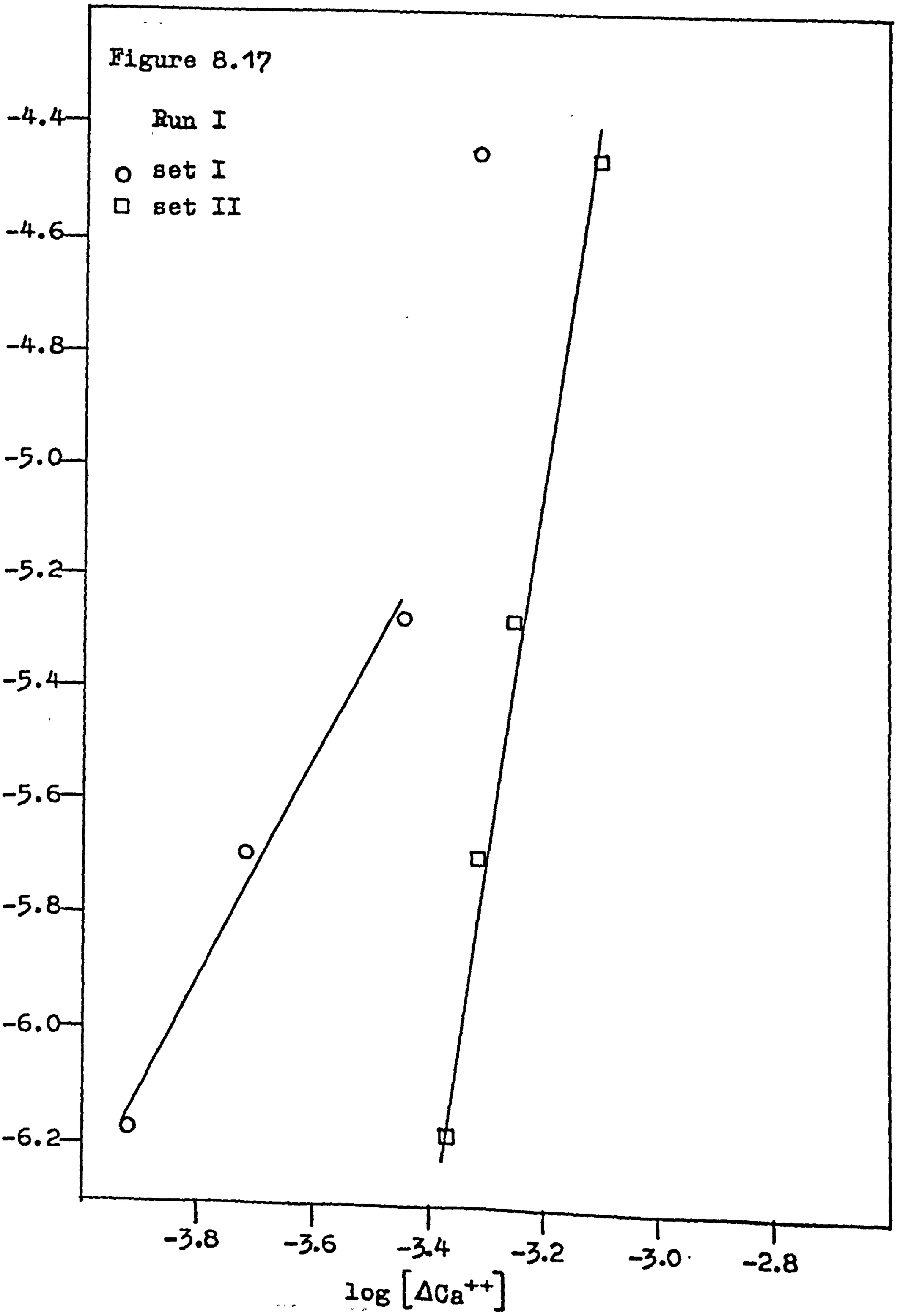
Run I
o set I
□ set II
(log dG/dt - log A)
-4.4
-4.6
-4.8
-5.0
-5.2
-5.4
-5.6
-5.8
-6.0
-6.2
-3.8
-3.6
-3.4
-3.2
-3.0
-2.8
log [ΔCa++]

Figure 8.18

Run V

○ set I

□ set II

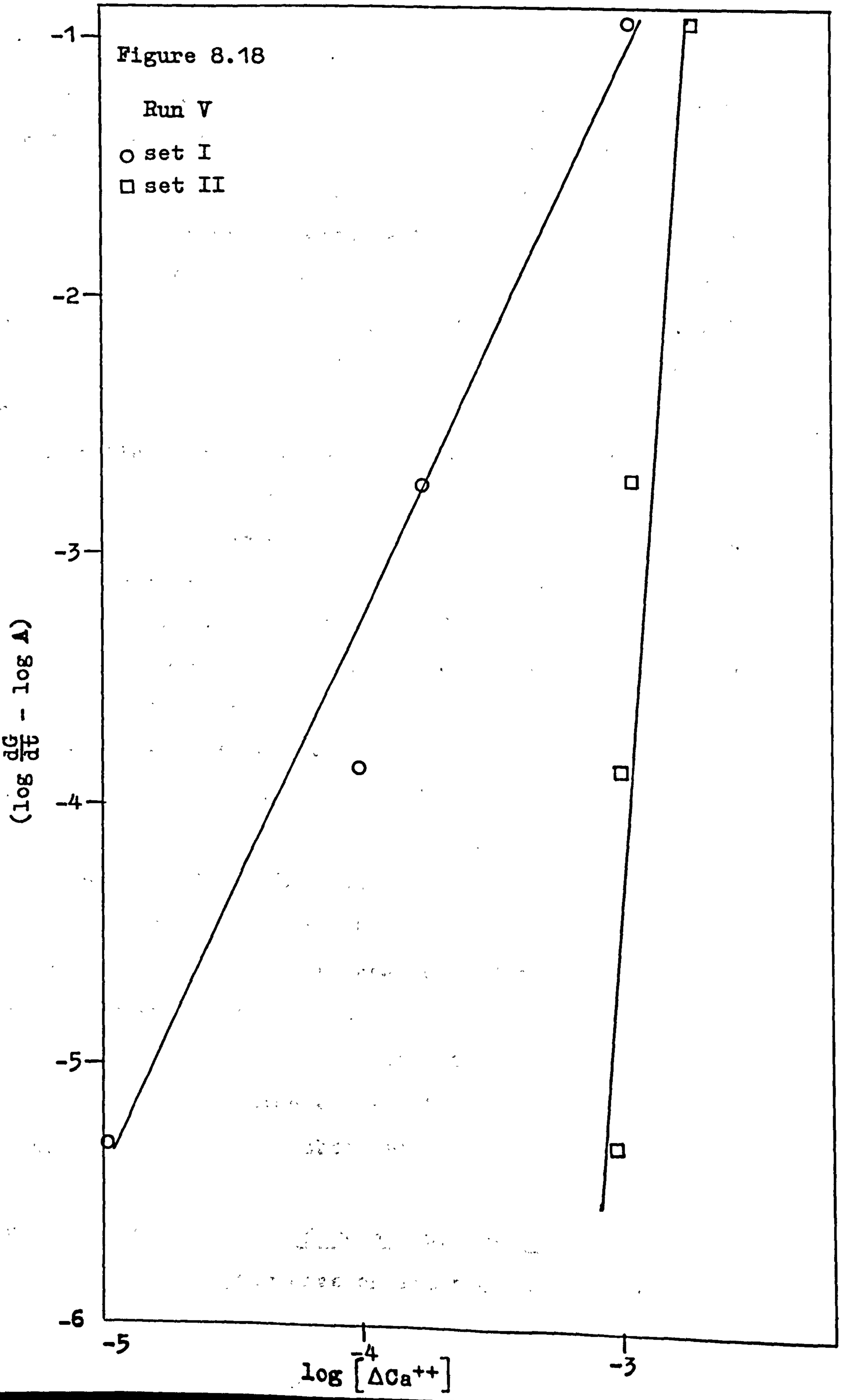

For both plots the slopes of lines corresponding to $[\Delta Ca^{++}] = ([Ca^{++}]_{t=t} - [Ca^{++}]_{theory})$ corresponded to a reaction order much higher than could reasonably be expected and in disagreement with Reddy's observation of second order for this precipitation whereas the slopes based upon the observed limiting solubilities were, within the wide scatter of experimental data, consistent with second order kinetics. As only part of the particle size distribution was amenable to the size analysis technique used, it is best to regard all results drawn from size distribution measurements with reservation. The increase in calculated particle yield with increasing time from particle size data (see table 8.5) may account for the non-linearity of I at 3 minutes but this is very speculative.

The values of the rate constant, k, calculated from the intercepts of curves I for each of these sets of data is 16.59 and 2.0×10^5 whilst that calculated for one set of Reddy's data is 0.6, all in units of $m^{-1}l^3moles^{-2}min^{-1}$.

In view of the enormous spread in this data and the indirect method of calculation, each step of which involves assumptions and errors it was decided to go no further with the calculation of reaction rate constants, although it does seem from the data obtained that a rate law second order in concentration and first order in surface area, as proposed by Reddy, is obtained in the present case.

8.2.1.2 Calculation of Data - Nucleation Rate

Coulter Counter size analysis data was also used to

calculate the nucleation rate employing the technique of Misra and White[176]. Performing a population balance on the growing crystal system and assuming that the McCabe linear growth rate law is obeyed, this technique permits evaluation of the number of nuclei present when those nuclei are too small to be counted and sized. The growth rate is determined by plotting cumulative number versus size graphs for the system at intervals of time during the crystallisation. If the McCabe ΔL law is obeyed the resulting curves should all be of the same shape, progressively displaced to higher size with increasing time.

Figure 8.19 shows a family of curves for Run I, the samples being taken at 3, 5, 10, 15 and 30 minutes. It will be noticed that the curves are not parallel and that the 5 minute line crosses the 3 minute line. The number of particles counted at the large end of the size range is very small and the subsequent statistical error is substantial. In order to obtain even this number of particles it was necessary to take such a large sample from the precipitation reactor that the level had dropped so low after withdrawal of five samples that the formation of a vortex about the stirrer became a problem. Also the size distribution of the growing particles is relatively narrow and using a Coulter Model TA-II which is pre-set to count 15 channels in increasing diameter ratio $\sqrt[3]{2}$, not many points occur on the portion of interest of each size distribution.

To enable the reaction to be followed over a reasonable

Figure 8.19

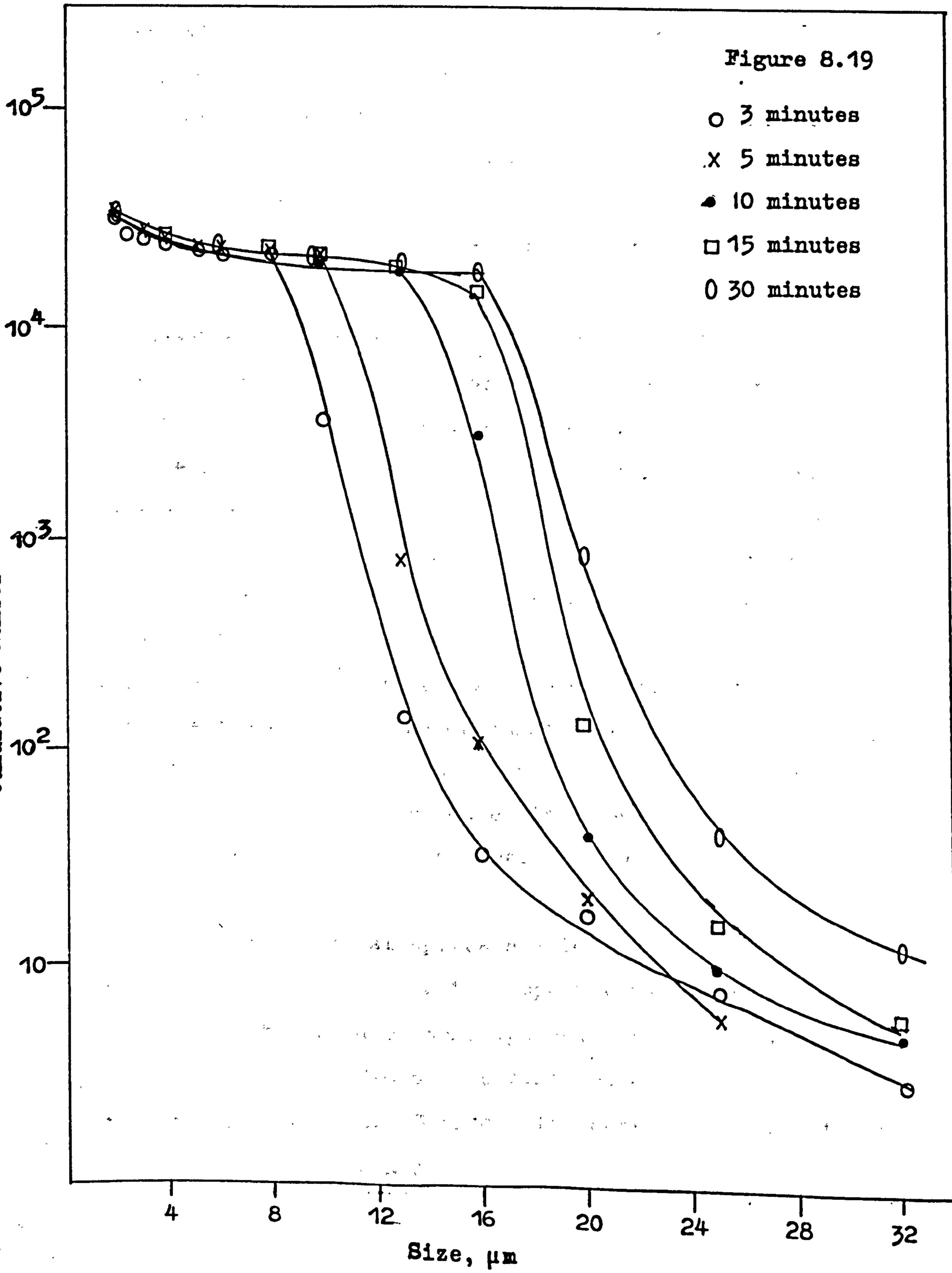
o 3 minutes
x 5 minutes
• 10 minutes
□ 15 minutes
0 30 minutes
Cumulative Number
10^5
10^4
10^3
10^2
10
4
8
12
16
20
24
28
32
Size, μm

length of time with samples at closely spaced time intervals, a group of three parallel runs A, B, C, were set up, samples being withdrawn at:-

		Sampling Time (minutes)
Run V	(A)	5 10 15 20 25 30
	(B)	25 30 35 40 45 50
	(C)	45 50 55 60 65 70

The overlapping runs at 25 and 30 and 45 and 50 minutes were to check on the consistency of the parallel experiments.

Figure 8.20 shows the duplicated analyses plotted as cumulative number undersize plots from which it can be seen that whilst the curves of each of a pair have a similar shape they are displaced with respect to one another.

Because that part of the size analysis curve of interest is very steep and covered at the most by only four size increments, the data was not considered precise or consistent enough for the calculation of nucleation rates. This technique has previously been applied to systems[176] where the reaction occurs more slowly and the particle size is larger so that a more accurate size distribution may be obtained.

Another empirical approach which correlates the desupersaturation rate to the supersaturation ratio, S_i, similar to that used by Randolph and Larson[179] was used for studying the effects of parameters on the crystallisation rate. Consider the general rate equation:-

$$-dm/dt = K S_i^n \quad \ldots\ldots\ldots\ldots\ldots\ldots\ldots\ldots \quad 8.4$$

Figure 8.20

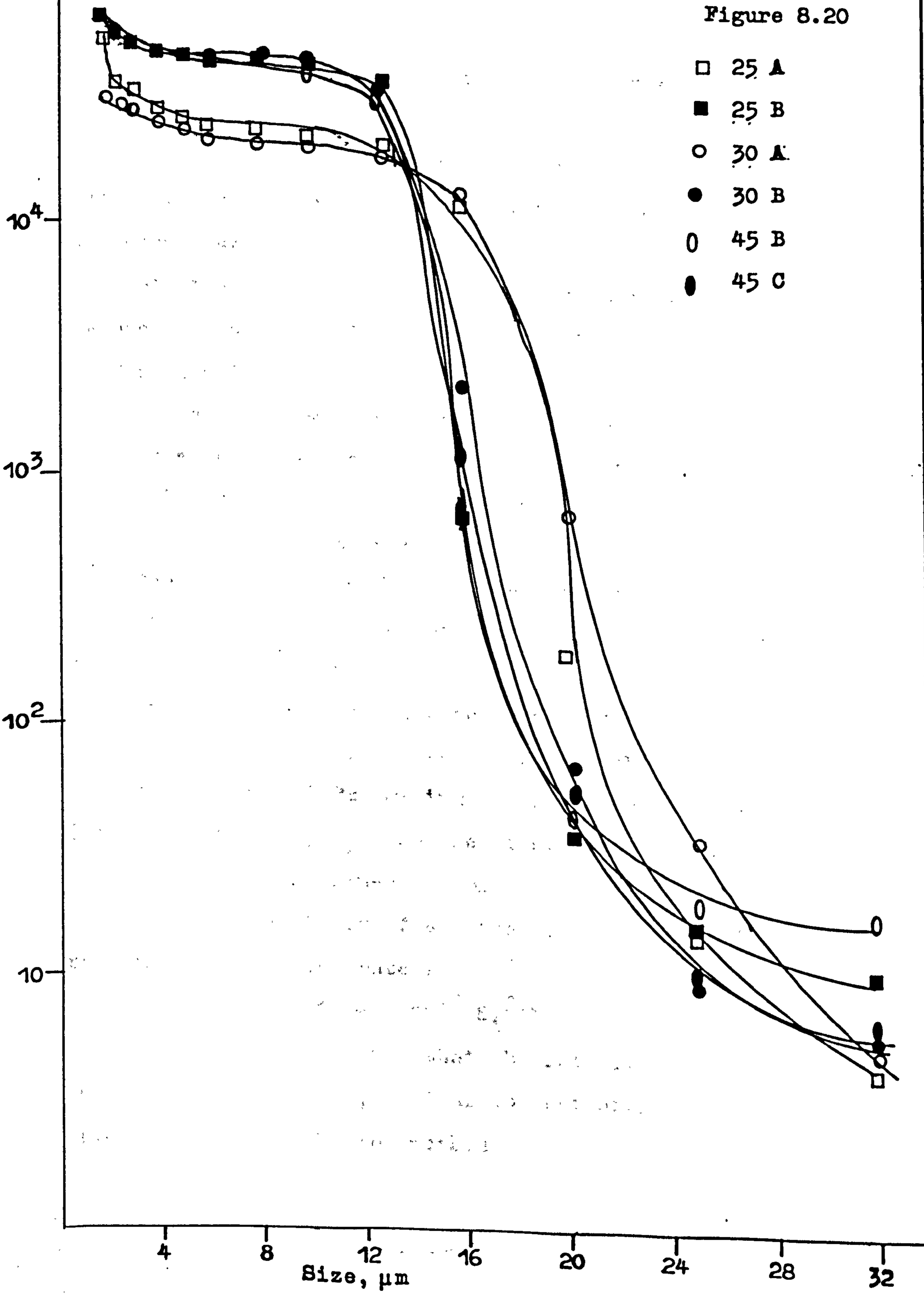
□ 25 A
■ 25 B
○ 30 A
● 30 B
0 45 B
● 45 C
Cumulative Number
10^4
10^3
10^2
10
4
8
12
16
20
24
28
32
Size, µm

where -dm/dt = is the desupersaturation rate.

K = is a rate constant.

n = is the order of crystallisation.

Table 8.7 shows the effect of supersaturation ratio, S_i, on the desupersaturation rate (-dm/dt). Where -dm/dt is the initial slope of the best straight line through the desupersaturation region. A typical straight line is shown in figure 8.21.

Table 8.7 shows the very strong dependence of the desupersaturation rate (-dm/dt) on the supersaturation ratio, S_i. The rate of desupersaturation increases as the supersaturation ratio increased. This shows the greater ease for nucleation at higher supersaturation ratios and is consistent with the values of the induction period and the half life time tabulated in table 8.3.

The desupersaturation rates (-dm/dt) and supersaturation ratio, S_i, tabulated in table 8.7 are plotted in figure 8.22, giving a relationship of log (-dm/dt) versus log S_i. The least square straight line was fitted to these experimental points. The equation representing the effect of supersaturation ratio, S_i, on the desupersaturation rate is:-

$$-dm/dt = 1.54 \times 10^{-9} S_i^{2.6} \quad \ldots\ldots\ldots\ldots\ldots 8.5$$

Equation 8.5 suggests that the rate lies between second and third order, similar to that obtained by the crystal size distribution method.

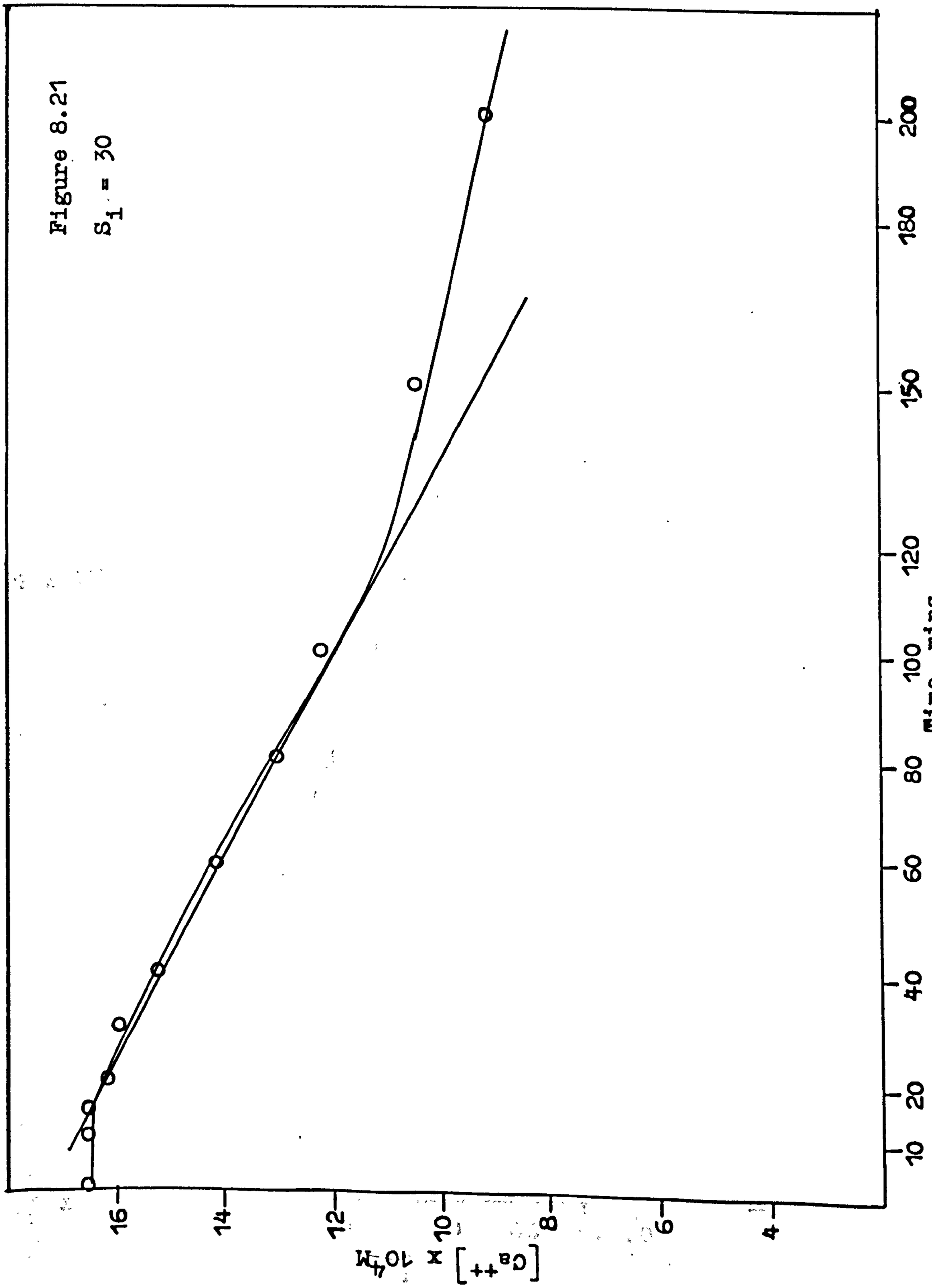
Figure 8.21
S_1 = 30
Time, mins.
10
20
40
60
80
100
120
150
180
200
$[Ca^{++}] \times 10^{4}M$
16
14
12
10
8
6
4

Figure 8.22

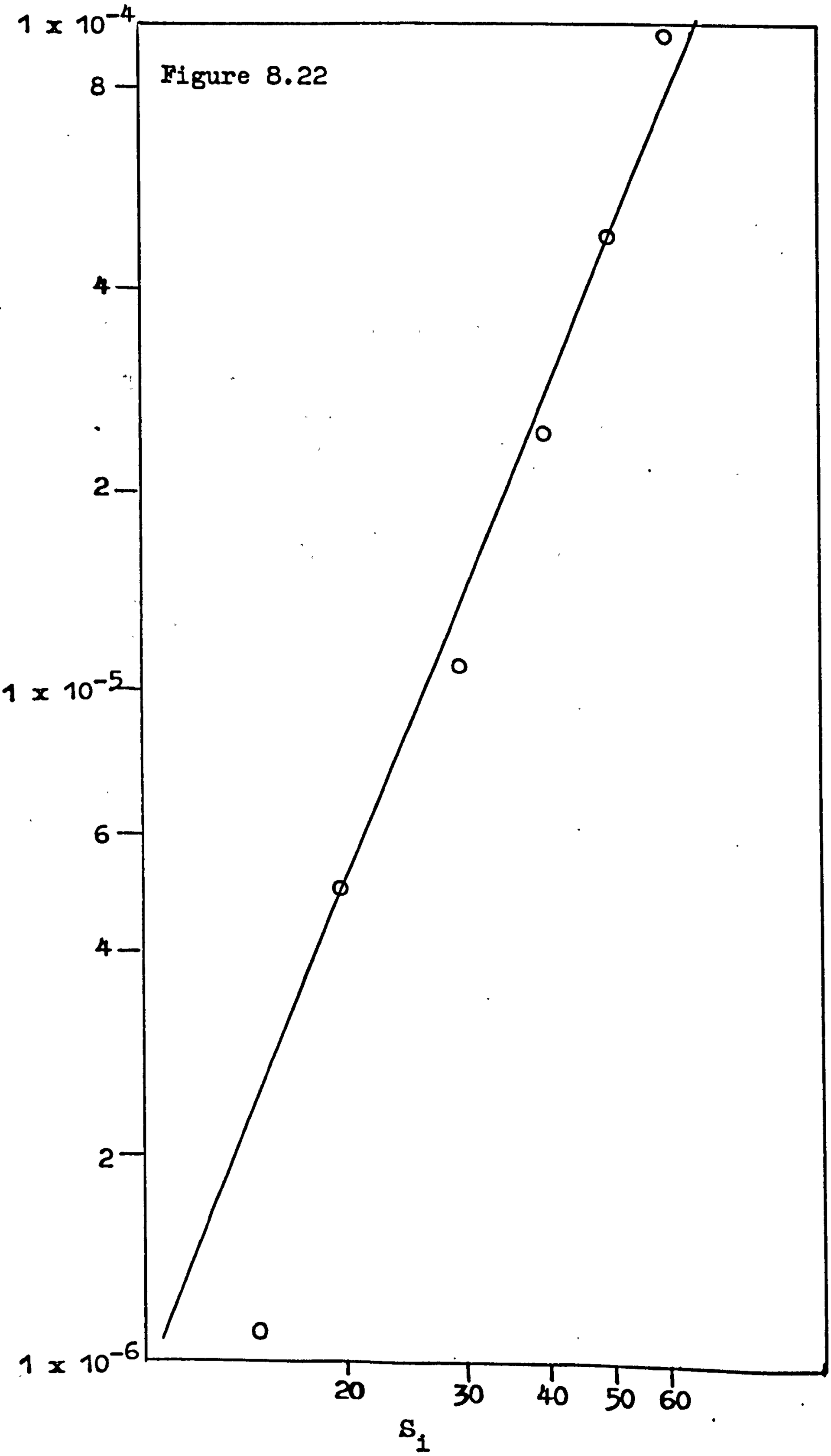

Table 8.7

S_i	$(-dm/dt) \times 10^6$	$\log S_i$	$\log (-dm/dt)$
15	1.2	1.1761	-5.92
20	5.0	1.301	-5.30
30	12.0	1.4771	-4.92
40	24.5	1.6020	-4.61
50	48.0	1.699	-4.32
60	98.0	1.7782	-4.01

8.2.2 Effect of the Presence of Seed Crystals During Desupersaturation

The precipitation of calcium carbonate in cold-lime softening is almost invariably carried out in a continuous flow reactor in which the reactants are added to an already formed suspension of growing crystals. The presence of seed enables crystal growth to occur at supersaturation corresponding to very low nucleation rates. Randolph and Larson theory[179] has suggested that the nucleation rate follows a law of the type:-

$$B^o = k S^i \quad \ldots\ldots\ldots\ldots\ldots\ldots\ldots\ldots\ldots\ldots \quad 8.6$$

from which the supersaturation dependence can be seen. To simulate the presence of seed in a precipitation reactor experiments were carried out in the presence of added calcium carbonate crystals.

A supersaturation ratio $S_i = 15$ was chosen for these studies as at this supersaturation a long induction period (170 minutes) was observed in the absence of seed crystals. The effect on the desupersaturation produced by introducing low and high concentration (0.1, 1.0, and 10% w/v) of seed was studied.

Table 8.8 and figure 8.23 show the results. Curve a is the desupersaturation curve in an unseeded system, and curve b represents three similar runs performed in the presence of 1% seed crystals. Curves c and d are for the results obtained when 0.1% and 10% seed crystals were introduced.

Table 8.8

	τ min	$t_{\frac{1}{2}}$ min	t_{∞} min	$[Ca^{++}]_{\infty} \times 10^{4}$ M	$-dm/dt$, M.min^{-1}
unseeded	170	280	≈ 1000	—	0.12×10^{-5}
0.1% seed	8	35	200	6.2	0.73×10^{-5}
1.0% seed	7	30	200	5.4	1.44×10^{-5}
10% seed	< 1	8	80	5.7	3.54×10^{-5}

Figure 8.23

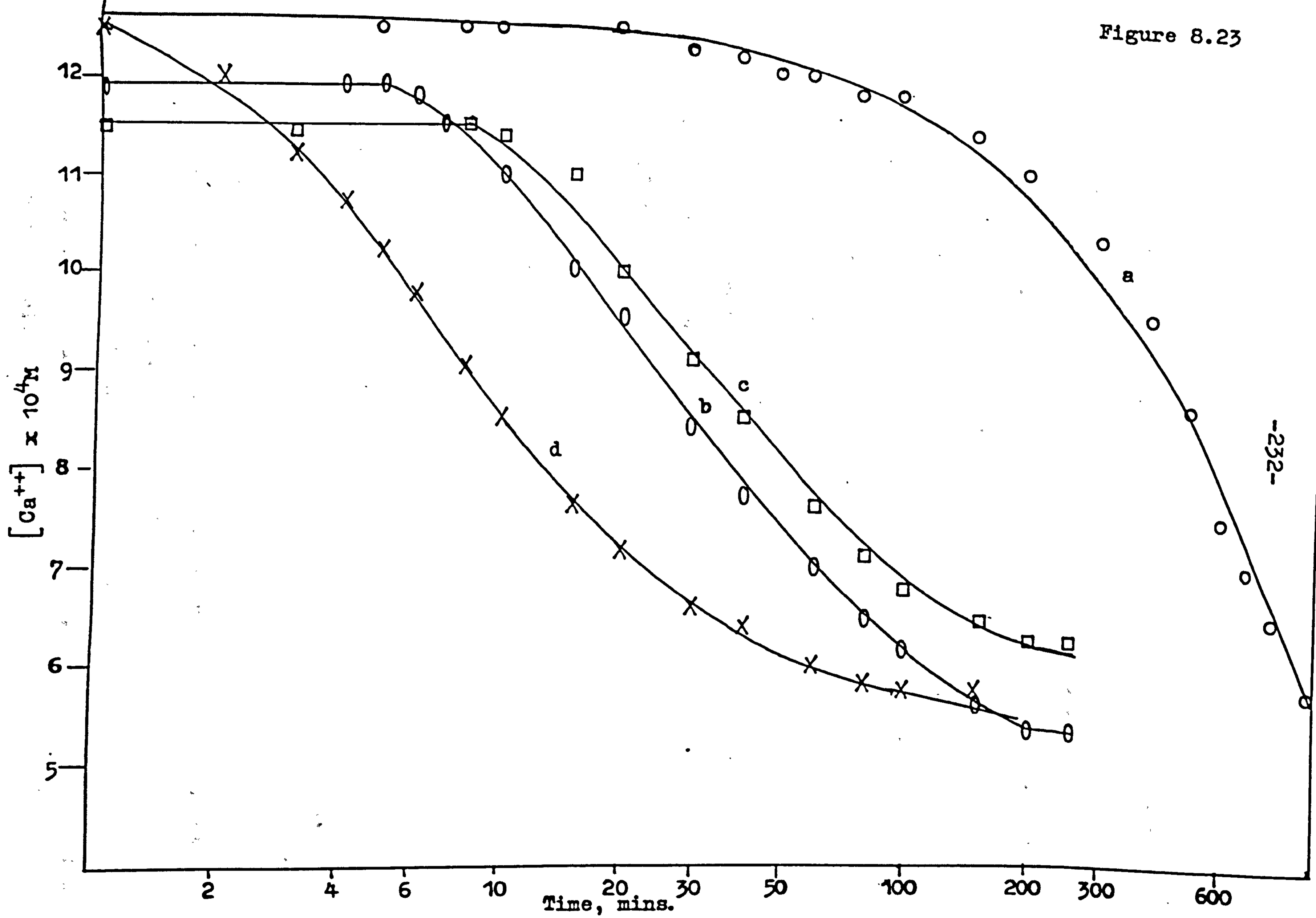
[Ca++] x 10^4M
12
11
10
9
8
7
6
5
a
b
c
d
2
4
6
10
20
30
50
100
200
300
600
Time, mins.

Table 8.8 and figure 8.23 summarise the large effects produced by just introducing a small quantity of seed crystals into the solution at the beginning of a run. The induction period, τ, decreased from about 170 minutes when no seed crystals were present to <1 minute when 10% (0.1gm) seed crystals were introduced; similarly the half life reduced from 280 minutes to 8 minutes. The rate of desupersaturation (-dm/dt) increases with the amount of seed introduced and it is almost increased by 30 times when 10% seed crystals were introduced comparing with that when no seed was present. This is probably due to the greater ease with which secondary nucleation occurs (see 4.5).

The total time for almost complete desupersaturation was also reduced when seed crystals were present (from $\approx$ 1000 to 80 minutes).

The effects produced by introducing a fixed number of seed crystals (1%$\approx$0.01gm) into solutions of different initial supersaturation ratio are shown in table 8.9.

As S_i is increased to the point where an induction period ceases to be observed, i.e. $S_i = 50$, $S_i = 60$, the addition of seed crystals has a negligible effect on $t_{\frac{1}{2}}$ whereas at lower S_i large effects are noticed. At $S_i = 20$ in the presence of 1% seed crystals for example, τ, is reduced from 50 to 7 minutes and $t_{\frac{1}{2}}$ from 180 to 25 minutes. It is possible that once a certain surface area of crystals had been created by nucleation and growth for $S_i \geqslant 50$, the solution continued to desupersaturate mainly through growth of these nuclei.

Table 8.9

Effects of 1% seed (0.01gm) on crystallisation of calcium carbonate

S_i	τ min.		$t_{\frac{1}{2}}$ min		t_∞ min	
	seeded	unseeded	seeded	unseeded	seeded	unseeded
5	>5hr.	>5hr.	——	——	——	——
10	30	5hr.	100	300	500	>1000
15	7	170	30	280	200	>1000
20	7	50	25	180	200	400
30	3	16	18	55	150	350
40	< 2	9	6	20	40	200
50	< 1	< 1	4	4	30	150
60	< 1	< 1	1	1	20	30

The effect of supersaturation ratio, S_i, on the desupersaturation rate (-dm/dt) in the presence of a fixed amount of seed crystals (1% = 0.01gm) is shown in table 8.10.

The values of log (-dm/dt) for seeded runs are plotted versus log S_i in figure 8.24. The equation representing the effect of supersaturation ratio, S_i, on the desupersaturation rate in the presence of 0.1gm seed crystals is:-

$$-dm/dt = 2.2 \times 10^{-8} S_i^{2.36} \quad \ldots\ldots\ldots\ldots\ldots 8.7$$

Though the presence of seed does not affect the order of crystallisation but the rate constant, k, is increased by ten times (see equation 8.5). This confirms the greater ease for precipitation of $CaCO_3$ in cold-lime softening in the presence of seeds (see 2.3).

8.2.3 Effect of the Presence of Additives During Desupersaturation

The principle object of this research was to see if trace quantities of added high molecular weight and natural organic substances would affect the rate of precipitation. The materials chosen for this were two anionic, one cationic and one nonionic synthetic flocculant of the type that might be used either in other stages of the water treatment process or to enhance the precipitation of calcium carbonate from the softening reaction. Starch, which can also be used as a flocculant, was used and an extract of water humic substance, an organic material present in many natural waters. Additional experiments

Table 8.10

		$(-dm/dt) \times 10^6$ M.min^{-1}		log (-dm/dt)	
S_i	log S_i	seeded	unseeded	seeded	unseeded
10*	1.0	——	——	——	——
15	1.1761	14.39	1.20	-4.84	-5.92
20	1.301	22.13	5.00	-4.65	-5.30
30	1.4771	57.63	12.0	-4.24	-4.92
40	1.6021	125.2	24.5	-3.90	-4.61
50	1.6989	267.0	48.0	-3.57	-4.32
60	1.7782	140.0	98.0	-3.85	-4.01

* It was not possible to find -dm/dt.

Figure 8.24

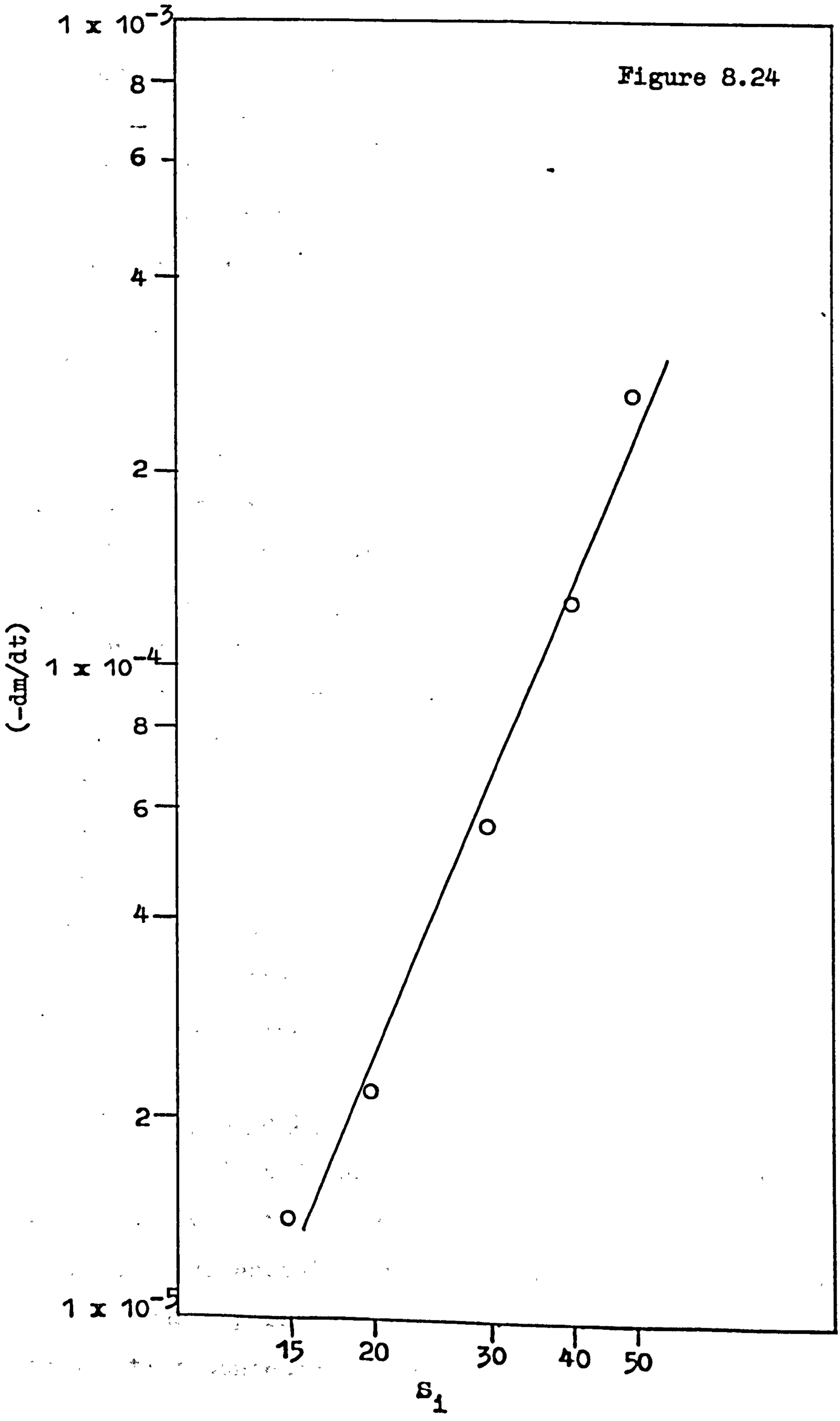

were carried out with added aluminium sulphate which is used as a coagulant in cold-lime softening and general water treatment. All the experiments were carried out under the same conditions, as described in 8.1.1. The experimental results have been grouped together according to the type of substitutent group attached to the polymer chain.

8.2.3.1 Flocculants Containing Poly (Acrylic Acid) Groups

8.2.3.1.1 Cationic Polyacrylamide

Table 8.11 and figure 8.25 compare the results of experiments with cationic polyacrylamide as additive with the results in the absence of additive. The effect of additive concentration on the crystallisation of $CaCO_3$ was followed in the presence of three different concentrations of cationic polyacrylamide (1, 2, 5 p.p.m.), holding the initial supersaturation ratio at 30.

The first effect observed is that the rate of desupersaturation (-dm/dt) is apparently unchanged and there is no apparent effect of the additive concentration on either the induction period or the half life.

8.2.3.1.2 Anionic Polyacrylamide

Figure 8.26 and table 8.12 show the results of experiments with two anionic polyacrylamides as additives, FA 200-5 (high anionic ratio) and FA 60H (normal anionic ratio). The supersaturation ratio, S_i, was fixed at 30 and the additive concentration used was 5 p.p.m.

Figure 8.25

S_1 = 30

Plus (+) PAM

○ 1 p.p.m.

□ 2 p.p.m.

0 5 p.p.m.

x no additive

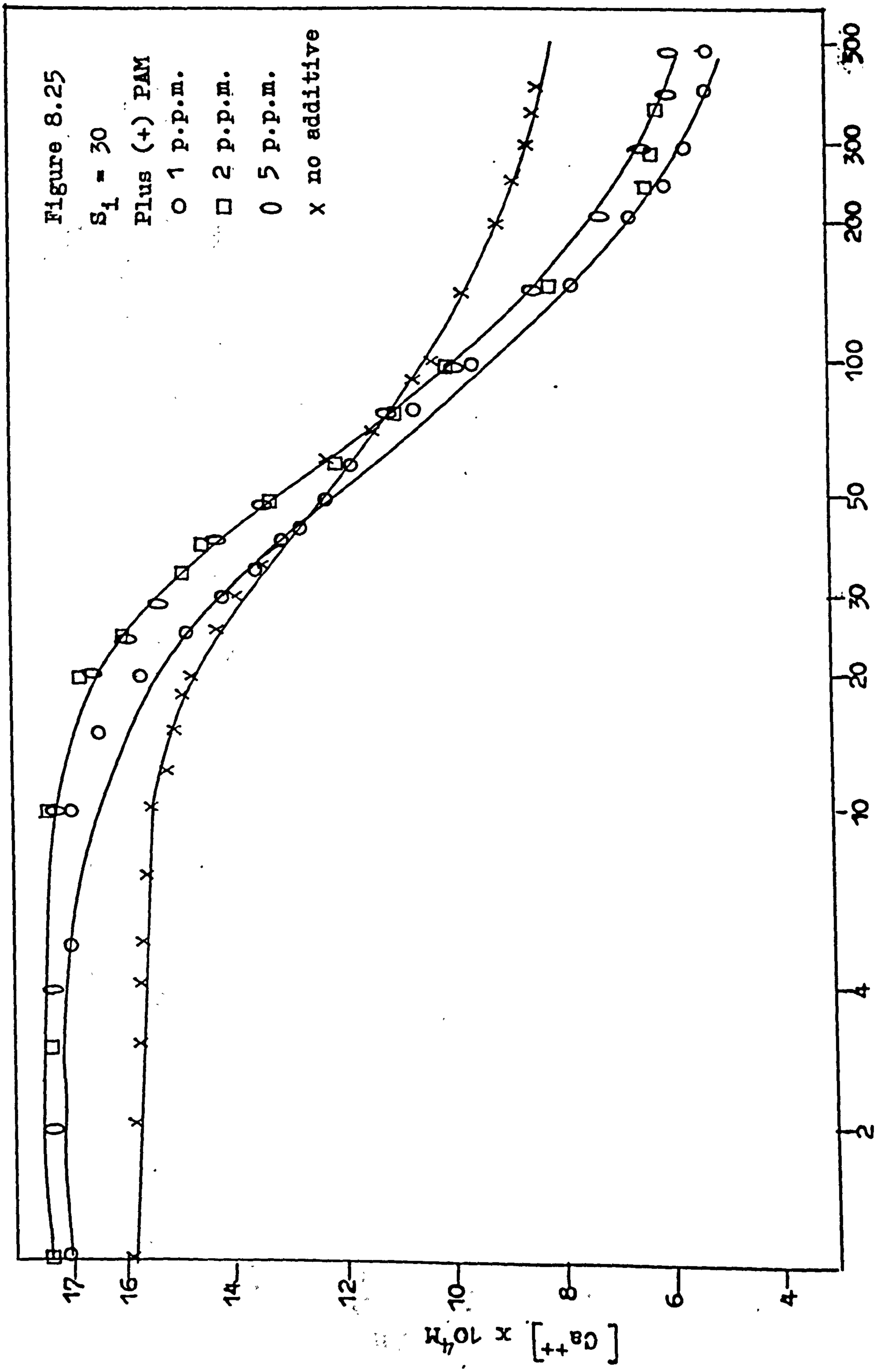

Figure 8.26

S_i = 30

○ 5 p.p.m. (-) PAM (L)

● 5 p.p.m. (-) PAM (H)

× without additive

$[Ca^{++}] \times 10^4 M$

18
16
14
12
10
8
6
4

2 4 6 10 20 30 40 60 100 200 300

Time, mins.

Table 8.11

(+) PAM p.p.m.	τ min	$t_{\frac{1}{2}}$ min	t_∞ min	$[Ca^{++}]_\infty \times 10^4 M$	$(-dm/dt)$ M.min^{-1}
0	16	55	350	8.0	12.0×10^{-6}
1	15	66	300	5.8	11.1×10^{-6}
2	18	66	300	6.2	10.8×10^{-6}
5	18	68	350	6.0	9.0×10^{-6}

Table 8.12

(-) PAM	τ min	$t_{\frac{1}{2}}$ min	t_∞ min	$[Ca^{++}]_\infty \times 10^4 M$	$(-dm/dt)$ M.min^{-1}
None	16	55	350	8.0	12.0×10^{-6}
(-) PAM (L)	15	60	350	8.5	11.9×10^{-6}
(-) PAM (H)	15	45	200	10.0	10.3×10^{-6}

The first point to note is that the anionic polyacrylamides have no significant effect on crystallisation of $CaCO_3$, neither the induction, τ , nor the half life, $t_{\frac{1}{2}}$ within the experimental error, being changed. These results show an interesting effect of anionic polyacrylamides, particularly FA 200-5, on the final calcium concentration, $\left[Ca^{++}\right]_{\infty}$, it being 10.0 x 10^{-4}M in the presence of (-) PAM (H) compared with $\left[Ca^{++}\right]_{\infty}$ = 8.0 x 10^{-4}M in the absence of additive. This may result from the formation of soluble complexes between Ca^{++} and acrylic acid/acrylamide copolymers. At 1g eq of Ca^{++} per 1.49 and 1.34 g eq acrylic acid respectively, the 0.84/0.16 and 0.36/0.64 acid/amide polymers complex approximately equal amounts of Ca^{++} per acid equivalent weight. As previously dicussed, no complex is formed by Dispex N-40 or the nonionic polyacrylamide and it would seem that both amide and carboxylic acid groups are necessary. Calcium is readily complexed by bidentate ligands, e.g. E.D.T.A. and in these cases stability constants may be calculated. As, however, the nature of the ligand is not known in the present case this is not possible. These complexes may have interesting practical consequences in the use of anionic polyacrylamides in Ca^{++} containing waters. The rate of desupersaturation (-dm/dt), is virtually unaffected.

8.2.3.1.3 Nonionic Polyacrylamide

A further set of experiments were carried out using a nonionic polyacrylamide flocculant as the additive. Those

experiments were carried out in the presence of 5 p.p.m. (O) PAM at a supersaturation ratio 30. The results are shown in figure 8.27.

It seems that polyacrylamide without ionisable groups behaves similarly to the polyacrylamide with ionisable groups previously discussed. The induction period, τ, and the half life, $t_{\frac{1}{2}}$ (16 and 55 minutes respectively) compared with 16 and 55 minutes in the absence of (O) PAM show a lack of effect on the precipitation process.

The law $\left[Ca^{++}\right]_{\infty}$ in the presence of (O) PAM (3.5×10^{-4}M) compared with $\left[Ca^{++}\right]_{\infty} = 8.0 \times 10^{-4}$M in the absence of (O) PAM cannot be explained.

8.2.3.1.4 Dispex N-40

Figure 8.28 shows the results when 5 p.p.m. Dispex N-40 was used as additive at a supersaturation ratio $S_i = 30$. The first point to note is that Dispex N-40 completely inhibited the crystallisation of $CaCO_3$ at this super-saturation ratio. Although no crystallisation occurred for five hours or so after mixing, it would have been incorrect to conclude from this that the crystallisation had been inhibited indefinitely.

8.2.3.2 Humic Substance

Figure 8.29 and table 8.13 show the results of experiments when humic substance was added to crystallisation runs at $S_i = 30$. These experiments were to simulate the effect of organic materials present in many natural waters

Figure 8.27

S_1 = 30

o 5 p.p.m. (O) PAM

x no additive

$[Ca^{++}] \times 10^4 M$

Time, mins.

Figure 8.28

S_1 = 30

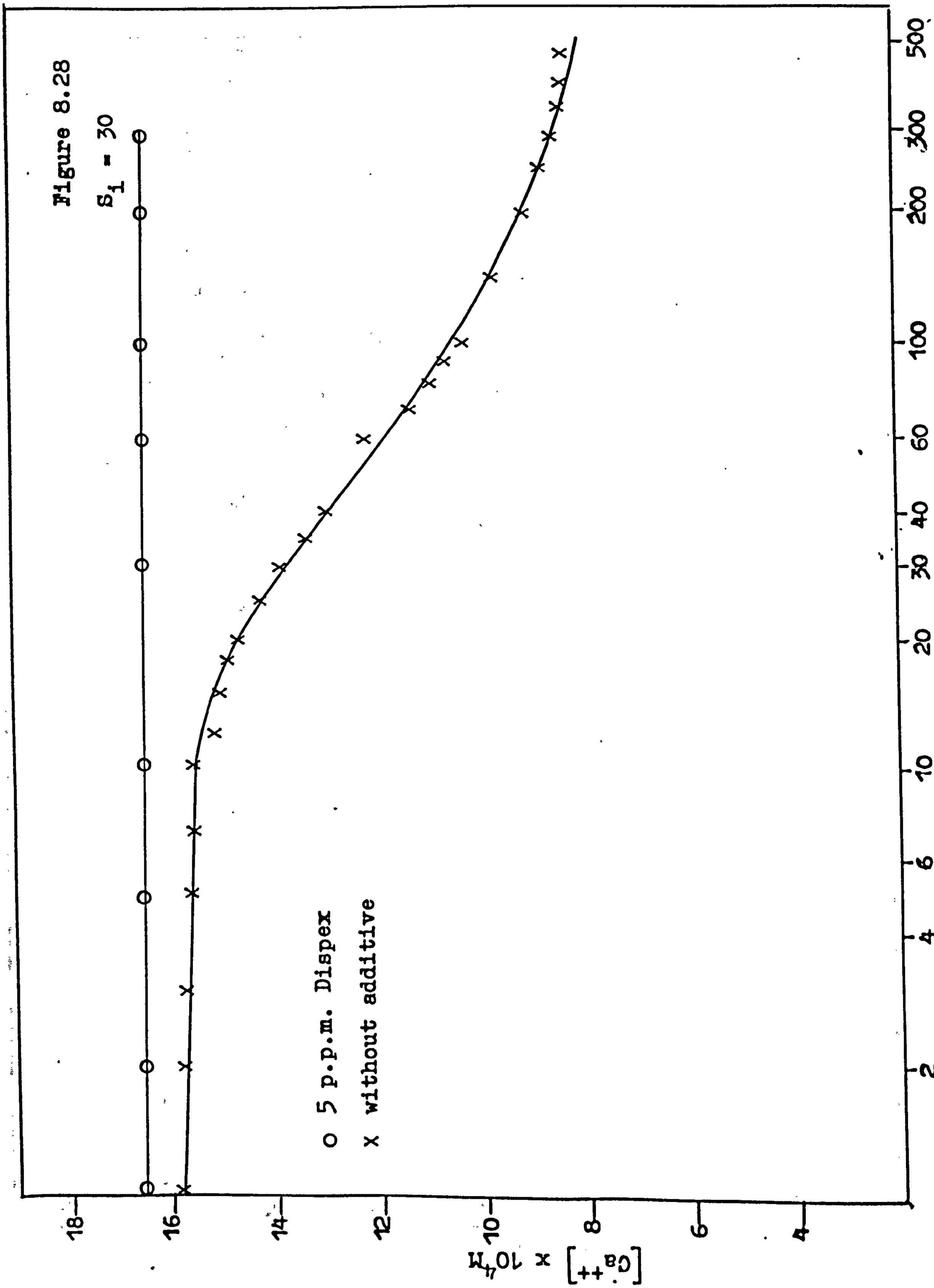

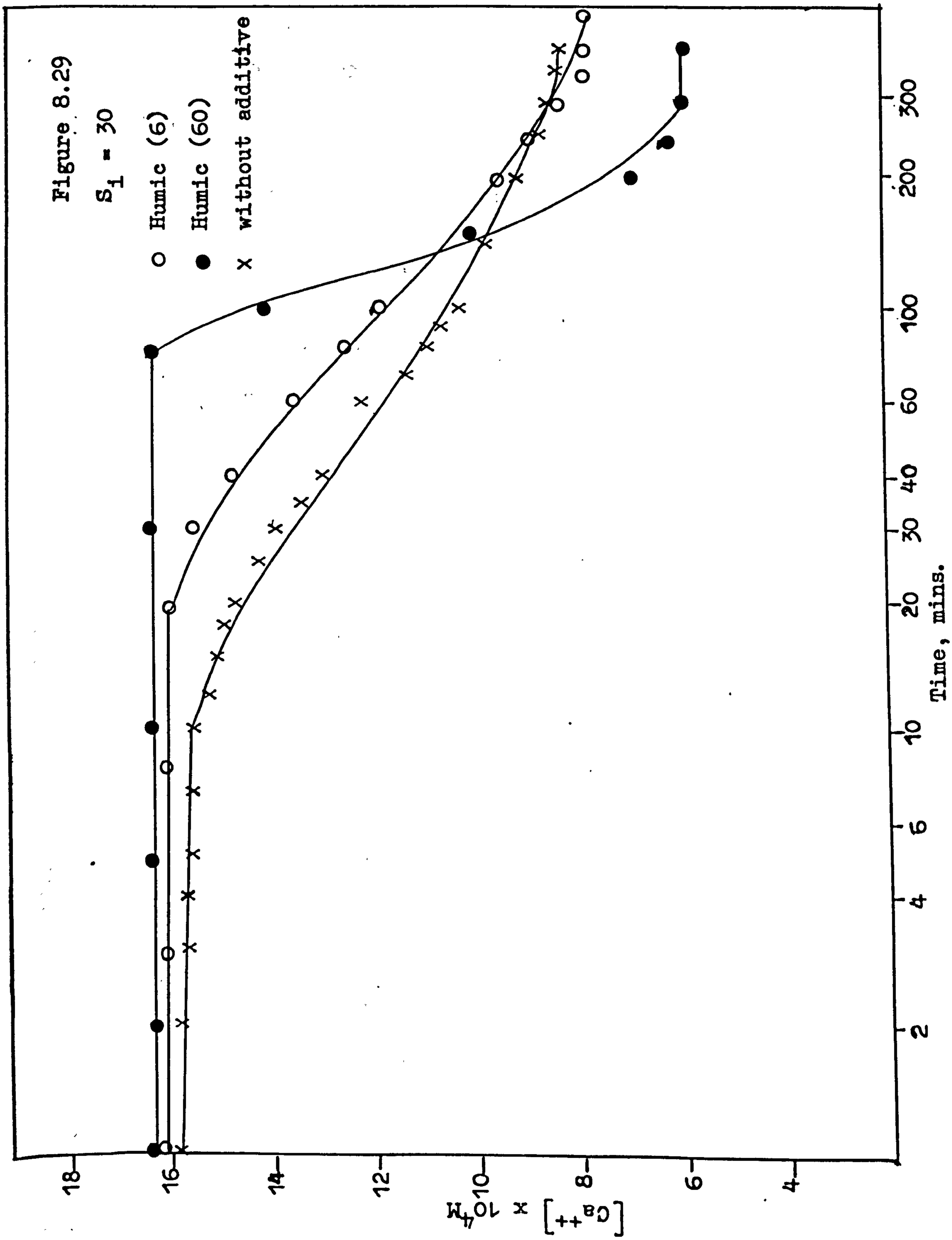
Figure 8.29
S_1 = 30
o Humic (6)
● Humic (60)
x without additive
Time, mins.
2
4
6
10
20
30
40
60
100
200
300
$[Ca^{++}] \times 10^4 M$
4
6
8
10
12
14
16
18

Table 8.13

H.S.	τ min	$t_{\frac{1}{2}}$ min	t_∞ min	$[Ca^{++}]_\infty$ x 10^4M	(-dm/dt) M.min^{-1}
None	16	55	350	8.0	12.0×10^{-6}
H.S. (60)	82	135	300	6.0	7.7×10^{-6}
H.S. (6)	28	95	350	8.0	5.5×10^{-6}

on the precipitation of $CaCO_3$ in cold-lime softening.

Humic substance at a concentration corresponding to 60 hazen units increased the induction period from 16 minutes to 82 minutes, and the half life was almost doubled. Because of the long induction period, 82 minutes, the rate of desupersaturation -dm/dt ($7.7 \times 10^{-6} M.min^{-1}$) was roughly estimated and three points are involved to fit the best straight line. Similarly, at a concentration corresponding to 6 hazen units the half life and the induction period are doubled. The rate of desupersaturation (-dm/dt) reduced from 12.0×10^{-6} to $5.5 \times 10^{-6} M.min^{-1}$.

8.2.3.3 Starch

Experiments using starch as an additive showed that a considerable amount of particles adhere to the wall of the precipitation vessel. At $S_i = 30$ the induction period, τ, (16 minutes to 23 minutes) and the half life, $t_{\frac{1}{2}}$, (55 to 76 minutes) were only slightly affected. The results are shown in figure 8.30.

8.2.3.4 Effects of Dispex N-40 and Humic Substance on Crystallisation of $CaCO_3$ at Supersaturation Ratio 40, 50, 60

Sections 8.2.3.1.1 to 8.2.3.1.3 show that at operating concentrations high molecular weight flocculants do not inhibit the precipitation of $CaCO_3$ from supersaturated solution whereas low molecular weight polyacrylate and humic substance do. It was decided to make a more detailed study

Figure 8.30

S_i = 30

O 5 p.p.m. Starch

X without additive

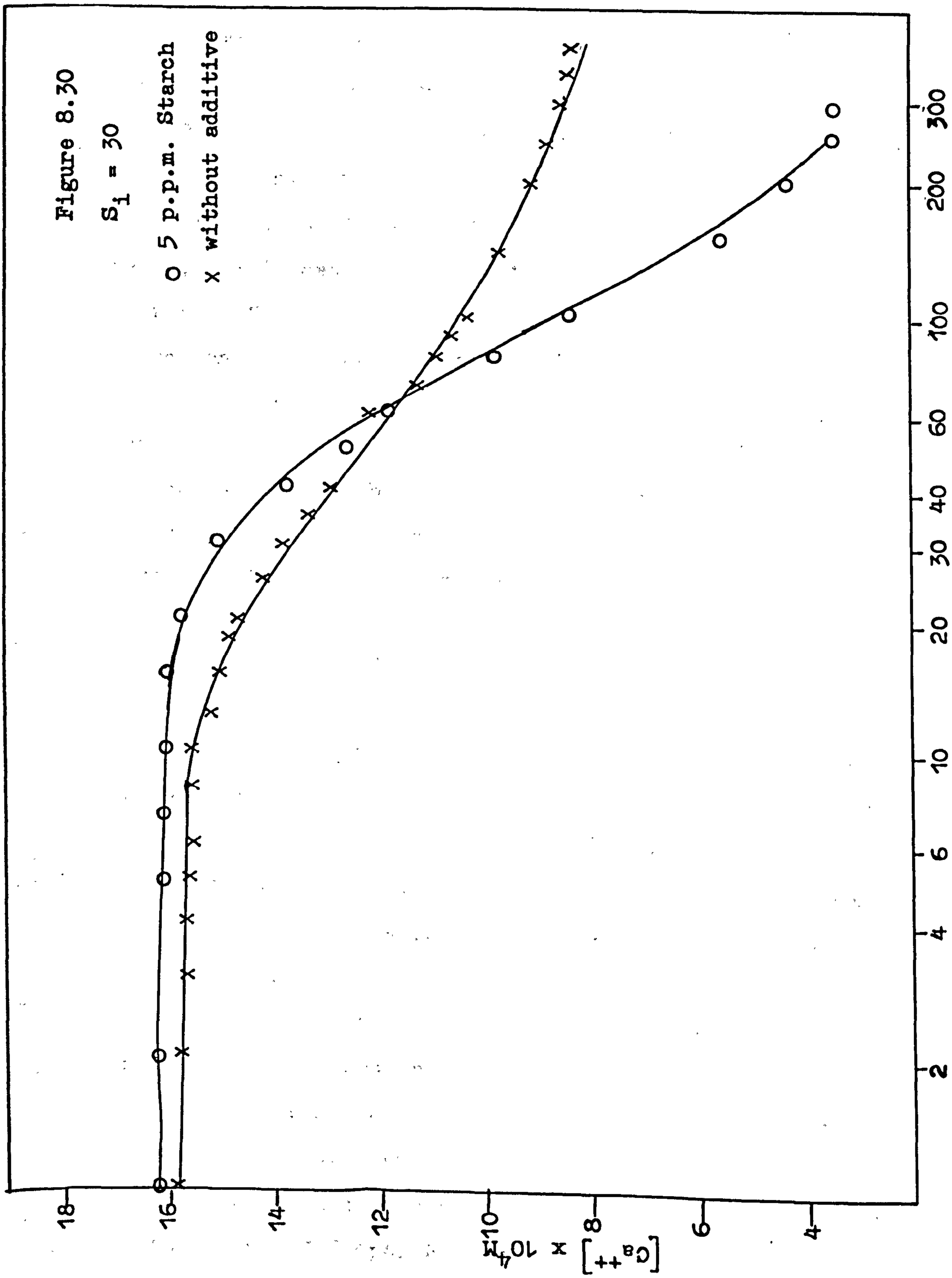

of the effects of these low molecular weight additives, especially at higher supersaturation ratios.

Tables 8.14 to 8.16 and figures 8.31 to 8.33 show the effect of humic substance and Dispex N-40 on the crystallisation of $CaCO_3$ at 40, 50, 60, supersaturation ratio, S_i. It can be seen that as the initial supersaturation increased from 40 to 60 the effects of the additives on the induction period and the half life decreased.

The first point which arises from the above results is that at a supersaturation 40, humic substance at a concentration of 6 hazen units increased the induction period from 9 to 20 minutes; similarly, the half life increased from 22 to 60 minutes comparing with experiments in the absence of humic substance. Whilst at supersaturation levels $S_i > 40$ the effect is not noticeable and there was more or less instantaneous precipitation.

Figures 8.31 to 8.33 and tables 8.14 to 8.16 show the dramatic effect of humic substance at a concentration of 60 hazen units and of 5 p.p.m. Dispex N-40. At a fixed supersaturation level, 60 hazen units of humic substance and 5 p.p.m. Dispex show the same trend, that is the induction period and the half life are increased. On the other hand, the effect of humic substance and Dispex N-40 on the rate of desupersaturation (-dm/dt) is very marked for all the conditions studied. At any given supersaturation level the rate of desupersaturation decreases in the order:- no additive > Humic Substance 6 hazen units > Humic Substance 60 hazen units $\approx$ Dispex N-40.

Table 8.14

S_i = 40 Effects of Inhibitors on Crystallisation of $CaCO_3$

Inhibitor	τ min	$t_{\frac{1}{2}}$ min	t_∞ min	$[Ca^{++}]_\infty \times 10^4 M$	$(-dm/dt)$ M.min^{-1}
none	9	22	150	9.5	24.5×10^{-6}
H.S. (6)	20	60	250	12.0	7.8×10^{-6}
H.S. (60)	47	85	300	8.8	14.3×10^{-6}
Dispex N-40 (5 p.p.m.)	48	88	250	9.0	15.7×10^{-6}

Table 8.15

S_i = 50 Effects of Inhibitors on Crystallisation of $CaCO_3$

Inhibitor	τ min	$t_{\frac{1}{2}}$ min	t_∞ min	$[Ca^{++}]_\infty \times 10^4 M$	$(-dm/dt)$ M.min^{-1}
none	1	4	85	2.5	48.0×10^{-6}
H.S. (6)	1	20	200	11.0	38.4×10^{-6}
H.S. (60)	12	40	300	10.0	23.7×10^{-6}
Dispex N-40 (5 p.p.m.)	11	60	200	4.0	22.2×10^{-6}

Table 8.16

S_i = 60 Effects of Inhibitors on Crystallisation of $CaCO_3$

Inhibitor	τ min	$t_{\frac{1}{2}}$ min	t_∞ min	$[Ca^{++}]_\infty$ x 10^4M	(-dm/dt) M.min^{-1}
none	1	2	30	2.3	98.0 x 10^{-6}
H.S. (6)	1	14	150	17.8	67.5 x 10^{-6}
H.S. (60)	12	22	150	12.0	32.2 x 10^{-6}
Dispex N-40 (5 p.p.m.)	11	60	200	4.0	33.7 x 10^{-6}

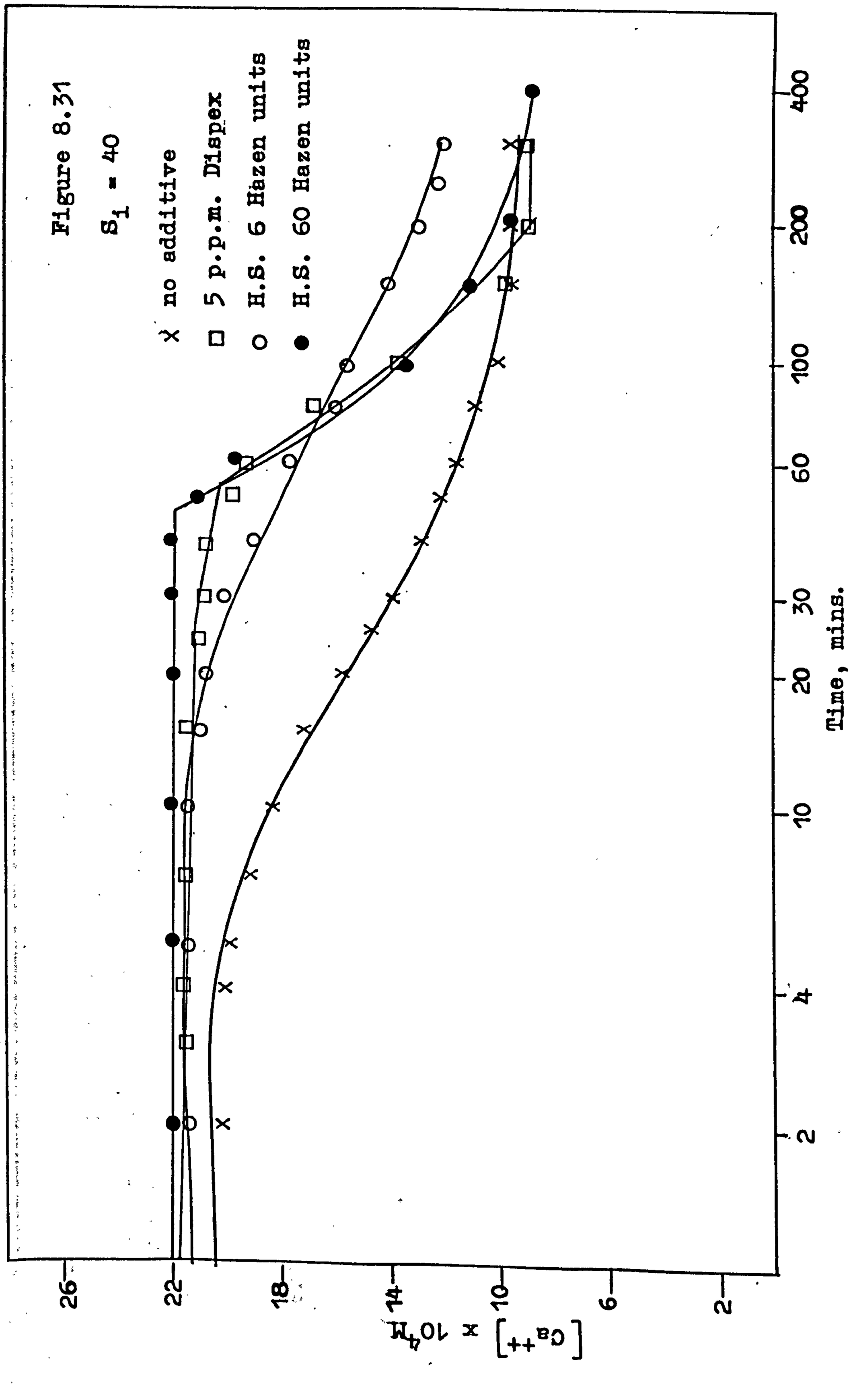
Figure 8.31
S_1 = 40
additive
p.p.m. Dispex
5 p.p.m. 6 Hazen units
H.S. 60 Hazen units
H.S.
no a
x
□
○
●
400
200
100
60
30
20
10
4
2
Time, mins.
26
22
18
14
10
6
2
$[Ca^{++}] \times 10^4 M$

Figure 8.32

S_1 = 50

x no additive

□ 5 p.p.m. Dispex N-40

○ H.S. 6 Hazen units

● H.S. 60 Hazen units

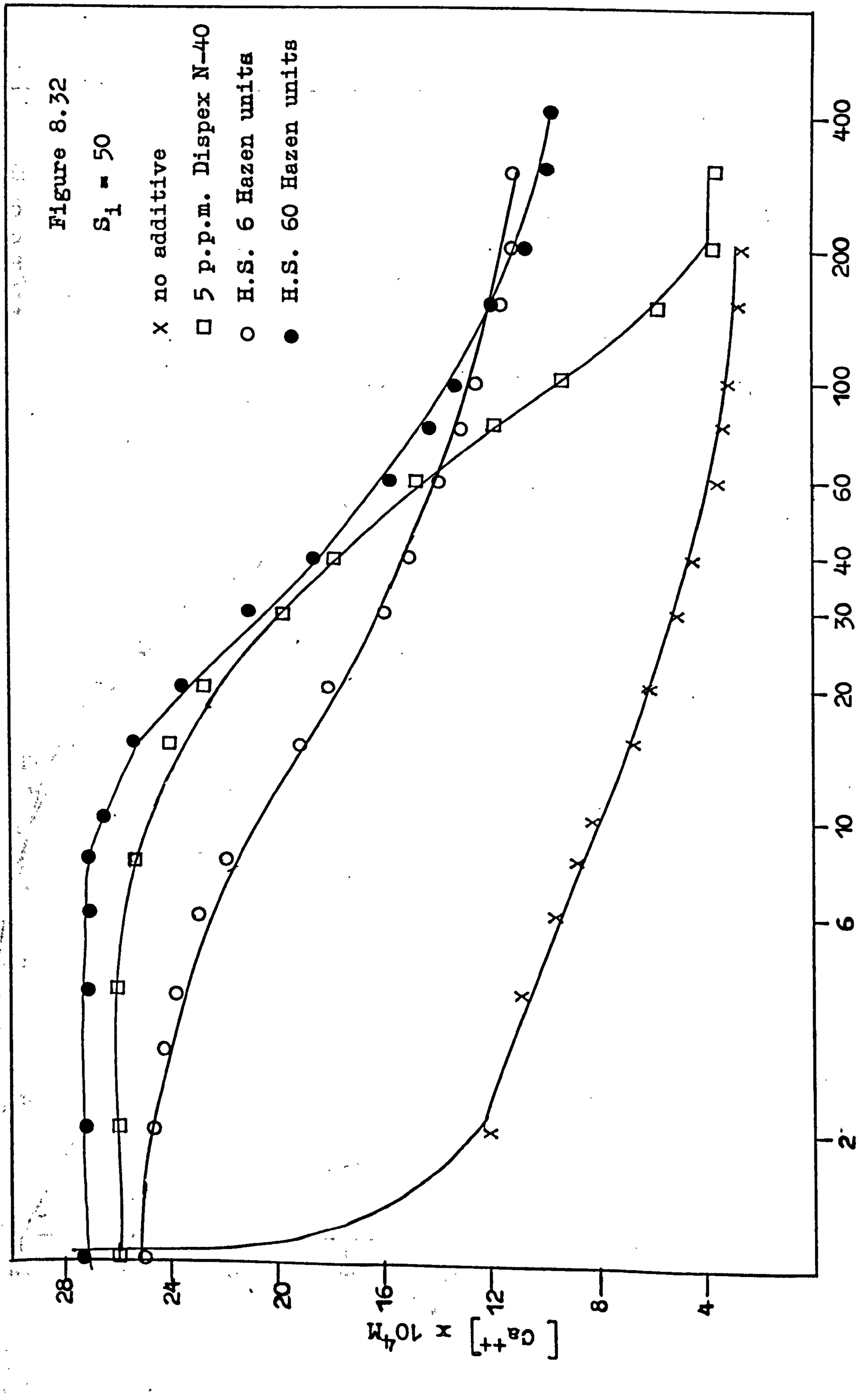

Figure 8.33

S_1 = 60

× no additive

□ 5 p.p.m. Dispex

○ H.S. 6 Hazen units.

● H.S. 60 Hazen units

Time, mins.

2 4 6 10 20 30 40 60 100 200

$[Ca^{++}] \times 10^4 M$

32 28 24 20 16 12 8 4

and the time interval during which precipitation was complete (t_∞) increased in the presence of the inhibitor.

The values of desupersaturation rates (-dm/dt) (shown in table 8.17) are plotted on a log-log basis (desupersaturation rate (-dm/dt) versus supersaturation ratio S_i) in figure 8.34. Fitting best straight lines through each set of data the following relationships were obtained:-

$$-dm/dt = 7.8 \times 10^{-12} S_i^{3.8} \text{ (H.S. 6)} \quad \ldots\ldots\ldots\ldots 8.8$$

$$-dm/dt = 7.1 \times 10^{-9} S_i^{2.1} \text{ (H.S. 60)} \quad \ldots\ldots\ldots\ldots 8.9$$

$$-dm/dt = 1.8 \times 10^{-9} S_i^{2.4} \text{ (Dispex 5 p.p.m.)} \quad \ldots\ldots 8.10$$

comparing these equations with that for crystallisation of $CaCO_3$ in the absence of the inhibitors:-

$$-dm/dt = 1.54 \times 10^{-9} S_i^{2.6} \quad \ldots\ldots\ldots\ldots\ldots\ldots 8.5$$

the reaction order, n, remains reasonably constant within the experimental errors except for humic substance (6 hazen units) which is anomalously high. This anomaly cannot be explained but could be due to the scatter of data in this type of experiment. An error in the slope of this line could also account for the anomalously low reaction rate constant found from the intercept.

8.2.3.5 Humic Substance (6) + Alum

Alum is used quite widely as a coagulant in water treatment process including lime softening. Its main use is the removal of colloidal substances which impart colour and turbidity to the raw water. The amount of coagulant required varies with the nature of the water, but a dose of approximately 10-30 p.p.m. is common.

Table 8.17

		$(-dm/dt) \times 10^6$			log $(-dm/dt)$		
S_i	log S_i	H.S. (6)	H.S. (60)	Dispex	H.S. (6)	H.S. (60)	Dispex
30	1.4771	5.5	7.7	——	-5.26	-5.11	——
40	1.6020	7.8	15.5	12.7	-5.11	-4.81	-4.89
50	1.6989	38.3	23.7	22.2	-4.42	-4.62	-4.65
60	1.7782	67.5	32.2	33.7	-4.17	-4.49	-4.47

Figure 8.34

○ H.S. (6)

● H.S. (60)

□ Dispex 5 p.p.m.

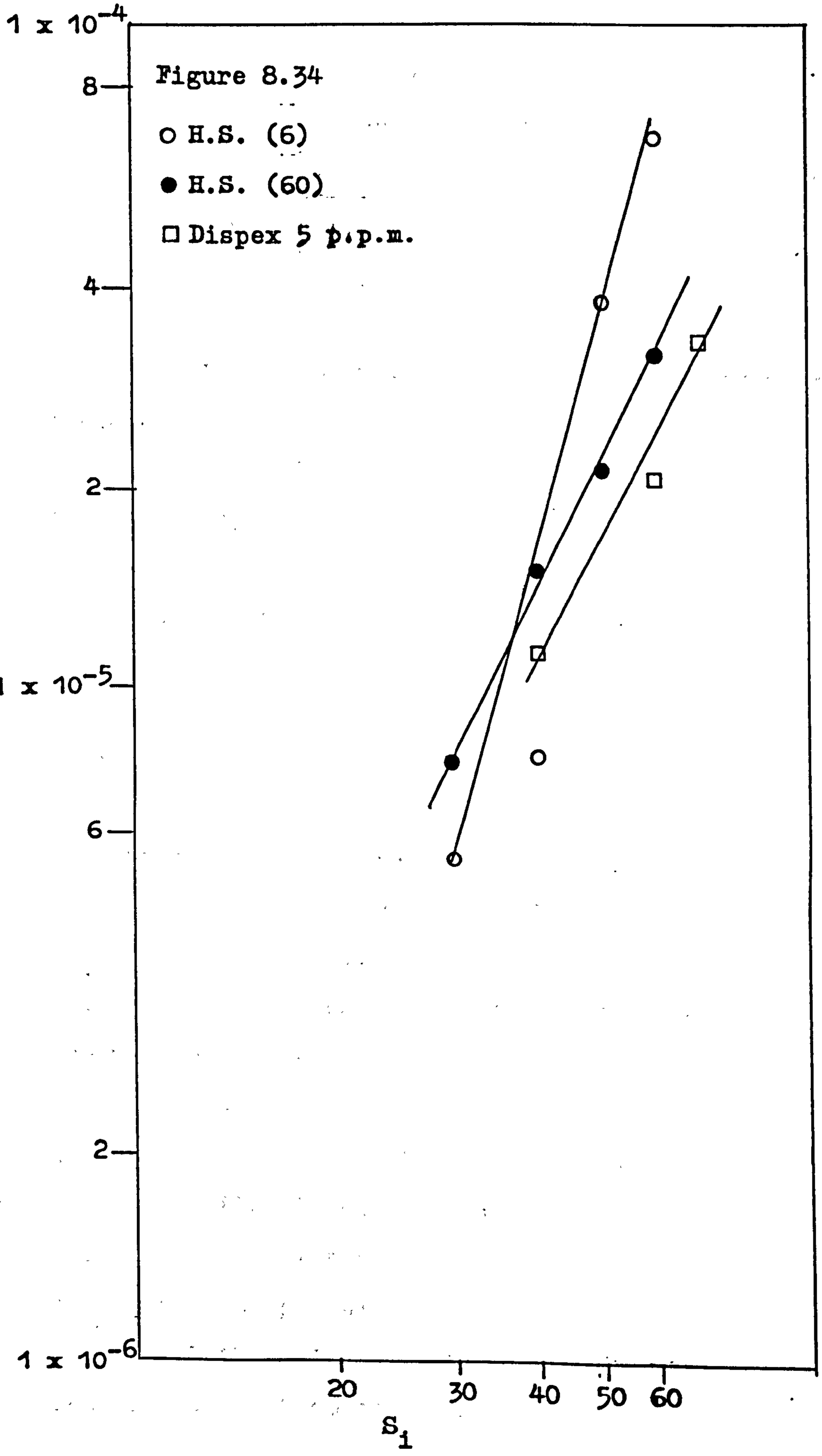

Crystallisation of calcium carbonate experiments were carried out in the presence of humic substance and Aluminium sulphate was added to see whether Alum inhibited the effects of humic substance on precipitation rate when employed in lime softening treatment of coloured water. Figure 8.35 shows the results of three runs of $CaCO_3$ precipitation at supersaturation 30 in the presence of humic substance at 6 Hazen units concentration with the addition of 10, 20, and 30 p.p.m. Alum. It can be seen that the induction period and half life (35 and 85 minutes respectively) are the same as that in the presence of 6 Hazen units humic substance. Similarly, the rate of desupersaturation ($-dm/dt = 5.1 \times 10^{-6} M.min^{-1}$) is almost constant comparing with the presence of 6 Hazen units of humic substance only ($-dm/dt = 5.5 \times 10^{-6} M.min^{-1}$), see table 8.13.

As mentioned in 3.4.3, the addition of an aluminium coagulant to water leads to the formation of a wide range of hydrolysis products, the proportions of which vary with pH. Aluminium hydroxide which is the main product at near neutral pH values, plays the main role in colour removing in natural water. Under the condition of lime softening where high pH values (10-11 pH) are found might it has been shown that Alum is not effective in coagulating the colloidal particles which impart colour. Hall and Packham[248] show that the optimum pH for colour removal is about 7, above pH 7 the colour removal declines owing to the ionisation of phenolic groups on the humic substance . .

Figure 8.35

S_1 = 30

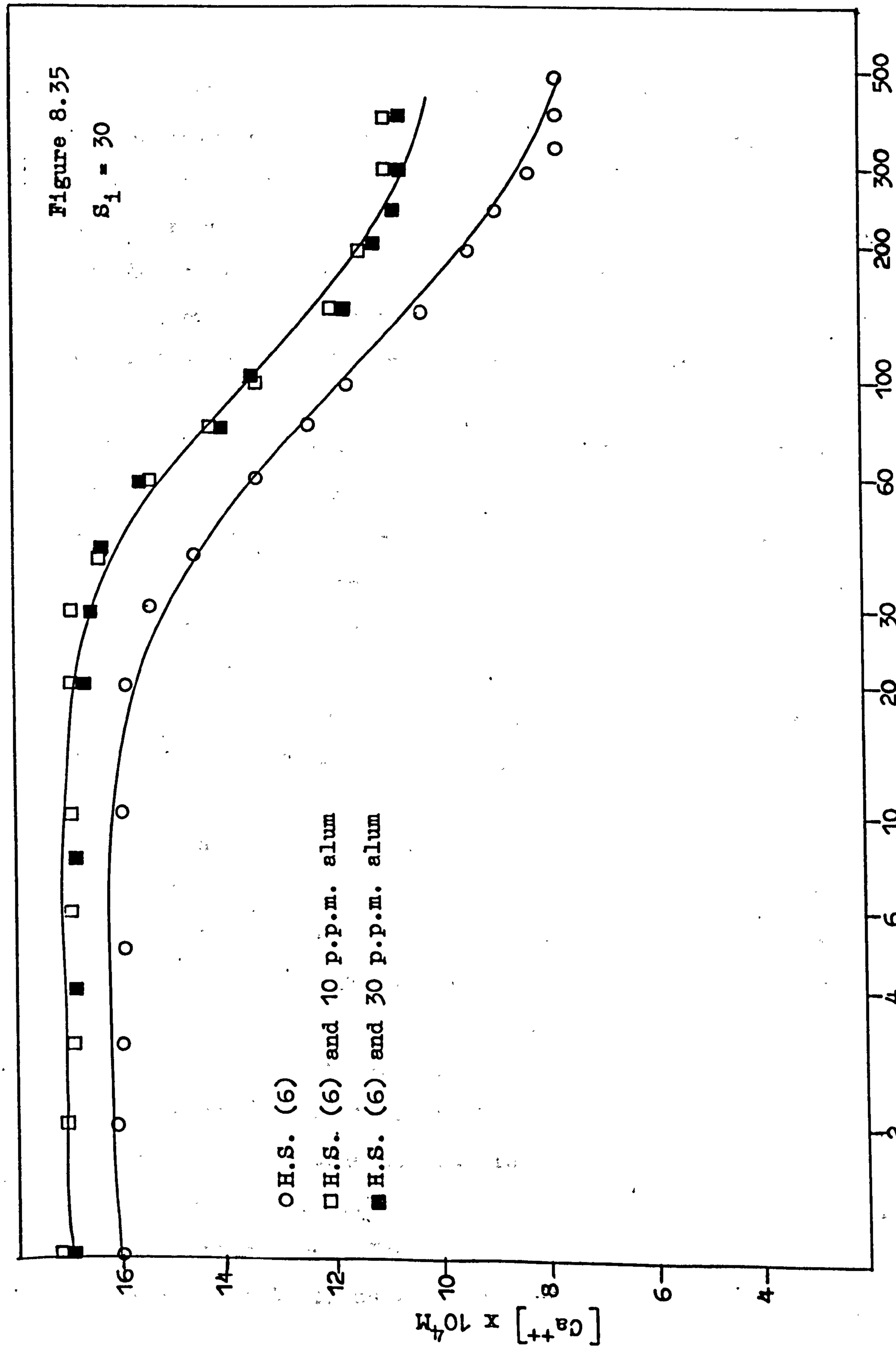

molecule that can form a soluble complex with aluminium. The present results show that the inhibiting effect of humic substance on calcium carbonate precipitation are still exerted by this aluminium complex or that the calcium complex known to be present is more stable. Figure 8.35 shows that increasing the coagulant dose to 30 p.p.m. does not affect the inhibiting action of humic substance.

8.2.4 Effect of the Presence of Seed Crystals and Additive

This section describes experiments in which the combined effects of organic additives and seed crystals were studied. In some cases the additive was allowed to adsorb on the seed before seed was added to the model crystalliser.

The results for seeded (0.01gm) calcium carbonate solutions in the presence of 5 p.p.m. additives are shown in table 8.18.

As in the unseeded case, the results in table 8.18 indicate that the molecular weight of the additive might be a determining factor in determining its effectiveness on calcium carbonate precipitation. The values of desupersaturation rate (-dm/dt) in the presence of flocculant are more or less indistinguishable from that without.

The results in table 8.18 also show when lower molecular weight organic materials are present in the supersaturated solution of $CaCO_3$, a marked reduction in the growth rate occurs. The induction period and half life increased ten times as a result of the presence of 5 p.p.m.

Table 8.18

S_i = 30

Additive	τ min	$t_{\frac{1}{2}}$ min	t_∞ min	$[Ca^{++}]_\infty$ x 10^4M	(-dm/dt) M.min^{-1}
none	3	18	150	8.2	57.0 x 10^{-6}
(+) PAM	<1	5	60	5.7	107.1 x 10^{-6}
(O) PAM	<1	5	60	7.0	91.2 x 10^{-6}
(-) PAM (L)	<1	5	30	10.0	80.5 x 10^{-6}
Starch	<2	5	80	6.6	100.0 x 10^{-6}
Dispex	30	50	100	15.0	3.0 x 10^{-6}
H.S. (60)	30	55	150	11.5	7.8 x 10^{-6}
H.S. (6)	4.5	11.0	60	11.8	18.0 x 10^{-6}

Dispex N-40 and of humic substance 60 Hazen units in experiments seeded with 0.01gm. Similarly the rate of desupersaturation reduced from 57 x 10^{-6}M.min^{-1} to 3 x 10^{-6}M.min^{-1} in the presence of 5 p.p.m. Dispex and to 7.8 x 10^{-6} and 18 x 10^{-6}M.min^{-1} in the presence of humic substance 60 and humic substance 6 Hazen units respectively.

In a further series of experiments, the effectiveness of the additives (5 p.p.m) on the crystallisation of calcium carbonate with large quantity of seeds (0.1gm) was examined. The results are shown in table 8.19.

The important feature that emerges from table 8.19 is that the effects of high molecular weight polyacrylamides on the induction period and half life are comparable in magnitude with those in table 8.18, i.e. crystallisation of $CaCO_3$ in the presence of the same quantity of PAM but with the addition of ten times more seeds (0.1gm).

The inductiom periods in the presence of flocculants were observed to be about four minutes and the half lives almost doubled with respect to the values in table 8.18.

To get a clear picture of the effect of an already adsorbed layer of a high molecular weight additive on the crystallisation of calcium carbonate in a recirculated sludge lime softening reactor, experiments were carried out with seed crystals pre-coated by adsorption by the additive.

Table 8.20 shows the results of experiments when 2 p.p.m. of high molecular weight polyacrylamide flocculants was allowed to adsorb on seed crystals (0.01gm) before the addition to the supersaturated solution. 2 p.p.m. of a

Table 8.19

Effect of 5 p.p.m. additive on crystallisation of $CaCO_3$ seeded with 10% (0.1gm) seeds.

$S_i = 30$

Additive	τ min	$t_{\frac{1}{2}}$ min	t_∞ min	$[Ca^{++}]_\infty \times 10^4 M$	$(-dm/dt)$ M.min^{-1}
none	<1	6	80	6.2	35.0×10^{-6}
(+) PAM	3.5	12	100	8.0	37.0×10^{-6}
(0) PAM	4	15	80	8.7	34.4×10^{-6}
(-) PAM (L)	5	16	100	9.6	29.6×10^{-6}
Starch	<1	11	60	8.0	66.6×10^{-6}
Dispex	4	20	100	8.5	25.1×10^{-6}
H.S. (60)	5	16	100	8.2	32.3×10^{-6}
H.S. (6)	<1	4	50	9.5	59.0×10^{-6}

stock polymer solution was added to a tube containing 0.01gm of seed crystals, and the tube was rotated for three hours in a thermostat bath at 25°C. The concentration of the polymers correspond to complete surface coverage of the seeds.

Table 8.20

Effect of pre-adsorbed seeds with high molecular weight PAM on crystallisation of $CaCO_3$.

$S_i = 30$

Polymer	τ	$t_{\frac{1}{2}}$	t_∞	$[Ca^{++}]_\infty$ M	Remarks
(O) PAM	9	17	40	15×10^{-4}	small amount removed
(-) PAM(H)	8	18	30	15.5×10^{-4}	small amount removed

The results in table 8.20 indicate that in the pre-adsorbed seed experiments, there are measureable delays in precipitation and reduction in the crystal growth rate.

8.3 General Discussion of Results

Sections 8.1 to 8.2 show the results of experiments to test the reproducibility of the experimental procedure and give accounts to attempt to establish a rate equation for the precipitation reaction so that the data may be presented as rate constants. Much absolute crystallisation rate data has been obtained by measuring the linear growth rates of collections or of single relatively large crystals which are growing slowly. This is not practicable for systems in which very many extremely small crystals are rapidly precipitated from a solution of very high supersaturation. An attempt to calculate growth rates based on particle size distribution measurements is shown in 8.2.1.1, but the results do not inspire confidence in the procedure. In order to compare results the parameters, γ , $t_{\frac{1}{2}}$, t_{∞} , and C_{∞} are used. A simplified form of rate equation based on the initial rate of removal -dm/dt was found useful and enabled comparisons between different experiments to be made and also showed that the order n in:-

$$-dm/dt = k\, S_i^{\,n} \quad \ldots\ldots\ldots\ldots\ldots\ldots\ldots\ldots \quad 8.4$$

was approximately 2 with respect to supersaturation ratio. Reddy[2] observed the rate law

$$dN/dt = k\, A_s \left[Ca^{++}\right]^2 \quad \ldots\ldots\ldots\ldots\ldots\ldots \quad 8.11$$

where A_s = is the area available for growth.

and k = is the reaction rate constant.

As a check on the precision of the measured precipitation rates comparisons were made with data given by Reddy[2]. The rate constant in equation 8.11 was

calculated for a seeded run at S_i = 30 on the basis of the initial removal rate and the surface area of added seed. This was compared with the rate constant of the first row of data in Reddy's table II, converting units and with data obtained from a plot in Reddy's figure 2 used to calculate the above rate constant. These values are shown in table 8.21.

Table 8.21

	k at 25°C ($moles^{-1}\ l^2\ m^{-2}\ min^{-1}$)
This work	2.6×10^2
Reddy - table II	7.1×10^2
Reddy - figure 2, 5 mins.	9.3×10^2
Reddy - figure 2, 20 mins.	2.9×10^2

The spread in data from Reddy, all from the same experimental run confirms the difficulty in obtaining precise rate information on reactions of this type. This is further demonstrated by the scatter in Reddy's figure 3. However, the good general agreement between the two sets of work carried out using different techniques in different laboratories is satisfying. Further rate constants could not be calculated in the present work because of lack of surface area data as previously discussed in 8.2.1.1. Because precipitation reactions are so very sensitive to conditions, e.g. stirring rate, presence of impurities and seed, it would be inadvisable to size reactor clarifiers for lime softening on the basis of laboratory measurements of reaction rate made in batch reactors. In the present

work a continuous reactor was not used because, apart from lack of time, it would have required volumes of reactant solutions that were impracticable to prepare because it had been decided to carry out all experiments on a pure calcium bicarbonate solution rather than a local mains water containing magnesium, sulphate hardness and unknown quantities of trace materials. This is not a limitation when performing trials on an existing water supply.

The results obtained do however demonstrate general trends that could be taken note of in the design and operation of full scale plant.

8.3.1 Factors Affecting Precipitation Rate

Because absolute rate constant data was not available this section will discuss the experiments in terms of the induction period, τ, the half life, $t_{\frac{1}{2}}$, and the initial removal rate -dm/dt. The experiments without seed and additive show the expected reduction in induction time and increase in desupersaturation rate with increasing supersaturation as is observed in all crystallisation studies.

The addition of seed crystals increases the precipitation rate and decreases the observed induction times. At the supersaturation range used in all these experiments $5 \leqslant S_i \leqslant 60$, 60 being a representative supersaturation level in cold lime softening practice, it would be expected that homogeneous nucleation would occur[74, 96]. It is possible that in the seeded systems the seed acts as secondary nuclei and this is supported by a marked reduction

in the observed induction times. For example, at $S_i = 10$ the induction period in the absence of seed exceeded five hours whereas with 0.005gm/l seed, τ, was reduced to 30 minutes. At high supersaturation in seeded systems it is possible that both primary and secondary nucleation is occurring simultaneously but the present work is not able to distinguish between these two mechanisms. In a recent study of the crystallisation of nickel ammonium sulphate in which a brief account is given of the effects of polyacrylamide flocculants, Mullin and Ang[74] are able to distinguish between different nucleation mechanisms on the basis of nucleation "order" and nucleation rate. The data in this work is not suitable for determination of order and a different type of experiment is required to determine nucleation rate.

The increased growth rate in seeded systems could be due to a greater surface area being available for growth in the initial stages of desupersaturation. The dependence of initial desupersaturation rate on seed area is shown by the comparison of rates given in table 8.21 and is the basis of Reddy's determination of second order reaction in the presence of sufficient seed to make the rate area insensitive.

Effects due to the presence of organic additives during precipitation are complex and because of the many ways (see 5.1) in which these materials may affect crystal growth it is not possible to assign specific mechanisms to the observed phenomena.

When used at concentrations of the order met with in flocculation practice, the four polyacrylamide derivatives tested did not appear to have any inhibition effect as shown by the parameters used to measure precipitation rate. However, experiments in which seed crystals were coated with anionic and nonionic flocculant prior to addition to the supersaturated solution showed an increased induction period and very little reduction in the level of super-saturation which is evidence that a layer of adsorbed macromolecule at the surface may have marked inhibiting effect. This is explained in the literature[187] as being due to an inhibition of the step motion in crystal growth. We know from the results of adsorption experiments (see 7.1 and 7.2) that all four flocculants tested do adsorb at the surface and are also effective flocculants, the nonionic and cationic materials exhibiting a reduction in cappillary suction time at an optimum concentration corresponding reasonably to monolayer coverage (see table 7.2). An interesting but unexpected result of the adsorption studies was the observation that anionic polyacrylamides, i.e. acrylamide/acrylic acid copolymers were capable of forming complexes with the calcium ion or calcium ion containing species. Hbwever, the effect of the flocculants on precipitation behaviour did not seem to depend on the ability to complex one of the precipitating ions.

In the case of the seeded runs it is possible to calculate the available surface at the beginning of desupersaturation. For the cationic polyacrylamide, the

quantity added corresponded to 263.0mg m^{-2} at 0.01gm added seed and 26.3 mg m^{-2} at 0.1 gm added seed, to be compared with a saturated monolayer coverage of 1.4mg m^{-2}. Hence the amount of polymer added was well in excess of that to saturate the surface. The most plausible explanation of the lack of inhibiting effect is that the polymer was not available at the surface, for adsorption during crystal growth although other mechanisms must be considered.

There are several theories for crystal growth (see 4.7) but an essential step in all of these growth mechanisms is transfer of the crystallising substance from the bulk of the solution to the surface of the growing crystal. The steps in a crystal growth process may be considered as:-

(1) Diffusion of crystallising species in bulk liquid,

(2) Diffusion of crystallising species through surface boundary layer or laminar film,

(3) Reaction of the crystallising species with crystal surface to produce new crystal material.

The demonstrated insensitivity of rate on stirring for the present system[155,161] suggests that (1) above is not important here but the film diffusion processes must not be disregarded.

The observed phenomena can be qualitatively explained on the basis of competitive diffusional processes if the reactions are assumed not to be entirely surface rate controlled. A general expression for the diffusionally controlled rate of mass transfer to a surface is:-

$$dm/dt = K_G A (C - C^*) \quad \ldots\ldots\ldots\ldots\ldots\ldots \quad 4.38$$

where A = is the surface area.

K_G = is the overall mass transfer coefficient.

C = is the solute concentration.

and C^* = is the concentration of a saturated solute.

The overall mass transfer coefficient K_G will depend on both the diffusion coefficient and surface reaction rate. In the present discussion only the former will be considered. A detailed treatment of the rate of diffusion of ions or molecules towards a growing crystal surface in this system is not possible because the fluid mechanical behaviour adjacent to the surface is not known. However, an estimate of the order of magnitude of effects due to concentration and diffusion coefficient may be calculated using von Smoluchowski's[249] treatment for the diffusion collision rate of spherical particles.

The number of particles striking a spherical shell is given by:-

$$I = 4\pi R.D\, N_o \quad \ldots\ldots\ldots\ldots\ldots\ldots\ldots\ldots \quad 8.12$$

where R = is the collision radius of the two particles experiencing collision.

D = is the sum of their diffusion coefficients.

and N_o = is the number of diffusing particles per unit volume.

For the present example the collision radius may be taken as the radius of the growing crystal. The diffusion coefficient of a spherical crystal may be calculated using the Stokes-Einstein[249] expression:-

$$D = \frac{k\,T}{6\pi r\eta} \quad \ldots\ldots\ldots\ldots\ldots\ldots\ldots\ldots \quad 8.13$$

which for a particle of 1 μm diameter in water at 25°C gives:-

$$D = 5.7 \times 10^{-11}\ m^2 s^{-1}$$

As this is significantly smaller than any of the other diffusion coefficients being considered, the collecting particle will be considered as stationary.

The diffusion coefficients of the polymer species are not accurately known but literature equations may be used to estimate them. A general equation for the diffusion coefficients of polymers is:-

$$D = K M^{-a} \quad \ldots\ldots\ldots\ldots\ldots\ldots\ldots\ldots\ 8.14$$

and for polyacrylamide and its derivatives Scholtan[250], has given:-

$$K = 8.46 \times 10^{-8}$$

$$a = 0.69$$

Using the manufacturers values of molecular weight for the polymers used the diffusion coefficients may be calculated as:-

Table 8.22

Polymer Designation	Description	Stated M.Wt.	$D \times 10^{12}$ $m^2 s^{-1}$
FA 200-5	Anionic, 84%	$5\text{-}10 \times 10^6$	2-1.25
FA 60H	Anionic, 36%	10^7	1.25
FO 115	Cationic, 20%	5×10^6	2.0
FA 20H	Nonionic,	10^7	1.25
Dispex N-40	Anionic, 99%	40,000	57.0
Starch			115.0

The value quoted for starch was taken from the Polymer Handbook[251] for a starch of molecular weight quoted as 5,000. The starch used in the present experiments was obtained from B.D.H. Ltd., and is of unknown type and molecular weight hence the above value is only a guide. There is no way, short of experimental determination, of knowing the diffusion coefficient of the humic substance used. On the basis of the quoted molecular weight range[43] 800-50,000, it would be expected to have a significantly higher diffusion coefficient than the high molecular weight macromolecules.

The diffusivity of $CaCO_3$ was approximated by using Nernst's[252] equation for diffusion of electrolytes at infinite dilution:-

$$D_o = 8.931 \times 10^{-14} T \left(\frac{l_+^o \, l_-^o}{\Lambda^o}\right)\left(\frac{Z_+ + Z_-}{Z_+ \, Z_-}\right) \ldots . \quad 8.15$$

where l_+^o and l_-^o are the cationic and anionic conductivities at infinite dilution $\Lambda^o = l_+^o + l_-^o$, and Z_+ and Z_- the corresponding ion equivalent charges.

Using $\left.\begin{matrix} l_+^o = 59.5 \\ l_-^o = 69.3 \end{matrix}\right]$ (253)

gives a corresponding diffusion coefficient of:-

$$D_o = 8.6 \times 10^{-10} \; m^2 \; s^{-1}.$$

The corresponding number concentration terms in equation 8.12 can be calculated from the weight concentrations and molecular weights:-

Table 8.23

	molecules m^{-3}
$CaCO_3$ at S_i = 30	$\sim 10^{23}$
PAM, M.Wt. 5×10^6 at 5 p.p.m.	6×10^{17}
Dispex N-40 at 5 p.p.m.	7.5×10^{20}

Substituting the corresponding diffusion coefficients and concentrations into equation 8.12 for the number of particles colliding by diffusion with a 1 μm sphere of $CaCO_3$ is:-

Table 8.24

	molecules s^{-1}
$CaCO_3$ at S_i = 30	5.4×10^8
PAM, flocculant	7.5
Dispex N-40	2.7×10^4

Although the Smoluchowski treatment is a gross over-simplification for the present system it does show what a wide range of collision rates can be calculated on the basis of concentration and diffusivity. A more complete treatment would require a knowledge of the thickness of the surface layer through which diffusion occurs, the local concentration gradients and the equations would have to be set up for a plane surface, not a spherical shell. However, the figures in table 8.24 do show that the probability of adsorption of a molecule of Dispex N-40 onto the surface of a growing $CaCO_3$ crystal is several orders of magnitude higher than that for a high molecular flocculant molecule.

By analogy humic substance and starch might be expected to be intermediate in behaviour between Dispex N-40 and $CaCO_3$ itself.

It is not possible to test the above hypothesis by altering reagent concentrations because a significant increase in the polymer concentrations would lead to a gel structure whilst a reduction in salt concentration would bring the system below supersaturation and no precipitation would occur at all.

The Smoluchowski treatment does not predict the McCabe ΔL law whereas a plane surface model would.

Upon adsorption the organic substances could have several effects including:-

(1) Inhibition of crystal growth by any of the mechanisms discussed in 5.2.

(2) Adsorption of macromolecules onto sub critical primary nuclei might inhibit the removal of those nuclei by Ostwald ripening. The pre-adsorption experiments show that an adsorbed layer inhibits secondary nucleation and growth and by analogy might be seen as inhibiting solution. One molecule of high molecular weight flocculant has been shown from the adsorption experiments to cover approximately 7×10^{-15} m^2. Converted to a spherical surface this corresponds to a radius of 2.4×10^{-2} μm, lying within the range of critical nuclear sizes calculated in section 8.2.1.1.

(3) Adsorption of flocculant and subsequent flocculation of particles. Flocculation was not apparent in the reactor, this probably being due to the amount of agitation induced by the stirrer. However, flocs of very small particles would not have been seen and would have been less sensitive to stirrer induced shear. It is possible that the subcritical nuclei could have been increased in size to above the critical size by flocculation. If it did occur this would have had the effect of reducing the induction time of experiments in the presence of flocculant. As this did not occur the effect must be disregarded in the absence of further evidence.

(4) Dispex N-40 is a proprietary stabilising agent that is believed to act by forming a highly charged adsorbed layer. Riley[229] has measured an electrophoretic mobility corresponding to a ξ potential of 76 mV on Dispex covered $CaCO_3$. This high surface potential subsequent upon adsorption could have the following effects:-

(a) prevention of particle aggregation,

(b) inhibition of adsorption of carbonate anions by charge repulsion.

At the pH of the precipitation experiments the carboxylic acid functions of the humic substance might be expected to behave in a similar way[234]. Ionic flocculants will also increase charge on adsorption and this effect may

inhibit flocculation. This was not seen in the present system.

The data in table 8.14 and 8.15 show that the main inhibiting effect of both Dispex N-40 and humic substance is to increase the induction time without markedly reducing the desupersaturation rate. This could be explained on the basis that nuclear growth by aggregation was important and was inhibited by the stabilising effects of the additives. Similar effects have been postulated[254] in emulsion polymerisation.

8.3.2 Factors Affecting Final Desupersaturation $[Ca^{++}]_\infty$

It is accepted in lime softening practice[12] that the final Ca salt level is at least five times that predicted from known solubility products. The present work confirms this although the experimental data shows considerable scatter. The residual Ca^{++} concentrations determined are shown in table 8.25. The experiments in section 7.1 which demonstrated the complexing Ca^{++} by some reagents may be considered as demonstrating that the Ca^{++} selective electrode was not sensitive to complexed Ca^{++}. The following trends may be noted from the data:-

(1) That in experiments without additive or seed the $[Ca^{++}]_\infty$ is lower as S_i is increased. Under these conditions theory would predict a greater homonucleation rate. If the general discrepancy between experiment and theoretical prediction were due to the presence of other inhibiting

Table 8.25

$[Ca^{++}]_\infty$ x 10^4M

S_i	$[Ca^{++}]_o$ x10^4M	None	H.S.(6)	H.S.(60)	(+) PAM	(-) PAM (H)	(-) PAM (L)	(0) PAM	Dispex	Starch
30	16.1	8,8	8.0	6.0	6,6.2, 5.8	10.0	0.5,0.5, 0.5,8.5.	3.5,3.0	——	3.8, 3.5.
40	21.5	8.5, 9.5.	12.0	8.8	6,7	——	——	——	9.0	——
50	26.8	2.2, 2.5.	11.0	10.0	——	——	——	——	4.0	——
60	32.2	2.3, 2.4.	17.8	12.0	——	——	——	——	4.0	——
30+ 1% seed	——	8.2	11.8	11.5	5.7	——	10.0	7.0	15.0	6.6
30+ 10% seed	——	6.2	9.5	8.2	8.0	——	9.6	8.7	8.5	8.0
30 pre-coated with seed (1%)	——	——	——	——	——	15.5	——	15.0	——	——

substances present in the materials used, e.g. in the lime used, the presence of larger numbers of seed crystals might compensate for this.

(2) That if humic substance, which markedly affects the induction period is present, $\left[Ca^{++}\right]_{\infty}$ is increased. This increase does not seem to be concentration dependent.

(3) With flocculating polymers that have an insignificant effect on rate, $\left[Ca^{++}\right]_{\infty}$ is not significantly different from experiments in the absence of polymer.

(4) Starch has no effect on $\left[Ca^{++}\right]_{\infty}$.

(5) Dispex N-40 has no significant effect on $\left[Ca^{++}\right]_{\infty}$ except for the run with 1.0% seed at $S_i = 30$. This anomaly cannot be explained.

(6) Precipitation in the presence of coated seed crystals and an excess of polymer hardly proceeds at all.

(7) There is no correlation between the complexing ability of a reagent and $\left[Ca^{++}\right]_{\infty}$. As remarked above humic substance has a marked inhibiting effect but this is not so with anionic polyacrylamides. With the latter the picture is confused by the data obtained at $S_i = 30$ where in three runs $\left[Ca^{++}\right]_{\infty} = 0.5 \times 10^{-4}M$ was obtained whereas a fourth run gave $8.5 \times 10^{-4}M$. This cannot be explained.

(8) Data for $\left[Ca^{++}\right]_{\infty}$ shows more scatter than found with rate terms for the corresponding experiments.

CHAPTER NINE

Conclusions and Suggestions For Further Work

9.1 Conclusions

(1) In an unseeded stoichiometric system, at 25°C, the rate of desupersaturation of a solution of calcium bicarbonate increases with increasing supersaturation level. The equation which correlates the desupersaturation rate with the supersaturation level is:-

$$-dm/dt = 1.5 \times 10^{-9} S_i^{2.6} \quad \ldots\ldots\ldots\ldots\ldots\ldots 8.5$$

(2) The induction period or time-lag before the onset of precipitation decreases with increasing supersaturation level, S_i. No induction period was observed in unseeded systems at supersaturation level, $S_i > 40$.

(3) The crystal growth kinetics, under the conditions used in this work, are independent of stirring rate.

(4) The induction period is decreased and the desupersaturation rate increased by the presence of seeded crystals. The effect of seeds is greater when a large number of seeds are introduced. However, the effect at supersaturation level $S_i > 40$ (spontaneous crystallisation in the absence of seeds) is less pronounced. An empirical relationship between the rate of desupersaturation (-dm/dt) and initial supersaturation level in the presence of 0.005gm seed l^{-1} is:-

$$-dm/dt = 2.2 \times 10^{-8} S_i^{2.36} \quad \ldots\ldots\ldots\ldots\ldots\ldots 8.7$$

(5) The presence of anionic, nonionic, and cationic polyacrylamides at normal flocculation concentration

do not inhibit the rate of desupersaturation.

(6) Dispex N-40 (sodium polyacrylate - M.Wt. 40.000) and humic substance (60 Hazen units) have a marked inhibiting effect on desupersaturation and humic substance (6 Hazen units) a less marked one. The main effect is to increase the induction time. The relationship between the rate of desupersaturation (-dm/dt) and the supersaturation level in the presence of 5 p.p.m. Dispex N-40 and humic substance (60 Hazen units) are:-

$$-dm/dt = 7.1 \times 10^{-9} S_i^{2.1} \text{ (H.S. 60)} \quad \ldots\ldots 8.9$$

$$-dm/dt = 1.8 \times 10^{-9} S_i^{2.4} \text{ (Dispex N-40)} \quad \ldots 8.10$$

(7) Prior contact of seed crystals with a high molecular weight flocculant has a marked inhibiting effect and causes only a slight reduction in the Ca^{++} concentration.

(8) The presence of aluminium sulphate does not prevent the inhibiting action of humic substance.

(9) Acrylic acid/acrylamide copolymers and humic substance are capable of complexing Ca^{++}.

(10) The ability of substance to complex Ca^{++} does not appear to be related to their ability to inhibit the desupersaturation of calcium carbonate solutions.

(11) Residual $\left[Ca^{++}\right]_{\infty}$ were significantly higher than predicted from solubility data but apart from a marked effect in the presence of humic substance no systematic correlations were apparent.

9.2 Suggestions For Further Work

Searches of the literature of crystallisation/ precipitation and water softening carried out during this work revealed many gaps in our understanding of the fundamentals concerned. This is due to the difficulties of studying the rapid precipitation of fine particles from a chemically complex system in which many ionic equilibria exist. To extend the present work to be of value in practical water softening operations where flocculants and other organic materials may be present it would be useful to investigate:-

(1) The kinetics of calcium carbonate precipitation in a mixed suspension mixed product removal crystalliser (MSMPR), i.e. a reactor clarifier im the presence of organic impurities.

(2) Other reactions occurring in cold lime softening, e.g. $Mg(OH)_2$ precipitation.

(3) The above reactions in the presence of fresh seeds generated in situ.

(4) The effect of temperature and other operating variables on the kinetics of cold lime softening.

REFERENCES

(1) Linstedt, K. D.; etal, J. Water Poll. Cont. Fed., 43 (8) (1971) 1661.

(2) Reddy, M. M.; In "Chemistry of Waste Water Technology" ed. Rubin, A. J., Ann Arbor Science 1978.

(3) Otsuki, A., and Wetzel, R. G.; Limnol. Oceanogr., 18 (1973) 490.

(4) Williams, F. V., and Ruehrwein, R. A.; Amer. Chem. Soc. 79 (1957) 4898.

(5) Akers, R. J.; "Flocculation" I. Ch. Eng., London 1975.

(6) Kitchener, J. A.; Br. Polym. J., 4 (1972) 217.

(7) Thomas, C. M.; Filtration and Separation, 3 (1966) 211.

(8) Gale, R. S., and Baskerville, R. C.; Filtration and Separation, 7 (1970) 37.

(9) Purchas, D. B.; Process Biochem., 3 (10) (1968) 17.

(10) Hamer, P.; Jackson, J; and Thurston, E. F.; "Industrial Water Treatment Practice", Butterworths 1961.

(11) Langmuir, D.; Geochim. Cosmochim. Acta, 32 (1968) 835.

(12) McGhee, T. J.; J.A.W.W.A., 67 (1975) 626.

(13) Greenfield, R. E., and Buswell, A. M.; J. Am. Chem. Soc. 44 (1922) 1435.

(14) McCauley, R. F., and Eliassen, R.; J. Am. W. Wks. Ass., 47 (1955) 487.

(15) Sauer, E., and Fischler, F.; Z. Angew. Chem., 40 (1927) 1176, 1276.

(16) Ranck, J. P.; Desalination, 6 (1969) 75.

(17) Judkins, Jr., J. F., and Wynne, Jr., R. H.; J. Am. W. Wks. Ass., 64 (1972) 306.

(18) Faust, S. D., and Orford, H. E.; Ind. Eng. Chemistry, 50 (1958) 1537.

(19) Judkins, Jr., J. F., and Parsons, W. A.; J. Water Poll. Cont. Fed., 41 (1969) 1625.

(20) Faust, S. D.; Orford, H. E.; and Parsons, W. A.; Sewage and Ind. Waste, 28 (1956) 872.

(21) Spaulding, C. H.; U.S. Patent 2,021,672 (Nov. 19, 1935).

(22) Behrman, A. S., and Green, W. H.; I. and E. C., 31 (1939) 128.

(23) Koyl, C. H.; U.S. Patents 653,011 (1900) and 677,669 (1901).

(24) Sutro, H. H., and Booth, L. M.; U.S. Patents 797,759 (1905).

(25) Green, W. H, and Behrman, A. C.; U.S. Patents 1,653,272 (1927).

(26) Degremont, G.; "Water Treatment Handbook" 4th ed. 1973.

(27) Lawrance, C. H.; J. Am. W. Wks. Ass. 55 (1963) 177.

(28) Langelier, W. F.; J. Am. W. Wks. Ass. 38 (1946) 169.

(29) Levchenko, V. M., and Bekman, V. V.; Geochemistry, 144 (1962) 169.

(30) Weber, Jr., W. J., and Stumm, W.; J. Am. Wks. Ass., 55 (1963) 1553.

(31) Adamson, A. W.; "Physical Chemistry of Surfaces", Interscience, New York 1960.

(32) Nancollas, G.; "Interaction in Electrolyte Solutions" Elsevier pub. comp. 1966.

(33) Langelier, W. F.; J. Amer. Wat. Wks. Ass., 28 (1936) 1500.

(34) Larson, T. E., and Buswell, A. M.; J. Am. W. Wks. Ass., 34 (1942) 1667.

(35) Fair, G. M.; Geyer, J. C.; and Okun, D. A.; "Water and Waste Water Engineering" Vol. 2, Water Purification and Waste Water Treatment and Disposal.

(36) Nordell, E.; "Water Treatment for Industrial and Other Uses" 2nd ed. 1961.

(37) Standard Methods for the Examination of Water and Waste Water. New York, N.Y., American Public Health Association, 13th ed. (1971).

(38) Schierholz, P. M.; Stevens, J. D.; and Cleasb, J. L.; J. Am. W. Wks. Ass., 68 (1976) 112.

(39) Stumm, W., and Morgan, J. J.; "Aquatic Chemistry" 1970.

(40) Harned, H. S., and Sholes, S. R.; J. Am. Chem. Soc., 63 (1941) 1706.

(41) Harned, H. S., and Hammer, W. J.; J. Am. Chem. Soc., 55 (1933) 2194.

(42) Harned, H. S., and Cook, M. A.; J. Am. Chem. Soc., 59 (1937) 2304.

(43) Wilson, A. L.; J. App. Chem., 9 (1959) 501.

(44) Fitch, E. B.; "Solid/Liquid Separation Equipment Scale-Up", Edited by Derek B. Purchas, 1977.

(45) La Mer, V. K.; J. Coll. Sci., 19 (1964) 291.

(46) Quoted in Perrin, J. Les Atomes, Paris 1913.

(47) Derajaguin, B., and London, L.; Acta. Physiochem. U.S.S.R., 14 (1941) 633.

(48) Verwey, E. J. W., and Overbeek, J.; "Theory of Stability of Lyophobic Colloid", Elsevier (1948).

(49) Franks, F., "Water A Comprehensive Treatise" Vol. 5 Water in Disperse System, N.Y. 1975.

(50) Hamaker, H. C.; Physica, 4 (1937) 1058.

(51) Visser, J.; Adv. Colloid Interface Sci., 3 (1972) 331.

(52) Gouy, G. J.; Physique, 9 (1910) 457.

(53) Chapman, D. L.; Phil. Mag., 25 (1913) 475.

(54) Stern, O.; Z. Electrochem., 30 (1924) 508.

(55) Gregory, J., in "The Scientific Basis of Filtration", ed. K. J. Ives, 1975.

(56) Schultze, H.; J. Prakt. Chem., 25 (1882) 431; 27 (1883) 320.

(57) Hardy, W. B.; Proc. Roy. Soc. London, 66 (1900) 110. Z. Phys. Chem., 33 (1900) 385.

(58) Powell, S. T.; "Water Conditioning for Industry", McGraw-Hill, N.Y. 1954.

(59) Weber, Jr., W. J. "Physicochemical Processes for Water Quality Control", 1972.

(60) Stumm, W., and Morgan, J. J.; J. A. W. Wks. Ass., 54 (1962) 971.

(61) Packham, R. F.; J. Coll. Sci., 20 (1965) 81.

(62) Stumm, W., and O'Melia, C. R.; J. A. W. Wks. Ass., 60 (1968) 514.

(63) Hahn, H. H., and Stumm, W.; J. Coll. Inter. Sci., 28 (1968) 134.

(64) Packham, R. F.; Water Research Association, 1973 TP100.

(65) Beardsley, J. A.; J. Am. W. Wks. Ass., 65 (1973) 85.

(66) Yadev, N. P.; Water Research Association, TP 71 1970.

(67) Ruehrwein, R. A., and Ward, D. W.; Soil Sci., 73 (1952) 485.

(68) Rebhum, M., and Wacks, A. M.; Int. Congr. Pure. Appl. Chem., (Moscow) A88, 1965.

(69) Linke, W. F., and Booth, R. B.; Trans. Am. Inst. Min. Metall. Eng., 217 (1959) 364.

(70) O'Melia, C.; In "Physiochemical Processes for Water Quality Control" Ed. Weber, W., 1972 New York.

(71) Camp, T. R., and Stein, P. C.; J. Boston Soc. Civ. Eng., 30 (1943) 219.

(72) Camp, T. R.; Trans. Am. Soc. Civ. Engr., 120 (1955) 1.

(73) Mullin, J. W.; "Crystallisation" Butterworth, London, 2nd. edn. 1972.

(74) Mullin, J. W., and Ang, H. M.; Farad. Diss. of the Chemical Soc., 141 (1976) No. 61.

(75) Glasstone, S.; "Textbook of Physical Chemistry", Macmillan, 2nd. edn., London, 1962.

(76) Ostwald, W. Z.; Physik. Chem., 22 (1897) 289.

(77) Gibbs, J. W.; 'Collected Works', Longmans Green, London, 1928.

(78) Miers, H. A.; J. Chem. Soc., 89 (1906) 413.

(79) Miers, H. A., and Isaac, F.; Proc. Roy. Soc., A79 (1907) 322.

(80) de Coppet, L. C.; Annls. Chim. Phys., 10 (1907) 457.

(81) Nyvlt, J.; In "Industrial Crystallisation", I. Chem. E. Symposium (1969) pp. 1-23.

(82) Palmer, R. C., and Batchelor, J.; I. Chem. E. Symposium (1969) pp. 227-235.

(83) Granqvist, C. G., and Buhrman, R. A.; J. Appl. Phys., 47 (1976) 2200.

(84) Ostwald, W. Z.; Phys. Chem., 34 (1900) 495.

(85) Freundlich, H.; "Colloid and Capillary Chemistry", Methuen and Co., London, 1926.

(86) Jones, W. J.; Z. Phys. Chem., 82 (1913) 448.

(87) Dundon, M. L., and Mack, E.; J. Amer. Chem. Soc., 45 (1923) 2479, 2650.

(88) Hulett, G. A.; Z. Physik. Chem., 37 (1901) 385.

(89) Knapp, L. F.; Trans. Far. Soc., 17 (1921) 457.

(90) Kolthoff, I. M.; J. Phys. Chem., 36 (1932) 860.

(91) Fischer, J.; Anal. Chem. Acta., 22 (1960) 501.

(92) Vonnegut, B.; J. Colloid. Sci., 3 (1948) 563.

(93) Collins, and Leinweber; J. Phys. Chem., 60 (1956) 389.

(94) Turnbull, D.; Acta Met., 1 (1953) 684.

(95) Johnson, R. A., and O'Rourke, J. D.; J. Amer. Chem. Soc., 76 (1954) 2124.

(96) Katz, J. L., and Virkler, T. L.; Far. Diss. of Chem. Soc., No. 61 (1976) 83.

(97) Pound, G. M., and La Mer, V. K.; J. Chem. Phys., 17 (1949) 1337.

(98) Volmer, M., and Flood, H.; Z. Phys. Chem., A170 (1934) 273.

(99) Kirkwood, J. G., and Buff, F. P.; J. Chem. Phys., 17 (1949) 338.

(100) Tolman, R. C.; J. Chem. Phys., 17 (1949) 333.

(101) Rastogi, R. P., and Bassi, P. S.; J. Scient. Ind. Res., A21 (1962) 463.

(102) Dunning, W. J.; "Chemistry of the Solid State", edited by W. F. Garner, CH. VI.

(103) Farkas, L.; Z. Physik. Chem., 125 (1927) 236.

(104) Van Hook, A.; "Crystallisation - Theory and Practice", Reinhold, London, 1961.

(105) Strickland-Constable, R. F.; "Kinetics and Mechanism of Crystallisation", Academic Press, London, 1968.

(106) Stevenson, D. G.; Trans. Instn. Chem. Engrs., 42 (1964) T316.

(107) Einstein, A.; Ann. Physik., 33 (1910) 1275.

(108) Volmer, M., and Weber, A.; Z. Physik. Chem., 119 (1926) 277.

(109) Christiansen, J. A.; Acta Chem. Scand., 5 (1951) 676.

(110) Christiansen, J. A., and Nielsen, A.; Z. Electrochem., 56 (1952) 465.

(111) Christiansen, J. A.; Acta Chem. Scand., 8 (1954) 909, 1665.

(112) O'Rourke, J. D., and Johnson, R. A.; Anal. Chem., 27 (1955) 1699.

(113) Szilard, L.; referred to in Farkas, ref. (103).

(114) Becker, R., and Döring, W.; Ann. Physik., 24 (1935) 719.

(115) Zeldovich, J. B.; Acta Physicochemica, U.R.S.S., 18 (1943) 1.

(116) Frenkel, J.; J. Chem. Phys., 7 (1939) 200.

(117) Bradley, R. S.; Quart. Rev. Chem. Soc., London, 5 (1951) 315.

(118) Turnbull, D., and Fischer, J. C.; J. Chem. Phys., 17 (1949) 71.

(119) Becker, R.; Ann. Physik., 32 (1938) 128.

(120) Bransom, S. H.; Dunning, W. J.; and Millard, B.; Dis. Far. Soc., 5 (1949) 83.

(121) Turnbull, D., and Vonnegut, B.; Ind. Eng. Chem., 44 (1952) 1292.

(122) Newkirk, J. B., and Turnbull, D.; J. Appl. Phys., 26 (1955) 579.

(123) Melia, T. P., and Moffitt, W. P.; J. Coll. Sci., 19 (1964) 433.

(124) Dunning, W. J., and Notley, N. T.; Z. Electrochem., 61 (1957) 55.

(125) Dunning, W. J., and Shipman, A. J.; 'Proc. Agric. Indust.', 10th International Congress, Madrid, 1954.

(126) Carten, V. A., and Herd, R. B.; Phil. Mag., 8 (1963) 1793.

(127) Carten, V. A., and Herd, R. B.; Phil. Mag., 14 (1966) 1243.

(128) Nielsen, A. E.; Acta Chem. Scand., 15 (1961) 441.

(129) Kuznetsov, V. D.; "Crystals and Crystallisation", (in Russian) Moscow, 1953.

(130) Volmer, M.; Z. Electrochem., 35 (1929) 555.

(131) Mason, R. E. A., and Strickland-Constable, R. F.; Trans. Far. Soc., 62 (1966) 455.

(132) Lal, D. P.; Mason, R. E. A.; and Strickland-Constable, R. F.; J. Crystal Growth, 5 (1969) 1.

(133) Melia, T. P., and Moffitt, W. P.; Ind. Engng. Chem. Fund., 3 (1964) 313.

(134) Chretien, A., and Heubel, J.; C.r.hebd. Seance. Acad. Sci., Paris, 239 (1954) 814; 242 (1956) 2837.

(135) Nielsen, A. E.; J. Colloid. Sci., 10 (1955) 576.

(136) Khamskii, E. V.; "Crystallisation from Solutions", A special research report translated from Russian p.45.

(137) Tovberg, J. A.; Z. Phys. Chem., 180A (1937) 93.

(138) Van Hook, A.; J. Phys. Chem., 44 (1940) 75.

(139) La Mer, V. K., and Dinegar, R. H.; J. Amer. Chem. Soc., 73 (1951) 380.

(140) La Mer, V. K., and co-workers; J. Amer. Chem. Soc., 72 (1950) 4847.

(141) de Coppet, L. C.; Bull. Soc. Chim., 17 (1872) 146.

(142) Tamman, G.; "Stakes of Aggregation", Van Nostrand, New York 1925.

(143) Van Hook, K. A., and Bruno, A. J.; Dis. Far. Soc., 5 (1949) 112.

(144) Turnbull, D.; Tran. Am. Inst. Min. Met. Engrs., 175 (1948) 774.

(145) Van Hook, K. A.; Ind. Eng. Chem., 36 (1944) 1042.

(146) Christiansen, J. A., and Nielsen, A.; Acta Chem. Scand., 5 (1951) 673.

(147) Nielsen, A. E.; "Kinetics of Precipitation", Pergamon Press, London, 1964.

(148) Dunning, W. J.; Diss. Fara. Soc., 5 (1949) 79.

(149) Nielsen, A. E.; "Crystal Growth", Proceedings of an International Conference on Crystal Growth, Boston, 1966; Pergamon Press, London, 1967.

(150) Felbinger, A., and Neels, H.; Kirstal und Tecknic, 1 (1966) 137.

(151) Kuznetsov, V. D.; "Surface Energy of Solids", Trans. 1967, London, H.M.S.O.

(152) Walton, A. G.; Anal. Chem. Acta, 29 (1963) 434.

(153) Matijevic, E.; Chimia Aarau, 9 (1955) 287.

(154) Gupta, Y. P., and Santhanam, A. T.; Acta Meta., 17 (1969) 419.

(155) Bircumshaw, L. L., and Riddiford, A. C.; Quart. Revs., 6 (1952) 157.

(156) Sears, G. W.; J. Chem. Phys., 32 (1960) 1317.

(157) Sears, G. W.; J. Chem. Phys., 29 (1958) 1045.

(158) Curie, P.; Bull. Soc. France. Mineral, 8 (1885) 145.

(159) Wulff, G.; Z. Kristallogr., 34 (1901) 449.

(160) Burton, W. K., and Cabrera, N.; Diss. Farad. Soc., 5 (1949) 333.

(161) Marc, R.; Z. Physik. Chem., 61 (1908) 385; 67 (1909) 470; 73 (1910) 685.

(162) Noyes, A. A., and Whitney, W. R.; Z. Physik. Chem., 23 (1897) 689.

(163) Nernst, W.; Z. Physik. Chem., 47 (1904) 52.

(164) Berthoud, A.; J. Chem. Phys., 10 (1912) 624.

(165) Valeton, J. J. P.; Z. Krist., 59 (1923) 135, 335; 60 (1924) 1.

(166) Friedal, G.; Bull. Soc. Franc. Mineral, 48 (1925) 12; 49 (1926) 87.

(167) Reddy, M. M., and Nancollas, G. H.; J. Coll. Inter. Sci., 36 (1971) 166.

(168) Marshall, R. W., and Nancollas, G. H.; J. Phys. Chem., 73 (1969) 3838.

(169) Bujac, P. D. B., and Mullin, J. W.; "Industrial Crystallisation", Inst. Chem. Engrs. Sympos., London (1969) 121.

(170) Davies, C. W., and Jones, A. L.; Diss. Far. Soc., 5 (1949) 103.

(171) Campbell, J. R., and Nancollas, G. H.; J. Phys. Chem., 73 (1969) 1735.

(172) Jenkins, J. D.; J. Am. Chem. Soc., 47 (1925) 903.

(173) Allen, T.; "Particle Size Measurements", Chapman and Hall, London, 1968.

(174) Power, H. E. C.; Int. Sug. J., 50 (1948) 149.

(175) Mullin, J. W.; Ind. Chemist, 36 (1960) 277.

(176) Misra, C., and White, E. T.; A. I. Ch. E., 67 (1971) 53.

(177) Larson, M. A., and Randolph, A. D.; Chem. Eng. Prog. Sym., 65 (1969) 1.

(178) Garside, J., and Jancic, S. J.; A. I. Ch. E. J., 22 (1976) 887.

(179) Randolph, A. D., and Larson, M. A.; "Theory of Particulate Processes", New York, N.Y. Academic Press, 1971.

(180) Suess, E.; Geochim. Cosmochim. Acta, 37 (1973) 2435.

(181) Meyers, P. A., and Quinn, J. G.; Limnol. Oceanogr., 16 (1971) 992.

(182) Whetstone, J.; Trans. Far. Soc., 51 (1955) 973.

(183) Michaels, A. S., and Colville, A. R.; J. Phys. Chem., 64 (1960) 13.

(184) Matijević, E., and Ottewill, R. H.; J. Coll. Sci., 13 (1958) 242.

(185) Jaffe, H., and Kjellgren, B. R. F.; Diss. Far. Soc., 5 (1949) 319.

(186) Egli, P. H., and Johnson, L. R.; "The Art and Science of Growing Crystals", ed. Gilman, J. J. Wiley (1963) page 194.

(187) Smith, B. R., and Alexander, A. E.; J. Coll. Int. Sci., 34 (1970) 81.

(188) Liu, S. T., and Nancollas, G. H.; J. Coll. Int. Sci., 44 (1973) 422.

(189) Bassett, H. N.; Steam Engr., 6 (1937) 406.

(190) Ermolenko, N. F., etal.; J. Appl. Chem. U.S.S.R., 10 (1937) 2009.

(191) Reitemeier, R. F., and Buehrer, T. F.; J. Phys. Chem., 44 (1940) 535.

(192) Raistrick, B.; Diss. Far. Soc., 5 (1949) 234.

(193) Miura, M., etal.; Kogyo Kagaku Zasshi, 66 (1963) 597.

(194) Kitano, Y., and Hood, D. W.; Geochim. Cosmochim. Acta, 29 (1965) 29.

(195) McCartney, E. R., and Alexander, A. E.; J. Coll. Sci., 13 (1958) 383.

(196) Miura, M., etal.; Bull. Chem. Soc. Japan, 39 (1966) 344.

(197) Orlov, P., and Rossiisk, Zh.; Fiz. Khim. Obshch., 28 (1896) 714.

(198) Buckley, H. E.; "Crystal Growth", Wiley, J., N.Y. 1951.

(199) Frondel, C.; Am. Mineral, 25 (1940) 91.

(200) Royer, L.; Compt. Rend., 180 (1925) 378.

(201) Walcott, A. J.; Am. Mineral, 2 (1926) 221, 259.

(202) Nancollas, G. H., and Reddy, M. M.; In "Aqueous-Environmental Chemistry of Metals", ed. Rubin, A. J., Ann. Arbor. Science Pub. Inc., 1974.

(203) Reddy, M. M., and Nancollas, G. H.; Desalination, 12 (1973) 61.

(204) Sears, G. W.; In "Growth and Perfection of Crystals", eds. Doremus, R. H. etal. N.Y.; Wiley, J., and Sons Inc., 1958.

(205) Volmer, M., and Schultze, W.; Z. Physik. Chem., A156 (1931) 1.

(206) Freundlich, H.; Z. Physik. Chem., 75 (1910) 245.

(207) Kuntze, G, H.; Nature, 211 (1966) 406.

(208) Chave, K. E., and Suess, E.; Trans. N.Y. Acc. Sci., 29 (1967) 991.

(209) Suess, E.; Geochimca. Cosmochimca. Acta, 34 (1970) 157.

(210) Kipling, J.; Adsorption From Solutions of Non-Electrolytes, Acd. Press, London, 1965.

(211) Langmuir, I.; J. Am. Chem. Soc., 40 (1918) 1361.

(212) Akers, R. J.; Unpublished.

(213) Silberberg, A.; J. Phys. Chem., 66 (1962) 1872, 1884.

(214) Silberberg, A.; J. Chem. Phys., 46 (1967) 1105.

(215) Silberberg, A.; J. Chem. Phys., 48 (1968) 583.

(216) Oden, S.; "Die Huminsaurem", Kolloidchem. Beih., 11 (1919) 75.

(217) Schnitzer, M., and Khan, S. U.; "Humic Substances in the Environment" N.Y. 1972.

(218) Packham, R. F.; Water Treatment and Examination, 17 (1968) 316.

(219) Black, A. P.; J. A. W. W. Ass., 55 (1963) 753, 897.

(220) Guy, R. D., Chakrabartie, C. L., and Schramm, L. L.; Can. J. of Chem., 53 (1975) 661.

(221) France, L. G., and Werner, H.; Anal. Chem., 49 (1977) 216.

(222) Van Dijk, H.; Geoderma., 5 (1971) 53.

(223) Schnitzer, M., and Skinner, S. I. M.; Soil Sci., 99 (1965) 278.

(224) Stevenson, F. J.; In "Environmental Biogeochemistry", ed. Nriagu, J. O.; Ann Arbor Science, Michigan, 1976.

(225) Singer, P. C.; In "Trace Metals and Metal Organic Interactions in Natural Waters", ed. Ann Arbor Science, Michigan, 1973.

(226) Mortvedt, J. J.; Giordano, P. M.; and Lindsay, W. L.; In "Micronutrients in Agriculture", ed. Soil Science Society of America, 1972.

(227) Kononova, M. M.; "Soil Organic Matter", The Academy of Science of the U.S.S.R., 1961.

(228) Akram, A.; Ph.D. Thesis, Loughborough University, 1975.

(229) Riley, P. W.; Ph.D. Thesis, Loughborough University, 1972.

(230) Scarlett, B.; Rippon, M.; and Lloyd, J.; Proc. Part. Size Anal. Conf., 1966.

(231) Brunauer, S., etal.; J. Am. Chem. Soc., 60 (1938) 309. For errata see Emmett, P. H., and Dewitt, T. W.; Ind. Eng. Chem. (Anal), 13 (1941) 28.

(232) Krieger, K. A.; Ind. Eng. Chem. (Anal), 16 (1944) 398.

(233) Packham, R. F.; Soc. Wat. Treat. Exam., 13 (1964) 316.

(234) Schnitzer, M.; In "Soil Organic Matter", Dev. Soil Sci., 1978.

(235) Analysis of Raw, Potable and Waste Waters; Department of the Environment, London, 1972.

(236) Attia, Y. A., and Rubio, J.; Br. Polym. J., 7 (1975) 135.

(237) Crummett, W. B., and Hummel, R. A.; J. A. W. Wks. Ass., 55 (1963) 209.

(238) Baskerville, R. C., and Gale, R. S.; "Water Pollution Cont.", 67 (1968) 233.

(239) Oliver, D. R.; Chem. Eng. Sci., 15 (1961) 230.

(240) Kwatra, B.; Ahuja, L. D.; and Pamakrishna, V.; J. Appl. Chem., 20 (1970) 123.

(241) Moody, G. J.; Personal Communication.

(242) Moody, G. J., etal.; Analyst, 95 (1970) 910.

(243) Instruction Manual for Coulter Counter Model TA-II, Harpenden, England.

(244) Miura, M., etal.; Kogyo Kagaku Zasshi, 66 (1960) 1543.

(245) Fleer, G. J.; Ph.D. Dissertation, Agricultural Univ., Wageningen, The Netherlands, 1971.

(246) Tadros, M. E.; Skalny, J.; and Kalyouncu, R. S.; J. Coll. Int. Sci., 55 (1976) 20.

(247) Nancollas, G. H., and Reddy, M. M., J. Coll. Int. Sci., 37 (1971) 824.

(248) Hall, E. S., and Packham, R. F.; J. A. W. Wks. Ass., 57 (1965) 1149.

(249) Kruyt, H. R.; "Colloid Science", V.1, Elsevier.

(250) Scholtan, W.; Makromolec. Chem., 14 (1954) 169.

(251) Polymer Handbook, Eds. Brandrup, J., and Immegut, E. H., 2nd. Ed. 1975, Wiley and Sons, Inc.

(252) Perry, R. H., and Chilton, C. H.; "Chemical Engineers' Handbook", 5th Ed. 1973, McGraw-Hill Ltd.

(253) Robinson and Stokes; "Electrolyte Solution", Butterworth, London, 1958.

(254) Goodwin, J. W., etal; Br. Polymer J., 5 (1973) 347.

Appendix One: Calculations For Achieving The Level of Initial Supersaturation Ratio, S_i.

(A) $Ca(HCO_3)_2$ concentration

The concentration of calcium bicarbonate stock solution is determined by titration (50) ml of the calcium bicarbonate solution with 0.1 N HCl to methyl orange end point.

e.g. 50ml sample required 9.05ml 0.1 N HCl.

HCO_3^- = 9.05 x 2 x 61.02 = 1.10446gm/l

$Ca(HCO_3)_2$ concentration = $\frac{1.10446 \times 162.04}{122.04}$

= 1.4665gm/l = 0.1466gm/100ml

(B) $Ca(OH)_2$ concentration

The concentration of $Ca(OH)_2$ stock solution is determined by titration (50) ml of the solution with 0.1 N HCl using phenolphthalein as indicator.

e.g. 50ml sample required 10.8ml 0.1 N HCl.

$Ca(OH)_2$ concentration = 10.8 x 0.0074 = 0.07992gm/100ml

(C) The Supersaturation Ratio, S_i

For each precipitation run

$$Ca(HCO_3)_2 + Ca(OH)_2 \longrightarrow 2CaCO_3 + 2H_2O$$

162.04 74.09 200

e.g. 0.1466gm/100ml $Ca(HCO_3)_2$ needs 0.1466 x $\frac{74.09}{162.04}$

= 0.0670gm/100ml

Volume of $Ca(OH)_2$ required to make 0.0670gm

= 0.0670 x $\frac{100}{0.07992}$

Volume $Ca(OH)_2$ required = 83.87ml

Supersaturation Ratio, $S_i = \frac{\text{total solute (gm)}}{\text{total water (gm)}} \times \frac{100}{C^*}$

Total amount of solute present = 0.1466 + 0.0670

= 0.2136gm

Let the mass of water to be added to the precipitation vessel for diluting the resultant reaction mixture to the desired supersaturation ratio, S_i, be W_{gm}.

The total amount of water present = 100 + 83.87 + W

C^*, the solubility of $CaCO_3$ at the experimental temperature and pH = 0.000633gm/100

$$S_i = \frac{0.2136}{183.87 + W} \times \frac{100}{0.000633}$$

To achieve a supersaturation ratio of 20 at 25°C

$$S_i\ 20 = \frac{0.2136}{183.87 + W} \times \frac{100}{0.000633}$$

W = 1503.33gm, i.e.,

mass of water required for diluting the reaction mixture to give S_i of 20 is 1503.33gm

Thus to create a supersaturation of 20 we require

Volume of water = 1503ml

Volume of $Ca(HCO_3)_2$ = 100ml

Volume of $Ca(OH)_2$ = 84ml

Appendix Two: Typical Calculation For The Mass of $CaCO_3$ Recovered.

Run I

$S_i = 60$

$[Ca^{++}]_o = 32.2 \times 10^{-4}M$

$(CaCO_3) = 32.2 \times 10^{-2}gm/l$

(A) The experimental calcium ion concentration in solution and the corresponding pH as a function of time are:-

Time (mins)	pH	$[Ca^{++}] \times 10^4 M$	$CaCO_3 \times 10^2 gm/l$
3	11.15	8.5	8.5
5	10.72	7.2	7.2
10	10.00	5.5	5.5
15	10.12	4.8	4.8

(B) The amount of solid $CaCO_3$ removed as a function of time:-

Time (mins)	$(CaCO_3)_B$ Precipitated
3	$23.7 \times 10^{-2}gm/l$
5	$25.0 \times 10^{-2}gm/l$
10	$26.7 \times 10^{-2}gm/l$
15	$27.4 \times 10^{-2}gm/l$

(C) From the size distribution the number of particles in 2 mls sample at a particular time as a function of size are:-

	Population No. (n)			
diameter, μm	3 mins	5 mins	10 mins	15 mins
2	2871	3175	4041	5381
2.52	1701	1337	1515	2208
3.17	1214	1290	1336	1687
4	1000	1259	1197	1304
5.04	817	1510	965	1040
6.35	765	1392	860	921
8	18414	1027	1511	1054
10.08	3449	12571	1476	2029
12.7	109	8082	15784	4743
16	15	85	3021	15093
20.16	10	15	30	123
25.4	5	5	5	10
32	1	1	3	2

(D) Since each channel in Coulter Counter TA-II displace the results on volume basis (see 6.6.1)

$$V = n_i \times \bar{V}_i$$

where V = is the volume of the particles.

n_i = is the number of particles in channel i.

$\bar{V}_i$ = is the average volume of channel i, for example,

$$\bar{V}_{10} = \frac{V_{10} + V_{11}}{2}$$

$$\bar{V}_{10} = \frac{4}{3} \left(\frac{d_{10} + d_{11}}{4}\right)^3$$ (assuming spherical particles)

$$\bar{V}_{10} = \frac{4}{3} \left(\frac{10.08 + 12.7}{4}\right)^3 \times 10^{-12} = 7.737 \times 10^{-10} \text{ cm}^3$$

The volumes of particles at a particular time as a function of size are:-

$$V = n_i V_i \times 10^{10}$$

diameter, μm	V, cm^3	3 mins	5 mins	10 mins	15 mins
2	6.044×10^{-12}	174	192	244	325
2.52	1.206×10^{-11}	41	161	183	266
3.17	2.412×10^{-11}	293	311	322	407
4	4.835×10^{-11}	484	609	579	630
5.04	9.671×10^{-11}	790	1460	933	1006
6.35	1.934×10^{-10}	1480	2692	1663	1781
8	3.868×10^{-10}	71225	3972	5845	4077
10.08	7.737×10^{-10}	26685	97262	11420	15698
12.7	1.547×10^{-9}	1686	125028	244178	73374
16	3.094×10^{-9}	464	2630	93470	466977
20.16	6.19×10^{-9}	619	929	1857	7614
25.4	1.238×10^{-8}	619	619	619	1238
32	2.474×10^{-8}	247	247	7421	495

(E) The total volume as a function of time is:-

Time (mins)	$V \times 10^{10}$, cm^3
3	104807
5	236112
10	368734
15	573888

(F) The mass of solid $CaCO_3$, m, = $V \times 2.713 \times \frac{1000}{2} \times 3$ gm/l

where 2.713 = the density of $CaCO_3$ gm/cm^3

3 = is the dilution factor

the mass of $CaCO_3$ removed as a function of time is:-

Time (mins)	$(CaCO_3)_F \times 10^2$, gm/l
3	4.265
5	9.608
10	15.00
15	23.40

(G) Comparing mass of solid $(CaCO_3)_B$ precipitated calculated from calcium ion concentration solution with mass of solid $(CaCO_3)_F$ calculated from size distribution, the mass yield from the size distribution as a function of time is:-

Time (mins)	$(CaCO_3)_B$ gm/l	$(CaCO_3)_F$ gm/l	mass particle yield
3	23.70×10^{-2}	4.26×10^{-2}	18%
5	25.00×10^{-2}	9.61×10^{-2}	38%
10	26.70×10^{-2}	15.00×10^{-2}	56%
15	27.40×10^{-2}	23.40×10^{-2}	85%

Appendix Three: Sample Calculation of The Rate of Crystal Growth.

Run I

$S_i = 60$

(A) The specific surface area $A = n_i \bar{A}_i$

where n_i = is the number of particles in channel i,

$i \geqslant 9$

$\bar{A}_i$ = is the average surface area of equivalent spherical particles in channel i, e.g.

$$\bar{A}_{10} = 4\pi \left(\frac{10.08 + 12.7}{4}\right)^2 \times 10^{-12}$$

$$= 4.076 \times 10^{-10} \text{ m}^2$$

The specific surface area of the particles at a sampling time as a function of size are:-

		A, at sampling time (min) x 10^6			
dia. μm	$\bar{A} \times 10^{12}$ m^2	3	5	10	15
8	256.74	47.28	2.64	3.88	2.71
10.08	407.56	14.06	51.23	6.02	8.27
12.7	646.92	0.7	52.23	102.11	30.68
16	1026.94	0.15	0.87	31.02	155.00
20.16	1630.26	0.16	0.23	0.47	2.00
25.4	2587.70	0.13	0.13	0.13	0.26
32	4105.50	0.04	0.04	0.12	0.08

(B) The total rea, A, has a function of sampling time is:-

Time (mins)	A x 10^2, m^2/l
3	0.94
5	1.61
10	2.16
15	2.98

(C) The linear growth rate $dG/dt = (dCa^{++}/dt)/A$

where $\frac{dCa^{++}}{dt} = \frac{d\ Ca^{++}}{dt} \times \frac{100}{2.71} \times 10^{-6}$

For example $\frac{d\ Ca^{++}}{dt}$ at 3 minutes sample time, which is the tangent to the Ca^{++} versus t graph (figure 8.16)

$= 0.86 \times 10^{-4}\ M.min^{-1}$.

100 = molecular weight of $CaCO_3$.

2.71 = calcium carbonate density gm/cm^3.

$$\frac{dCa^{++}}{dt} = 0.86 \times 10^{-4} \times \frac{100}{2.71} \times 10^{-6} = 3.173 \times 10^{-9}\ m^3\ min^{-1}$$

$$\frac{dG}{dt} = \frac{3.17 \times 10^{-9}}{0.94 \times 10^{-2}} = 3.37 \times 10^{-7}\ m\ min^{-1}$$